Institute of Aircraft Design
Lehrstuhl für Luftfahrtsysteme

Vertiport Sizing and Layout Planning through Integer Programming in the Context of Urban Air Mobility

Master Thesis

Submitted in partial fulfillment of the requirements for the degree M.Sc. Mechanical Engineering at the Department of Mechanical Engineering of the Technical University of Munich.

Supervised by Prof. Dr.-Ing. Mirko Hornung
Lukas Preis, M.Sc.
Institute of Aircraft Design

Submitted by Manuel Hack Vázquez
Student ID: 03662303

Submitted on September 1, 2021

Sequential number LS-MA-2102-EX

Kurzfassung

Auf der Suche nach einem Transportmittel mit dem Potenzial Reisezeiten zu verkürzen und die Umwelt zu schonen, ist ein Konzept, dass seit den 1950er Jahren untersucht wird, wieder in den Fokus gerückt: Urban Air Mobility (UAM). Aufgrund seiner Vorteile hat der städtische Luftverkehr das Potenzial, das bestehende Verkehrssystem zu bereichern. Eine der größten, aber gleichzeitig am wenigsten untersuchten Hürden ist die, für das UAM-Netz erforderliche Infrastruktur. Kernstück der Infrastruktur sind die Flughäfen für elektrisch senkrecht startende und landende Vehikel, die so genannten Vertiports. Die Identifizierung und Auswahl möglicher Vertiport-Standorte ist bereits untersucht worden. Eine Forschungslücke zeigt sich jedoch im Bereich der Dimensionierung von Vertiports, die insbesondere in städtischen Gebieten aufgrund des begrenzten Platzangebots wichtig ist. In dieser Arbeit wird daher eine auf Integerprogrammierung basierende Methode vorgestellt, die es erlaubt, automatisch ein Vertiport-Design für ein gegebenes Gebiet zu erstellen und dessen möglichen Durchsatz abzuschätzen. Mit Hilfe der in MATLAB implementierten Methode zur Vertiport-Dimensionierung wurden Sensitivitätsstudien durchgeführt. Die Prozesszeiten (einschließlich der Ein- und Ausstiegszeiten sowie der An- und Abflugzeiten), die Größe der Vehikel, die zu verwendenden Topologien sowie die geometrischen Spezifikationen wurden für 1000 Flächen unterschiedlicher Größe und Form variiert. Daraus resultierten mehr als 25 Millionen Kombinationen der verschiedenen Parameter, die in den Studien analysiert wurden. Die Ergebnisse deuten darauf hin, dass im Vergleich zu den fünf anderen untersuchten Vehikel, die höchsten Durchsätze mit dem von Airbus entwickelten Vehikel erzielt werden können. Bei Turnaround-Zeiten von etwa 10 Minuten wurde ein stündlicher Passagierdurchsatz von über 0,14 Passagieren pro Quadratmeter Vertiport-Fläche erreicht. Bei sehr kurzen Abfertigungszeiten sind bis zu 0,4 Passagiere pro Stunde und Quadratmeter möglich. Es zeigt sich auch, wie wichtig es ist, bei der Planung eines Vertiports, die zu erwartenden Prozesszeiten zu berücksichtigen. Lange Start- und Landezeiten reduzieren tendenziell die Anzahl der Gates pro Pad, während die Turnaround-Zeiten diese erhöhen. Die Ergebnisse zeigen, dass in Abhängigkeit von

diesen Prozesszeiten und der Wahl des Fahrzeugs, Verhältnisse zwischen einem und maximal sieben Gates pro Pad wünschenswert sind.

Schlagwörter: Urban Air Mobility, electric Vertical Take-Off and Landing, Vertiport

Abstract

In the search for a mode of transportation that has the potential to reduce travel times and is environment-friendly, a concept that has been studied since the 1950s has come back into focus: Urban Air Mobility (UAM). Due to its advantages, urban air transportation holds the potential to enrich the existing transportation system. One of the biggest, but at the same time least studied challenges is the infrastructure needed for the UAM network. The centerpiece of the infrastructure are the airports for electrical vertical take-off and landing vehicles, the so called vertiports. The identification and selection of possible vertiport locations has already been investigated. However, a research gap in the area of dimensioning of vertiports, which is particularly important in urban areas due to the limited available space, becomes apparent. In this work, therefore, a method based on integer programming is presented, which allows to automatically create a vertiport design for a given area and to estimate its possible throughput. Using a method for vertiport sizing, which is implemented in MATLAB, sensitivity studies were conducted. The process times (including boarding and deboarding times and arrival and departure times), the size of the vehicles, the topologies to be used, as well as the geometric specifications were varied for 1000 areas of different sizes and shapes. As a result, more than 25 million combinations of the different parameters were obtained and analyzed in the study. The results suggest, that compared to the five other investigated vehicles, the highest throughputs can be achieved with the vehicle designed by Airbus. For turnaround times of about 10 minutes, an hourly passenger throughput of over 0.14 passengers per square meter of vertiport footprint was reached. With very low processing times up to 0.4 passengers per hour and sqaure meter are possible. It is also shown how important it will be to consider the expected process times when planning a vertiport. Long take-off and landing times tend to reduce the number of gates per pad, in contrast to turnaround times, which increase them. The results show that, depending on these process times and the choice of vehicle, ratios between one and a maximum of seven gates per pad are desirable.

Keywords: Urban Air Mobility, electric Vertical Take-Off and Landing, Vertiport

Table of contents

List of Figures XI

List of tables XIII

Symbol directory XVI

1 Introduction 1

1.1 Urban mobility challenges 1

1.2 Urban Air Mobility as potential solution 2

1.3 Potential of Urban Air Mobility 4

1.4 Motivation 6

1.5 Objective 7

1.6 Thesis outline 8

2 State of the Art 9

2.1 UAM Vehicles 9

2.1.1 Architecture of Vertical Take-Off and Landing Vehicles 9

2.1.2 Propulsion Systems for Vertical Take-Off and Landing Vehicles 11

2.2 Airport Planing 12

2.2.1 Airfield Design 17

2.2.2 Airfield Capacity 18

2.2.3 Taxiway Capacity 19

2.2.4 Apron Capacity 20

2.2.5 Airport Facilities 22

2.3 Heliport Design Guidelines 23

2.3.1 Vertiport site selection 26

2.3.2 Layout and design of heliport components 28

2.3.2.1 Pad 30

2.3.2.2 Gate 34

2.3.2.3 Taxiway 35

2.4 Vertiports 37

3 Methods **41**
3.1 UAM Planning Tools . . . 41
3.1.1 Vertiport Simulation . . . 42
3.1.2 Location Identification . . . 44
3.2 Identification of Research Gap . . . 45
3.2.1 Existing Vertiport Design Tool . . . 45
3.2.2 Weaknesses of Existing Vertiport Design Tool . . . 47
3.3 Extended Area to Throughput Method . . . 48
3.3.1 Vertiport Airfield Model . . . 48
3.3.1.1 Mathematical Formulation . . . 49
3.3.1.2 Assumptions and Simplifications . . . 50
3.3.2 Implementation of Model . . . 51
3.3.2.1 Main . . . 51
3.3.2.2 Layout Calculation . . . 54
3.3.2.3 Throughput Calculation . . . 59
3.3.2.4 Taxiway length . . . 62
3.3.3 Layout Configurations . . . 66
3.3.3.1 Single Topology . . . 66
3.3.3.2 Satellite Topology . . . 71
3.3.3.3 Linear Topology . . . 73
3.3.3.4 Pier Topology . . . 75
3.3.4 Inputs and Outputs . . . 79
3.4 Graphical User Interface for Layout Design . . . 83
3.5 Throughput to Area Method . . . 86
3.5.1 Model . . . 87
3.5.2 Implementation . . . 87
3.5.3 Inputs and Outputs . . . 90

4 Results and Discussion **93**
4.1 Area to Throughput . . . 93
4.1.1 Study with version one . . . 93

4.1.1.1 Experimental Setup 93
4.1.1.2 Results 94
4.1.2 Study with improved version 98
4.1.2.1 Experimental Setup 99
4.1.2.2 Results Research Questions on Shape of Area and Topology of Layout 101
4.1.2.3 Results Research Questions on Throughput of Layout 110
4.1.2.4 Results Research Questions on resulting Layout . . . 116
4.1.2.5 Results Research Questions on Bottleneck of Layout 122
4.2 Real World Scenario 127
4.2.1 Experimental Setup 128
4.2.2 Best Vehicle 131
4.2.3 Resulting Designs 132
4.3 Throughput to Area 136
4.3.1 Experimental Setup 137
4.3.2 Results 138

5 Conclusion **145**

6 Summary **147**

7 Outlook **150**

Bibliography **152**

A Appendix: Vertiport Layouts **A-1**

B Appendix: Area to Throughput Study with improved version **B-1**

C Appendix: Area to Throughput Real World Scenario **C-1**

D Appendix: Throughput to Area Study **D-1**

List of Figures

1.1 Vertiport design from 1951 [15] and today [16] 2
1.2 Potential time savings through UAM [11] 4

2.1 Most common VTOL concepts [45] 10
2.2 Vertiport model from Lilium [14] A - pad; B - gate; C - terminal; D - taxiway 29
2.3 Measures of a VTOL [87] 30
2.4 Structure and measures of a pad 31
2.5 Structure and measures of a gate 34
2.6 Structure and measures of a taxiway 36
2.7 Four vertiport topologies 40
2.8 Process steps at a vertiport for an eVTOL [88] 40

3.1 UAM Planning Tools 41
3.2 Flowchart of the main function of the area to throughput method 52
3.3 Flowchart of the function to calculate the single topology of the area to throughput method 55
3.4 Flowchart of the function to calculate the satellite topology of the area to throughput method 56
3.5 Flowchart of the function to calculate the linear topology of the area to throughput method 57
3.6 Flowchart of the function to calculate the pier topology of the area to throughput method 58
3.7 Flowchart of the processes a VTOL goes through on a vertiport 60
3.8 Distances for vertiport processes 61
3.9 Distances for taxiing at satellite topology 63
3.10 Distances for taxiing at linear topology 64
3.11 Distances for taxiing at pier topology 66
3.12 Configuration of four pads as single topology in line 67
3.13 Configuration of n_{Pads} as single topology in line 68
3.14 Configuration of n_{Pads} as single topology with more than one line . . . 70

3.15 Corner and middle pads in satellite topology 71
3.16 Configuration linear topology with $gate2pad$ ratio of three 74
3.17 Configuration pier topology with $gate2pad$ ratio of n_{pads} one line 76
3.18 Configuration pier topology with $pad2taxi$ of two 78
3.19 Output sheet of GUI before placing elements 84
3.20 Notification box when number of pads is exceeded 85
3.21 Flowchart throughput to area approach 89

4.1 Throughput for different vehicles out of study with version one of area to throughput approach 95
4.2 Distribution of topologies over the surface for vehicle from Uber 96
4.3 Distribution of topologies over the surface for different vehicles 97
4.4 Distribution of topologies over the surface for the vehicle of eHang with side ratios of two to three and $t_{turn,passenger} = 15\ s$ and $t_{T\&L} = 30\ s$ . . 104
4.5 Distribution of topologies over the surface and different side ratios $t_{turn,passenger} = 15\ s$ and $t_{T\&L} = 30\ s$ 105
4.6 Distribution of topologies over the surface and different side ratios $t_{turn,passenger} = 15\ s$ and $t_{T\&L} = 90\ s$ 107
4.7 Distribution of topologies over the surface and different side ratios $t_{turn,passenger} = 90\ s$ and $t_{T\&L} = 30\ s$ 108
4.8 Distribution of topologies over the surface and different side ratios $t_{turn,passenger} = 90\ s$ and $t_{T\&L} = 90\ s$ 109
4.9 Hourly passenger throughput for different vehicles and $t_{turn,passenger} = 60\ s$ and $t_{T\&L} = 30\ s$ and $t_{turn,fix} = 0\ min$ 112
4.10 Hourly passenger throughput for different vehicles and process times and $t_{turn,fix} = 0\ min$ 113
4.11 Hourly passenger throughput for different vehicles and process times and $t_{turn,fix} = 10\ min$ 115
4.12 Topology layout for CityAirbus for $t_{turn,passenger} = 30\ s$ and $t_{turn,fix} = 0\ min$ 118

4.13 Topology layout for CityAirbus for different process times and $t_{turn,fix} = 0\ min$ 119
4.14 Topology layout for eHang for different process times and $t_{turn,fix} = 0\ min$ 121
4.15 Bottleneck distribution for eHang for $t_{turn,passenger} = 90\ s$ and $t_{turn,fix} = 0\ min$ and $t_{T\&L} = 60\ s$ 123
4.16 Bottleneck distribution for eHang for different process times and $t_{turn,fix} = 0\ min$ and $t_{T\&L} = 60\ s$ 124
4.17 Bottleneck distribution for VoloCity for different process times and $t_{turn,fix} = 0\ min$ and $t_{T\&L} = 60\ s$ 126
4.18 Bottleneck distribution for Lilium for different process times and $t_{turn,fix} = 0\ min$ and $t_{T\&L} = 60\ s$ 127
4.19 UAM network of real world scenario [118] 129
4.20 Locations of real world scenario [118] 130
4.21 Pier topology layout for Tempelhof for CityAirbus 133
4.22 Pier topology layout for Kanzleramt for CityAirbus 134
4.23 Linear topology layout for Alexanderplatz for CityAirbus 136
4.24 Best topology for desired throughput for vehicle of Airbus 139
4.25 Best topology for desired throughput for all vehicles 140
4.26 Comparison for area needed for $t_{T\&L} = 60\ s$ and $t_{turn,passenger} = 30\ s$ 142
4.27 Comparison for area needed for different process times 143

A.1 Layouts single topology for one, two and three pads A-1
A.2 Layouts single topology for four pads A-2
A.3 Layouts satellite topology for two pads A-3
A.4 Layouts satellite topology for three pads A-4
A.5 Layouts satellite topology for four pads in quadratic configuration . . . A-5
A.6 Layouts satellite topology for four pads in linear configuration A-6
A.7 Layouts satellite topology for n pads in linear configuration A-6
A.8 Layouts satellite topology for n pads in quadratic configuration A-7
A.9 Layouts linear topology for one, two, three and four pads in one row for given x_{min} A-8

A.10 Layouts linear topology for one, two, three and four pads in two rows for given x_{min} A-9
A.11 Layouts pier topology for one and two pads for $pad2taxi = 1$ A-10
A.12 Layouts pier topology for three pads for $pad2taxi = 1$ A-11
A.13 Layouts pier topology for four pads for $pad2taxi = 1$ A-12
A.14 Layouts pier topology for n pads for $pad2taxi = 1$ A-13
A.15 Layouts pier topology for n units in linear configuration for $pad2taxi = 2$ A-14
A.16 Layouts pier topology for n units in quadratic configuration for $pad2taxi = 2$ A-15

B.1 Eperimental setup of study with improved version of area to throughput B-1
B.2 Hourly passenger throughput for different vehicles and process times and $t_{turn,fix} = 5\ min$ B-2
B.3 Hourly passenger throughput for different vehicles and process times and $t_{turn,fix} = 15\ min$ B-3
B.4 Hourly passenger throughput for different vehicles and process times and $t_{turn,fix} = 20\ min$ B-4
B.5 Topology layout for Lilium for different process times and $t_{turn,fix} = 0\ min$ B-5
B.6 Topology layout for Uber for different process times and $t_{turn,fix} = 0\ min$ B-6
B.7 Topology layout for Boeing for different process times and $t_{turn,fix} = 0\ min$ B-7
B.8 Topology layout for VoloCity for different process times and $t_{turn,fix} = 0\ min$ B-8
B.9 Bottleneck distribution for Uber for different process times and $t_{turn,fix} = 0\ min$ and $t_{T\&L} = 60\ s$ B-9
B.10 Bottleneck distribution for Boeing for different process times and $t_{turn,fix} = 0\ min$ and $t_{T\&L} = 60\ s$ B-10
B.11 Bottleneck distribution for CityAirbus for different process times and $t_{turn,fix} = 0\ min$ and $t_{T\&L} = 60\ s$ B-11

C.1 Eperimental setup of real world scenario of area to throughput approach C-1

D.1 Eperimental setup of throughput to area approach D-1

List of tables

2.1 Aiport planning in USA and rest of world [52] 15
2.2 Planning factors for airport facilities [55] 23
2.3 Minimum safety area width depending on markings for general aviation heliport [71] 32
2.4 Comparison pad measures of FAA and ICAO 33
2.5 FATO minimum separation distances for simultaneous operations . . . 33
2.6 Comparison gate measures of FAA and ICAO 35
2.7 Taxiway dimensions for FAA [71] 36
2.8 Taxiway dimensions for ICAO [72] 37

3.1 Overview of variables in mixed integer programming problem formulation 50
3.2 Inputs stored in parameter file for area to throughput method 79
3.3 Structure of the area file for a square with side length of 10 meters . . 81
3.4 Outputs stored in results file for area to throughput method 82
3.5 Output of center-position extraction for elements out of GUI 86
3.6 Vehicles implemented in the throughput to area approach 88
3.7 Inputs stored in parameter file for throughput to area method 90
3.8 Outputs stored in results file for area to throughput method 91

4.1 Vehicles considered for study of the area to throughput approach . . . 93
4.2 Parameters for study with version one of the area to throughput approach 94
4.3 Parameters for study with improved version of the area to throughput approach 99
4.4 Considered parameters for research questions on shape of area and topology of layout of the area to throughput approach 102
4.5 Considered parameters for research questions on throughput of layout of the area to throughput approach 111
4.6 Considered parameters for research questions on resulting layout of the area to throughput approach 117

4.7 Varied parameters for real world scenario of the area to throughput approach 128
4.8 Fixed parameters for real world scenario of the area to throughput approach 130
4.9 Hourly throughput for different locations and vehicles 131
4.10 Varied parameters for sensitivity study with throughput to area approach 137
4.11 Fixed parameters for sensitivity study with throughput to area approach 138

Symbol directory

Abbreviations . .

AAM ..... Advanced Air Mobility
ATC ..... Air Traffic Control
ATM ..... Air Traffic Management
BMVI ..... Bundesministerium für Verkehr und Digitale Infrastruktur
CCC ..... Capacity Coverage Chart
ConOps ..... Concept of Operations
DLR ..... Deutsches Zentrum für Luft- und Raumfahrt
EASA ..... European Union Aviation Safety Agency
EPSG ..... Cartesian Gauss-Krüger Coordinate System
EU ..... European Union
eVTOL ..... electric Vertical Take-Off and Landing Vehicle
FATO ..... Final Approach and Take-Off Area
GDP ..... Gross Domestic Product
GIS ..... Geographic Information System
GUI ..... Graphical User Interface
IATA ..... International Air Transport Association
ICAO ..... International Civil Aviation Organization
IFR ..... Instrument Flight Rules
IMC ..... Instrument Meteorological Conditions
LuftVG ..... German Air Traffic Act
LuftVZO ..... Luftverkehrs-Zulassungs-Ordnung
MD ..... Maximum Dimension
MRO ..... Maintanance, Repair and Overhaul
MSL ..... Mean Sea Level
MTOM ..... Maximum Take-Off Mass
NAS ..... National Airspace System
NASA ..... National Aeronautics and Space Administration
NATA ..... National Air Transportation Association
OSM ..... OpenStreetMap
PHC ..... Practical Hourly Capacity
PT ..... Positioning Time
RCE ..... Remote Component Environment
RFI ..... Request for Information

SA	Safety Area
SBT	Stand Blocking Time
SME	Subject Matter Expert
SOT	Scheduled Occupancy Time
STOL	Short Take-Off and Landing
TLOF	Touchdown and Lift-Off Area
TTS	Tip-to-Tip Span
UAM	Urban Air Mobility
UCD	Undercarriage Dimension
UTM	Unmaned Traffic Management
VBA	Visual Basic for Application
VMC	Visual Meteorological Conditions
VTOL	Vertical Take-Off and Landing Vehicle
WLC	Weighted Linear Combination

Indices

$calc$	calculated value	$[-]$
$FATO$	final approach and take-off area	$[-]$
$height$	height	$[-]$
$long$	expansion in long direction	$[-]$
max	maximum dimension	$[-]$
min	minimum dimension	$[-]$
SA	safety area of pad	$[-]$
SG	safety area of gate	$[-]$
$short$	expansion in short direction	$[-]$
$T\&L$	take-off and landing process	$[-]$
$turn$	turnaround process	$[-]$
TW	taxiway	$[-]$
$unit$	unit consisting of pad, gates and taxiway	$[-]$
$width$	width	$[-]$

Latin Symbols

A	area	$[m^2]$
$gate2pad$	gate to pad ratio	$[-]$
l	length	[m]
n_i	number of i	$[-]$

$pad2taxi$	pad to taxi ratio	$[-]$
t	time	[s]
$taxi2gate$	taxi to gate ratio	$[-]$
v	speed	[m/s]
x	distance between two FATOs	[m]

1 Introduction

1.1 Urban mobility challenges

With more than four billion people, over half of the world's population lives in cities at this point in time. According to The World Bank [1], over $80\ \%$ of the world's gross domestic product (GDP) is generated in these cities, making them the epicenters of economic activity. However, the large population and economic potency of cities leads to an increasing burden of traffic, which is largely responsible for air pollution [2].

In the U.S. just the transportation sector is responsible for $29\ \%$ of greenhouse gas emissions, causing more emissions than electricity generation ($28\ \%$) or industrial production ($22\ \%$). In Europe, as much as $30\ \%$ of greenhouse gases are attributable to the transportation sector, of which $72\ \%$ are caused by road transport [3].

In addition to the impact on the environment, growing traffic has a particular impact on people's quality of life in the form of congestion. Getting to work is considered a time eater for millions of people worldwide [2]. Studies show that since 1982, as cities have grown and megacities have emerged, the impact of congestion has grown rapidly [4]. On average, drivers in London spend 227 hours per year in congestion at a speed of $11\ \mathrm{km/h}$ [5]. Globally, people in major cities spend an average of 160 hours annually in congestion. This is equivalent to 21 working days a year lost on the way to work [6, 7].

Thus, congestion not only results in a loss of lifetime, but also leads to significant financial losses. In the U.S., according to Schrank et al. [8], 8.8 billion hours of work time and 3.3 billion gallons of fuel were wasted due to congestion in 2017, resulting in a financial loss of US$179 billion. The loss is expected to increase by $32\ \%$ by 2025. The Centre for Economics and Business Research forecasts that Germany, England, France, and the United States will lose US$4.4 trillion between 2013 and 2025 [9]. Congestion therefore results in less time with family, less time at work to drive our economy, more money spent on gasoline, and a significant increase in our stress levels which also negatively impacts physical health according to a study in the American Journal of Preventative Medicine [10, 11].

In addition, many roads are needed to carry this large traffic load. Therefore, for an average city, about $50\ \%$ of the public land is obstructed by roads and thus important living space is lost [12]. Especially considering that by 2050 the world population is expected to grow to 10 billion and $70\ \%$ of these people are expected to settle in cities [13]. This will lead to a further intensification of the problems and therefore action is needed.

1.2 Urban Air Mobility as potential solution

In the search for a mode of transportation that has the potential to reduce travel times and is environmentally sustainable, a concept that has been studied since the 1950s [14] has come back into focus, Urban Air Mobility (UAM). New technologies in the areas of propulsion, battery technology, sensor technology, microprocessors and advances in automation offer the potential to revive this old idea on a new scale. Figure 1.1 compares a vertiport design from 1951 with one from today.

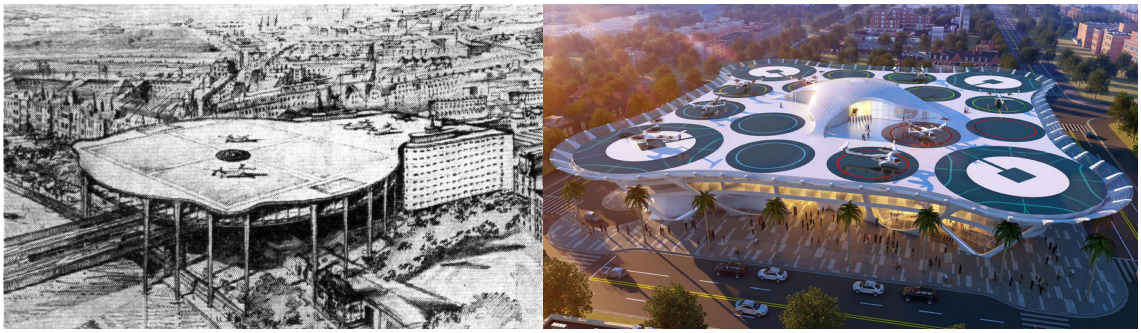

Figure 1.1: Vertiport design from 1951 [15] and today [16]

In particular electric vertical take-off and landing vehicles (eVTOL) are considered promising [17], as electric propulsion is expected to reduce greenhouse gases, and expansion into 3D space can counteract problems such as congestion or the buildup of potential living space.

Further the area of automation in particular offers opportunities. Not only travel costs could be reduced, but the use of infrared and electro-optical cameras as well as long range radar can also lead to a gain in safety. This is due to the fact that a large part of aircraft accidents are caused by human error [18] and it would be possible

to make VTOLs twice as safe as driving a car [11]. Further, pilot training time can be shortened through reduced skill requirements, as well as pilot mission time can be increased through the technical assistance provided through automatization. New propulsion concepts as well as VTOL architectures, as presented in section 2.1, offer further advantages in the areas of safety and environmental compatibility.

Moreover, benefits are predicted, especially in inter- and intra-city transport within a radius of 80 to 800 km [19]. According to Anand et al. [20], the introduction of UAM will lead to the reduction of congestion, travel time, and greenhouse gas emissions. It will also make it easier to reach remote locations. For example, according to Duvall et al. [21], the transportation of medicines or even other goods with time-brisance of delivery can be transported quickly and safely.

Uber is also predicting time savings [11]. A trip from San Francisco Marina to work in downtown San Jose usually takes two hours; with UAM, the distance can be covered in 15 minutes. Or one can save almost four hours for a round trip between downtown São Paulo and the suburbs in Campinas (see figure 1.2). For example, an eVTOL air taxi can transport passengers from Charles de Gaulle Airport in Paris to Orleans (160 km by road or 133 km by air) in about 35 minutes, instead of the two hours it takes today by car [2]. Brown et al. [7] also provide an overview of the potential time savings that can be achieved by implementing UAM in various cities around the world. It shows that travel times can be reduced by over $70\ \%$.

Figure 1.2: Potential time savings through UAM [11]

The use of airspace also reduces the reliance on roads, rail, bridges or tunnels and thus, according to Brown et al. [7], financial savings of 70 to $75\ \%$ can be achieved through reduced expansion and maintenance of the ground transportation network in terms of infrastructure. The possibility that the roofs of parking garages, existing helipads, or unused land near highway interchanges can be used for take-off and landing pads represents another opportunity for savings [11].

1.3 Potential of Urban Air Mobility

Due to its advantages, urban air transportation holds the potential to enrich the existing transportation system. Altran [2] estimates that eVTOLs are expected to reach a market value of up to US$322 billion by 2030. Hader et al. [22] also forecast annual revenue generated by UAM travel of US$90 billion by 2050. In contrast, cabs are predicted to have a market value of US$300 billion by 2030. Morgan Stanley [23] forecasts a total global market addressable by UAM of US$1.5 trillion by 2040, with

optimistic forecasts seeing a market value of up to US$2.9 trillion.

These forecasts are based on studies of the potential demand for UAM services and a whole new world of business across multiple sectors which get accessible by the implementation of UAM. Such as the study by Anand et al. [20], which examined global demand for UAM. For the study, 542 cities were examined in the time frame from 2035 to 2050. It found that, depending on the fare, up to 227 billion passenger trips will be made annually by 2035, and that the number is expected to increase to over 405 billion by 2050. Related to this, Hader et al. [22] predicts that over 160.000 UAM vehicles will be in operation for passenger transportation by 2050.

Despite the lack of an already proven business model, investors are betting on the UAM industry, due to the positive forecasts. According to a market study conducted by Booz Allen Hamilton [24] on behalf of the NASA, as of September 2018, more than 70 global manufacturers, investors, operators, suppliers, and governments have invested more than US$1 billion in UAM technologies. In the first half of 2020 alone, investments in startups reach US$907 million, 20 times the investments from all of 2016, and more investments are expected [22]. In addition to startups such as Lilium [14] or eHang [25, 26], existing large companies have also recognized the potential of UAM. Among them are Airbus, Boeing, Hyundai, Toyota and Uber [27].

But governments also see the potential. For example, the European Union (EU) has established the EIP-SUM-AC UAM Initiative [28]. Moreover, the National Aeronautics and Space Administration (NASA), launched the Advanced Air Mobility (AAM) National Campaign [29], and the European Commission initiated the Horizon 2020 project [30] to further advance research in UAM [31, 32]. The German government is also stepping up its efforts for UAM projects. In Ingolstadt, for example, the requirements for the use and integration of vertiports in the new Ingolstadt central station are to be researched and developed as part of a use case [33]. Ingolstadt has also agreed to be a pilot city for UAM as part of the UAM initiative [34]. But Ingolstadt is not the only city promoting the development of UAM, cities like Munich, Frankfurt or Hamburg are also contributing [35]. In addition, there are a large number of calls for proposals by the Bundesministerium für Verkehr und digitale

Infrastruktur (BMVI) [36, 37, 38]. In total, according to Hader et al. [22], there were approximately 110 ongoing projects dealing with UAM for passenger transport at the end of 2020. And despite the COVID-19 pandemic, we continue to see growth in the number of projects. In this context, Butterworth-Hayes [35] provides an overview of UAM projects worldwide in its 'Global Urban Air Mobility project report' published in March 2019. By pushing UAM technology forward, a possible launch seems not too far in the future. For example, Uber plans to launch its UAM service as early as 2023 [39]. Altran [2] equates the importance of UAM adoption to the shift from horse-drawn carriages to automobiles that occurred in the late 1800s.

1.4 Motivation

However, in order to make this leap in transportation, there are still some hurdles to overcome.

The main challenges can be categorized into two groups, technical and non-technical [20]. The technical challenges include the Air Traffic Control (ATC) needed for a UAM network, battery technologies to power the vehicles, or even the development of a fast and reliable communication network as the 5G network seems to be [11]. On the other hand, the non-technological challenges include regulatory and certification issues, competition with existing transportation modes, social acceptance, and the necessary infrastructure [20].

One of the biggest, but at the same time least studied challenges is the infrastructure needed for the UAM network [40]. The vehicles needed for UAM are already well advanced in their development, in contrast, the study of infrastructure requirements has been mostly secondary in research [41]. Therefore, the necessary infrastructure to support and enable the transportation of people and cargo is not yet in place [7]. Duvall et al. [21] further reiterate the urgency of infrastructure development because the timeframes for planning, building, and acquiring space for infrastructure are long. Consequently, infrastructure planning must begin now. Duvall et al. [21] aptly compare - If we wait until the first air mobility vehicles are operational, they will become the equivalent of a bridge to nowhere, expensive technological marvels that

serve no purpose. That means VTOL hubs with take-off and landing pads as well as charging infrastructure must be planned now for the means of transportation of the future, the so-called vertiports.

1.5 Objective

This work arises from the importance of the topic UAM and the associated infrastructure. The identification and selection of possible vertiport locations has already been investigated, however, a research gap in the area of dimensioning of vertiports [25], which is particularly important in urban areas due to the limited available space, becomes apparent. Therefore, in the context of the following work, an existing vertiport design tool is extended to allow automated planning of UAM infrastructure. The tool allows to derive both the maximum possible throughput from the available land mass and the minimum required footprint for a given throughput. Furthermore, resulting from a parameter study, characteristic values for the planning of vertiports and the estimation of possible throughputs will be derived.

The objective of this thesis is to provide a tool that allows the automated evaluation of a large number of possible locations based on current and potential guidelines and thus to provide more clarity in the field of vertiport infrastructure planning. It can also provide the link between existing tools that deal with either the selection of a suitable site or the simulation of an existing vertiport or vertiport network, but not the actual design of the vertiport on a particular site.

Within the scope of this work, answers to the following research questions shall be found:

- Which topologies should be preferred for the planning of new vertiports?
- In which relation should the individual components of a vertiport stand to each other?
- Which vehicle types are most promising for the UAM network of the future?
- Which regulations should be concretized for an efficient vertiport network?
- How do different process times affect the profitability of vertiports?

- Which area size is required for a desired passenger throughput?

It must be emphasized that at this time there are no clear guidelines for the design and planning of a vertiport. However, it is believed that the use of guidelines for heliport design is a good approximation. Further, it should be clarified that only the airfield of the vertiport is examined and neither the airspace surrounding the vertiport nor the terminal for passenger processing is addressed. Nevertheless, the results of this work could provide important guidance for binding vertiport design guidelines and thus pave the way for a functioning UAM infrastructure.

1.6 Thesis outline

The rest of this thesis is structered as follows.

The following chapter presents the state of the art in UAM vehicles and vertiports. Furthermore, standards in airport planning and guidelines for the infrastructure design of heliports are presented.

The chapter 'Methods' starts with an introduction to already existing tools for UAM planning, divided into simulation of vertiports, identification of locations and tools for the design of vertiports. Then, the methods created in the context of this thesis are presented.

The next chapter presents the results obtained from the studies carried out with the previously created tools. Here, different scenarios were run through and the results evaluated.

In the following chapter, the results are discussed and conclusions are drawn based on them with regard to the predefined research questions.

In the last two chapters, the results are summarized and an outlook on further research steps and possible approaches for improving the methods developed are discussed.

2 State of the Art

The following chapter provides an overview of the state of the art in the areas of UAM vehicles and vertiports. Furthermore, standards in airport planning and guidelines for the infrastructure design of heliports are presented.

2.1 UAM Vehicles

This thesis is primarily concerned with the UAM infrastructure: the vertiports. Since VTOLs are the vehicles that use them and they are a key component of the UAM network, a little insight is also given on them. In order to use the aircraft in an urban environment different conditions have to be met. The most important factor is safety as for all aviation systems, but another important point is to keep the impact on the environment as low as possible [42]. For this, the most important feature is low noise development. The importance of this aspect can be seen in the example of New York City where a ban on inner-city flights is already being discussed due to noise pollution [18]. In this context, the different designs and propulsion systems of VTOLs are presented below.

2.1.1 Architecture of Vertical Take-Off and Landing Vehicles

The design of VTOLs for passenger transportation is still a relatively new field of research [43, 44] and six design components can be distinguished: payload, speed, range, noise safety and costs.

The four most common types of VTOL aircraft architectures are shown in figure 2.1. The respective choice affects the design components and thus defines the cruise and hover efficiency and the noise emissions of an aircraft. Particular attention must be paid to the safety and noise of the vehicle as part of the conceptual design as mentioned earlier [45].

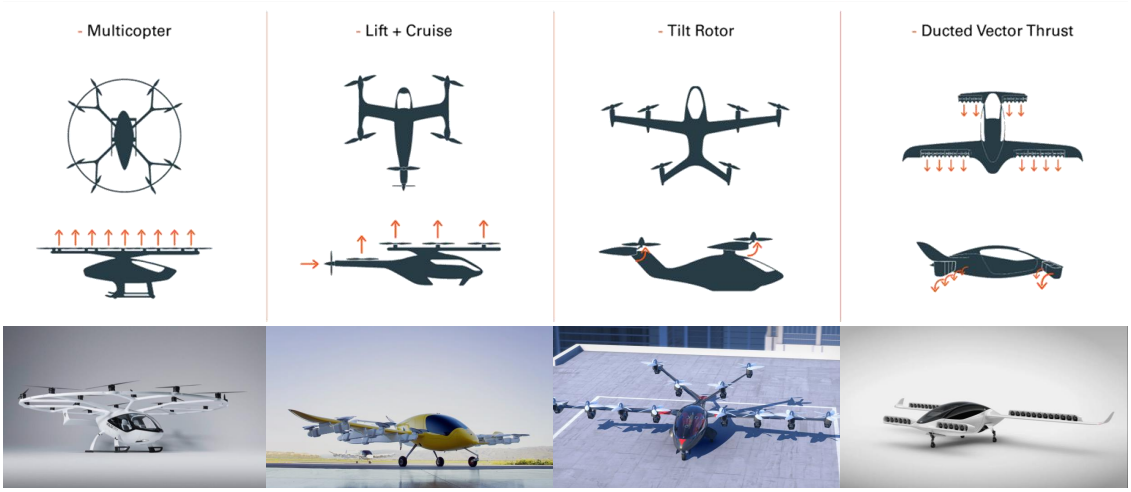

Figure 2.1: Most common VTOL concepts [45]

The first VTOL architecture category is the multicopter. This configuration is relatively simple and can be efficient in vertical take-off and landing as well as hovering due to low disc-loading. Since this configuration has no wings, it often has deficits in cruise efficency, which limits its application to an urban environment [45]. Pradeep and Wei [46] give a detailed insight into multicopter architecture. An example of such a multicopter would be the Volocopter [18].

The lift and cruise architecture is the second category of VTOLs [45]. This architecture represents a fusion of multicopter and aircraft. It combines the capability of vertical take-off and landing with the flight characteristics of an aircraft. To maximize range for these concepts, the number of blades per propeller is reduced and shorter chords are used minimize drag during cruise flight. The small size of the propellers poses a major challenge in terms of noise emissions due to the increased blade tip speeds. An example of an aircraft with such a lift and cruise architecture is the Cora Kitty Hawk [47].

The tilt rotor architecture, in which either the wings and propellers or only the propellers can be tilted, represents the third category [45]. In this category, the propeller axis is rotated 90° when the aircraft transitions from hover to forward flight. In general, this architecture allows a propeller to be designed which is more optimal than would be possible with a lift and cruise architecture of aircraft. However, it must be noted that

this results in a higher technical complexity, a larger overall size and a higher weight due to the tilt and pitch mechanism. As the hover process requires the propellers to be large, with low tip speed, either a gearbox is required or, the motors need to be large and heavy, to produce the low-speed torque. Hendricks et al. [48] give a design evaluation of tilt rotor aircraft. An example of an aircraft with such a tilt rotor architecture is the Joby S2 [49, 50].

The three categories of VTOL presented above rely on a propeller-based propulsion system [45]. The fourth category of VTOL are known as ducted fan architectures. A major advantage of ducted fans over propellers is that the duct acts to significantly mitigate noise. This is achieved by the presence of the duct and by acoustic liners mounted within them. This is particularly noticeable when the payload of the aircraft is increased. When the payload of a propeller-driven aircraft is raised, the only way to keep the noise level constant is to increase the size of the propellers. When the payload is raised on a ducted fan the disc loading can be raised and the duct and acoustic treatment is used to limit the increase in noise. This results in a ducted fan aircraft having a payload which is approximately $40\ \%$ higher than a propeller aircraft for a fixed footprint. Further advantages of ducted fans are, that blade tip losses are reduced, and the presence of a stator row removes exit swirl. The main disadvantage of ducted fans is that due to the higher disk load, the power required for hovering is higher than for propeller-driven aircraft. Two aircraft types can be distinguished for ducted fans. To minimize aerodynamic interactions for one type the ducted fan is located away from the airframe. In the second variant, there is a tight aerodynamic coupling, as the fan is closely connected to the fuselage and the wings. The Lilium Jet, is an example of the second type of ducted fan concept.

2.1.2 Propulsion Systems for Vertical Take-Off and Landing Vehicles

In addition to the vehicle architectures, different propulsion systems can be distinguished. A distinction is made between electric propulsion systems, cumbustion engines and mixed systems [42]. Significant noise reductions can be achieved by using low disk-loading propulsors and new propulsion configurations. In this context,

all-electric propulsion systems seem superior to conventional combustion propulsion systems. Hybrid-electric propulsion systems offer the potential to reduce noise while delivering better flight performance. Hybrid propulsion uses electric propulsion for take-off and landing and conbustion engines for endurance flights. For VTOL aircraft, the power needed for vertical take-off is much greater than the power needed to cruise. This power-matching problem can be solved with a balanced hybrid-electric propulsion system. However, there is a trade-off between take-off weight, wing loading, battery technology and range.

The advantage of electric propulsion over conbustion engines is that electric propulsion systems have a higher power to weight ratio. For example, electric propulsion provides about $5\ \mathrm{kW/kg}$, whereas a conbustion engine provides only about $1\ \mathrm{kW/kg}$. Another advantage is that electric propulsion can operate for short periods in overload configurations. Short missions off up to $80\ \mathrm{km}$ favor fully electric propulsion systems, as this configuration avoids the complexity of a hybrid [11]. But results indicate that hybrid-electric propulsion systems must be considered for future mid-range VTOL aircraft, as it combines the advantages of both propulsion systems. To enable widespread use of electric propulsion in aviation, according to Finger et al. [42] the electric batteries must provide an energy density of 400 to $500\ \mathrm{W\,h/kg}$ at pack level, which is about twice what is possible today. Uber plans to achieve an energy density at pack level of $400\ \mathrm{W\,h/kg}$ by 2023 [11]. Improvements are also expected in the area of electric motors, which can currently provide a power of $5\ \mathrm{kW/kg}$ and are expected to double to $10\ \mathrm{kW/kg}$. It can already be seen that short distance flights in the range of $50\ \mathrm{km}$ are possible with VTOLs with pure electric propulsion. Further, Finger et al. [42] note that with continued progress in electric motor and battery technology, there is the possibility of developing new VTOL aircraft that operate much more efficiently than conventional propulsion systems.

2.2 Airport Planing

Vertiports can be defined as a combination of conventional heliports with the throughput of classic commercial airports [51]. Therefore, in the following, the most important

considerations in the planning of such a commercial airport are presented.

Neufville et al. [52] explain that an airline's fleet is described by the total number of aircraft and the specific types of aircraft that are operated. Each aircraft type has different technical and performance characteristics, usually defined by range and size. Range describes the distance an aircraft can travel with passengers and/or cargo. Size is defined as the cargo or seating capacity.

Flight and fleet planning is one of the core issues that an airline must address if it is to achieve profitable flight operations. Such planning usually starts more than a year in advance of planned flights and follows the four following key questions:

1. How many flights should be operated per day and route?
2. What are the take-off and landing times of the aircraft?
3. What type of aircraft is used for each departure?
4. How are the available aircraft routed through the airline's network?

Since this work is concerned with the design of a vertiport, it is more important to know the operations at the airport. Neufville et al. [52] explain that much of the uncertainty and volatility in flight operations is due to activities at the airport. These include the handling of passengers and baggage and also the processes that the aircraft goes through.

Restrictions are caused, for example, by the existing gates, which in turn must be adapted to the size of the aircrafts. If a gate is too small, for example, it cannot be used by aircraft of a certain size. The same applies to take-off and landing areas as well as taxiways, which can also be influenced by weather conditions.

Also important are the turnaround processes that accompany each arriving and departing aircraft. These include the boarding and deboarding of passengers, the loading and unloading of baggage, and the preparation of the vehicle for the next flight. These preparations include cleaning, security checks and refueling or charging of the aircraft.

Due to the complexity and large number of variables, buffers are planned for the

processes, but it is important to ensure that these are not too large. Because in addition to delays, processes that are completed faster than planned also lead to problems.

Further, international conditions must be considered, as there are significant differences from country to country in many aspects of airport planning, design, and management. Nevertheless, air transport is a global business with remarkably similar international standards. For example, in general reliance is placed on aircrafts from a few manufacturers such as Airbus or Boeing. Moreover, many of the international requirements are set by two organizations, the FAA and ICAO. The FAA has a dominant role because the U.S. is the largest single market in aviation and spends the most money and research on establishing standards. According to Neuville et al. [52], this also results mostly in the FAA setting standards that are later adopted by the ICAO. However, there are major international differences in terms of the landside characteristics of airport planning, design, and management.

One difference can be seen in the check-in area, as employees stand in the U.S. while they sit in Europe. This appears to be a small difference, but it is crucial in the design of the facilities. Another difference between the two markets is that in Europe, airlines have little influence on the design of airport infrastructure. In contrast, airlines in the U.S. can participate in the construction of airports and make arrangements. The following table 2.1 shows some differences in airport planning and design between the U.S. and the rest of the world.

Table 2.1: Aiport planning in USA and rest of world [52]

Area of Practice	**Common Practice in USA**	**Common Practice in Rest of World**
Facility construction	Generous airfield paving to facilitate aircraft ground operations	Restricted amount of paving for taxiways and aircraft aprons
	Emphasis on private cars, automobile access, parking	Emphasis on collective transportation, rail access
Planning	Suggestive	Directive
Operations	Airlines usually schedule freely as they whish	Airports allocate landing and take-off slots
	No discriminatory pricing; all users have access	Peak-hour pricing, small aircraft often excluded
	Airport operator has small staff; Most services contracted out	Airport operator is a big employer; airport offers most services

To develop airports the approach of dynamic strategic planning is recommended unlike traditional master planning. The reason therefore is, that the airport and aviation industry are highly uncertain, and planners, designers and managers consequently need to consider many different possibilities. Dynamic strategic planning leads planners to anticipate the range of possible futures and scenarios of operation – instead of merely a single forecast. This is needed because airport professionals must assume that the future reality can be different from what seems most likely at present.

Based on the ICAO [53] an airport master plan presents the planner's conception of the ultimate development. It should involve three essential notions.

1. Ultimate vision, that is, a current view of the possible long-term future. (e.g. 20 years)
2. Development, that is, the buildings, runways, and other physical facilities – not operational concepts or management issues
3. Specific airports, not to regional or national aviation system

However, as already mentioned, master planning is often no longer up to date. One

of the central messages of Neufville et al. [52] is, that while planning airports the forecasts most of the time will be wrong. Starting with the coast estimation, where estimates of construction costs for major projects are notoriously inaccurate. Resulting in differences between estimated and actual costs of $30\ \%$ on standard projects being common. Therefore, it is suggested to just focus on the first two decimals of the forecast and to use large ranges, on the order of $\pm 30\ \%$ or more over 20 years.

As good planning needs to deal with reality. For airport systems, the fundamental reality is that future forecasts are highly unreliable. Forecasting errors of $20\ \%$ or more after only 5 to 10 years is normal, and errors for longer-term forecasts are usually worse.

To prevent these problems the concept of dynamic strategic planning is suggested for airport planning. In this concept it is convenient to start with a SWOT analysis. Starting with the possible strengths and weaknesses of the planned airport, both internally and regarding its competition. Followed by analyzing the opportunities and threats for the airport in terms of new markets, mergers, technologies etc.

Moreover, it is essential to maintain a flexible approach, as it is impractical to build now the facilities that will meet all eventualities. For example, facilities cannot be large enough to handle the highest expected traffic volumes on the one hand, but small enough to avoid unnecessary expenditures if traffic volumes remain constant or decrease only slightly on the other. A common approach is to establish a middle course. In the process of dynamic strategic planning, an inventory of existing conditions should be made. Further, a forecast of future traffic volumes and possible scenarios for the major components should be conducted. Based on the forecast, the facility requirements suitable for the several possible levels and types of traffic should be determined. Knowing the facility requirements afterwards several alternatives will be developed to carry out a comparative analysis. On the basis of analysis, the first-phase development, that enables subsequent and appropriate responses to the possible future conditions will be selected.

When planning an airport, it is not sufficient to consider only components that directly affect the airport, such as air traffic or finances. The impact on the environment must

also be considered and solutions must be found to prevent or mitigate it as good as possible. Key issues mentioned by Neufville et al. [52] include noise pollution from aircraft, air and water quality, climate change, and impacts on wildlife.

2.2.1 Airfield Design

The geometric design of an airfield should consider flexibility, operational efficiency, and the potential for future growth. The design should also be compliant with an extensive set of design standards and proposed practices, provided by international and national civil aviation organizations and intended to promote a maximum level of safety. The most influential sets of design standards are those of the FAA and the ICAO.

Geometric design plays a central role in airfield planning, as it affects every aspect of airport operations. Due to the high importance of safety for aviation operations, the given design standards must be strictly followed, as already mentioned.

Neufville et al. [52] state, that despite the extensive set of guidelines, airport planners must still exercise a great deal of judgement in making critical design choices:

- How much land should be acquired or reserved for a new airport?
- What should be the overall geometric layout of runways, taxiways, and aprons?
- What size of aircraft should the airfield be designed for?
- How should the construction of airside facilities be phased?

Taxiways can be extensive and complex and are therefore costly to build and maintain. Yet they are considered late in the planning of airfields. The take-off and landing areas and gates are determined first, and the taxiways are then designed so that they connect the desired components. This is a costly approach, as it leads to increased operating costs. On average, one minute of taxi time saves about US$10 million per year in direct costs to the airline, which equates to about US$100 million in capital investment.

2.2.2 Airfield Capacity

The subject of airfield capacity is a fundamental topic to modern airport planning and design. The capacity of the airfield and especially of runway systems typically determines the ultimate capacity of an airport. The runway can be associated with the pads of this thesis.

The principal measure of the capacity of a runway system is the maximum throughput capacity. It indicates the average number of movements (arrivals and/or departures) that can be performed on the runway system in one hour in the presence of continuous demand, while adhering to all the separation requirements imposed by the air traffic management (ATM) system. To estimate the number of hourly movements with consideration of acceptable levels of delay, the practical hourly capacity (PHCAP) was implemented. Typically, it is equal to 80 to $90\ \%$ of the maximum throughput.

Through the capacity coverage chart (CCC) the range of capacities available at an airport over a long period of time, such as one year, and the frequency with which these capacities are available can be summarized. An operations mix of $50\ \%$ arrivals and $50\ \%$ departures and the runway configuration in use at any given time is the one that provides the highest capacity under the prevailing conditions is assumed by the CCC.

Moreover, it is important to distinguish between the static capacity of an apron, that is defined as the number of aircraft that can be stationed there at any instant, and the dynamic capacity, which shows the number of aircraft that can be served at the apron per unit of time. The dynamic capacity depends on the stand blocking time (SBT) or turnaround time.

The principal bottleneck of an airfield system is usually the runway, since this is where traffic is reduced from the three-dimensional airspace to a single runway and the final approach airspace.

Neufville et al. [52] identified several factors affecting the capacity of a runway system. First the number and geometrical layout of the Runways. Second every ATM system specifies a set of required minimum separations between aircraft flying under

instrument flight rules (IFR). The separation requirements for airplanes operating to or from parallel runways can range from 762 m or more. The needed separation of pads for parallel operations of VTOLs is smaller and will be presented in the following section 2.3. Other factors affecting the possible throughput are the visibility which is depending on ceiling, and precipitation, the wind direction and strength, the mix of aircraft as well as the mix and sequencing of arrivals and departures.

A simple mathematical model is originally developed by Blumstein [54] to calculate the capacity of a single runway. This model follows three steps:

1. For all possible pairs of aircraft classes (i, j) and for all permissible pairs of movements ("arrival followed by arrival", "arrival followed by departure", etc.) where an aircraft of type i is immediately followed by an aircraft of type j, the expected time separation $t_{i,j}$ between successive movements must be calculated. This must be done while respecting and taking into account the ATM separation rules. It should be noted that the average time separation $t_{i,j}$ is greater than or at best equal to the minimum separation $T_{i,j}$ between successive movements for this pair of aircraft, since the expected time separation $t_{i,j}$ also includes deviations from the optimal separation due to, for example, human factors.
2. The probability $p_{i,j}$ of occurrence of each of the expected time intervals $t_{i,j}$ determined in step 1 shall be calculated.
3. Compute the overall expected time of the interval between any two consecutive movements,

$$E[t_{ij}] = \sum_{i=1}^{k} \sum_{j=1}^{k} p_{ij} t_{ij} \tag{2.1}$$

and from that the maximum throughput capacity $\mu = \frac{1}{E[t_{ij}]}$

2.2.3 Taxiway Capacity

The capacity of the taxiway can be determined, by the number of aircraft per hour that can taxi from the apron areas to the runway and vice versa. For example, if

aircraft travel on the taxiway at a speed of 36 km/h and the separation between (nose of) successive aircraft on the taxiway is a conservative 400 m, the flow capacity of the taxiway is 90 aircraft per hour, far more than a runway can typically handle and therefore usually not the bottleneck.

2.2.4 Apron Capacity

The capacity of aprons in contrast to the taxiway system can occasionally be a constraining factor on the overall capacity of space constrained airports. An apron consists of the stands designated for the aircraft and taxilanes, which are the corridors the aircraft utilize to reach the stands. The stands can be associated with the gates of this thesis. Neufville et al. [52] explain, that there are two ways of defining the apron capacity. First is the static capacity which is classified as the number of stands at hand. This number indicates the maximum amount of aircraft that can be occupying simultaneously the apron at any given instant. On the other hand, there is the dynamic capacity which is defined as the number of hourly aircraft that can be accommodated at the stands. This approach is more consistent with the throughput notion of the runway.

When calculating dynamic capacity, the time an aircraft spends on a stand must be taken into account, from the time of entry to the time of departure. The minimum interval consists of the sum of two components, which can be complemented by considering buffer times (BT).

1. The turnaround time, which is the amount of time that an aircraft is scheduled to spends at the stand. Refered to as scheduled occupancy time (SOT).
2. The positioning time (PT) needed to position the aircraft into and out of the stand. In this time the stand is unavailable to other aircraft.

The dynamic capacity is calculated in four steps:

1. Subdivision of arriving aircraft into k classes depending on criteria such as aircraft size and/or flight type and/or airline. It should be noted that the classes established for calculating apron capacity do not necessarily correspond to the

classes established for calculating runway capacity.

2. For each class i, the average time between stand occupancies is estimated as the sum of SOT, PT, and BT for the class. This sum is called the stand blocking time (SBT).
3. Calculate the expected average SBT for airport stands according as

$$E[SBT] = \sum_{i=1}^{k} p_i SBT_i \tag{2.2}$$

where p_i is the fraction of arriving aircraft that belong to class i.

4. The dynamic capacity of the apron is then approximately equal to $\frac{n}{E[SBT]}$ aircraft per hour.

For an adequate determination of the possible capacity, possible delays must also be taken into account. The consideration of these can be done by means of the following steps.

1. All possible runway configurations and the weather conditions under which they can operate must be identified.
2. For each of these configurations, the maximum throughput per hour must be calculated.
3. Based on weather records and taking into account local guidelines, the approximate percentage that each of the configurations is used per year must be determined. At airports where the highest capacity configuration is selected at any time, this step is equivalent to determining the CCC.
4. Creation of typical daily profiles of demand on the runway system (hourly number of arrivals and departures, mix of aircraft types, seasonal variations in profiles).
5. Estimation of delays associated with all applicable combinations of demand profiles and runway configurations used.
6. Estimation of total delay statistics based on the results of Step 5 and the frequency of use of each runway configuration determined in Step 3.

2.2.5 Airport Facilities

Beside of the planning of an airport airfield, the planning of airport facilities is needed. Neufville et al. [52] states, that planers should design them for peak traffic but not for the absolute maximum traffic. To check plans rapidly, it is possible to estimate peak loads by using rules of thumb, such as the following two which are meant for airports with an anual traffic of about 10 million per year:

$$\text{average paeak-day traffic} \approx \frac{annual\ traffic}{300} \tag{2.3}$$

$$\text{design paeak-hour traffic} \approx \frac{annual\ traffic}{3000} \tag{2.4}$$

The design peak day can be defined eather as the 10th, 15th, or 30th busiest day of the year. Or the 90th or 95th percentile busiest day of the year, that is, a day whose traffic load is exceeded by only 36 or 18 days in the year.

For the design peak hour, Neuville et al. [52] define that it corresponds to the 20th, 30th, or 40th busiest hour of the year, or the '$5\ \%$ busiest hour,' i.e., an hour chosen so that all the busiest hours of the year together handle $5\ \%$ of the annual traffic volume.

The International Air Transport Association (IATA) [55] for example provides guidelines for spaces to be provided for passengers in different functions in m$^2/passenger$ based on levels of service standards ranging from excellent to unacceptable. Another important factor in the design of airport facilities is the dwell time. The dwell time refers to the typical length of time passengers stay in an area waiting for service. Based on this time and the before metioned IATA guidelines the size of waiting areas can be calculated.

In this context the following table 2.2 shows some planning factors for specific facilities.

Table 2.2: Planning factors for airport facilities [55]

Item	Area	Per	Remarks
Check-in counters	0.42 m^2		Based on 3.5 min/passenger
Check-in queues	0.87 m^2		7.5 m depth
Circulation	1.4 m^2	Peak-hour	12 m after check-in
Arrival hall	1.35 m^2	passenger	-
Toilets	0.31 m^2		Based on comparable airports
Baggage claim	7.65 m^2		Based on comparable airports
Concessions	900 m^2	Million annual	Based on comparable airports
Public circulation	900 m^2	passengers	-
Gate lounges	1.25 m^2	Seats in aircraft using gate	90 % load factor, 80 % seating, and 20 % standing

2.3 Heliport Design Guidelines

As early as 1970, Allen and Simpson [51] stated that appropriate government agencies should develop mandatory guidelines for the location, design, and operations of vertiports to ensure safe and efficient processes, minimize undesirable environmental impacts, and provide for orderly, trouble-free growth of the UAM system in the coming decades. Currently, however, according to the National Air Transportation Association (NATA) [56], there are no comprehensive policy guidelines or regulatory requirements that govern the design and operation of vertiports. There is a lack of mandatory design standards, building codes, best practices, or fire codes necessary to evaluate a vertiport and its operation as safe based on objective measures. This lack of regulation is a problem because many municipalities are unwilling to issue the necessary permits or licenses to construct vertiports and this discourages early investments.

The wide variety of different eVTOLs and lack of proven approaches makes it difficult to develop regulatory procedures and policy guidance. Therefore, in 2019, the FAA [51] issued a Request for Information (RFI) to the eVTOL industry to initiate this

process.

However, it can be assumed that specific regulations for the operation and infrastructure of eVTOLs will be based on already existing regulations. Given the physical characteristics of eVTOLs and their vertical flight capability, the vehicle most comparable to an eVTOL is the helicopter [41]. Thus, the closest infrastructure for UAM is the one which supports helicopter operations, that are consequently heliports and helistops [51].

Based on these assumptions, the NASA [57] is developing a Concept of Operations (ConOps) for the deployment and integration of UAM into the National Airspace System (NAS). These define roles and responsibilities for all stakeholders associated with UAM operations.

In this context, the FAA is responsible for creating a regulatory framework and developing operating rules. Here, the responsibilities of operators and other stakeholders of manned and unmanned UAM vehicles are regulated and an Unmanned Traffic Management (UTM) concept is developed [58]. The NASA is also developing different concepts of airspace regulation whether for manned [59] or unmanned [60, 61] vehicles. In relation to UTM, a paper by Jiang et al. [62] was published which provide further suggestions for a possible design. The German Aerospace Center (DLR) has also published rules for regulating UAM airspace in the form of a blueprint [63, 64].

In the context of this work, regulations in the field of airspace are largely negligible. In contrast, regulations of ground infrastructure play a central role. Different organizations and papers that publish codes and regulations for heliport construction are presented below.

Allen and Simpson [51] studied the design of vertiports as early as 1970 and analyzed possible flight deck configurations, among other things. Cohen's paper [65] addresses the challenges of placing UAM infrastructure and presents guideline values for the size of vertiports in different scenarios. Peisen et al. [66, 67, 68], on behalf of the NASA and the FAA, published initial studies to determine the location of vertiports and their design requirements. They also summarized the results of vertiport feasibility studies

funded by the FAA in 1988.

Many papers and guidance documents follow NASA and FAA guidance [69, 70, 71]. Among them, for example, Ashford et al. [84] and Taylor et al. [17].

According to the FAA Heliport Design Advisory Circular [71] vertiports must have at least one touchdown and liftoff area with some key elements. The basic elements of a vertiport are a clear approach/departure path, a clear area for ground maneuvers, a final approach and take-off (FATO) area, a safety area, and a wind cone. The FAA also has specifications regarding processes, fire protection, parking and much more [70].

In addition to the FAA, EASA and the ICAO have also published rules for the design of heliports. Ploetner et al. [27], like Feldhoff and Roque [41], for example, base their work in the area of vertiport design on the basic design principles and regulations for heliports of the ICAO [72, 73, 74, 75]. According to these, a vertiport consists of landing fields, taxiways, parking gates and space for passenger processes. Depending on the level of service, space for vehicle maintenance and charging stations will also be considered. However, the ICAO regulations have been adapted to the basic requirements of § 6 of the German Air Traffic Act (LuftVG) and § 44 et seq. of the German Luftverkehrs-Zulassungs-Ordnung (LuftVZO) and are only applied as far as they do not contradict German law.

The EASA for example provides certification specifications and associated guidance material for the design of surface-level helipads or parts thereof located at aerodromes [76].

Due to the similarity of vertiports and the flight deck of aircraft carriers in many areas, it is recommended by the NATA [56] to consider the manuals of the U.S. Navy [77, 78] or the navies of other nations [79] when planning vertiports. In addition, it is emphasized that the International Fire Code [80, 81] and the International Building Code [82] must always be followed when designing vertiports [56]. In addition to these international requirements, local requirements must also be considered. For example, the State of California has certain requirements for helipad carriers. These are based on sound

studies, land use compatibility studies, and environmental impact reports, all of which are described in the Caltrans Airport Land Use Planning Handbook [83].

In the following, the regulations for the planning of a heliport will be discussed in more detail since the planning of a vertiport can be derived from it.

2.3.1 Vertiport site selection

Ashford et al. [84] explain that one of the most important aspects of planning and designing a heliport is the selection of a suitable site. Site selection should be conducted with the goal of maximizing ease of use, vehicle safety, and community acceptance.

Various sources of information should be consulted for an initial investigation, including land use and transportation plans. These studies may contain information about land use projections, travel origins and destinations, travel time data for traffic, and others. Further an analysis of available wind data is needed to determine the desirable orientation of heliports. In addition, road and aeronautical maps and land costs should be evaluated for potential locations. Another approach for site review, is to inspect the area from the air with a helicopter to evaluate potential flight obstacles, available emergency landing sites along approach routes, wind turbulence, and other aspects related to aerial navigation.

Before a final comparison of alternative sites is made, the sites should be thoroughly inspected. The following eight factors should be considered as part of identifying these potential sites:

1. Desired type and layout of the heliport
2. Convenience of the users
3. Obstruction of the airspace
4. Coordination with other aircraft movements
5. Direction of the prevailing winds
6. Social and environmental factors
7. Turbulences
8. Visibility

Desired type and layout of the heliport: The dimensions of the take-off and landing area of a helipad depends on the size of the largest helicopter to be served. The resulting required space is crucial for the selection of a suitable location.

Convenience of the users: Because excessive delays and inconvenience due to difficult heliport accessibility, negate the advantage of time savings and convenience of a helicopter, Ashford et al. [84] recommend that for short-haul transports such as those performed by helicopters, landing sites should be located as close as possible to the actual origin and destination of people. Therefore, it is recommended that the areas with the highest demand, should be identified through traffic studies. In addition, it is helpful to compare total travel time with that of other modes to forecast helicopter use.

Obstruction of the airspace: In order to identify the potential danger to helicopter flights from physical objects surrounding the heliport such as buildings, masts, towers and the like at an early stage, studies must be carried out in this regard. For these studies, the FAA [71] and ICAO [72], for example, have defined departure and approach corridors that must be kept clear.

Coordination with other aircraft movements: To ensure that the use of the proposed heliport does not interfere with the take-off, flight and landing operations of other airports, investigations must also be carried out. This aspect is particularly important if the proposed site is located at or in the immediate vicinity of an existing airport. In this case, the use of the airspace must be cleared by the appropriate authority. For U.S. airspace, the FAA is responsible for this.

Direction of the prevailing winds: Preferably, helicopter take-off and landing operations should be conducted into the wind. In the event that other factors permit, approach and departure areas should therefore be oriented so that take-off and landing operations can be performed into the wind.

Social and environmental factors: People often find the noise generated by helicopter rotors unpleasant. At the same time, as shown under 'convenience of users', heliports are to be placed near population centers. This constellation poses a par-

ticular challenge in the selection of a suitable heliport location. Therefore, special attention should be paid to minimizing the impact of helicopter noise in the immediate vicinity of the heliport.

In addition to noise pollution, water and air quality, land use, and other social and environmental factors should also be considered. For example, in the United States, building plans must undergo an environmental review. For this, the FAA provides guidance materials that show how to consider environmental impacts [85, 86].

In general, municipal zoning regulations allow heliports to be used in industrial, commercial, manufacturing, agricultural, and non-residential zoning districts. However, it will be necessary to seek amendments to existing zoning regulations to allow the construction of required heliports in residential areas as well. Restrictions on the height of buildings in helicopter approach departure corridors should also be included in the zoning regulations.

Turbulences: Especially for elevated heliports, surrounding buildings or structures may cause disturbing wind turbulence. Test flights or simulations may be required to determine the nature and extent of turbulence. These tests may reveal that for a site, problematic turbulences only occur above certain wind speeds. In this case, the FAA [71] recommends that heliport operations should only be authorized within a range of predetermined wind speed.

Visibility: Particularly on buildings of $30\ \mathrm{m}$ or higher, elevated heliport operations may be limited due to low clouds. Other visibility obstructions such as fog, smoke or glare may also cause the exclusion of potential heliport locations.

2.3.2 Layout and design of heliport components

In the context of this work, the focus is less on the site selection and more on the layout and design of the vertiport, which can be further derived from that of a heliport.

Ashford et al. [84] explain that the size and shape of a heliport and the type of services offered depend on three main factors:

1. Size and type of site available.
2. Dimensions and performance characteristics of the helicopters to be served.

3. Number, size and location of buildings and other objects in the vicinity of the heliport.

The FAA, EASA and ICAO provide specifications for the core elements of a vertiport, these are the take-off and landing areas with the associated safety areas (pads), dimensions of taxiways, standing areas for the vehicles (gates) and approach and departure lanes to be complied with. A model of a possible vertiport with the core operational components just presented is shown in figure 2.2, although it should be noted that the model presented does not conform to FAA design standards. The individual components are shown in more detail below, along with institutional regulations.

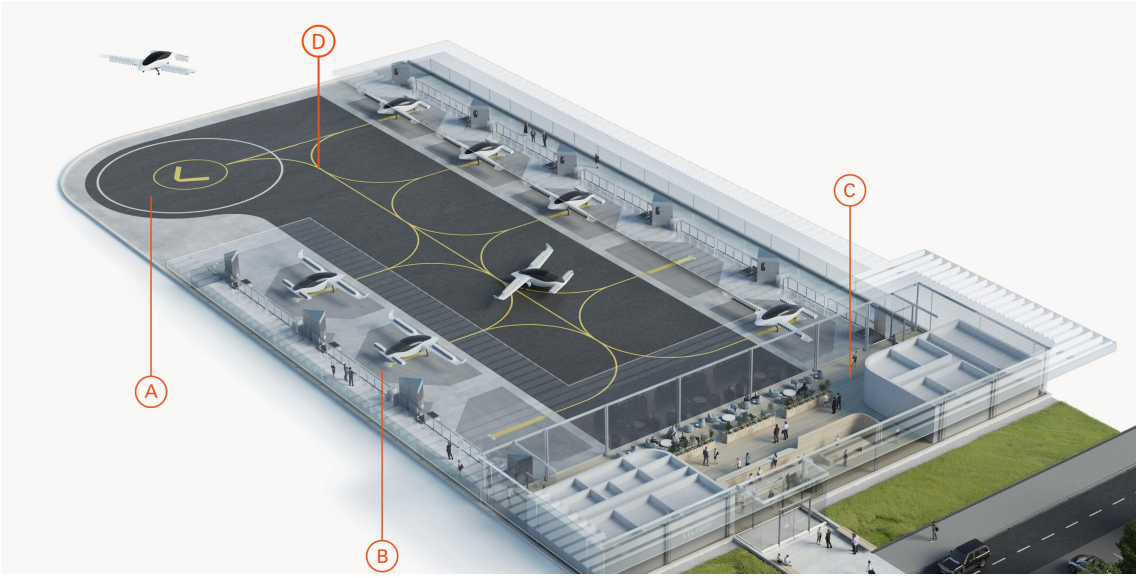

Figure 2.2: Vertiport model from Lilium [14] A - pad; B - gate; C - terminal; D - taxiway

It is important to note that the design guidelines are designed relative to helicopter dimensions. Therefore, they must be transferred to VTOLs for application to vertiports. Therefore, the following dimensions are specified for the rest of the paper:

- **Tip-to-Tip Span (TTS):** The TTS is defined as the maximum distance between the edges of any rotor or propeller arc [88].
- **Maximum Dimension (MD):** The MD is defined as the largest dimension of the vehicle including all rotating and fixed components [88]
- **Undercarriage Dimension (UCD):** The UCD is defined as the length or width

(whichever is larger) of the undercarriage of the aircraft [84]

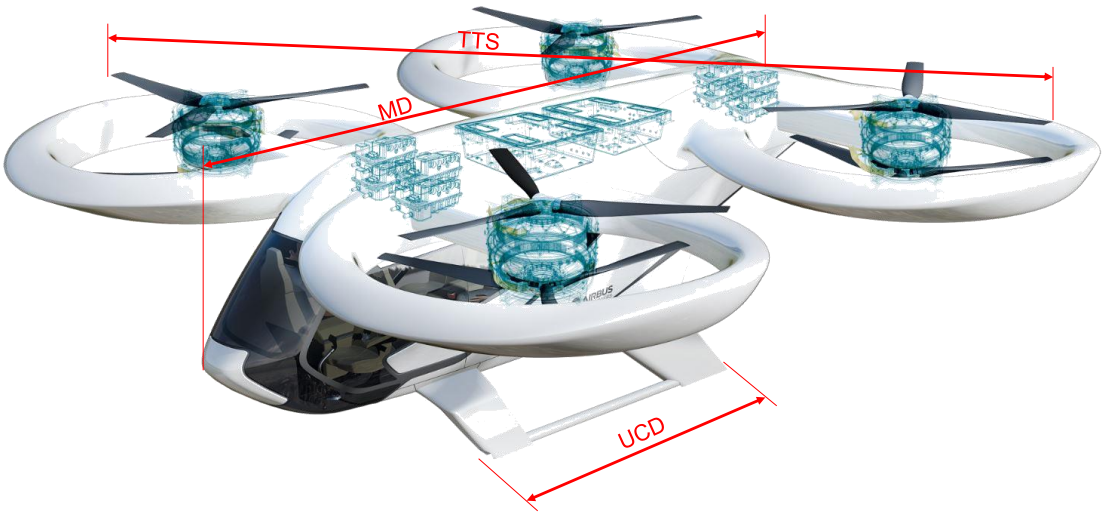

Figure 2.3: Measures of a VTOL [87]

2.3.2.1 Pad

A pad consists of three components and is defined as the area designated for aircraft landing and take-off. The touchdown and lift-off area (TLOF) is generally a load bearing surface on which the aircraft lands and/or takes off. This area, in turn, is within the final approach and take-off area (FATO), a defined area over which the pilot completes the final phase of the approach in the form of a hover or a landing and from which the take-off is initiated. Finally, the safety area (SA) is located around the FATO. The SA is the area on a helipad that surrounds the FATO and serves to reduce the risk of damage to helicopters that inadvertently stray from FATO [89]. Figure 2.4 outlines a pad, its structure and its measures.

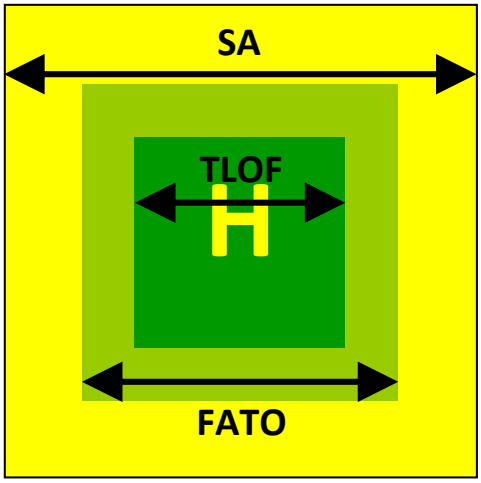

Figure 2.4: Structure and measures of a pad

The FAA [71] states that the TLOF of general aviation heliports may be placed on the ground, elevated structures, or roofs. However, it should be noted that the ground must be load bearing and capable of supporting the dynamic load of the helicopter. The dimensions of the TLOF are based on the dimensions of the helicopter to serve and the minimum dimension (length, width, or diameter) should be at least equal to the TTS. The TLOF can be designed to be rectangular or circular. According to the FAA, both designs can provide advantages. A square TLOF provides better guidance for the pilot, where a circular FATO is more visible in an urban environment. If the entire TLOF is not paved, care must be taken to ensure that the size of the paved area is no smaller than twice the UCD. In case the FATO surrounding the TLOF is not load bearing and it is an elevated heliport, the minimum dimension of the TLOF must be increased to the MD of the vehicle. Assuming an elevated TLOF (min 1.2 m), the FAA recommends installing safety nets, which should not be narrower than 1.5 m and must be able to withstand at least 122 kg/m^2.

The FATO should not be smaller than 1.5 times the MD of the aircraft. Regardless of the shape of the TLOF, the FATO can also be either rectangular or circular. The FAA further recommends that a longer rectangular FATO be provided when located at altitudes above 1000 ft MSL to provide a greater margin of safety and operational

flexibility. However, this is only a recommendation. The minimum distance between the TLOF and the FATO shall not be less than the ¾ MD - ½ TTS.

The SA surrounding the FATO spans in all directions to the same extent and its dimension is highly dependent on the safety markings present. The different dimensions of the SA are shown in table 2.3. The special feature of the SA is that there is an option to let the safety area extend into the free airspace.

Table 2.3: Minimum safety area width depending on markings for general aviation heliport [71]

SA width	TLOF perimeter	FATO perimeter	'H' marking
max(1/3 TTS; 6 m) [a]	yes	yes	yes
max(1/3 TTS; 9 m) [a]	yes	yes	no
max(1/2 TTS; 6 m)	no	yes	yes
max(1/2 TTS; 9 m)	no	yes	no

[a] Also applies when the FATO is not marked. FATO has not to be marked if:

a) the FATO (or part of the FATO) is non-load bearing surface.

b) the TLOF is elevated above the level of a surrounding load-bearing area.

The ICAO recommendations [84] for the geometric design of heliports according to international standards, have significant differences to the previously cited FAA standards. ICAO [90] distinguishes between three helicopter classes in the specifications for heliport dimensions. For performance class 1 helicopters, a FATO with a size equal to the MD is sufficient. For helicopters of per performance class 2 and 3, the maximum take-off mass (MTOM) is further differentiated. If the MTOM is less than or equal to 3175 kg, a FATO with a minimum dimension of 0.83 times MD is sufficient. If the MTOM is higher, the size of the FATO must be 1.5 times MD.

The TLOF must be large enough to enclose a circle of at least 0.83 times MD of the largest helicopter that is to approach it. If the TLOF is within the FATO, the center of the TLOF must be at least 0.5 times MD from the edge of the FATO. It is further emphasized that the TLOF may take any shape, as long as the above-mentioned requirements are met.

Unlike the FAA, the ICAO SA must be solid. For helicopters of all three performance

classes flying under visual meteorological conditions (VMC), the SA should extend beyond the edge of the FATO by at least 3 m or 0.25 times MD, whatever is bigger. For a rectangular FATO, the edge length should not be less than 2 times MD, and for a circular FATO, the radius should not be less than 2 times MD. If, on the other hand, the pad is to be approached in instrument meteorological conditions (IMC), the SA must extend laterally by at least 45 m on each side of the centerline and be at least 60 m away from the edges of the FATO in the longitudinal direction.

As an overview, the dimensions for the pad are summarized in table 2.4.

Table 2.4: Comparison pad measures of FAA and ICAO

Organisation	**TLOF**	**FATO**	**SA**
FAA [71]	TTS	1.5 x MD	max(1/3 TTS; 6 m)
ICAO [72]	0.83 x MD	MD to 1.5 x MD	FATO + max(6 m; 0.5 x MD) but min 2 x MD

In addition to the dimensions just presented, it must also be noted that safety distances between the pads must be maintained for simultaneous operation. The minimum distance is always defined from FATO edge to FATO edge. The FAA notes, that if the heliport operator intends to use the pads for simultaneous operations, a minimum distance of 61 m shall be provided between the edges of the FATOs. EASA and ICAO, on the other hand, make the distance dependent on the mass of the helicopter. The following table 2.5 summarizes the minimum distances for the three organizations.

Table 2.5: FATO minimum separation distances for simultaneous operations

Helicopter mass	**Distance between FATO edges**	
	EASA [76] and ICAO [72]	**FAA [71]**
$x < 3175$ kg	60 m	61 m
3175 kg $\geq x < 5760$ kg	120 m	
5760 kg $\geq x < 10000$ kg	180 m	
10000 kg $\geq x$	120 m	

2.3.2.2 Gate

A gate is the place to which the vehicle taxies to perform various processes. These processes include, for example, the boarding and deboarding of passengers, the loading and unloading of baggage, as well as the recharging and/or fueling of the vehicle. A gate is circular and consists of an inner standing area for the vehicle and is surrounded by an additional area for taxi movements and processes [89]. Figure 2.5 outlines a gate, its structure and its measures.

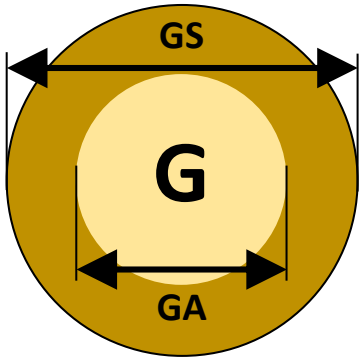

Figure 2.5: Structure and measures of a gate

Ashford et al. [84] state that in certain circumstances, gates for helicopters may be required at general aviation heliports if the facility is expected to be used by more than one helicopter. In certain circumstances, helicopters may also park on the pad or perform the turnaround process. However, such a practice is undesirable, according to Ashford et al. because it prevents the area from being used by other helicopters for take-offs and landings.

In contrast to this work, the FAA refers to stands rather than gates, but means the same component. FAA regulations [71] state that for heliports, the size of the gates depend on the number and size of helicopters to be accommodated. The FAA states that gates must be designed to accommodate the full range of size and weight of expected traffic. The size of the gates can be individualized to the vehicle that will be parked there, according to the FAA. However, the spacing between gates should be based on the largest helicopter. Further, the turn radius of helicopters when designing

gates for wheeled helicopters should be considered, because ground taxi turns of wheeled helicopters are significantly larger than a hover turn. Therefore, the size of the gate is at least the size of the MD and around there must be a minimum distance of 3 m for ground taxi operations and the greater of 3 m or one third of the TTS for hover taxi operations.

In the ICAO Heliport Manual [73], gates are referred to as stands. It specifies that a gate shall be large enough to enclose a circle of at least 1.2 times MD of the largest helicopter for which the gate is intended. In addition, if turns are to be made on the gate, the gate and the enclosing safety area shall not be less than 2 times MD. Moreover, the safety area shall not be narrower than 0.4 times MD. It is also stated that when the gates are operated simultaneously, the safety area of the gates and that of the associated taxiways must not overlap. When the gates are intended to be used for ground taxi operations by wheeled helicopters, the dimension of the gate shall take into account the minimum turn radius of wheeled helicopters the gate is intended to serve. EASA [76] follows the same standards as the ICAO.

As an overview, the dimensions for the gate are summarized in table 2.6.

Table 2.6: Comparison gate measures of FAA and ICAO

Organisation	**GA**	**GS**	
		GS for ground taxi	**GS for hover taxi**
FAA [71]	MD	MD + 6 m	MD + 2 max(1/3 TTS; 3 m)
ICAO [72]	1.2 x MD	2 x MD	

2.3.2.3 Taxiway

The taxiway represents the path that connects pads and gates. The taxiway includes the travel lane and requires safety clearances on both sides [89]. Figure 2.6 outlines a taxiway, its structure and its measures.

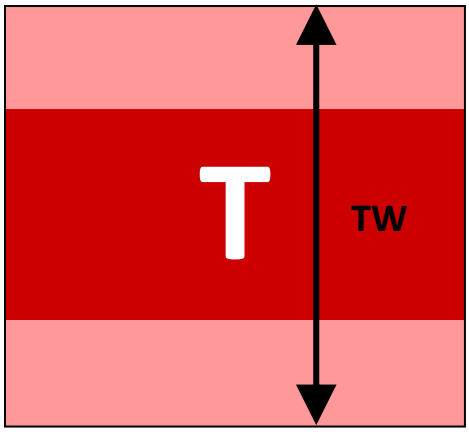

Figure 2.6: Structure and measures of a taxiway

The FAA [71] also defines the width of taxiways. Taxiway dimensions depend on helicopter size, taxiway markings, and type of taxing (ground taxi or hover taxi). These dimensions are specified in table 2.7. Normally, hover taxi requirements determine the width of the taxiway. However, if the fleet consists of a combination of large ground taxi helicopters and smaller hover taxi helicopters, the larger aircraft may dictate the width of the taxiway. If wheeled helicopters perform taxiing without touching the surface, the facility should be designed with a width for hover taxiways rather than ground taxiways. If visibility of the centerline marking cannot be assured at all times, e.g., in locations where snow or dust frequently obscure the centerline marking and it is not possible to remove it, the minimum taxiway dimensions should be set as if no centerline marking were present.

Table 2.7: Taxiway dimensions for FAA [71]

Taxiway type	Minimum width of paved area	Centerline marking	Total taxiway width
ground	2 x UCD Unpaved	Painted None	1.5 x TTS
hover	2 x UCD Unpaved	Painted None	2 x TTS

The ICAO [72] also distinguishes between ground and hover taxiing. In contrast to the FAA, the width of the taxiway for taxiing is determined on the basis of the maximum width of the helicopter. The width of the taxiway should be 1.5 times the MD. For hover taxiing, the factor used to determine the taxiway increases from 1.5 to 2. The paved area of the taxiway should not be narrower than 1.5 times the width of the UCD. The taxiway dimensions are summarized in the table 2.8.

Table 2.8: Taxiway dimensions for ICAO [72]

Taxiway type	Minimum width of paved area	Total taxiway width
ground	1.5 x UCD Unpaved	1.5 x MD
hover	1.5 x UCD Unpaved	2 x MD

ICAO further distinguishes air transit routes, which allow movements of the helicopter at a height of less than 30 meters above the ground at speeds above $37\ \mathrm{km/h}$. If the air transit route is to be used only during the day, the width of an air transit route must not be less than seven times the maximum total width of the helicopters for which the air transit route is intended. If night operations are also desired, the factor must be increased to ten.

2.4 Vertiports

UAM is a subcategory of AAM and is considered an innovative concept that provides a safe and efficient transportation system for manned and unmanned aircraft in an urban environment [43, 57]. Kohlman and Patterson [91] additional explain that it is a transportation concept through which flying vehicles can be used to transport people and cargo at low altitudes over cities. The NATA [56] further specifies that UAM is an on-demand air transportation system that connects urban core areas with residential suburbs and rural areas through the use of eVTOLs. For the purposes of this thesis, the following section will discuss the UAM infrastructure.

NASA [57] describes that an UAM aerodrome is one that meets the capability re-

quirements to support UAM departure and arrival operations. These aerodromes are referred to as vertiports. The term vertiport is composed of "verti-cal" and "air-port" and describes a new type of infrastructure element that supports the take-off and landing of tiltrotor aircraft and rotorcraft, enabling intra- and inter-urban air mobility [92]. Tayor et al. [17] generalize that it is an airport type for aircraft that land and take-off vertically. In addition to take-off and landing, operations at a vertiport include vehicle loading, passenger boarding and deboarding, pre- and post-flight inspections, and aircraft maintenance.

There are a variety of locations that can be considered for vertiports, including rooftops, land along waterfronts, space over highways, and unused land at existing airports [69, 84]. Vertiports are comparable to conventional heliports. However, they are larger, because they are intended to have a passenger handling capacity similar to commercial airports [92]. Nevertheless, the vertical take-off and landing capability of eVTOLs allows vertiports to be designed more compactly than commercial airports with similar throughput [51].

Lineberger et al. [40] explain that a vertiport requires different infrastructure components depending on its intended use and distinguish three types:

- Large vertiports should be placed on the periphery of urban areas to serve as central locations for UAM infrastructure. These vertiports should provide the infrastructure for maintenance, repair and overhaul (MRO) of the eVTOLs and a central citywide control system for their operation. For a working UAM network, each city should have at least one vertiport that meets these specifications.
- Further vertiports are located in the heart of the city and serve as major sites for both cargo and passenger boarding and deboarding and take-offs and landings. They have space to accommodate multiple eVTOLs at the same time and usually are equipped with fast charging and/or refueling systems, have basic security checkpoints, and the capacity to carry out minor MRO operations.
- The smallest vertiports consist of only one or two landing pads. They are used only for picking up and setting down passengers and cargo and serve as con-

necting points between the larger vertiports.

The FAA, the European Union Aviation Safety Agency (EASA) and the International Civil Aviation Organization (ICAO) provide specifications for the core elements of a vertiport, these are the take-off and landing areas with the associated safety areas (pads), dimensions of the taxiways, standing areas for the vehicles (gates) and approach and departure lanes to be complied with. Depending on the arrangement of the components of the pads in relation to the gates, four common topologies can be derived [92]:

- Single topology: The single topology consists only of a pad with no additional gates. Boarding and deboarding takes place directly at the pad (see figure 2.7a).
- Satellite topology: The satellite topology is similar to the single topology except that a pad is surrounded by gates. The gates are located directly adjacent to pads and therefore do not need to be accessed via a taxiway. Boarding and deboarding takes place at the gates (see figure 2.7b).
- Linear topology: In the linear topology, pads are positioned side by side along a line. Determined by the shape of the area up to two rows are possible with the arrival and departure corridors of the two rows facing in opposite directions. Gates are located directly adjacent to pads and therefore do not need to be accessed via a taxiway. Boarding and deboarding takes place at the gates (see figure 2.7c).
- Pier topology: Unlike the other topologies, the pier topology does not require the gates to be placed directly next to the pads. The gates are connected to the pads via a taxiway. Thereby it has to be distinguished how many pads share a taxiway and how the gates will be arranged at the taxiway. Boarding and deboarding takes place at the gates (see figure 2.7d).

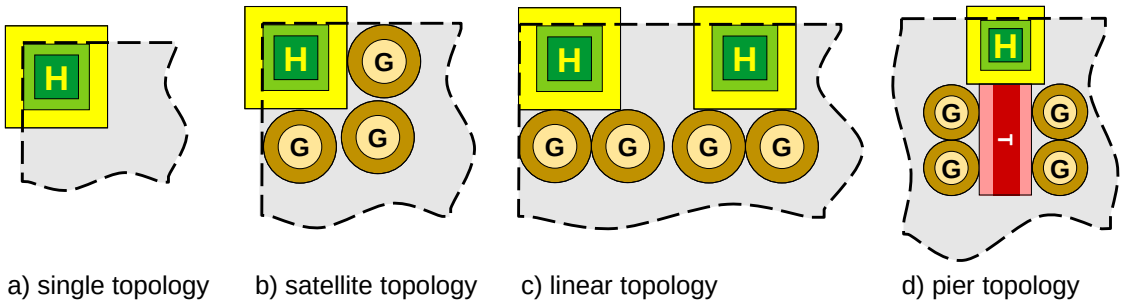

a) single topology b) satellite topology c) linear topology d) pier topology

Figure 2.7: Four vertiport topologies

For further investigations, it is also important to consider which processes an eVTOL goes through at a vertiport. In this context, Preis [88] defines that for an eVTOL the processes at a vertiport start with the arrival, followed by the taxiing to the gate, where the turnaround process takes place. After the turnaround process is completed, the taxiing is done back to the pad from where the departure is performed. The individual process steps are shown graphically in figure 2.8. Such a traversal of all process steps is defined by Preis [88] as a vehicle throughput and also in the context of this thesis a throughput is interpreted according to this definition.

Figure 2.8: Process steps at a vertiport for an eVTOL [88]

3 Methods

In the following chapter, the methods developed in the context of this work are presented. Before that, there is an insight into methods that have already been used.

3.1 UAM Planning Tools

Vertiport design is complex due to dynamic operations. A helipad is not a vertiport, and the analyses and specifications performed for helipads are therefore not fully transferable for the high throughput expected for vertiports with optimal design. Technological advances in the development of eVTOLs are expected to provide them with better flight and navigation capabilities than helicopters and thus infrastructure specifications will need to be adjusted [41]. Therefore, there is a knowledge gap for architectural firms in the process of planning and configuring operational areas on vertiports. Consequently, there is a need to fill the knowledge gap with a simulation of vertiport designs and their operations to compare the operational differences of the designs, including noise, safety, and throughput [17]. For the complete simmulation of a vertiport, three areas must be considered. First, the identification of the location, followed by the sizing and design of the vertiport for the given area. Once these two points are fulfilled, the vertiport can be simulated. The three steps are shown in figure 3.1.

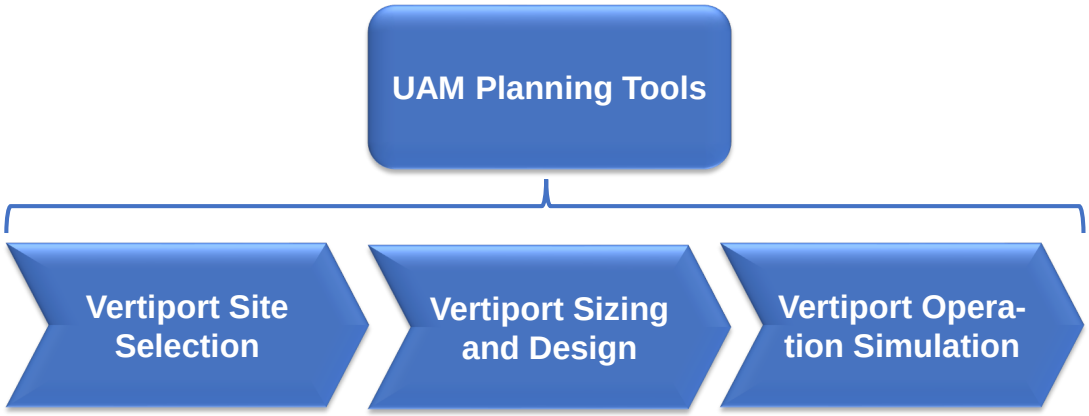

Figure 3.1: UAM Planning Tools

Various studies have already been conducted and programs developed in this regard, some of which are briefly reviewed below. The paper of Postoriono and Sarné [32]

provides a good overview of different simulation methods.

3.1.1 Vertiport Simulation

Amirzada [93] developed an agent-based modeling and simulation framework for simulating vertiport processes. The program builds on MATSim [94] and is based on the knowledge of the location and number of pads and gates as well as stands to simulate the processes on the vertiport to the second.

In their paper, Glaab et al. [95] investigate the noise impact of implementing a UAM operation for New York in cooperation with the NASA, the Intelligent Automation Inc , and the Port Authority of New York and New Jersey. For the study, flight paths were simulated using the Metrosim tool and these were used to determine the noise impact for the New York urban area for different scenarios.

Guerreiro et al. [96] present in their paper a mission planning algorithm developed by the NASA for UAM operations research. The algorithm plans conflict-free routes for a given set of UAM passenger trips. Further on-demand operations are assumed, and flights are prioritized on a first-come, first-served basis. In a follow-up work [97], the program was used to evaluate and compare the capacity and throughput of different vertiport configurations. Inputs given for individual vertiports are the number of take-off and landing slots and stand areas. The study was simulated based on a UAM demand scenario. It has been shown that the first-come-first-served scheduling approach for vertiports can have a detrimental effect. Nevertheless, a throughput of $80\ \%$ or more of peak throughput was achieved for most vertiport configurations.

Kleinbekman et al. [98] present a tool to optimally and efficiently coordinate arrivals and departures of eVTOLs in the context of on-demand air mobility in cities. They anticipate that the arrival phase will be the main bottleneck for vertiport operations. In the context of the study, a hexagonal vertiport network with vertiports with two landing points is investigated. The case study was done by using a new airspace design for the vertiport terminal area and a novel rolling horizon scheduling algorithm. Simulation results show that up to 50 seconds of delay per eVTOL can be expected during commuter peak hours and less than 10 seconds of delay, during off-peak hours.

In their paper, Niklaß et al. [99] investigate all relevant effects as well as interactions in an UAM system. In this context, a collaborative system-of-systems modeling approach for UAM is presented. A previously developed pool of low-fidelity physical analysis components is integrated into a Remote Component Environment (RCE) workflow engine. The developed pool includes demand forecast, trajectory, vertiport, and cost modeling as well as air traffic flow and capacity management. The system module is applied to a 24-hour simulation for three UAM networks in Hamburg.

Rothfeld et al. [100] present a methodology for simulating on-demand UAM air vehicle deployment in an urban traffic environment. The tool represents a MATSim extension and aims to allow easy adjustment of vehicle parameters and parameters of the necessary VTOL infrastructure to perform sensitivity analyses and thus make conclusions about the overall UAM system. The use of the UAM extension is intended to provide urban transportation and planning stakeholders with an open-source framework to evaluate potential UAM realizations.

Yang et al. [101] design a centralized computational guidance algorithm to enable safe and efficient on-demand autonomous flight operations for eVTOLs in a UAM network. The presented approach formulates the problem as a Markov decision process and subsequently solves it using the online MonteCarloTree Search algorithm. A coordination mechanism is also designed to coordinate multiple eVTOLs in parallel. This is achieved, by generating real-time actions that all aircraft follow. The algorithm can guide all aircraft to their respective destinations while avoiding potential conflicts between them. To test the performance of this algorithm, an airspace simulation was created. The results show that this algorithm results in all aircraft reaching their destinations, with conflicts occurring in only $0.2\ \%$ of flights.

Postorino and Sarné [32] analyze different UAM scenarios using an agent-based approach with different traffic conditions. Preliminary results focusing on travel costs show that they depend on the average distances traveled and the location of vertiports acting as transfer nodes between air and ground modes.

3.1.2 Location Identification

For a meaningful use of the tools just presented and to obtain realistic results, it is important to know the location of the vertiports and to position them efficiently. In this context, there are already studies and tools dealing with the determination of the location of the take-off and landing points for a functioning UAM network. Peisen and Ferguson [68] conclude in their studies that vertiports must be located as close as possible to the center of demand.

Rath and Chow [102] develop a program to determine the location of vertiports. They rely on a novel application of the classical hub-location problem to properly evaluate the access distance of travelers from other zones to vertiports. They were thus able to reduce the cost compared to the clustering approach from the literature [103]. An experimental application to New York City showed that their new method outperformed that of Rajendran and Zack [103] by $7.4\ \%$.

Arellano [104] develops a semi-automatic method for placing UAM stations in the Munich metropolitan area. The method follows a geographic information system (GIS) multi-criteria decision analysis framework and analyzes GIS data for factors positive for UAM to subsequently make placement recommendations, with the goal of maximizing coverage of demand points.

In his work, Fadhil [105, 106] presents a GIS-based analysis for vertiport location selection. The suitability analysis is done using the weighted linear combination (WLC) method to find suitable areas for UAM ground infrastructure. The weightings of the factors for the WLC are selected by interviewing experts in the field of UAM infrastructure. For validation, the method was applied to the cities of Munich and Los Angeles.

Lippoldt et al. [92] present a method for locating infrastructure elements in the UAM field that identifies mobility hotspots in Bavaria. The determined hotspots can subsequently be used to derive the optimal locations for vertiports.

3.2 Identification of Research Gap

The approaches just presented can be used to determine the optimal location for vertiports, but it cannot be determined whether they can be reasonably implemented at these locations. Therefore, in order to create a realistic simulation of a vertiport network, the actual possible design is of central importance. In this context, there are some publications dealing with the design of vertiports [17, 68, 89]. However, except for the work of Preis [92, 88] on which this thesis is based, no publication could be found during the literature review that shows an automated procedure for the creation of vertiport designs.

Nevertheless, a comparable tool exists that allows for the design of short take-off and landing (STOL) infrastructure. The code developed by Robinson et al. [107] allows predictions to be made on the sizing of runways based on a given area and thus whether the given area is suitable for an airport.

3.2.1 Existing Vertiport Design Tool

In the context of this thesis, the work of Preis [92, 88] is continued and the existing program is improved and further developed.

The existing MATLAB-based code is able to determine the possible VTOL throughput for a surface based on read-in surfaces and different input parameters. In the following, the functionality of the tool is presented.

The first component of the code are the input variables. The area to be analyzed is read in as a csv-file and contains the coordinate points of the polygon area to be analyzed. It is possible determine the area by QGIS [108] or create it manually. For the calculation of the possible throughput, the vehicle dimensions must also be specified. Within the scope of the code, it is the TTS and the MD.

Furthermore, the operation parameters of the vertiport to be designed must be specified. It has to be selected which type of taxiing will be applied at the airport. The code allows to choose between hover and ground based on the FAA [71, 89] standards. Further the process times have to be set. Namely, approach and departure time, taxi

time and turnaround time. As last input it is possible to select if parking for cars is considered on the given area or not.

Based on the just mentioned parameters, the dimensions for the vertical transport components are calculated using the FAA specifications [71, 89]. The dimmensions for pad, gate and taxiway are determined. In addition, the size of the parking spaces is determined.

A car parking area represents the place where passengers can park their private vehicles. The dimensions for these parking spaces are in accordance with the regulations for parking garages [109]. A parking lot requires an access road, since in the context of this work it is assumed that two rows of parking lots face each other. Parking lots can share an access road and therefore, a car parking unit consists of one parking space and half an access road.

After having determined the size of the components, units of pad, gate and taxiway are formed based on four possible defined topologies, and it is calculated how many can be placed on the given area. We are talking about the four already known topologies: single, satellite, linear and pier.

In this first approach developed by Preis was assumed that for the single and satellite topology, a maximum of four units can be placed based on the approximate assumption of a rectangular area. This means, one in each corner as long as sufficient area is available. Since the safety areas of the pads may extend beyond the base area, their areas are only calculated proportionally. In the case of a linear topology, the maximum straight line within the area is required in addition to the base area to calculate the number of units that can be placed. Based on this straight line, the number of pads that can be placed in a row is calculated. Subsequently, it is determined whether a second row of pads and gates can also be positioned in the area. If this is the case, two rows of pad/gate units are assumed, otherwise one. The pier topology is characterized by the fact that there is no fixed number of units. The maximum quantity of units is limited only by the available footprint.

In the developed method it is possible to choose whether the bottleneck should be at

the gates or at the pad. According to the choice, the gate to pad ratio is determined. For the other topologies a fixed gate to pad ratio is assumed.

Using the number of components calculated as explained earlier, in the next step the throughput of the designed vertiport is determined. The assumption is made that all pads and gates can be operated in parallel. Therefore, by adding up the times for the individual processes of take-off and landing, taxi time, and turnaround time, the hourly vehicle throughput can be calculated. In addition to the computationally possible throughput, the function also outputs the limiting component, which as previously mentioned is important in the context of the calculations for the pier topology.

After successful dimensioning the vertiport for the four possible topologies, the results are returned as a table. In the case that parking spaces are to be considered, the number of them is calculated based on the throughput. The assumption is made that a certain number of passengers travel to the vertiport by vehicle and thus depend on a parking space. For simplicity, one passenger per vehicle is assumed. In the following, the layout is adjusted until the vertiport components and the parking spaces required for the resulting throughput fit on the given area.

3.2.2 Weaknesses of Existing Vertiport Design Tool

Since this is a simplified model, it has been extended by a few components in the course of this thesis. On the one hand, the process times were broken down further and are no longer assumed to be fixed process times but are dependent on, for example, the length of the taxiway and the associated taxispeed or the turnaround time depends on the number of passengers a vehicle carries.

Furthermore, the fixed gate to pad ratios were abolished and made variable. Thus, the ratio is chosen to achieve maximum throughput. In addition, the limitation on the maximum number of pads for the single and satellite topologies has been removed. Moreover, the calculation of the pier topology has been refined. Because it is not realistic to cover the entire available area with pad/gate units. Rather, the pads are to be positioned only at the edge of the area to ensure obstacle-free approach and departure paths. Furthermore, the v2.0 also takes into account the minimum dis-

tances that must be maintained between pads to enable parallel operation. Another enhancement is that it tries to capture the actual shape of the surface and not only its size.

In the following chapter this improved version is presented.

3.3 Extended Area to Throughput Method

As explained earlier, the 'Area to Throughput' method generates a vertiport design proposal based on a given area. This proposal contains information on the favored topology and the potential throughput of the selected area. In addition to the area, factors such as the selected vehicle type or even desired safety distances of the individual pads and the choice of parking situation for passenger cars, have an impact on the resulting design proposal. In the following, the model with its assumptions and simplifications is presented and its implementation and in- and outputs are displayed.

3.3.1 Vertiport Airfield Model

The problem of maximizing the possible throughput of a given surface is presented in this paper as a mixed integer programming problem. To solve it, the branch-and-bound approach is used. For many models, linear programming is reasonable and realistic because decision variables need not represent integers. However, if the decision variables are to take integers it is a (linear) integer programming problem. It is a mixed integer program if some but not all variables are integers. This is the case in this approach to vertiport dimensioning, since, for example, the number of elements or even the throughput may only take on integer values, but values for areas or even the length dimensions of the components cannot take on integer values. Branch-and-bound essentially means that after a top-layer formulation of the problem is defined, it is subdivided into several subcategories that are optimized in an iterative manner based on given factors. [110]

3.3.1.1 Mathematical Formulation

Based on the model from Preis [88] the following is developed. In this thesis the subcategories are the four defined topologies of a vertiport. The utility function aims to maximize the hourly throughput T. Here, a throughput is defined as the traversal of the process from approach to departure in which three different elements of the vertiport (index i), namely pad, gate, and taxiway are occupied for different durations. The number of different elements n_i is determined by the vertiport layout. The possible throughput depending on a particular element is calculated by multiplying the element n_i by one hour and dividing by the blocking time $t_{block,i}$ that the respective element is occupies in a process run. To calculate the blocking time, the different process times $t_{i,j}$ must be summed up for each element. The index j stands for the process, which can be e.g. landing, taxiing or turnaround. The total throughput for the vertiport design corresponds to the smallest element-specific throughput T_i. This element therefore also represents the operational bottleneck. The times needed for each process step are given, as well as on which element they take place.

$$
\begin{aligned}
maximize\ \ T & \\
subject\ to\ \ T & = min_{\forall i} T_i, \quad i = pad, gate, taxiway \\
with\ \ T_i & = \frac{n_i * 1h}{\sum_j t_{i,j}}
\end{aligned}
$$

To determine the number of elements n_i, the auxiliary unit n_{unit} is used, which consists of a pad and the associated gates and taxiways. The number of associated elements varies depending on the topology and layout of these. This results in the factor $c_{i,pad}$ which indicates the number of respective elements per pad. Depending on dimensions of the vehicle to be used, each element has certain dimensions and an area A_i. Accordingly, the area of a unit is the sum of all products of A_i and c_i. Depending on the general conditions given area A_{total}, and the maximum and minimum extent of this area l_{min} and l_{max}, as well as the minimum distance x_{min} to be maintained between two pads, the maximum number of possible units n_{units} is deter-

mined iteratively. Based on n_{units} and the individual factor c_i, the number of respective elements n_i can be inferred. Table 3.1 lists all variables, including a description and their possible range of values.

$$
\begin{aligned}
n_i &= \lfloor n_{unit} c_{i,pad} \rfloor \\
with \;\; n_{unit} &= \left\lfloor \frac{A_{total}}{A_{unit}} \right\rfloor \\
and \;\; A_{unit} &= \sum_i A_i c_{i,pad}
\end{aligned}
$$

Table 3.1: Overview of variables in mixed integer programming problem formulation

Description	Formula sign	Range of values
hourly throughput	T	$\in \mathbb{Z}_+$
process times	t	$\in \mathbb{Q}_+$
number of elements	n	$\in \mathbb{Z}_+$
physical area	A	$\in \mathbb{Q}_+$
ratio between element a and b	$c_{a,b}$	$\in \mathbb{Q}_+$
index indicating element	i	$\in (pad, gate, taxiway)$
index indicating process	j	$\in (landing, taxiing, turnaround...)$

3.3.1.2 Assumptions and Simplifications

Since a complete representation of the reality would be desirable but not feasible within the scope of this work, some assumptions and simplifications were made, which are presented below. First of all, the standards for the calculation of the individual components are based on the FAA guidelines. The choice to use the FAA guidelines is based on the statement of Neuville et al. [52] that mostly the FAA is setting standards that are later adopted by the ICAO. In addition, many other studies are already based on the FAA standards as already seen in section 2.3.

Further, the calculation of throughput assumes full utilization and that no delays

occur. The turnaround time also does not include times specifically for loading, maintenance, cleaning, servicing, or anything else. These are assumed together by a fixed invariant time. In contrast, the passenger-related turnaround time is variable and depends on the number of passengers per vehicle. However, this simplification should be valid, since it is a method for dimensioning a vertiport and not a simmulation of the prevailing processes. Furthermore, the vertiport is considered as a closed or isolated system. This means that no environmental influences are taken into account. Thus, surrounding buildings, winds or other phenomena do not play a role in the design. The area under study is assumed to be simplified as a rectangle, and furthermore, no 'mixing' is possible in the design layout. This means that the vertiport cannot be designed for several vehicles at the same time, only for one pre-selected vehicle. Also, no topologies can be mixed in the sense of increasing throughput, or individual pad, gate units can not have larger or smaller gate to pad ratios in a design, these are fixed. Finally, it should be noted that only the design of the airfield is done. The terminal or other fascilities are not considered.

3.3.2 Implementation of Model

The implementation of the previously presented model is done in MATLAB and is performed by means of a mainfile. The central components of the mainfile represent two additional functions. First, the function that generates the layout for each topology. On the other hand the throughput function which calculates the potential throughput for the given layout. In the following sections, the structure of the mainfile and the functionality of the functions are described.

3.3.2.1 Main

As just explained, the model is implemented in a mainfile, which is presented in the following. The flow of the code is visualized in figure 3.2.

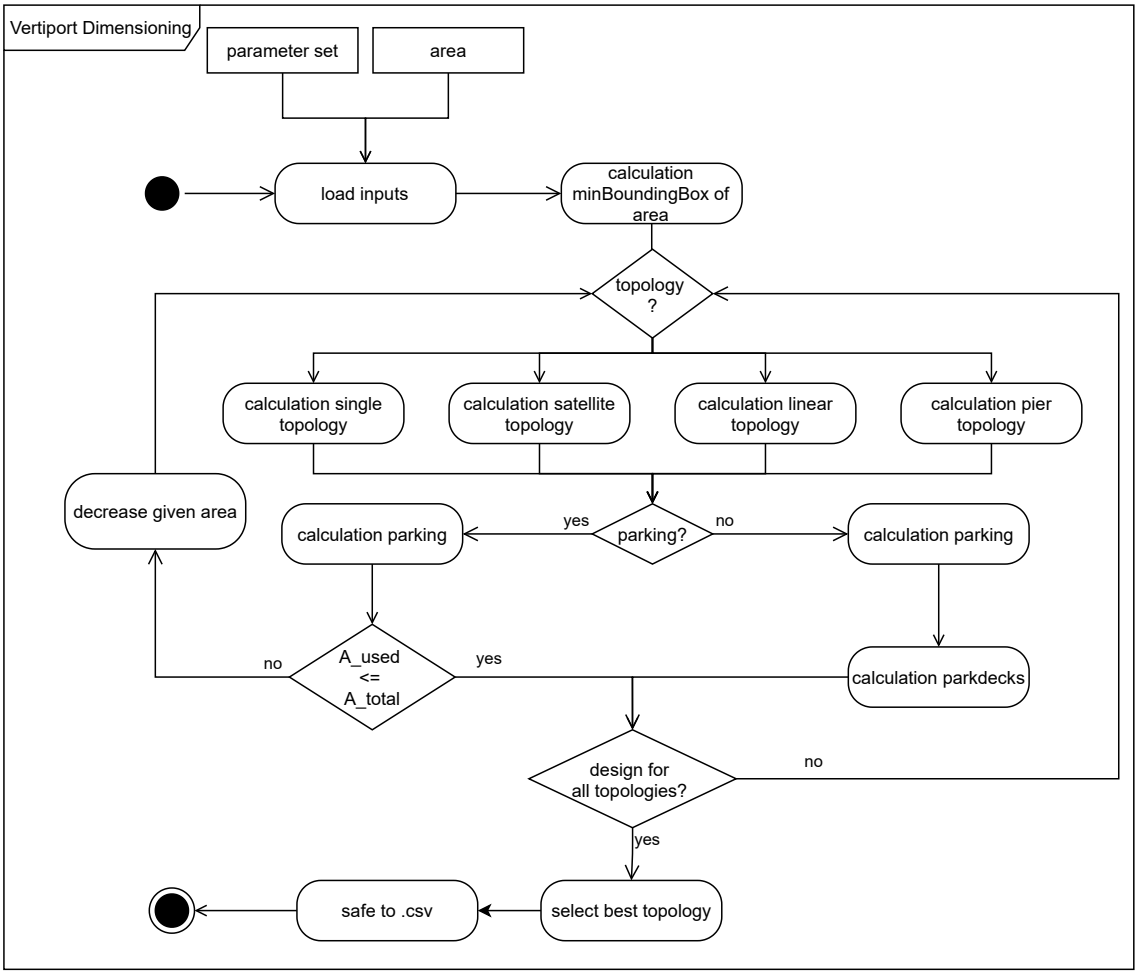

Figure 3.2: Flowchart of the main function of the area to throughput method

After starting the program, first of all the inputs are loaded, which consist of previously defined surfaces and a parameter set. In addition to the selection of the desired parameter set and the surfaces to be examined in this respect, the user is offered the possibility to choose for which topologies the examination is to take place and in which folder structure the results are to be stored.

After the initialization of the code the processing of the input data takes place. In the first step, the area to be examined is analyzed and therefore fed into a function that generates a minimum bounding rectangle that spans the area. The code for this function is based on the open-source code provided by Nguyen et al. [111]. By applying the function, the shape of the originally fed polygon can be reduced to a rectangle. From this, the minimum and maximum extent of the area can be determined for the

following calculations, l_{min} and l_{max}. In addition, the function returns the area of the surface to be examined, A_{total}.

Based on this information, the previously selected topologies are then calculated. In the following, the functions for the creation of the topology and surface conditional designs are briefly described. For an explicit presentation of the individual layouts, please refer to the following chapter 3.3.3 and the appendix A.

For the calculation of the design proposal, the dimensions of the individual components must first be determined. The components include the pad with its TLOF, FATO and SA as well as the gate and the dimensions of the taxiway. The information from the input parameter set, which consists of the vehicle dimensions and the type of movement on the taxiway (ground or hover), serves as the basis for the calculation. The determination of the dimensions for the individual vertiport components is the same for all topologies, with the exception that for the single topology no calculation of the gates needs to be performed and only for the pier topology the dimensions for the width of the taxiway is required. The following procedures for creating a design proposal differ from topology to topology and are therefore presented separately in section 3.3.2.2.

With the calculated values for the created designs, the possible throughput for the determined layout is calculated. In addition to the layout, the throughput also depends on the different process times on the vertiport. The process times include the take-off and landing time, the time required for taxiing and how long the turnaround process takes. A detailed overview of the calculation of the throughput is given in section 3.3.2.3.

After successful calculation of the layout and the corresponding throughput, there are two options depending on the input parametes. On the one hand, parking spaces can be included in the available area or it is determined how many parking spaces are required for the determined layout and how many parking levels or parking decks would have to be provided accordingly under the given area. In either case, the parking function is used to calculate the number of parking spaces and the size of the parking area from the determined passenger volume and the modeshare. The

modeshare refers to the percentage of people who drive to the vertiport and therefore need a parking space. Based on the research of Wang et al. [112] in relation to park and ride, it is assumed that a modeshare between 0.2 and 0.3 is realistic.

If the parking area is to be included in the available area, it is determined whether the sum of parking and airfield area can be accommodated in the area under study. If this is not the case, the area under investigation is reduced, leaving the external dimensions, i.e. l_{min} and l_{max}, the same. With these new input parameters, a new layout is determined. This process is repeated until both, the parking area and the terminal area can be placed on the area under investigation.

Depending on the topologies selected at the beginning to be calculated, this process is repeated for each topology. When for each topology a possible design with associated throughput has been determined, the design with the highest passenger throughput is selected and saved as the best result for given parameters and area in a csv-file. Depending on the given areas and parameter sets, this procedure is run through for each of these configurations.

3.3.2.2 Layout Calculation

In this section, we will go into more detail on how layouts are calculated for each topology. We will start with the single topology, followed by the satellite, linear and pier topologies.

Single Topology

In the case of the single topology, the various possible configurations are run through in a loop. Figure 3.3 shows the sequence of the design determination.

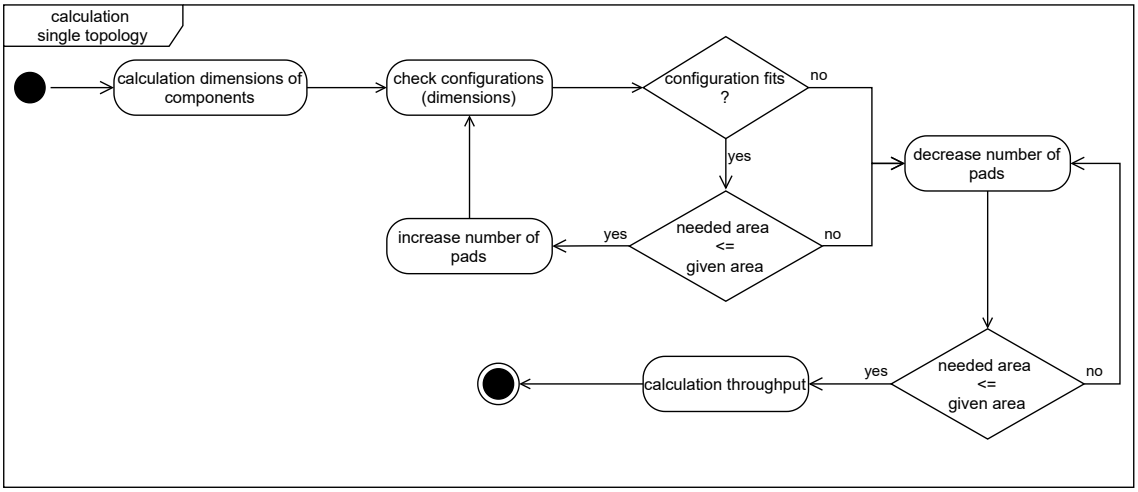

Figure 3.3: Flowchart of the function to calculate the single topology of the area to throughput method

The loop starts with the assumption that the possible number of pads is one. This assumption is first checked against the outer dimensions l_{min} and l_{max} of the area under investigation. If the dimensions of the design proposal are smaller than those of the surface, it is checked whether this also applies to the existing and required surface. If this is the case, the number of pads is increased until one of the two conditions does not apply. If one of the two conditions does not apply, the number of pads is decreased again. If the reason for the exit of the loop was a not fit due to the dimension of the configuration the reduction of the pads leads to the selection of the last fit configuration. If the available area is not sufficient for the configuration, the reduction of the pads can take into account the actual shape of the area to be examined, which is not necessarily reflected by the bounding rectangle.

Satellite Topology

The procedure for determining the layout for a satellite topology is shown in figure 3.4.

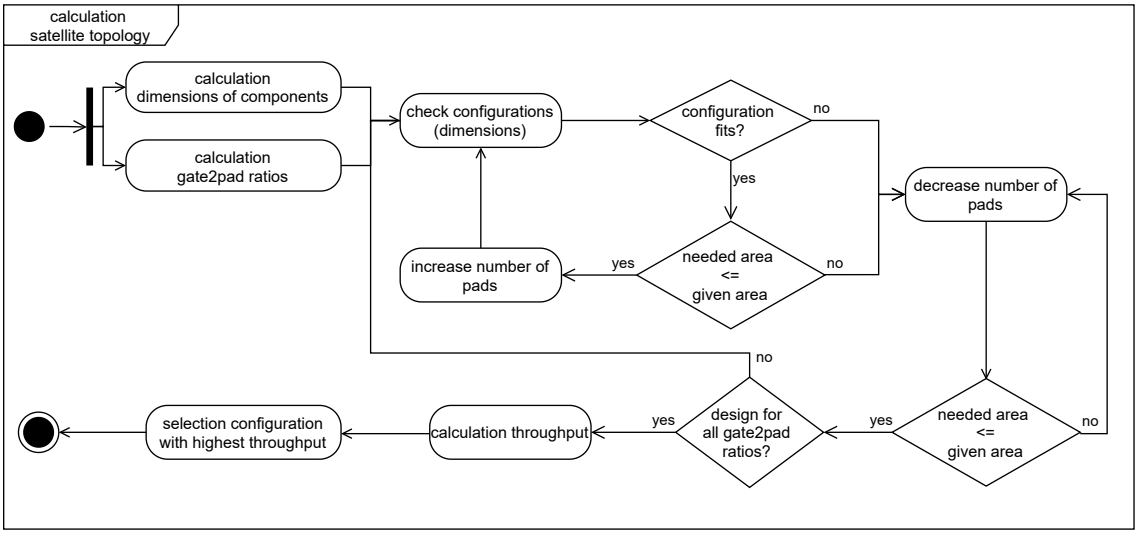

Figure 3.4: Flowchart of the function to calculate the satellite topology of the area to throughput method

The satellite topology calculation function first calculates the possible $gate2pad$ ratios for the two possible units, a corner and a middle unit. A pad can be placed either in a corner or along a straight line of the given area, resulting in either more or less space for positioning gates. To calculate the optimal $gate2pad$ ratio, the bottleneck of the corner unit is calculated using the throughput function. The operation of the function just mentioned will be shown later. If the resulting bottleneck is the pad, the number of gates is reduced until the pad is just the bottleneck. If it results that the gate is the bottleneck, the determined $gate2pad$ ratio represents the best possible ratio. Due to the defined geometry of a satellite topology, the number of gates cannot be increased to cause the pad to become the bottleneck. If after this procedure the number of gates of a center unit is smaller than that of a corner unit, the $gate2pad$ ratio of the corner unit is adjusted to that of the center unit. Once the optimum $gate2pad$ ratio is known, the individual configurations are calculated as before for the single topology, as shown in section 3.3.2.2. In comparison with the single topology, the intermediate results of the configurations are documented. After calculating the throughput of the different configurations, the one with the highest potential throughput is selected. By varying the $gate2pad$ ratios used and by changing the number of corner or center units, the designs can achieve higher or lower throughputs.

Linear Topology

The linear topology calculation is represented in figure 3.5.

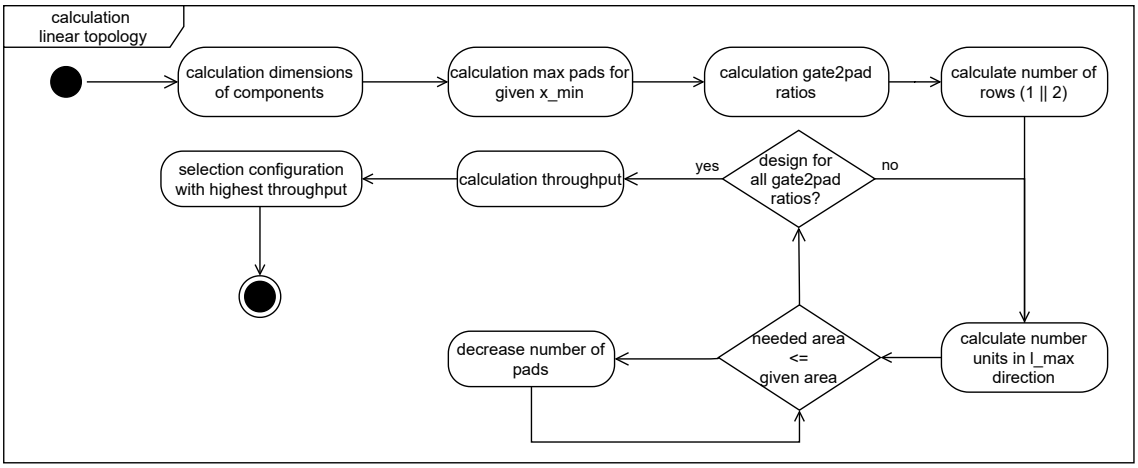

Figure 3.5: Flowchart of the function to calculate the linear topology of the area to throughput method

The first step of the calculation process is to determine how many pads can be placed along the long side of the surface with given safety distance x_{min}.

Depending on the calculated number of pads and the length l_{max}, a $gate2pad$ ratio is calculated afterwards. For this ratio the bottleneck for one unit of pad and gates is calculated. If the resulting bottleneck is the gate, the number of gates is successively increased until the pad is the new bottleneck. As the number of gates increases, the calculated distance that must be maintained between two pads can exceed the value x_{min}. In this case all $gate2pad$ ratios are saved. If the bottleneck is the pad, the number of gates is decreased until just the pad is the bottleneck. And this is stored as the optimal ratio. Now the calculated $gate2pad$ ratios are used to determine how many units can be placed along the long side of the given area and these are then multiplied by the number of possible rows to calculate the total number of pads. As for the previously presented topology functions, the number of units is reduced until the required area matches the available area. As a final step, the throughputs for the different $gate2pad$ ratios and their corresponding pad counts are calculated. The configuration that promises the highest throughput is then selected as the best alternative.

Pier Topology

Figure 3.6 ilustrates the process of determinig the layout of a pier topology.

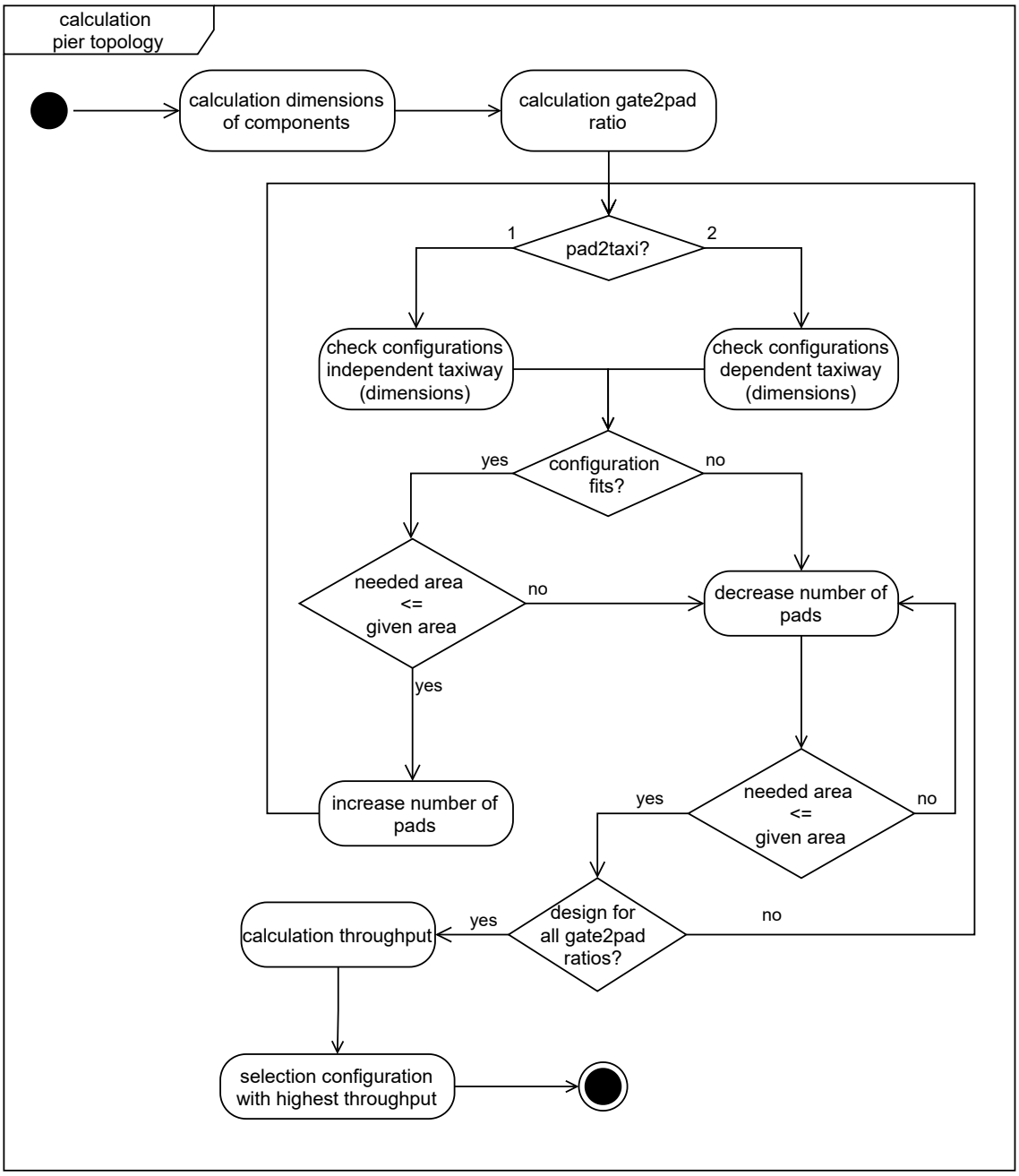

Figure 3.6: Flowchart of the function to calculate the pier topology of the area to throughput method

The design of the pier topology starts with the determination of the $gate2pad$ ratio.

An initial ratio of two is assumed which, as already known from the calculation for the linear topology, is either increased or decreased depending on the bottleneck. Also special to the pier topology is that a taxiway is always included in the design. Therefore, the applicable $pad2taxi$ ratio must be checked prior to design. In the context of this code, the ratios of one and two were implemented. Subsequently, for the different $gate2pad$ ratios, the configuration is determined that allows the placement of the most pads depending on l_{min} and l_{max}. Afterwards the known procedure of reducing the units is done until the available area matches the required one. Then the possible throughputs of the determined layouts are calculated in order to select the one with the highest throughput as the best one.

3.3.2.3 Throughput Calculation

As part of creating the layout, the average hourly throughput for vehicles and passengers is calculated. The input variables needed to calculate the hourly throughput are, the number of pads and gates as well as the associated topology. In addition, the different distances within the taxi process are important. These are divided into the path from the pad to the taxiway, the length of the taxiway and the path from the taxiway to the gate. Furthermore, certain durations are attributed to the individual processes on the vertiport. These include landing and departure times or the turnaround time. The time for the taxi process is variable compared to the other processes, as it depends on the length of the taxiway and the taxi speed already mentioned. The assumed processes are shown in figure 3.7. The processes known from figure 2.8 were further split to obtain a higher level of detail in the throughput calculation.

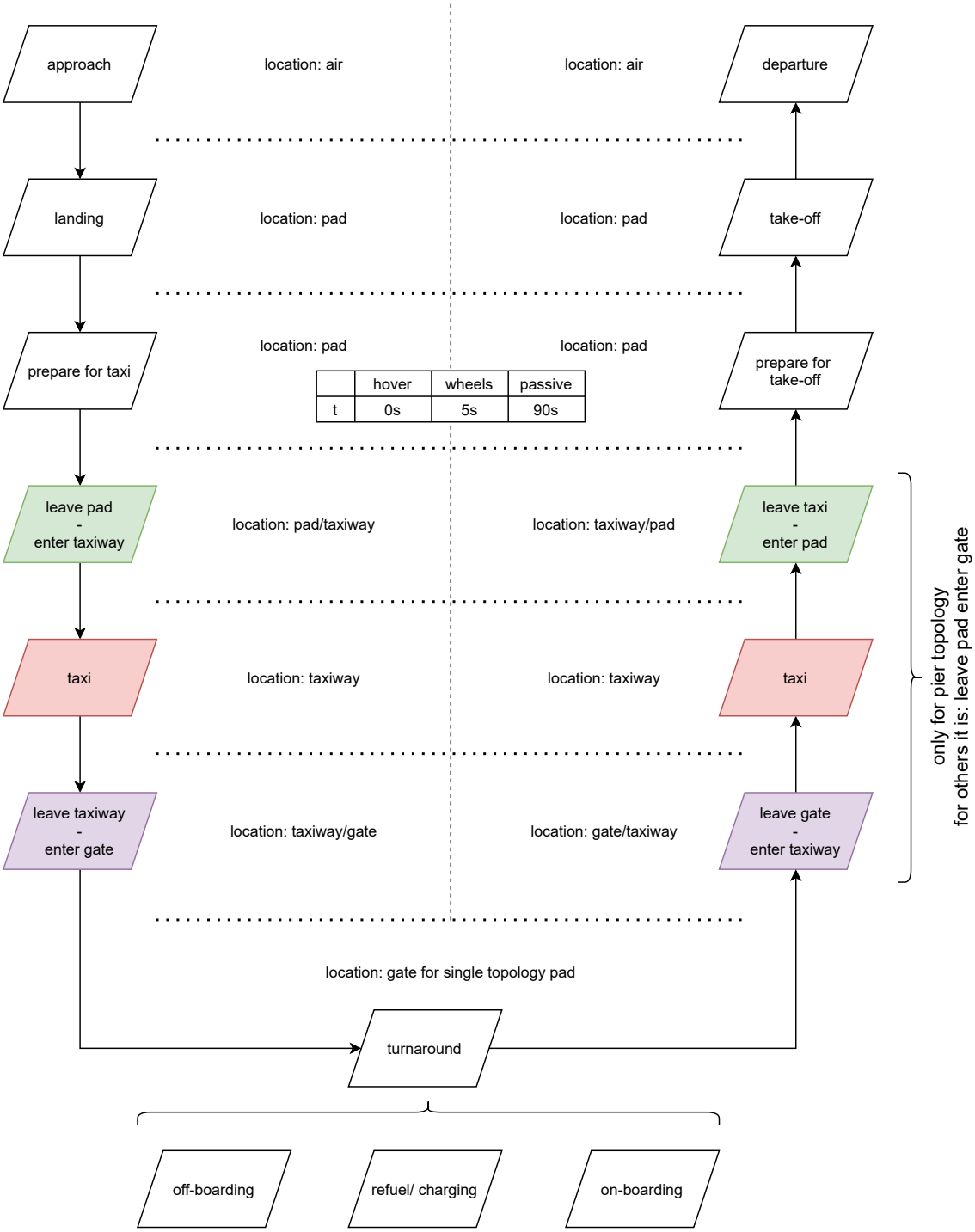

Figure 3.7: Flowchart of the processes a VTOL goes through on a vertiport

The initial process is the approach to the vertiport. Since the vehicle is in the air at this time, it is not considered for the vertiport throughput, as is the departure process. Once the landing is initialized, the pad is considered occupied until the vehicle touches

down. Then the preparation for the taxiing process begins. Here it is distinguished whether the vehicle performs the taxiing in hover mode, by actively driving (wheels) or in passive form. The associated times can also be seen in figure 3.7.

As soon as the vehicle leaves the pad and enters the taxiway, both elements are considered occupied. The time needed for this depends on the taxi speed and the length of the path from the center of the pad to the taxiway. The different lengths of the paths are shown schematically in figure 3.8 and color coded in accordance with figure 3.7. The time that the taxiway is considered occupied depends on its length and the taxi speed. The same applies to the process of driving up to the gate. In the opposite direction, when leaving the gate, the same process take place. It is to be noted that the full process run takes place only for the pier topology, since for the other topologies no separate taxiway is assumed. Therefore, for the satellite and linear topology the process taxiing is omitted. For the single topology, the turnaround process is initiated directly after landing and therefore takes place at the pad.

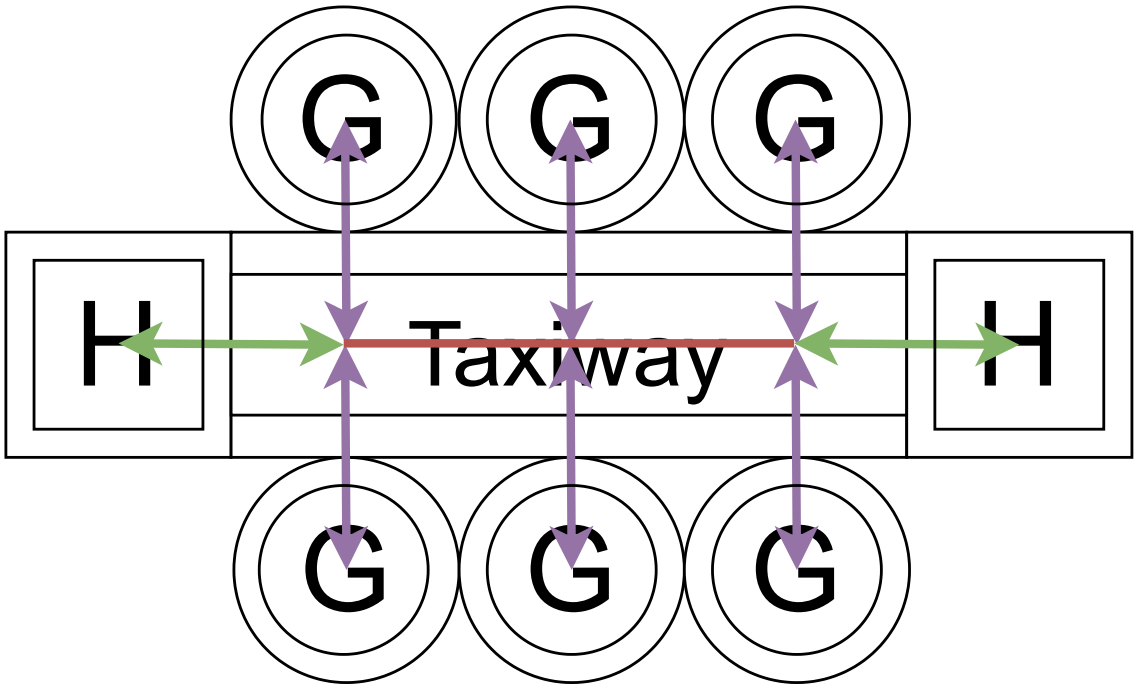

Figure 3.8: Distances for vertiport processes

The path from the pad to the taxiway is defined as the sum of the radius of the pad and the gate. The path from the taxiway to the gate is defined as the sum of the radius

of the gate and half the width of the taxiway. How the length of the taxiway is defined is shown later in section 3.3.2.4 for all topologies.

The turnaround process for the presented method consists of two components. One is the variable turnaround time, which depends on the number of passengers per vehicle and the assumed time for boarding and deboarding. On the other hand a fixed turnaround time is reserved for refueling or loading of the vehicle, cleaning, security checks or maintanance. The occupancy time of the gate results from the respective larger turnaround time.

After returning to the pad, the occupation of the pad ends at the moment when the take-off is completed and the departure is initiated.

Within the function, a distinction is first made whether it is the pier topology or another. In the case of the pier topology, the times for reaching and leaving the taxiway as well as the time on the actual taxiway must be considered as part of the taxi time. For the satellite or linear topology, a direct connection between the pad and the gate is assumed for simplicity and thus there is no classical taxiway and no time is spent on it. For a better understanding, please refer to the next section in which the calculation of the taxiway is presented. With the knowledge of the taxi time, the number of hourly taxiing processes that are possible on the vertiport is then calculated. For the pads and gates, the determination of the possible hourly processes is done in the same way. Then the process counts are compared and the component that has the lowest number of processes is identified as the bottleneck. Based on the bottleneck, it can be said that the process count reflects the maximum possible vehicle throughput. With this throughput and the knowledge of the number of passengers per vehicle, the passenger throughput can be calculated.

3.3.2.4 Taxiway length

As shown before, the length of the taxiway is essential to calculate the throughput. There are four approaches for determining this depending on the topology in the context of this work. In the case of a single topology, there is no taxiway since all processes take place on the pad.

In the case of a satellite topology, the shortest and longest taxi distances are assumed, and an average value is determined from these. See figure 3.9 and the resulting equation 3.1. The mean value is independent of the number of gates in the case of the satellite topology and is always calculated in the same way.

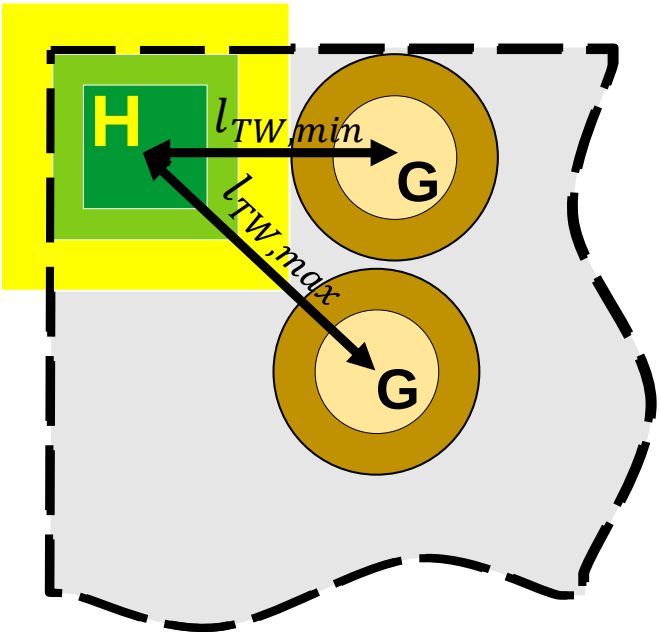

Figure 3.9: Distances for taxiing at satellite topology

Based on the above assumptions, the following formula is used to calculate the length of the taxiway in the satellite topology.

$$l_{TW,satellite} = \frac{l_{TW,max} + l_{TW,min}}{2} \tag{3.1}$$

For the linear topology, on the other hand, the number of gates is also considered because of the way they are lined up. Consequently, the distance from the center of the pad to the center of the respective gate is determined for each gate and an average value is calculated from this. Figure 3.10 schematically illustrates the calculation for the linear topology. As for the satellite topology, a direct connection between pad and

gate is assumed, without a physical taxiway.

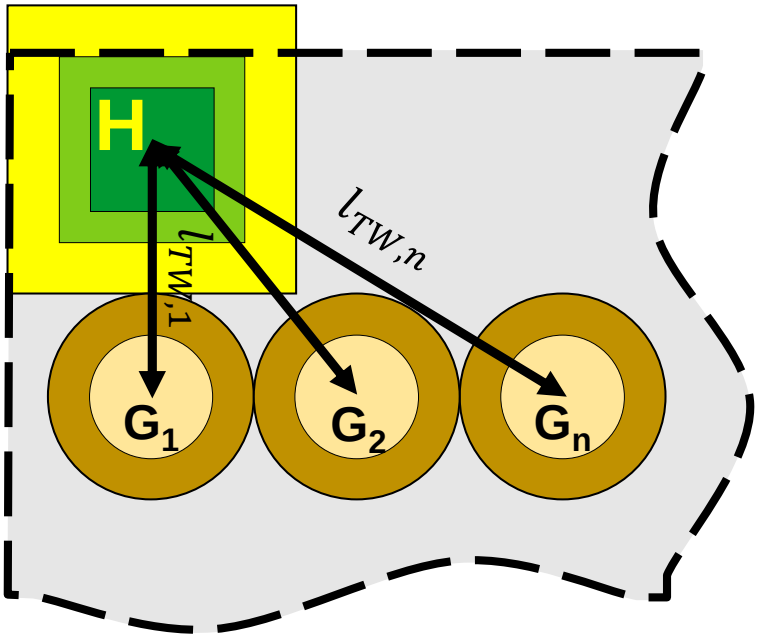

Figure 3.10: Distances for taxiing at linear topology

Based on the above assumptions, the following formula is used to calculate the length of the taxiway in the linear topology.

$$l_{TW,linear} = \sum_{i=1}^{n} \frac{l_{TW,i}}{gate2pad} \tag{3.2}$$

For the pier topology, the taxiway is divided into three sections, the path from pad to taxiway, the taxiway itself, and the path from taxiway to gate. The path from pad to taxiway is the same as the path from the center of the pad to the taxiway. For the path from the gate to the taxiway it is the same except that it starts from the center of the gate (see figure 3.8). For the actual taxiway again, an averaged value is used, consisting of the shortest and longest taxiway distance. For the taxiway calculation, the $pad2taxi$ ratio must also be considered. If this is one, the maximum taxiway length

is equal to:

$$
\begin{aligned}
l_{TW,min} &= l_{GS} \\
l_{TW,max} &= l_{GS} * (\lceil n_{Gates} * taxi2gate \rceil - 1) \\
l_{TW,pier} &= \frac{l_{TW,min} + l_{TW,max}}{2}
\end{aligned}
\tag{3.3}
$$

On the other hand, with a $pad2taxi$ ratio of two, it is necessary to distinguish what the layout of the pier unit looks like. There are two options. First is that the departure paths of the pads face into oposite directions (see figure 3.8). For this constelation the taxiway length can be calculated as seen in equation 3.3.

If the departure paths of the pads face into the same direction there is the need of a connection piece. And there are two options to be considered (see firgure 3.11). If the $gate2pad$ ratio is represented by a uneven number or the $taxi2gate$ ratio is one, as can bee seen in figure 3.11a the taxiways can be connected directly resulting the length of the taxiway being calculated as follows:

$$
\begin{aligned}
l_{TW,min} &= l_{GS} \\
l_{TW,max} &= 2 * (l_{GS} * (\lceil n_{Gates} * taxi2gate \rceil - 1) + x_{min} \\
l_{TW,pier} &= \frac{l_{TW,min} + l_{TW,max}}{2}
\end{aligned}
\tag{3.4}
$$

Else (see figure 3.11b) the taxiway length is calculated as follows:

$$
\begin{aligned}
l_{TW,min} &= l_{GS} \\
l_{TW,max} &= 2 * (l_{GS} * (\lceil n_{Gates} * taxi2gate \rceil - 1) + l_{TW,width}) + x_{min} \\
l_{TW,pier} &= \frac{l_{TW,min} + l_{TW,max}}{2}
\end{aligned}
\tag{3.5}
$$

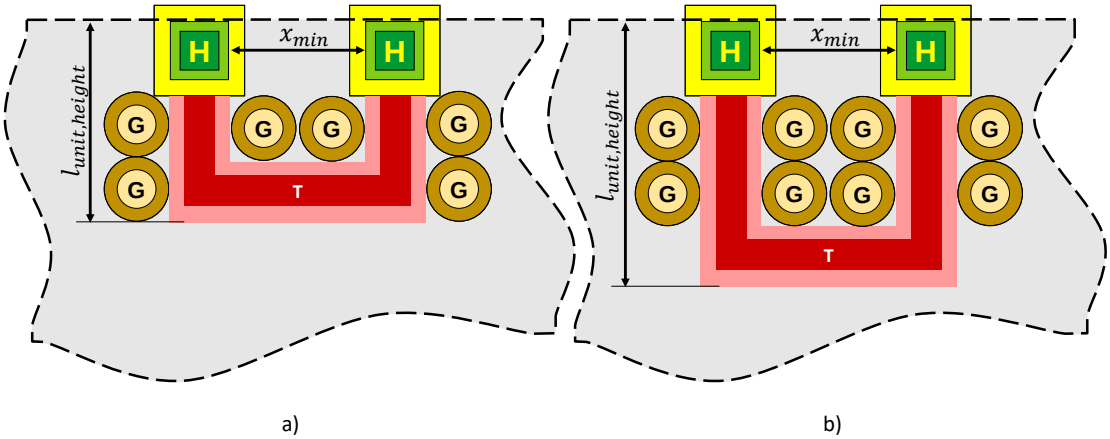

Figure 3.11: Distances for taxiing at pier topology

3.3.3 Layout Configurations

As already shown in the implementation section, different configurations for the given area are checked for the four topologies and the number of units to be placed. In order to keep the given dimensions of the area and any safety distances, different formulas are used as a basis. The following sections will therefore go into detail about how the configurations of the individual topologies can look and how they are calculated.

3.3.3.1 Single Topology

Due to its structure, the single topology has the simplest calculation basis. For a single pad, the footprint of the FATO is required. For two or more pads, it should be noted that space for the SA must be taken into account between the two pads in addition to the area of the FATO. For the arrangement of three pads, two different configurations can already be distinguished. The pads can either be positioned in a row or in a triangular configuration. The same is true for the positioning of four pads, which can be arranged in a square or in a row. For smaller configurations like these, no x_{min} has to be considered yet, since the arrangement does not result in any overlap of the approach and departure paths of the pads, an example of this is the linear arrangement of the single topology with four pads, with the assumed approach and departure paths shown in figure 3.12. The dotted line represents the minimum area needed for placing the configuration. For the other configurations with their assumed

approach and departure paths, please refer to the appendix A.1.

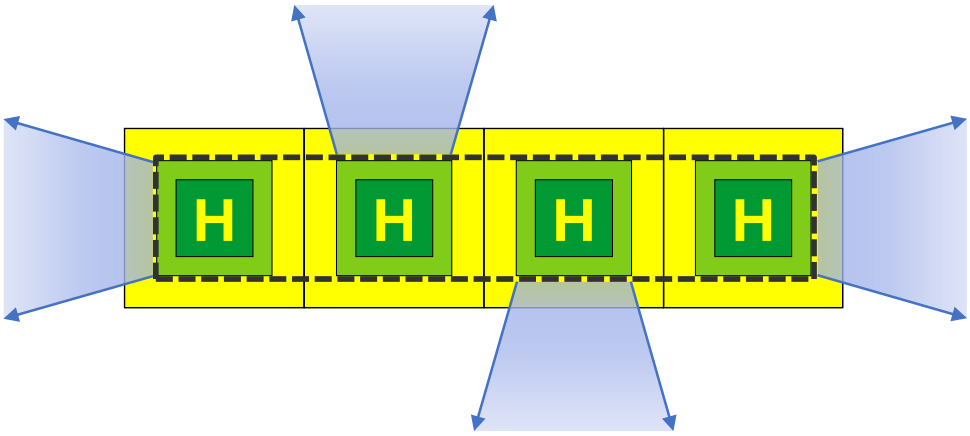

Figure 3.12: Configuration of four pads as single topology in line

As soon as the number of pads exceeds four, it is no longer possible to circumvent the minimum distances for simultaneous pad operation by the orientation of the approach and departure paths (see figure 3.13). Therefore, for the single row arrangement, there are two formulas for calculating the length l_{width} that $n_{Pads,long}$ need to be placed. The variable $n_{Pads,long}$ indicates how many pads can be placed along the long side of the given area. For an odd number of pads applies,

$$l_{width} = (l_{FATO} + 3l_{SA}) + (x_{min,calc} + l_{FATO}) * \left\lceil \frac{n_{Pads,long} - 4}{2} \right\rceil - l_{SA} \tag{3.6}$$

and for an even number

$$\begin{aligned} l_{width} = (l_{FATO} + 3l_{SA}) + (x_{min,calc} + l_{FATO}) * \left\lceil \frac{n_{Pads,long} - 4}{2} \right\rceil \\ - l_{SA} + \frac{x_{min,calc} + l_{FATO}}{2} \end{aligned} \tag{3.7}$$

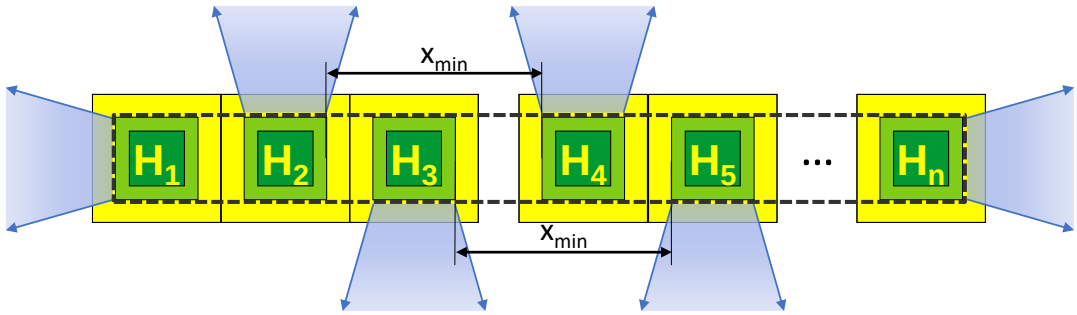

Figure 3.13: Configuration of n_{Pads} as single topology in line

The calculation is based on the assumption that by alternating the direction of the approach and departure lanes, a $x_{min,calc}$ only needs to be maintained between every second pad. In this case, the number of pads is increased as long as the condition $l_{width} \geq l_{max}$ is met. The variable $x_{min,calc}$ represents the minimum distance between the FATOs of two pads. However, if the given x_{min} is greater than this distance, $x_{min,calc}$ takes the value of x_{min}.

$$x_{min,calc} = max(x_{min,calc}; l_{SA} - l_{FATO}) \tag{3.8}$$

However, it must be noted that if the pads are placed in only one row, due to the alternating of the arrival and departure paths x_{min} must only be maintained between every second pad. Therefore $x_{min,calc}$ in this context corresponds to

$$x_{min,calc} = max(x_{min,calc}; 2l_{SA} - l_{FATO}) \tag{3.9}$$

If there is room for two pads in the short direction l_{min} of the area, the directions of the approach and departure paths of the pads can no longer be alternated, since pads are not to be overflown. Therefore, $x_{min,calc}$ must be considered already from a number of three pads in a row. And the number of pads along the long side of the

surface l_{max} is calculated as follows

$$\begin{aligned} l_{max} &\geq (n_{Pads,long} - 1)x_{min,calc} + n_{Pads,long} l_{FATO} \\ l_{max} &\geq n_{Pads,long}(l_{FATO} + x_{min,calc}) - x_{min,calc} \end{aligned} \tag{3.10}$$

$$n_{Pads,long} = \left\lfloor \frac{l_{max} + x_{min,calc}}{l_{FATO} + x_{min,calc}} \right\rfloor \tag{3.11}$$

As soon as more than two pads can be positioned in l_{min}, the number of pads is also calculated in this direction using the approach of equation 3.11, resulting in equation 3.12. The configuration is shown in figure 3.14

$$n_{Pads,short} = \left\lfloor \frac{l_{min} + x_{min,calc}}{l_{FATO} + x_{min,calc}} \right\rfloor \tag{3.12}$$

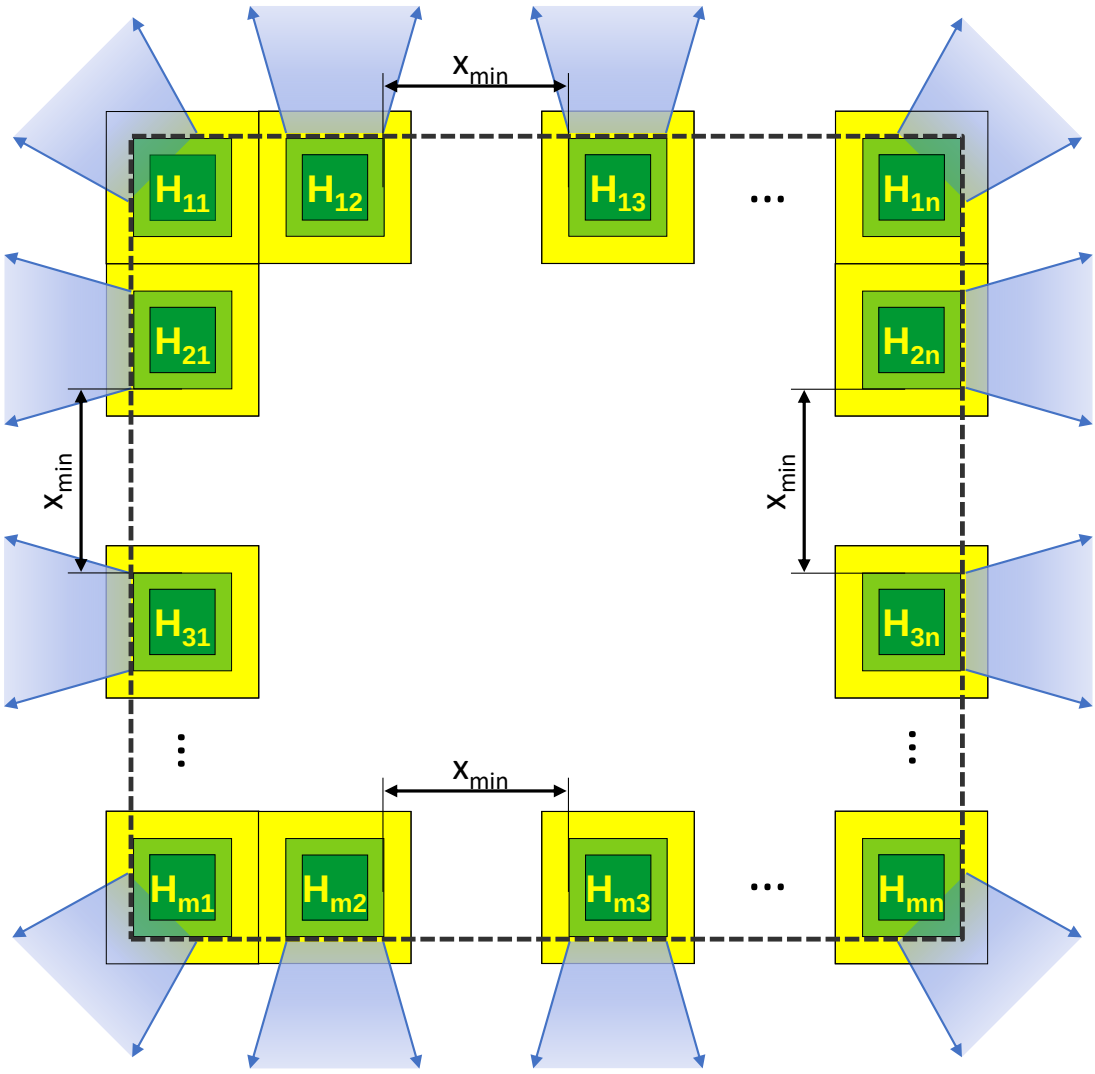

Figure 3.14: Configuration of n_{Pads} as single topology with more than one line

The resulting total number of pads, is calculated for up to two rows of pads in l_{min}

$$n_{Pads} = n_{Pads,short} * n_{Pads,long} \tag{3.13}$$

and for more than two rows

$$n_{Pads} = 2 * (n_{Pads,long} * (n_{Pads,short} - 2)) \tag{3.14}$$

Since this assumes a square arrangement, which cannot necessarily be adhered to in terms of the real area shape, the required area is compared with the available area in the last step. In case the available area is exceeded, the number of pads is reduced until this is no longer the case and consequently the total number of possible pads is obtained.

3.3.3.2 Satellite Topology

Satellite topology configurations are similar to single topology configurations. However, the special feature in the calculation of satellite topology configurations is that a distinction is made between corner pads (see figure 3.15a) and center pads (see figure 3.15b). Based purely on the position, more gates can be placed around a center pad than around a corner pad. If it turns out that center pads can generate higher throughput due to their larger gate to pad ratio, these must be taken into account as part of the configurations. Consequently, there are pure corner pad, center pad or mixed configurations. As already explained in the context of the single topology, up to four pads can be arranged either individually, in pairs, in a triangular or quadrilateral configuration, or in a single row. For the graphical representation, please refer to the appendix A.2.

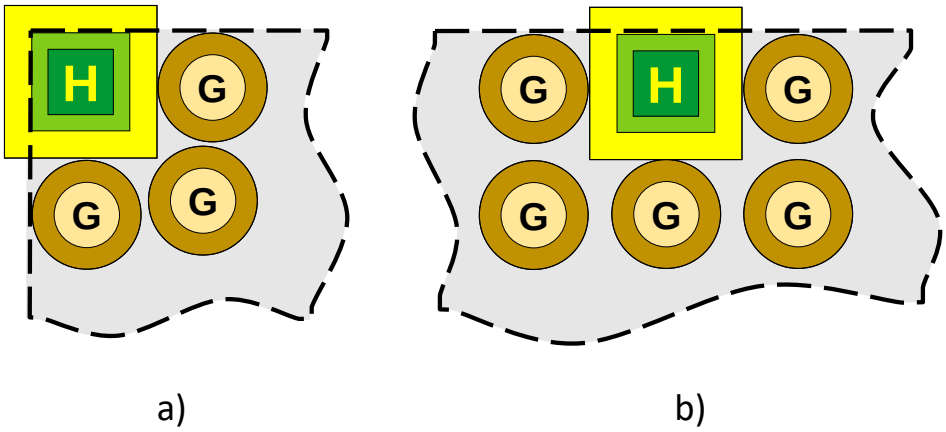

Figure 3.15: Corner and middle pads in satellite topology

In the case of a single row arrangement, the directions of the approach and departure

lanes are alternated to reduce the expansion due to the minimum distances. If the case applies that center pads achieve a higher throughput than corner pads, it must be checked whether there is enough space in l_{min} direction for the width of a center pad. If both requirements are met, the single row configuration is calculated purely with center pads, otherwise a mixed shape is calculated for which corner pads are used at the edges.

In the case that more than four pads can be placed, it is no longer possible to circumvent the minimum distances for simultaneous pad operation by the orientation of the approach and departure paths. Therefore, for the single row arrangement, two formulas result for calculating the length l_{width} that $n_{Pads,long}$ need to be placed. For an odd number of pads applies,

$$l_{width} = (l_{FATO}+3l_{SA}+6l_{GS})+(x_{min,calc}+l_{FATO})*\left\lceil\frac{n_{Pads,long}-4}{2}\right\rceil-2l_{GS}-l_{SA} \quad (3.15)$$

and for an even number

$$\begin{aligned} l_{width} = (l_{FATO} + 3l_{SA} + 6l_{GS}) + (x_{min,calc} + l_{FATO}) * \left\lceil\frac{n_{Pads,long}-4}{2}\right\rceil \\ - 2l_{GS} - l_{SA} + \frac{x_{min,calc} + l_{FATO}}{2} \end{aligned} \quad (3.16)$$

As for the single topology, the number of pads is increased as long as the condition $l_{width} \geq l_{max}$ is met. Since in the case of the satellite topology the pads are surrounded by gates, in the case of the single row configuration $x_{min,calc}$ must be calculated as follows

$$x_{min,calc} = max(x_{min}; l_{SA} - l_{FATO} + 2l_{GS}) \quad (3.17)$$

However, it must be noted that if the pads are placed in only one row, due to the alternating of the arrival and departure paths x_{min} must only be maintained between every second pad. Therefore $x_{min,calc}$ in this context corresponds to

$$x_{min,calc} = max(x_{min}; 2l_{SA} - l_{FATO} + 4l_{GS}) \quad (3.18)$$

When the short side of the area offers enough space for more than one unit of pad and gates, the number of pads along the long side $n_{Pads,long}$ can be calculated based on $x_{min,calc}$ in the same way as in the single topology case (see equation 3.11). The same is true for $n_{Pads,short}$ (see equation 3.12). As a distinction is made between center and corner pads, the number of these must also be calculated individually in order to subsequently calculate a coherent throughput. Since it is assumed that for configurations with more than four pads that have more than one row, the corners are equipped with corner pads, $n_{Pads,corner} = 4$ and the number of center pads is calculated as follows:

$$n_{Pads,middle} = 2 * ((n_{Pads,long} - 2) + (n_{Pads,short} - 2)) \tag{3.19}$$

As a square arrangement is assumed here, which cannot necessarily be adhered to in terms of area, the required area is compared with the available area in the final step. If the available area is exceeded, the number of center pads is reduced until this is no longer the case. To calculate the total number of pads, the number of corner and center pads must now be added together.

3.3.3.3 Linear Topology

A special feature of linear topology is that there can be at most two rows of pads positioned along the long side of the given surface (see figure 3.16).

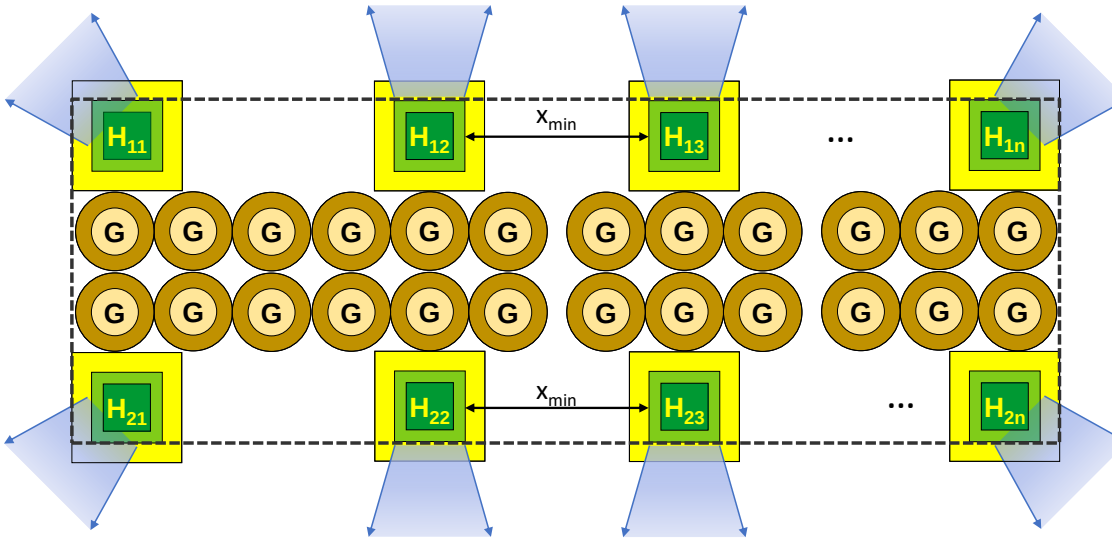

Figure 3.16: Configuration linear topology with $gate2pad$ ratio of three

However, to determine the constellation with the highest throughput, it is first calculated how many units out of pads and gates can be positioned along the long side l_{max}. To calculate this, the minimum distance that the FATOs of two pads must have from each other to enable simultaneous operation must be determined. Therefore, depending on the $gate2pad$ ratio results:

$$x_{min,calc} = max\left(x_{min}; l_{SA} - l_{FATO}; gate2pad * l_{GS} - \frac{l_{SA} - l_{FATO}}{2}\right) \tag{3.20}$$

The three components of the equation 3.20 are on the one hand the given minimum distance, the SA of each pad that must separate them minimally and the length of the gates lined up, which can exceed the two previous values and thus represents $x_{min,calc}$. With the $x_{min,calc}$ calculated in this way, the number of pads along l_{max} is obtained:

$$\begin{aligned} l_{max} &\geq n_{Pads,long} l_{SA} + (n_{Pads,long} - 1) * (x_{min,calc} - (l_{SA} - l_{FATO})) \\ l_{max} &\geq n_{Pads,long} * (x_{min,calc} + l_{FATO}) - (x_{min,calc} - l_{SA} + l_{FATO}) \end{aligned} \tag{3.21}$$

$$n_{Pads,long} = \left\lfloor \frac{l_{max} + x_{min,calc} - l_{SA} + l_{FATO}}{l_{FATO} + x_{min,calc}} \right\rfloor \tag{3.22}$$

If there is enough space in direction l_{min} of the area for a second row, $n_{Pads,long}$ is multiplied by two to calculate the total number of pads. For the linear topology the direction of the approach and departure lines can not be alternated, because it is not allowed to fly over gates. In the last step, to ensure that the required area matches the existing area, the number of units out of pads and gates is reduced until the required area is less than or equal to the existing area.

3.3.3.4 Pier Topology

The pier topology is the only topology that explicitly requires taxiways. Thus, the ratios of pad to taxiway and also gate to taxiway play an important role in the calculation of the configurations. The ratio of gate to taxiway primarily influences the length of the taxiway. For the actual arrangement of the pads, the ratio of pad to taxiway plays a more important role, because it determines how many pads share a taxiway net. In the context of this work, only the ratio of one pad to one taxiway and two pads to one taxiway is considered. As for the single and satellite topologies, pads can be positioned in different arrangements for a ratio of one without having to consider the minimum distance x_{min}. This behaves as before for a maximum number of four pads.

If the number of four pads is exceeded, the safety distances must be taken into account in both rectangular and single row arrangements (see figure 3.17). Therefore $x_{min,calc}$ must be calculated as already known. Note that the type of taxiing, whether ground or hover, affects the length of the distance, since in hover mode the taxiway must be wider. Therefore, for the calculation of the number of pads in single row configuration $x_{min,calc}$ is calculated as follows.

$$x_{min,calc} = max(x_{min}; 2 * (l_{GS} + x_{hover}) + 2l_{GS} + l_{TW,width}) \tag{3.23}$$

In this context, x_{hover} represents the distance between the outer edge of the taxiway and the FATO.

$$x_{hover} = \frac{l_{TW,width} - l_{FATO}}{2} \tag{3.24}$$

If it is possible to have more than one unit consisting of pads and gates in l_{min} as for

the other topologies $x_{min,calc}$ has to be calculated differently and is

$$x_{min,calc} = max(x_{min}; 2 * (l_{GS} + x_{hover})) \tag{3.25}$$

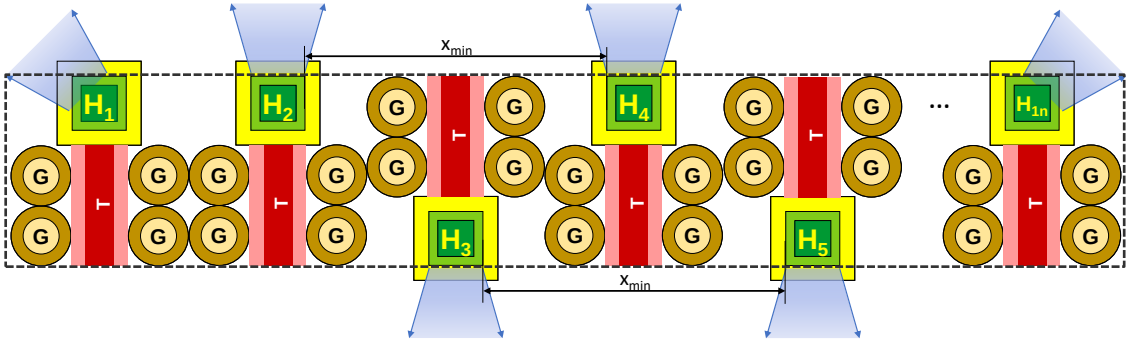

Figure 3.17: Configuration pier topology with $gate2pad$ ratio of n_{pads} one line

For the single row arrangement, this results in two formulas for calculating the length l_{width} that $n_{pads,long}$ need to be placed. For an odd number of pads applies,

$$\begin{aligned} l_{width} = (6l_{GS} + 4l_{TW,width} + 2x_{hover}) + x_{min,calc} * \left\lceil \frac{n_{Pads,long} - 4}{2} \right\rceil \\ + l_{FATO} \left(\left\lceil \frac{n_{Pads,long} - 4}{2} \right\rceil - 1 \right) \end{aligned} \tag{3.26}$$

and for an even number

$$\begin{aligned} l_{width} = (6l_{GS} + 4l_{TW,width} + 2x_{hover}) + x_{min,calc} * \left\lceil \frac{n_{Pads,long} - 4}{2} \right\rceil \\ + l_{FATO} \left(\left\lceil \frac{n_{Pads,long} - 4}{2} \right\rceil - 1 \right) + \frac{l_{FATO} + x_{min.calc}}{2} \end{aligned} \tag{3.27}$$

As for the single and satellite topologies, the number of pads is increased as long as the condition $l_{width} \geq l_{max}$ is met. If more than one row is possible, the number of pads

is calculated as follows:

$$\begin{aligned} l_{max} \geq\ & 2 * (l_{GS} + l_{FATO} + x_{hover}) + x_{min,calc}(n_{Pads,long} - 1) \\ & + l_{FATO}(n_{Pads,long} - 2) \\ l_{max} \geq\ & 2 * (l_{GS} + x_{hover}) + n_{Pads,long}(x_{min,calc} + l_{FATO}) - x_{min,calc} \end{aligned} \tag{3.28}$$

$$n_{Pads,long} = \left\lfloor \frac{l_{max} - 2 * (l_{GS} + x_{hover}) + x_{min,calc}}{l_{FATO} + x_{min,calc}} \right\rfloor \tag{3.29}$$

If the number of placeable pad gate units exceeds two $n_{Pads,short}$ is calculated as follows:

$$n_{Pads,short} = 3 + \left\lfloor \frac{l_{min} - 2 * max(l_{FATO} + x_{min}; l_{unit,height} + l_{GS} + x_{hover}) - l_{FATO}}{l_{FATO} + x_{min,calc}} \right\rfloor \tag{3.30}$$

In the calculation, $l_{unit,height}$ represents the height of a pier unit (see figure 3.11), or the minimum distance that must be maintained in order not to cause overlaps in the placement of pads along l_{min} with those along l_{max}.

$$l_{unit,height} = l_{FATO} + \frac{l_{SA} - l_{FATO}}{2} + l_{GS} * \lceil gate2pad * taxi2gate \rceil \tag{3.31}$$

If the configuration has a pad to taxiway ratio of two, the calculation must also be adjusted. In this case, two basic units are distinguished, see figure 3.18. Due to this fact, pads can only be placed in groups of two. For the type of unit seen in figure 3.18a there is the possibility to position them in a single row, therefore the number of pads would be calculated as follows:

$$n_{units} = \left\lfloor \frac{l_{max} + x_{min,calc} - 2 * (l_{GS} + x_{hover})}{l_{FATO} + x_{min,calc}} \right\rfloor \tag{3.32}$$

$$n_{Pads} = 2n_{units} \tag{3.33}$$

The configuration shown in figure 3.18b can also be accommodated in a single row, but is not as efficient in terms of the space required. Therefore, the number of pads

along l_{max} for more than three units is calculated as follows:

$$n_{units,long} = \left\lfloor \frac{l_{max} - 2 * (l_{GS} + x_{hover}) - 3 * (x_{min,calc} + l_{FATO})}{2 * (l_{FATO} + x_{min,calc})} \right\rfloor \tag{3.34}$$

$$n_{Pads,long} = 2n_{units,long} \tag{3.35}$$

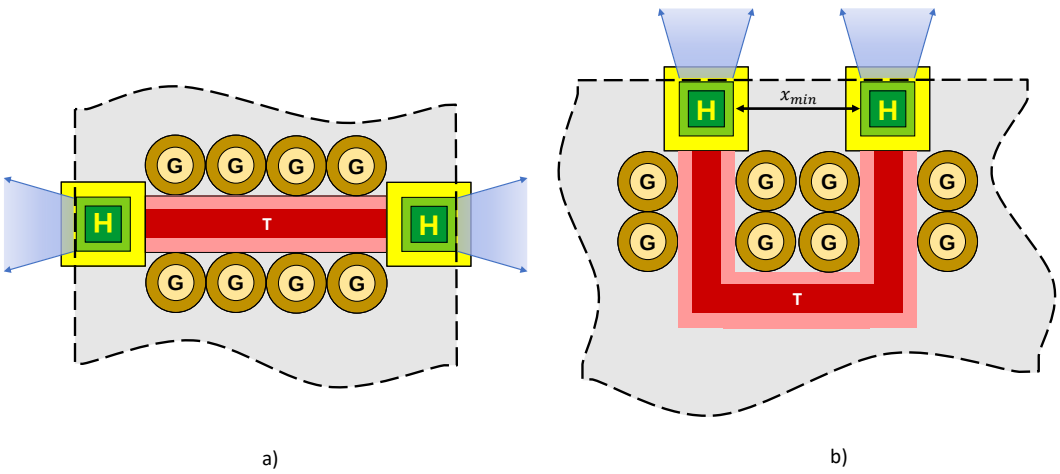

Figure 3.18: Configuration pier topology with $pad2taxi$ of two

To determine the number of pads along the short side l_{min}, the height of one unit must be determined. As can be seen in figure 3.11, two possibilities of the taxiway arrangement can be distinguished. On the one hand, if the number of gates is odd or the $taxi2gate$ ratio is one, the connecting taxiway can be positioned between the two pads, see figure 3.11a. Otherwise, it must be "attached", see figure 3.11b. The height of the unit is calculated in the first case the same way as in equation 3.36.

In the second case, the height of the unit corresponds to:

$$l_{unit,height} = l_{FATO} + \frac{l_{SA} - l_{FATO}}{2} + l_{GS} * \lceil gate2pad * taxi2gate \rceil + l_{TW,width} \tag{3.36}$$

The number of pads along the short side of the face can be calculated for more than

three units using equation 3.36.

$$n_{units,short} = 3 + \left\lfloor \frac{l_{min} - (x_{min,calc} + 2l_{FATO}}{2l_{FATO} + 2x_{min,calc}} - \frac{2 * max(l_{FATO} + x_{min}; l_{unit,height} + l_{GS} + x_{hover})}{2l_{FATO} + 2x_{min,calc}} \right\rfloor \tag{3.37}$$

$$n_{Pads,short} = 2n_{units,short} \tag{3.38}$$

Depending on $n_{Pads,short}$ and $n_{Pads,long}$ the total number of pads can now be determined. Accordingly, this is calculated as follows:

$$n_{Pads} = n_{Pads,short} * n_{Pads,long} \qquad for\ n_{Pads,short} < 3 \tag{3.39}$$

$$n_{Pads} = 2 * ((n_{Pads,short} - 2 * pad2taxi) + n_{Pads,long}) \qquad for\ n_{Pads,short} \geq 3 \tag{3.40}$$

3.3.4 Inputs and Outputs

In the following, the in and outputs of the method just described are presented. Beginning with the inputs. In the following table the input variables, which are stored in the parameter file, are presented with a description.

Table 3.2: Inputs stored in parameter file for area to throughput method

variable	description
Parameter ID	The parameter ID is the identifier by which the different parameter combinations can be distinguished.
unit	Here by entering 'ft' or 'm' it is indicated whether the following measurements are given in feet or meters.
l_{TTS}	The TTS of the vehicle under investigation is specified here. The dimension is to be given in the unit as specified under the input 'unit'.
l_{MD}	The MD of the vehicle under investigation is specified here. The dimension is to be given in the unit as specified under the input 'unit'.
$n_{passengers}$	The passenger capacity of the vehicle under investigation is specified here.

variable	description
x_{min}	Here the minimum distance between two pads is specified to allow parallel operation. The dimension is to be given in the unit as specified under the input 'unit'.
taximode	For the taximode there are two choices ('hover' and 'ground') depending on how the taxiing process should be done on the planned vertiport.
car parking	By setting this variable to 'true', parking spaces in the given area will be taken into account. If the variable is set to 'false', it will be calculated how many parking spaces are needed for the achieved passenger throughput as parking decks below the given area.
modeshare	The modeshare refers to the percentage of people who reach the vertiport with their own car and therefore need a parking space.
$t_{landing}$	This variable specifies how long a landing process takes. The time must be specified in seconds.
$t_{takeoff}$	This variable specifies how long a take-off process requires. The time must be specified in seconds.
$t_{prepare4taxi}$	This variable specifies the time that the vehicle needs after landing to initialize the taxiing process. The time must be specified in seconds.
$t_{prepare4takeoff}$	This variable specifies the time that the vehicle needs to initialize the take-off after taxiing. The time must be specified in seconds.
v_{taxi}	This variable indicates the speed at which the vehicles move along the taxiway. The speed must be specified in meters per second.
$t_{turn,fix}$	Here is specified how much time should be considered for the fixed turnaround time. So how long the loading, security checks, maintainance etc. need. The time is to be specified in seconds.
$t_{turn,passenger}$	The time specified here indicates how long it takes per passenger for the boarding or deboarding process to take place. The time is to be specified in seconds.

variable	description
$taxi2gate$	This ratio specifies how many gates per taxiway section are to be considered in the pier topology. It is the choice between the values 0.5, if two gates meet a taxiway section or one, if one gate meets a taxiway section.
$pad2taxi$	This ratio specifies how many pads share a taxiway in the pier topology. It is currently possible to choose between one and two.

In addition to the input variables just shown, a surface must also be fed in as an input parameter. The surfaces are read in as polygons. The coordinates of the polygon are read out for a real area with the help of QGIS [108] in the cartesian Gauss-Krüger coordinate system (EPSG). In the case of self-created areas, it should be noted that the coordinates of the individual points of the polygon are specified in meters. Table 3.3 shows how the csv-file containing the area must be structured. The name of the csv-file acts as the ID of the area.

Table 3.3: Structure of the area file for a square with side length of 10 meters

ID	x-coordinate	y-coordinate
1	0	0
2	0	10
3	10	10
4	10	0

After running the program, an output file is generated that contains the data listed in table 3.4.

Table 3.4: Outputs stored in results file for area to throughput method

value	description
Parameter ID	The parameter ID is the identifier by which the applied parameter combination can be distinguished.
Area ID	The area ID is the identifier by which the used area can be distinguished.
unit	Here the unit in which the length measurements are given is specified. Currently, the values are always given in meters.
l_{TTS}	The TTS of the examined vehicle is specified here. The dimension is given in the unit specified under the parameter 'unit'.
l_{MD}	The MD of the examined vehicle is specified here. The dimensions are given in the unit specified under the parameter 'unit'.
A_{total}	The total area of the studied area is given here in square meters.
l_{max}	Here the maximum extension of the examined area is given. The dimension is given in meters.
topology	This parameter specifies the topology for which the results were obtained. This parameter can take the values: 'single', 'linear', 'satellite' and 'pier'.
n_{Pads}	Here the number of pads needed for the determined layout is specified.
n_{Gates}	Here the number of gates needed for the determined layout is specified.
throughput vehicle	The hourly vehicle throughput as specified by the given input parameters and the determined vertiport design is given here.
throughput passengers	The hourly passenger throughput as specified by the given input parameters and the determined vertiport design is given here.
bottleneck	This specifies which element of the vertiport represents the opperational bottleneck.
gate2pad satellite_corner	The gate to pad ratio for corner units in the satellite topology is specified here.

value	description
gate2pad satellite_middle	The gate to pad ratio for middle units in the satellite topology is specified here.
gate2pad linear	The gate to pad ratio for the linear topology is specified here.
gate2pad pier	The gate to pad ratio for the pier topology is specified here.
$A_{parking}$	Specifies the area allocated to parking spaces in square meters.
$n_{parking,spots}$	Specifies how many parking spaces are required for the created design.
$n_{parking,decks}$	Specifies how many parking decks are needed to place the determined number of parking spaces. If the parking spaces are to be placed on the analyzed area, this parameter takes the value zero.
taxi mode	Here is specified for which taximode the vertiport was designed.
$A_{airfield}$	Here the size of the area required for the placement of the vertiport components for the specified design is shown in square meters.
A_{used}	Here is indicated how large the used area is. That is the sum of $A_{airfield}$ and $A_{parking}$. If the parking spaces were planned in the form of parkdecks, then $A_{parking}$ takes the value zero.
A_{unused}	This indicates the size of the area to which no specific use is attributed and which is therefore categorized as unused.

3.4 Graphical User Interface for Layout Design

In order to visualize the results of the area to throughput approach, a graphical user interface (GUI) has been created. This GUI uses Microsoft Publisher as an interface and was programmed in Visual Basic (VBA). As input for the GUI serve the results, which emerge from the area to throughput tool, as well as the associated input variables. After reading in the result file to be visualized, step-by-step the creation of the result sheet which can be seen in figure 3.19 takes place.

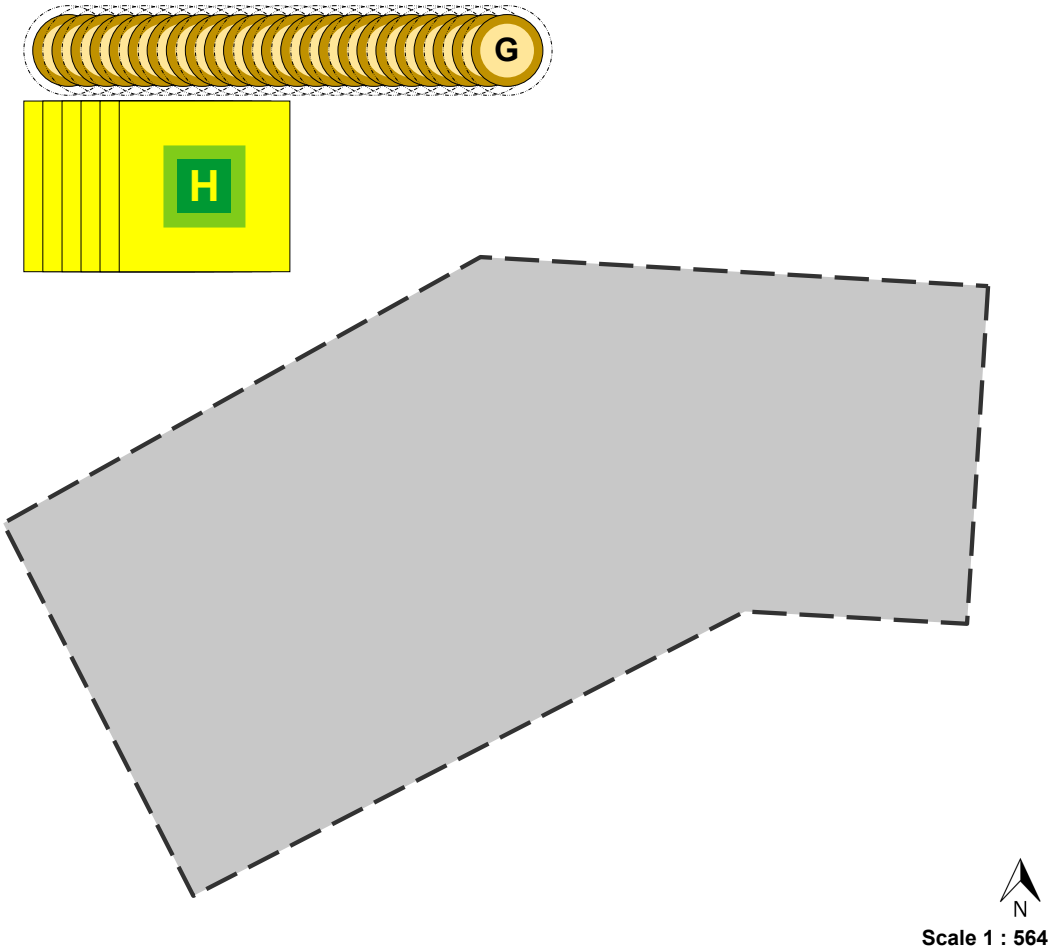

For the area 'BER_Tempelhof_31468', based on the given parameters 'P01' out of Parameterset_Real_World_Scenario a maximum VTOL throughput of 135 vehicles per hour was determined. This corresponds to 270 passengers per hour. Under the given parameters, a satellite topology is recommended. The gates represent the limiting factor for the throughput. For corner pads a gate2pad ratio of 4 and for middle pads one of 4 is applied. To achieve the given throughput, it is assumed that the required 54 car parking spaces for this configuration are placed on 1 parking deck(s) over an area of 1025 square meters below the given area.

Figure 3.19: Output sheet of GUI before placing elements

As the first step the GUI asks for the language in which the results should be presented. It is possible to choose between the languages German and English. In addition, in the VBA macro must be indicated which parameter set is to be visualized.

If these inputs are made, the visualization is built up step by step. In the first step the examined surface is plotted. The dimensions of the area are already scaled down before plotting. This means that the dimensions for the area, given in meters, are taken

as centimeters, and reduced by a factor of five. Accordingly, there is a scale of 1:500. This is done in order to be able to place the areas on a sheet of the format DIN A4. Since the VBA macro works with the unit pt and not in cm, a further conversion takes place. One cm corresponds to about 28.3464566929 pt. If the area is nevertheless too wide or long to be placed on a page of the size DIN A4, the scale is adjusted so that this becomes possible. In addition, the surface is moved to the coordinate origin an centered on the page. Since the coordinates of the area polygon are already given in the EPSG coordinate system, no further transformation is necessary here. The scale and a north arrow are positioned to the right under the plotted area (see figure 3.19).

Next, the other elements are plotted using the previously determined scale. These include pads, gates and parking spaces. Their dimensions are taken from the input variables. The individual elements are also color coded to distinguish their individual components, such as FATO, TLOF and SA for a pad.

If the critical case occurs that the number of pads exceeds a predefined quantity, a notification box is plotted (see figure 3.20). This informs that the critical maximum of pads for visualization has been exceeded and indicates the number of each component for the design proposal.

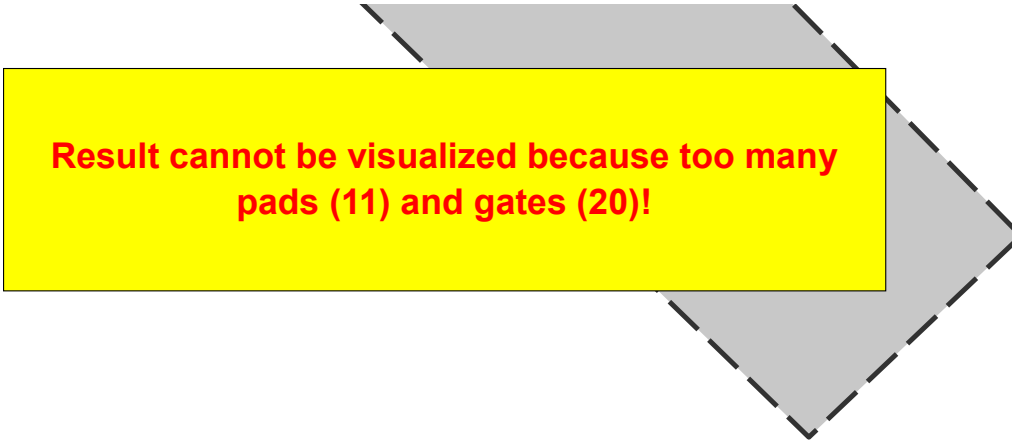

Figure 3.20: Notification box when number of pads is exceeded

In the last step, a text field is placed that contains the core information about the design proposal. These are the area and parameter identification numbers, the name of the selected parameter set, the topology, the bottleneck, and the projected through-

puts for passengers and vehicles, aswell as informations about the gate to pad ratio and the parking situation (see figure 3.19).

A new page is then generated on which the next design suggestion is visualized. This process is repeated until all results for the selected parameter set have been evaluated.

At the current stage of development, automated positioning of components on the surface according to the defined design specifications is not yet possible, so this must be done manually. The positioning is possible by drag and drop. After successful placement of the pads and gates, it is possible to read out their position in relation to the surface and save it in a csv-file. The reading of these positions is automated. First, it is determined which geometries are pads and gates. Then a table is generated in which the x-coordinates and y-coordinates of the center point and the type of component are stored. After reading out the coordinates, they are converted back to the original scale and the table is saved as a csv-file. The structure of the file can be seen as an example in table 3.5.

Table 3.5: Output of center-position extraction for elements out of GUI

x-coordinate	y-coordinate	element
22	34	pad
40	50	gate
10	10	gate

3.5 Throughput to Area Method

As explained earlier, the 'Throughput to Area' method provides the required size of an area and its dimensions to achieve a given throughput. Moreover, it suggests which topology is best suited to achieve this throughput. In addition to the throughput, factors such as the selected vehicle type or even desired safety distances of the individual pads have an impact on the resulting area size. In the following, the model with its assumptions and simplifications is presented and its implementation and in-

and outputs are displayed.

3.5.1 Model

The purpose of the throughput to area model is to determine how a given throughput can be achieved given a set of constraints. In abstract terms, the throughput to area model is the counterpart to the area to throughput model. As in the previously presented model, the approach is an optimization problem. The goal is to find the smallest possible area that can serve a given throughput. Here, the constraints to be met include the design standards specified by the FAA [71]. In addition, the specifications of the four predefined topologies must be met.

Within the framework of this model, there are also some limitations that had to be made in order not to exceed the scope of this work. Firstly, only rectangular shapes are assumed when determining the area. This means that for example any circular ones that might achieve a higher throughput per area unit are not considered. However, it is assumed that this is a valid simplification, since vertiports will be built on building roofs, especially in urban environments, and thus will mostly have a square footprint. In addition, pads with their fixed $gate2pad$ ratio are considered as units, so for a satellite topology with a $gate2pad$ ratio of three, a unit would consist of one pad and three gates. In contrast to the area to throughput model, the ratio of gate to pad is not searched for, which generates the best value in the area to throughput ratio, but an 'optimal' ratio is assumed in which the pad represents the bottleneck. Furthermore, the vertiport is designed as a closed or isolated system and, accordingly, without interaction with its environment. This means that the environment is not taken into account. For the throughput this means that there is always a $100\ \%$ utilization without delays and for the dimensioning neither surrounding buildings nor wind conditions are considered.

3.5.2 Implementation

The implementation of the previously presented model is done in MATLAB and is performed by means of a mainfile. The central component of the mainfile is the function

that generates the layout for each topology based on the given throughput and from this returns the needed area to achieve this throughput.

After starting the code, the user can choose between two modes to run the code. On the one hand, the standard mode can be selected, which provides a fixed set of parameters for dimensioning and opens an input field in which the desired throughput per hour is to be entered. On the other hand, the professional mode can be selected, which allows the user to define the parameter values in a previously created Excel file and thus to run through several configurations in one run. The user is then prompted to select the vehicles for which the surface is to be calculated from a list. It is also possible to select which of the four known topologies should be taken into account. In the current version the vehicles listed in the following table 3.6 with the associated dimensions are available for selection.

Table 3.6: Vehicles implemented in the throughput to area approach

Vehicle	Nr. of Passengers [a]	TTS	MD
eHang [113]	2	5.61 m	5.61 m
CityAirbus [113]	5	8.00 m	8.00 m
Airbus Vahana [44]	2	6.25 m	6.25 m
Boeing Aurora [113]	4	9.14 m	9.14 m
Lilium Jet [20]	6	11.00 m	11.00 m
Volocopter 2x [89]	2	9.15 m	9.15 m
Volocopter VC200 [44]	2	9.15 m	9.15 m
VoloCity [114]	2	11.30 m	11.30 m
Uber eCRM-004 [115]	5	15.24 m	15.24 m
Joby S4 [89]	5	10.40 m	10.40 m
Cora Kitty Hawk [89]	2	11.00 m	11.00 m
AeroMobil 3.0 [116]	2	2.24 m	6.00 m

[a] The number of passengers always corresponds to the total number of seats, regardless of whether the vehicle can fly autonomously or not.

After successful input of the variables these are run through in the context of a loop and the associated results are stored in csv-files. First the different parameters are

run through. For each parameter set, each vehicle and for each vehicle, each of the selected topologies is examined. In this context the function is initialized, which outputs the necessary dimensions of the surface for the desired throughput based on the parameter set, the selected vehicle and the topology. The structural design of the function can be seen in figure 3.21.

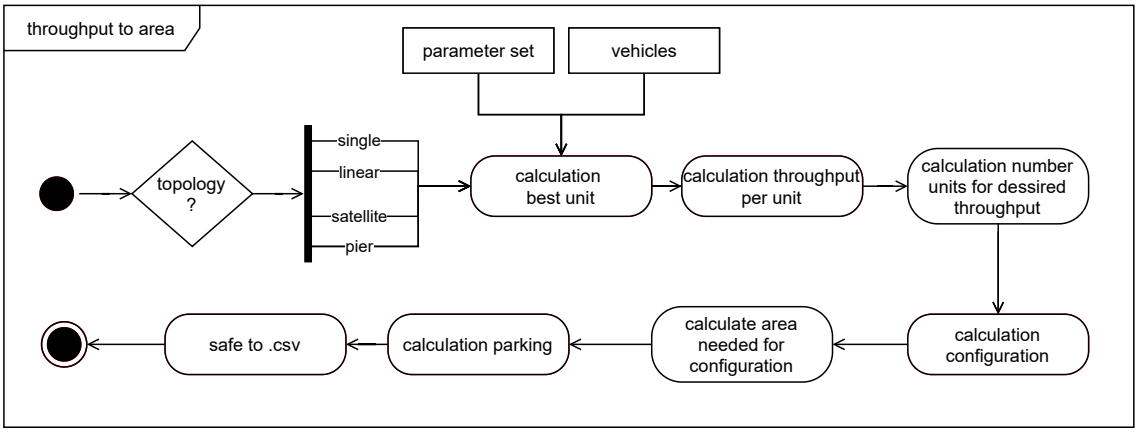

Figure 3.21: Flowchart throughput to area approach

As part of the function, the 'optimal' ratio of gates to pads is first calculated. This is done by assuming an initial ratio of one, which is increased until the bottleneck is the pad. Based on the resulting unit of the topology, the throughput of this unit is calculated, using the same function as presented in section 3.3.2.3. Subsequently, it is determined how many of these units are needed to achieve the desired throughput. It can happen that a higher throughput than the desired throughput is achieved, because as already explained each unit is a fixed constellation of pads and gates and splitting of the units into fragments is not realistic. With this number of required units, the configurations already known from section 3.3.3 are determined in dependence of the input parameters and abstracted from it how large the required area is and which outer dimensions it needs, in order to guarantee the safety distances between the pads. However, only two-row configurations are considered, since these are the ones that take up the least space and this is the goal of the optimization. Afterwards, the number of parking spaces and the area required for them are calculated for the desired throughput. These results are all saved in the form of a csv-file.

3.5.3 Inputs and Outputs

In the following, the in and outputs of the method just described are presented. Beginning with the inputs. In the following table 3.7 the input variables, which are stored in the parameter file, are presented with a description. It can be seen that the input variables are similar to those of the area to throughput method. However, it should be noted that in this method the vehicle properties are not read in via the parameter file, but are loaded separately via the vehicle list already presented in table 3.6. The biggest difference, however, is that instead of an area, the desired throughput has to be specified. Furthermore the variable 'car parking' is omitted, since the option is not available to consider parking spaces on the plan area.

Table 3.7: Inputs stored in parameter file for throughput to area method

variable	description
Parameter ID	The parameter ID is the identifier by which the different parameter combinations can be distinguished.
throughput	The desired hourly throughput that the user wants to achieve must be specified here. It should be noted that throughput in this method always means passenger throughput.
x_{min}	Here the minimum distance between two pads is specified to allow parallel operation. The dimension is to be given in meters.
taximode	For the taximode there are two choices ('hover' and 'ground') depending on how the taxiing process should be done on the planned vertiport.
modeshare	The modeshare refers to the percentage of people who reach the vertiport with their own car and therefore need a parking space.
$t_{landing}$	This variable specifies how long a landing process takes. The time must be specified in seconds.
$t_{takeoff}$	This variable specifies how long a take-off process requires. The time must be specified in seconds.

variable	description
$t_{prepare4taxi}$	This variable specifies the time that the vehicle needs after landing to initialize the taxiing process. The time must be specified in seconds.
$t_{prepare4takeoff}$	This variable specifies the time that the vehicle needs to initialize the take-off after taxiing. The time must be specified in seconds.
v_{taxi}	This variable indicates the speed at which the vehicles move along the taxiway. The speed must be specified in meters per second.
$t_{turn,fix}$	Here is specified how much time should be considered for the fixed turnaround time. So how long the loading, security checks, maintainance etc. need. The time is to be specified in seconds.
$t_{turn,passenger}$	The time specified here indicates how long it takes per passenger for the boarding or deboarding process to take place. The time is to be specified in seconds.
$taxi2gate$	This ratio specifies how many gates per taxiway section are to be considered in the pier topology. It is the choice between the values 0.5, if two gates meet a taxiway section or one, if one gate meets a taxiway section.
$pad2taxi$	This ratio specifies how many pads share a taxiway in the pier topology. It is currently possible to choose between one and two.

After running the program, an output file is generated that contains the data listed in table 3.8.

Table 3.8: Outputs stored in results file for area to throughput method

value	description
Parameter ID	The parameter ID is the identifier by which the applied parameter combination can be distinguished.
topology	This parameter specifies the topology for which the results were obtained. This parameter can take the values: 'single', 'linear', 'satellite' and 'pier'.

value	description
vehicle	The name of the vehicle for which the calculations were made is listed here.
l_{TTS}	The TTS of the examined vehicle is specified here. The dimension is given in meters.
l_{MD}	The MD of the examined vehicle is specified here. The dimension is given in meters.
n_{seats}	The passenger capacity of the examined vehicle is specified here.
A_{total}	The total area required to achieve the stated hourly passenger throughput is given here in square meters.
area height	Here, the height of the area required to achieve the desired passenger throughput is specified. The specification is made in meters.
area width	Here, the width of the area required to achieve the desired passenger throughput is specified. The specification is made in meters.
given throughput	The throughput desired by the user is specified here.
calculated throughput	Here you can see the calculated throughput. This throughput is usually higher than the desired throughput. An exact achievement of the desired throughput is often not possible due to the design of the vertiport with fixed pad/gate units.
n_{Pads}	Here the number of pads needed for the determined layout is specified.
n_{Gates}	Here the number of gates needed for the determined layout is specified.
$A_{parking}$	Specifies the area allocated to parking spaces in square meters.
$n_{parking,spots}$	Specifies how many parking spaces are required for the dessired throughput.

4 Results and Discussion

In the following chapter, the results obtained for the studies with the developed tools are presented and analysed. Starting with the results from the 'Area to Throughput' approach and followed by the results from the 'Throughput to Area' approach.

4.1 Area to Throughput

In the following, the results obtained from three studies conducted with the 'Area to Throughput' approach are presented.

4.1.1 Study with version one

This study was conducted using the first version of the area to throughput tool presented in section 3.2.1. The goal of the study was to get a feeling for which areas and vehicles have the highest throughputs and which topology to choose.

4.1.1.1 Experimental Setup

In order to conduct the study, the following vehicles were varied (see table 4.1).

Table 4.1: Vehicles considered for study of the area to throughput approach

Vehicle	Nr. of Passengers [a]	TTS	MD
eHang [113]	2	5.61 m	5.61 m
CityAirbus [113]	5	8.00 m	8.00 m
Boeing Aurora [113]	4	9.14 m	9.14 m
Lilium Jet [20]	6	11.00 m	11.00 m
VoloCity [114]	2	11.30 m	11.30 m
Uber eCRM-004 [115]	5	15.24 m	15.24 m

[a] The number of passengers always corresponds to the total number of seats, regardless of whether the vehicle can fly autonomously or not.

Regarding the parameters, it should be said that fixed values were assumed here and only the areas were varied. For the investigation 964 rectangular surfaces were used, which have an area of 2000 to 50000 m^2 and which consist of four side ratios. The

aspect ratios were from one to one, one to two, one to three and two to three. The other parameters are shown in the table below.

Table 4.2: Parameters for study with version one of the area to throughput approach

Parameter	Value	Unit
$t_{T\&L}$	60	s
t_{turn}	5	min
t_{taxi}	15	s
Taximode	hover	-
$pad2taxi_{satellite}$	2	-
$pad2taxi_{linear}$	1.5	-
$pad2taxi$	1	-
$taxi2gate$	0.5	-
bottleneck	pad	-
Topology	single; satellite; linear; pier;	-

As already can be seen, for this study fixed gate to pad ratios are given for the satellite and linear topology and for the pier topology the number of gates is chosen so that the pad represents the bottleneck. Likewise, the turnaround time as well as the taxi time assumes the same value for all constellations. In the following, the results of the study are presented.

4.1.1.2 Results

First, the throughputs achieved by the different vehicles are examined. For this purpose, the hourly passenger throughputs of the six vehicles have been plotted in the following figure 4.1. Along the y-axis, the hourly passenger throughput per square meter is plotted and along the x-axis the size of the area for which the throughput was achieved. The different vehicles are color coded.

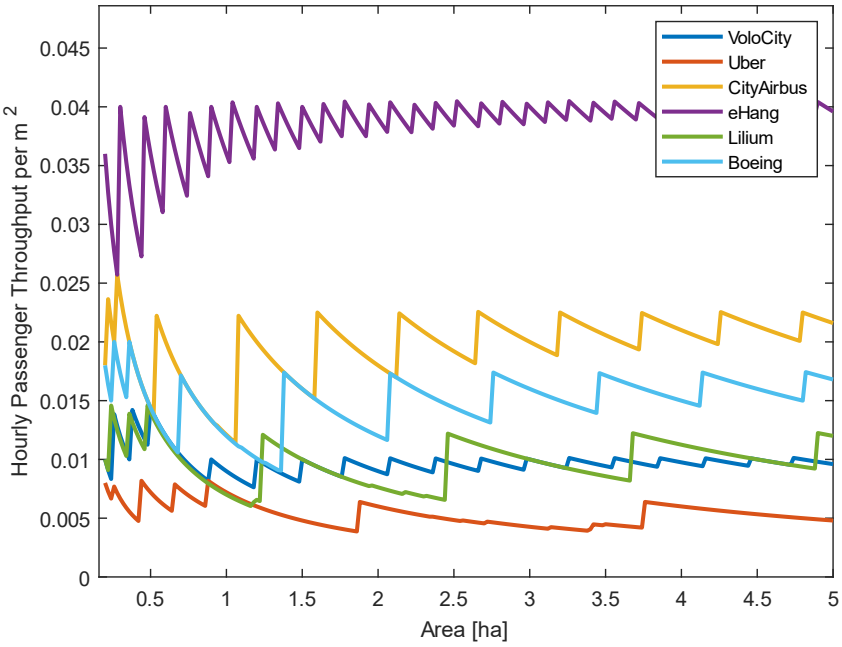

Figure 4.1: Throughput for different vehicles out of study with version one of area to throughput approach

It can be observed that for all surfaces, the vehicle of eHang generates the largest throughputs. The vehicle is followed by that of Airbus. This shows that the throughput in this case seems to depend mainly on the size of the vehicle, since it is the smallest and second smallest vehicle. The largest vehicle that of Uber accordingly delivers the lowest throughputs. A zigzag pattern can be seen for all vehicles. This most likely stems from the fact that whenever there is enough new space for a new unit of pads and gates, the throughput increases again. Further, it can be observed that for eHang's vehicle, the hourly throughput per square meter settles at about 0.04 passengers. This is likely due to the fact that in the first version of the area to throughput method for the pier topology, there are no limits on the pads. Accordingly, they can be distributed over the entire area, but this is unrealistic because it would result in overlapping arrival and departure paths or flying over the pads, which is not allowed for safety reasons. For a realistic design, it would have to be assumed that the pads would only be placed at the edges of the areas and that, as the area increases, a larger area would have to be left free in the middle, thus reducing the throughput per square meter.

The study also investigated which topologies generate the highest throughputs. For this purpose, the following plot shows how often which topology generates the highest throughputs for each area (see figure 4.2). For the vehicle of Uber it can be seen that for small areas the single topology provides the best results. However, once the areas become larger than 0.4 ha, the satellite topology is the best choice. This continues until an area size of about 1.8 ha is reached. After that, the satellite topology is replaced by the pier topology. In the range between about 2.3 and 3.7 ha the linear topology is the best, before it is replaced by the pier topology again. With the linear topology, 'steps' can be seen in the plot, this is probably due to the shape of the surfaces. Thus the linear topology has an advantage with smaller surfaces only if these are long and with increasing size the shape of the surface plays a subordinate role, since also not more than two rows of pads are placeable in this topology.

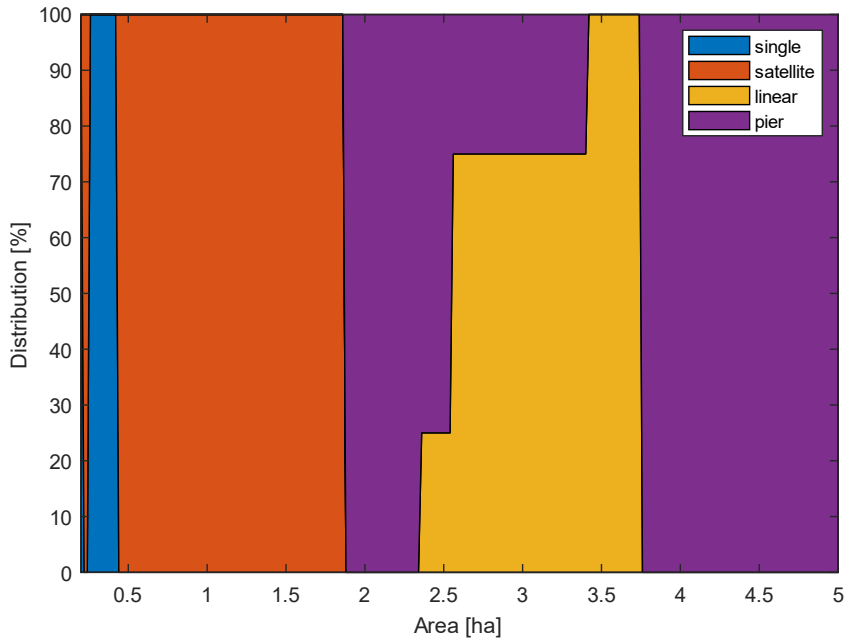

Figure 4.2: Distribution of topologies over the surface for vehicle from Uber

For a better classification of the results, the results of all vehicles have been juxtaposed in the following figure 4.3. Here it can be observed that only for the vehicle of Uber the single topology is relevant. For small areas, the satellite topology is rather preferred. From a certain size of the area, this is then replaced by the pier topology. This can be due to the limitation to a total of four satellite units per area. Accord-

ingly, it can be seen that for large areas the pier topology always provides the highest throughputs.

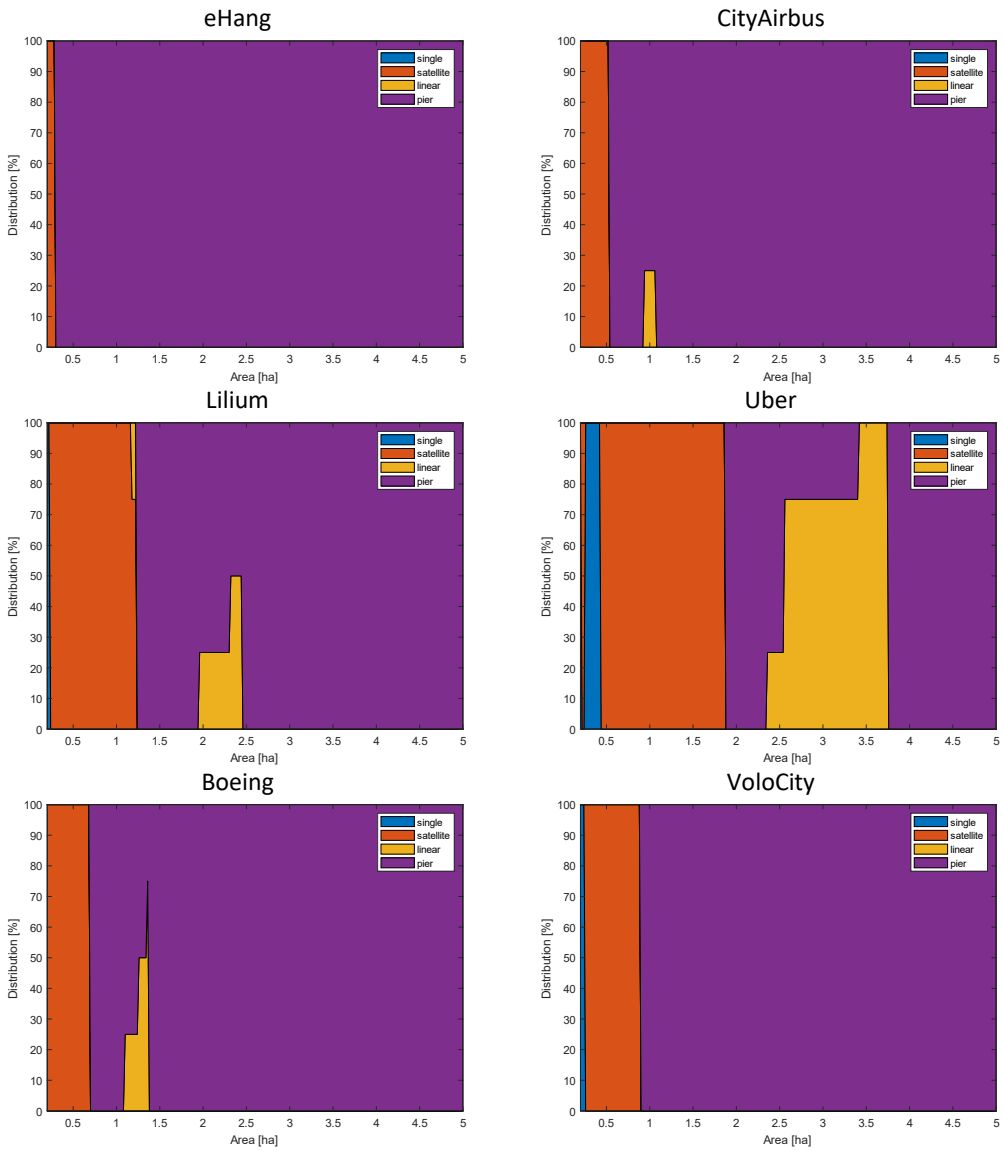

Figure 4.3: Distribution of topologies over the surface for different vehicles

However, the results are not necessarily reliable, since many parameters were not taken into account. For example, it can be assumed that the taxi process is much longer for the pier topology than for the other topologies. Furthermore, the pier topology is the only one that allows an unrestricted amount of pads per area and thus clearly is the only topology that can further increase its throughput as the area

grows. With the satellite topology, for example, as soon as there is room for four pads, a further increase in the vertiport footprint is not worth considering, since it is not allowed to place more pads and thus the generated throughput stagnates. For this and other reasons this method has been extended and in the following chapter the results obtained with this improved version are presented.

4.1.2 Study with improved version

This study was conducted using the area to throughput tool and a summary of the experimental setup can be seen in appendix B.1. The objective of the study was to obtain answers to the following research questions:

1. How does the area size and shape influence the topology selection?
2. Which topology is favorable for which area?
3. How much is the throughput dependent on the area-shape?
4. Which vehicle leads to highest throughput based on variation of turnaround times and areas?
5. What is the influence of different boarding and deboarding times depending on the vehicle?
6. How is the influence of the fixed turnaround time compared with the variable one?
7. How big is the impact of the take-off and landing time depending on the other process times and the vehicle?
8. What are the most common gate to pad ratios for each topology?
9. How do different take-off and landing times influence the vertiport layout?
10. How do different process times influence the vertiport layout?
11. What is the most common bottleneck?

4.1.2.1 Experimental Setup

To find answers to the presented research questions, the available variables were varied as in table 4.3.

Table 4.3: Parameters for study with improved version of the area to throughput approach

Parameter	Value Range	Unit	Combinations
Area (size)	200 to 50000 in steps of 200	m^2	250
Area (side ratio)	1:1; 1:2; 1:3; 2:3	m	4
Vehicle (size & passengers)	6 representative	m & $n_{passengers}$	6
x_{min}	0; 30; 61	m	3
$t_{T\&L}$	30; 60; 90	s	3
$t_{turn,passenger}$	15; 30; 60; 90	s	4
$t_{turn,fix}$	0; 5; 10; 15; 20	min	5
Taximode	hover; ground;	-	2
$t_{prepare4taxi}$	0; 5; 90	s	3
$pad2taxi$	1; 2	-	2
$taxi2gate$	0.5	-	1
Topology	single; satellite; linear; pier;	-	4
Total			25.92 million

A total of 1000 rectangular areas with different aspect ratios and sizes were generated for the study in order to investigate the effects of different parameters on the resulting throughput and the preferred topology. The areas had a size of 200 to 50000 m^2, which was increased in steps of 200 m^2. In addition, four different aspect ratios were assumed for each area size, as shown in table 4.3. The areas were assumed to be of these dimensions because they are assumed to approximate those available in an urban environment. The assumption is based on the fact that in urban environments, building on rooftops is preferred and building footprints tend to be rectangular.

In order to get an overview of which vehicles generate high throughputs, vehicles that are currently planned or already being developed were selected. The focus was on covering the widest possible range of vehicle size and passenger capacity. The vehicles considered in the study are listed in table 4.1. It is known that there are other vehicles that have the potential to go into series production for UAM operations but are not explicitly considered in the study because their dimensions and passenger numbers are similar to a vehicle already considered. The examples of Lilium Jet and Joby Aviation are worth mentioning in this context. Further it has to be noted, that the number of passengers always corresponds to the total number of seats, regardless of whether the vehicle can fly autonomously or not. The reason for this simplification is that at this point in time, and probably in the near future, none of these vehicles will perform autonomous flights with passengers. In the future, however, this may be realistic for all. Therefore, the same assumption was made for all vehicles, regardless of the current published development status, for better comparability.

Three values were varied for the minimum distance x_{min} that must be maintained between the pads for parallel operation. One is the value of 61 m specified by the FAA [71] and then two others. The other two values are based on the assumption that, due to the superior flight characteristics of eVTOLs compared to helicopters [26], these safety distances may be halved or even eliminated in the future.

Within the framework of the pier topology, the variable ratio of pad to taxiway was also varied. The distinction was made that each pad has its own taxiway or two pads share a taxiway. The ratio of gates per taxiway section was assumed to be two gates per section, as single-sided use is considered unrealistic.

In addition to the physical parameters just presented, the parameters affecting the processes on the vertiport were also varied.

The choice of take-off and landing time was assumed to be 60 s, following Vascik and Hansman [89]. In order to take into account developments in the future that do not necessarily coincide with the current assumptions, a higher and a lower take-off and landing time were assumed. For simplicity and to support the interpretability of the results, it was assumed that the take-off time and the landing time are the same.

For the time needed for a turnaround process, the fixed time as well as the turnaround time per passenger varied. As it is not yet clear how the charging of the eVTOLs at the Vertiport will take place (battery change or fast charging) or to what extent cleaning, maintenance and safety checks will have to be carried out and how long these will take accordingly, the author has varied a range of times that are considered realistic. These times range from 0 to 20 min. The turnaround time per passenger of 60 s is based on the assumptions of Guerreiro et al. [97] and again faster as well as slower times were assumed to investigate their impact on the vertiport design and the throughput to be achieved.

For the taxiing process, a distinction is made between ground and hover taxiing. This also results in different times for the preparation time required to initiate the taxiing process. In hover mode this is zero. If ground taxiing is assumed, a further distinction must be made as to whether it is passive or active. This results in two further times of 90 s in passive mode and 5 s in active mode. Despite the three modes of traction, a uniform taxi speed of 2.4 m/s is assumed, based on subject matter expert (SME) interviews provided by Zelinski [117].

In order to provide an overview that is as complete as possible, a distinction was also made between all four topologies.

The number and size of parking spaces were not considered in the context of this study. Therefore, for performance reasons, no parking spaces were assumed in the given area and the modeshare was also not varied.

In total, the variation of all parameters results in 25.92 million combinations. After selecting the topologies with the highest throughput for each parameter, 6.48 million combinations remain. These results are referred to as best results. Running the study in its entirety took about 24 hours and 35 minutes. Accordingly, 293 parameter combinations can be run through per second.

4.1.2.2 Results Research Questions on Shape of Area and Topology of Layout

The following section will present the results based on research questions one through three, which have already been presented. For the sake of clarity, the questions are

listed again here:

- How does the area size and shape influence the topology selection?
- Which topology is favorable for which area?
- How much is the throughput dependent on the area-shape?

These research questions focus on how the size and shape of the given surface affects the choice of the desirable topology. For completeness, the influence of process times and the choice of vehicle were also taken into account.To better evaluate the results, they were filtered according to the research questions. The best results were used for this investigation, since the desire is to determine under which conditions which topology provides the best results. The process time $t_{turn,fix}$ was assumed to be 0 s in this context, as this better allows to evaluate the effects of increasing turnaround times. Furthermore, the surfaces were sorted according to their aspect ratios in order to be able to assess the effect of different shapes of the surfaces. Table 4.4 provides an overview of the variables included in this study.

Table 4.4: Considered parameters for research questions on shape of area and topology of layout of the area to throughput approach

Parameter	Values	Unit
Areas	splited into the different side ratios	m^2
Vehicles	all	-
Topologies	only the best	-
$t_{turn,passenger}$	15; 30; 60; 90	s
$t_{turn,fix}$	0	min
$t_{T\&L}$	30; 60; 90	s
x_{min}	30	m
Taximode	hover	-

Different plots were created for the evaluation of the results. In this thesis, however, a selection is presented in the following to give an overview of the results. If interested, the other plots are attached to the data CD. The vehicles of eHang, Lilium and the VoloCity were selected as representative. The choice was made this way because

it covers a large spectrum. First, eHang and VoloCity have the same low passenger capacity of two, but they differ greatly in size. Lilium, on the other hand, has a relatively large passenger capacity of six, but at the same time is comparable in size to the VoloCity.

Figure 4.4 shows the results obtained for the vehicle of eHang with a surface aspect ratio of two to three and assuming that the turnaround time per passenger is 15 s and the take-off and landing time per vehicle is 30 s. Along the x-axis the different areas are plotted and along the y-axis the percentage distribution of the topologies. The different topologies are color coded. It can be seen that up to a total area of about 3 ha, the single topology generates the highest throughputs. After that it can be seen that for about half of the results the single topology dominates and for the other half the pier topology. The dominance of the single topology is most likely due to the low passenger capacity and at the same time low turnaround and take-off and landing time. Due to these circumstances, it does not make sense to construct space-consuming gates for the turnaround process, since this is completed within 60 s and, in the case of the single topology, the time for taxiing is also saved. Thus, an entire process run would be finished within 120 s and the pad would be free for the next vehicle. As already mentioned, the pier topology is also used for larger areas, since the area no longer seems to be such a critical factor and the redistribution of the turnaround processes to gates therefore has advantages without the disadvantage of having to reduce the number of pads.

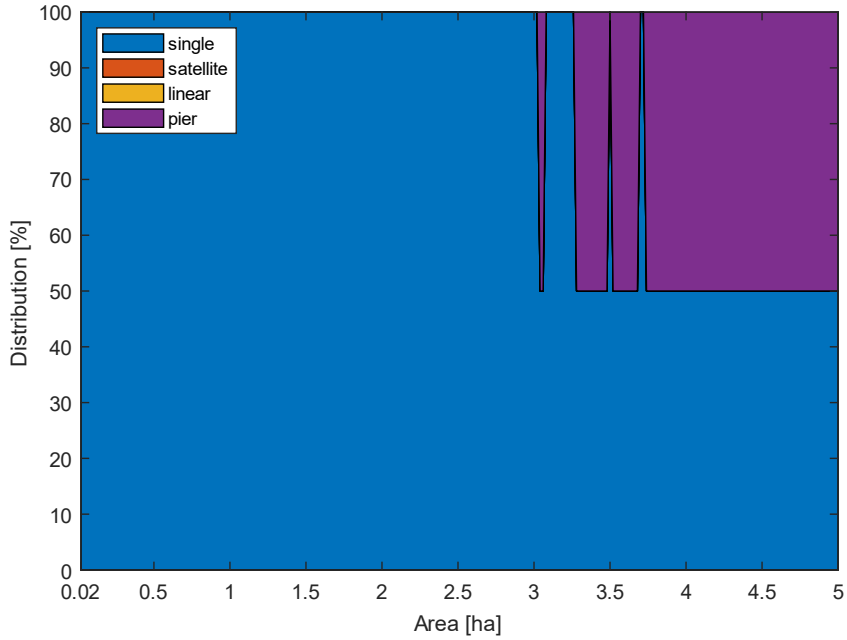

Figure 4.4: Distribution of topologies over the surface for the vehicle of eHang with side ratios of two to three and $t_{turn,passenger} = 15\ s$ and $t_{T\&L} = 30\ s$

To put the results in relation to the other vehicles, the following figure 4.5 shows the results for the three vehicles selected as representative at a $t_{turn,passenger}$ of 15 s and a $t_{T\&L}$ of 30 s. These are the shortest process times studied in each case. From top to bottom are the different aspect ratios and from left to right are the three vehicles.

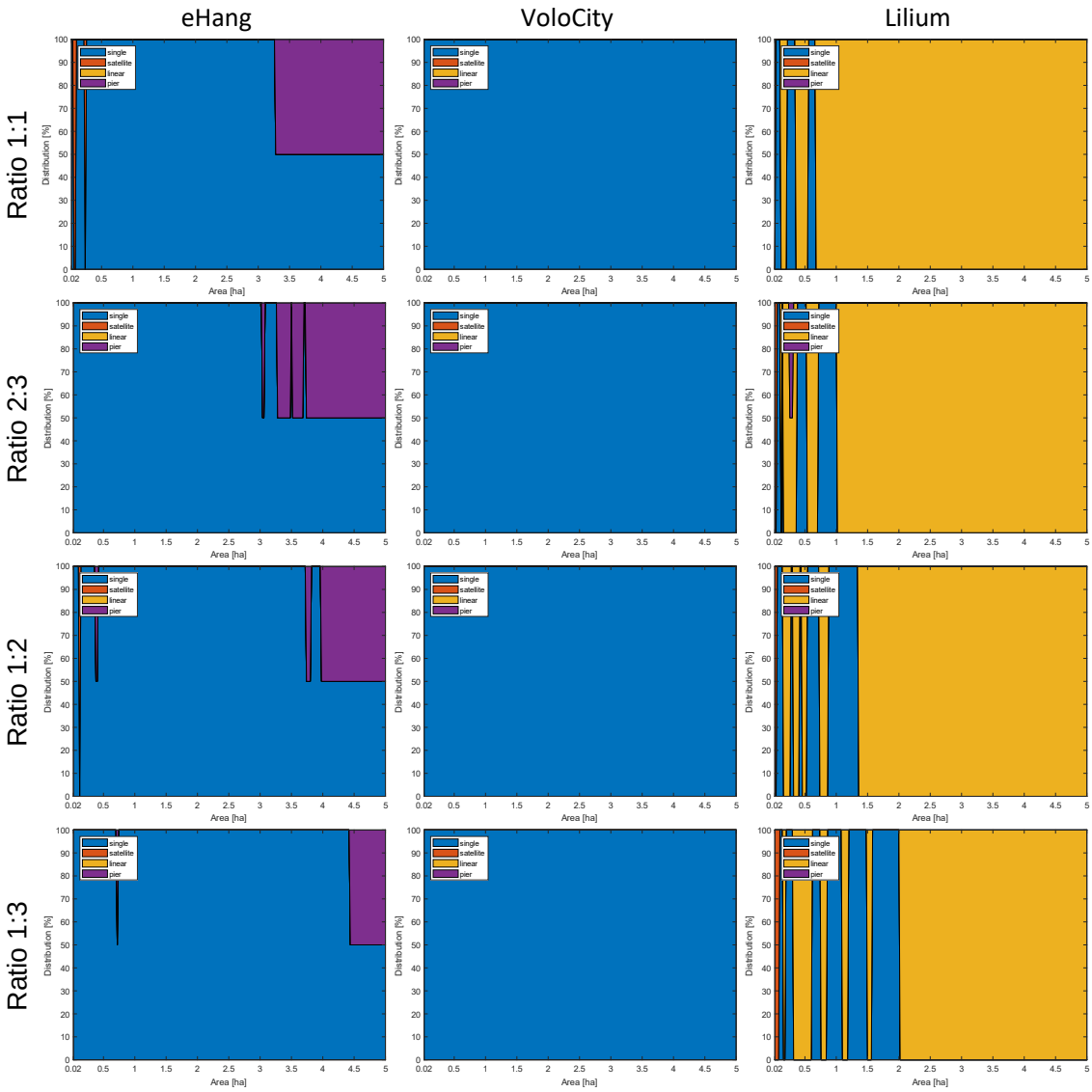

Figure 4.5: Distribution of topologies over the surface and different side ratios $t_{turn,passenger} = 15\ s$ and $t_{T\&L} = 30\ s$

It can be observed that for VoloCity the single topology is the best choice. The situation is similar for the eHang vehicle, but for larger areas the pier topology also seems to achieve good throughputs. However, as the aspect ratio increases, the use of the pier topology becomes profitable only for larger areas. At a side ratio of 1:1, the pier topology is still used for an area of 3.5 ha, and at a side ratio of 1:3 it is only used from 4.5 ha. For the Lilium Jet, on the other hand, it can be observed that primarily the linear topology has its strengths. But also the single topology has its strengths

especially for smaller areas. Surprising is to see that especially longer surfaces take over the dominance of the linear topology only from an area of 2 ha. One reason can be that the width of the surface is large enough to place a second row of the linear topology and thus it can only then unfold its full potential.

In the next figure 4.6, the $t_{T\&L}$ was increased to 90 s. Here it can be seen that the single topology now dominates for the Lilium Jet as well. It can be assumed that due to the high take-off and landing time it is more profitable to construct many take-off and landing areas and to make the turnaround directly at the pads due to the short turnaround time. It is also interesting to see that for the vehicle of eHang and the VoloCity, the increase in take-off and landing time has almost no effect on the choice of topology. The reason can be that due to the low passenger capacity and the fast $t_{turn,passenger}$, further increasing the $t_{T\&L}$ has no effect because the pad has already been the bottleneck before. And the design of the vertiport always has the pad as the core component.

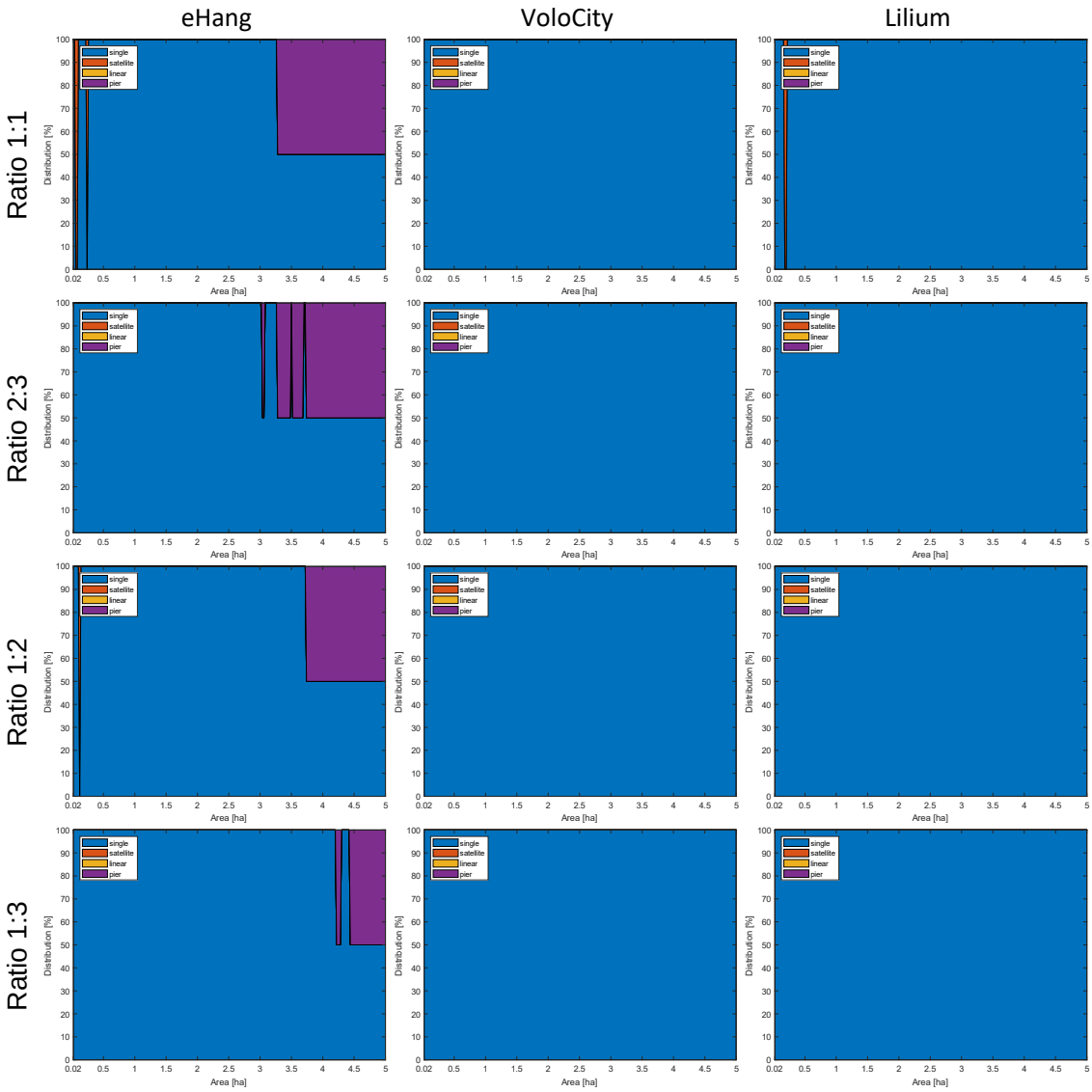

Figure 4.6: Distribution of topologies over the surface and different side ratios $t_{turn,passenger} = 15\ s$ and $t_{T\&L} = 90\ s$

When examining figure 4.7, for which the $t_{turn,passenger}$ was increased to 90 s and the $t_{T\&L}$ is again at 30 s, larger changes can be perceived. For all vehicles, it can be seen that for a square area, the satellite topology dominates from an area of about 2.2 ha at the latest. For the vehicle of eHang, the linear topology becomes more dominant for longer areas but shares the dominant position with the pier topology for larger areas. The VoloCity also has a large dominance of the linear topology. However, for smaller areas the single topology also seems to be good. For the Lilium Jet, no

clear tendency can be seen, except that the single topology is negligible. Especially for longer surfaces, there is a significant variation between the satellite, linear and pier topologies. In general, the satellite topology seems to be the best topology in comparison of the three somewhat more often.

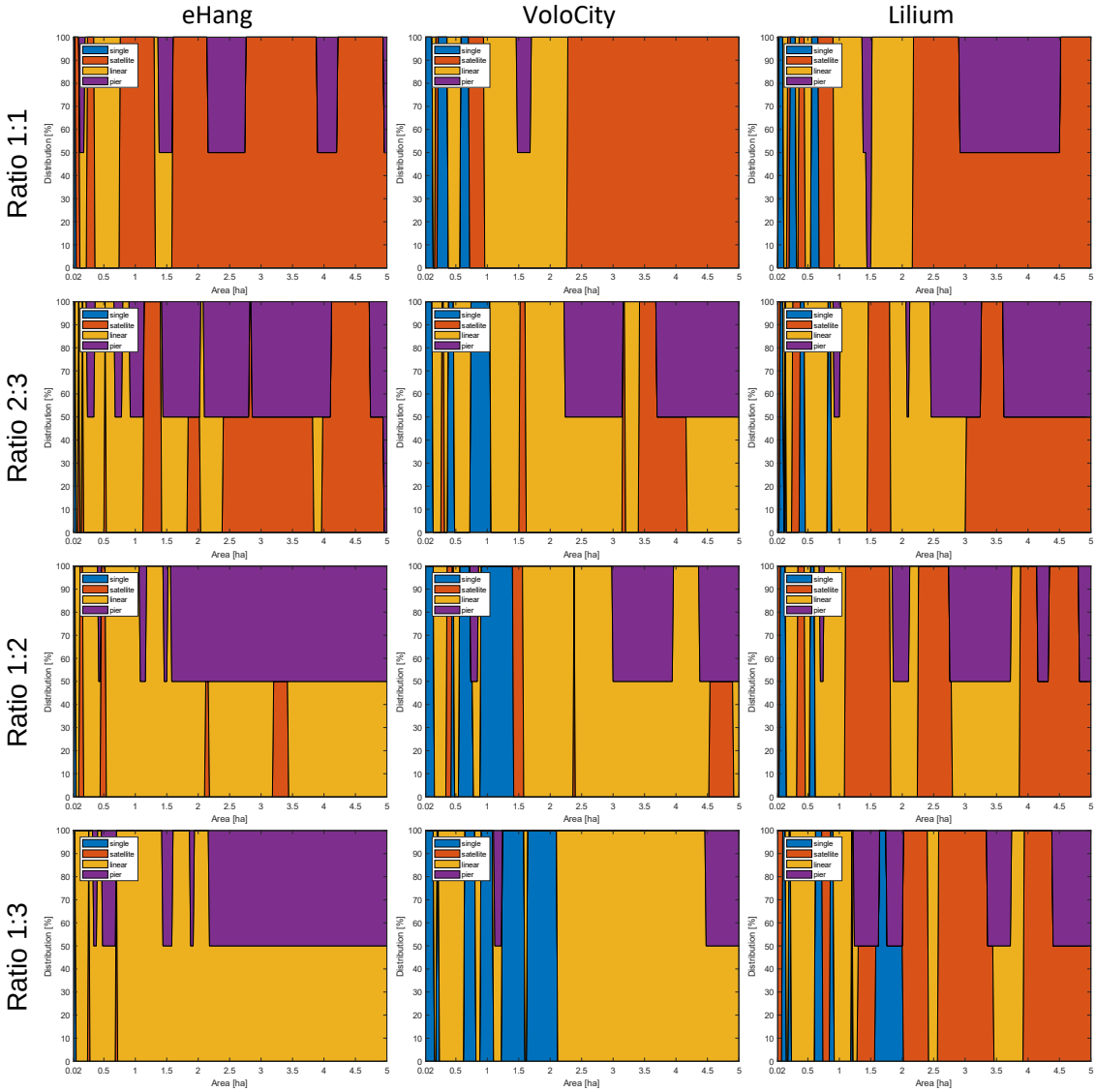

Figure 4.7: Distribution of topologies over the surface and different side ratios $t_{turn,passenger} = 90\ s$ and $t_{T\&L} = 30\ s$

In figure 4.8, a process time of 90 s is assumed for $t_{turn,passenger}$ and $t_{T\&L}$. In this case, the linear topology clearly seems to dominate for eHang and the VoloCity. For eHang it can be seen that for larger areas the pier topology also has importance, but

as the length of the area increases the importance of the pier topology decreases. For the VoloCity, a tendency towards the single topology can again be seen for small areas. For Lilium Jet, on the other hand, the single topology is negligible. In addition, large parallels to figure 4.7 can be seen. This allows the conclusion that especially the choice topology of Lilium Jet depends on $t_{turn,passenger}$ due to its high passenger capacity.

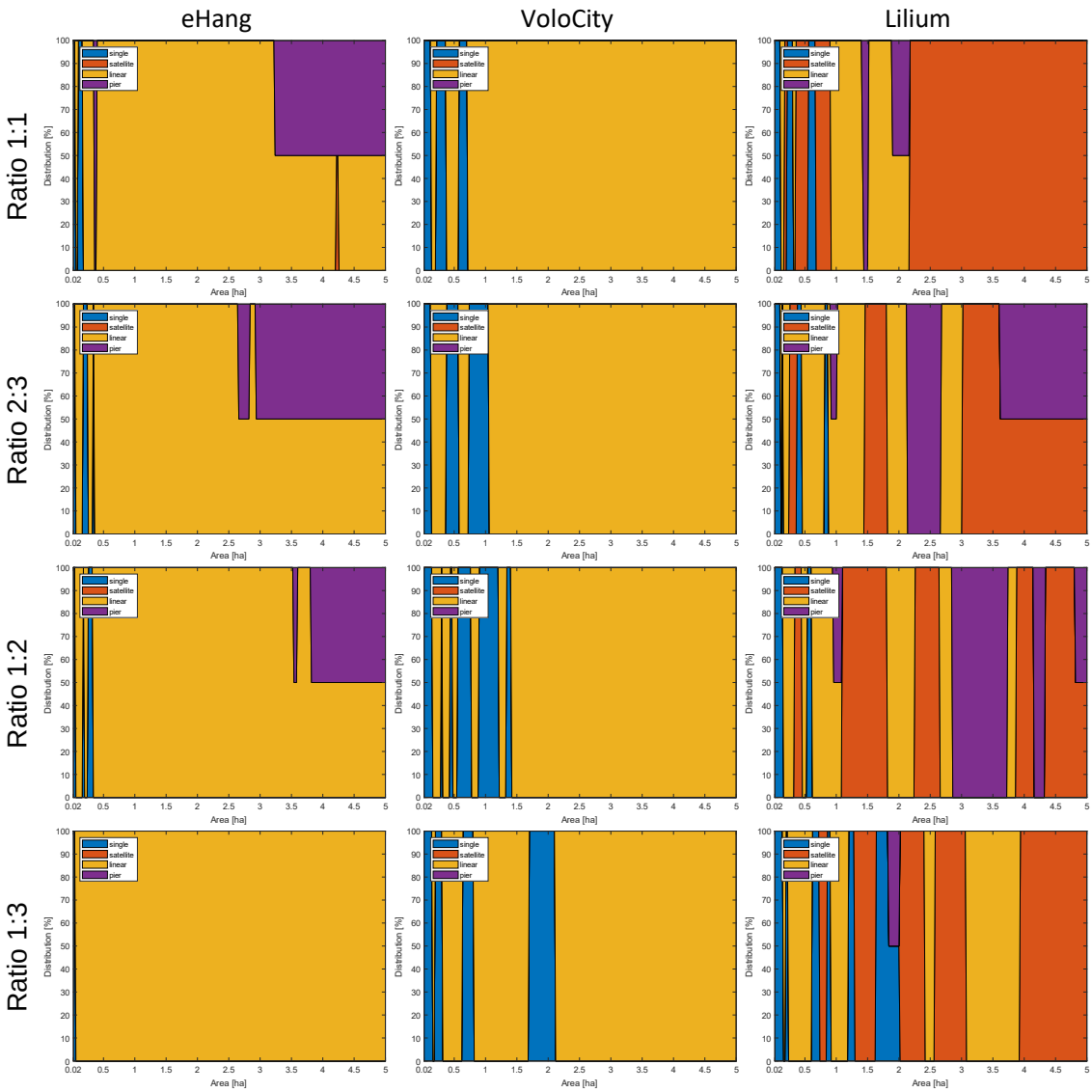

Figure 4.8: Distribution of topologies over the surface and different side ratios $t_{turn,passenger} = 90\ s$ and $t_{T\&L} = 90\ s$

4.1.2.3 Results Research Questions on Throughput of Layout

The following section will present the results based on research questions four through six, which have already been presented. For the sake of clarity, the questions are listed again here:

- Which vehicle leads to highest throughput based on variation of turnaround times and areas?
- What is the influence of different boarding and deboarding times depending on the vehicle?
- How is the influence of the fixed turnaround time compared with the variable one?
- How big is the impact of the take-off and landing time depending on the other process times and the vehicle?

These research questions focus on how different vehicles and turnaround process times affect the hourly passenger throughput. The hourly vehicle throughput is neglected, since the passenger throughput is the key criterion for assessing the performance of a vertiport. The changes in turnaround process times and vehicles are considered together because they are in direct influence to each other. According to the $t_{turn,passenger}$ each passenger needs to enter and leave a vehicle, the number of passengers per vehicle has a direct impact on the total turnaround time and thus the throughput. In addition, the influence of take-off and landing time is investigated in comparison to these variables. In order to better evaluate the results, they were filtered according to the research questions. For these research questions, a x_{min} of 30 m was generally assumed. According to current FAA guidelines [71], there would need to be a separation of at least 61 m for simultaneous operation of two pads. However, since eVTOLs have superior flight characteristics compared to helicopters, a smaller value for x_{min} is assumed. Furthermore, in order not to cause mixing of the different parameters, the taximode is set as hover. It should also be noted that only the best results were used for the analysis. Table 4.5 shows which variables have been included in this investigation.

Table 4.5: Considered parameters for research questions on throughput of layout of the area to throughput approach

Parameter	Values	Unit
Areas	all	m^2
Vehicles	all	-
Topologies	only the best	-
$t_{turn,passenger}$	15; 30; 60; 90	s
$t_{turn,fix}$	0; 5; 10; 15; 20	min
$t_{T\&L}$	30; 60; 90	s
x_{min}	30	m
Taximode	hover	-

In this context, the following figure 4.9 shows the throughputs of the six vehicles plotted over the areas for a $t_{turn,fix}$ of 0, a $t_{turn,passenger}$ of 60 s and $t_{T\&L}$ of 30 s. Along the x-axis of the plot the size of the area in hectares is plotted. Along the y-axis the hourly passenger throughput per square meter is plotted. This unit was chosen to keep throughput comparable across area size, as it is evident that larger areas generate higher throughputs. The different vehicles are color coded.

It can be seen that eHang's vehicle generates the highest throughput with this constellation of parameters for most areas. Up to an area of about one hectare, the throughput is generally between 0.09 and 0.1 passengers per hour per square meter of area. In second position is the CityAirbus, which reaches a maximum throughput of about 0.07. It can be observed that the throughput per square meter for eHang's vehicle decreases rapidly compared to the others as the area increases after the one hectare mark. This results in the vehicle from Airbus taking the position of the vehicle with the highest throughput per area unit from an area size of about 3 hectares. To put the drop in throughput in relation to area size, it drops by about $55\ \%$ for eHang, and only about $30\ \%$ for the CityAirbus. In descending order in terms of throughput, Airbus' vehicle is followed by Boeing's, Lilium's, Volocopter's, and Uber's. The strength of the eHang for this constellation of parameters is probably that the low passenger capacity means that the turnaround time can be kept short and the fast take-off and landing

time means that a large number of flights can be made. In contrast, the CityAirbus can probably hardly benefit from the fast take-off and landing time, since due to the large passenger capacity, the turnaround process takes about 10 minutes. In this time alone, two vehicles from eHang, each with two passengers, would have landed and taken off again, without taking into account the use of gates.

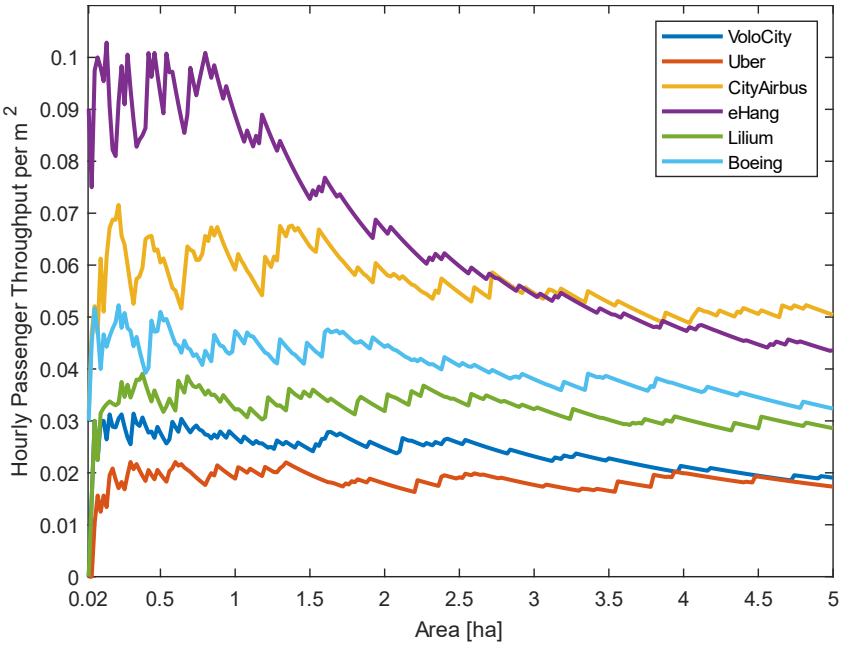

Figure 4.9: Hourly passenger throughput for different vehicles and $t_{turn,passenger} = 60\ s$ and $t_{T\&L} = 30\ s$ and $t_{turn,fix} = 0\ min$

In order to put the results in relation to each other and to observe how changes in process times affect the obtained throughputs, the plots are placed side by side in the following. Figure 4.10 only shows results for a $t_{turn,fix}$ of $0\ min$. Along a row, the assumed $t_{T\&L}$ increases from left to right. The assumed $t_{turn,passenger}$ increases from top to bottom.

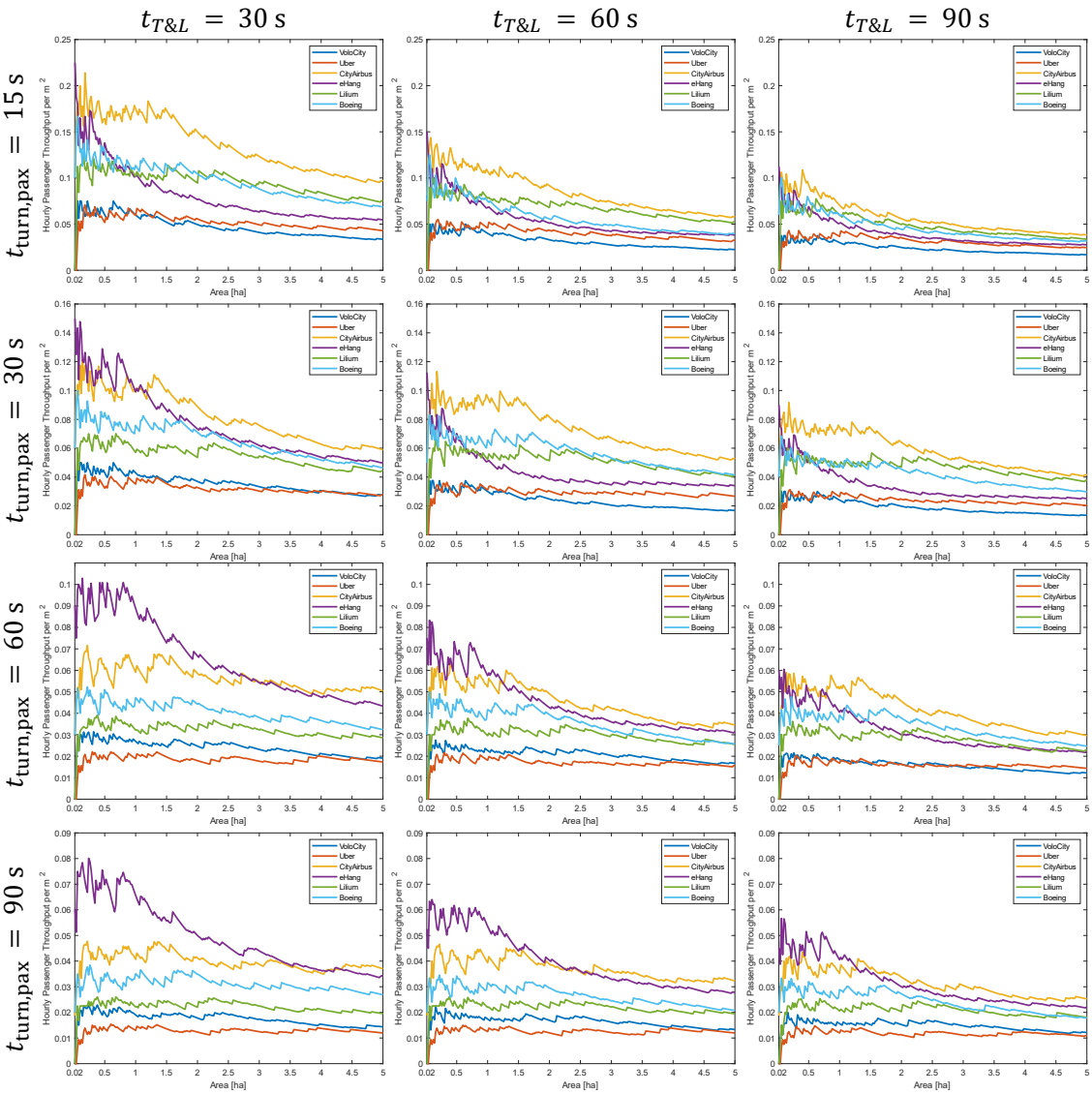

Figure 4.10: Hourly passenger throughput for different vehicles and process times and $t_{turn,fix} = 0\ min$

Analyzing the results, it can be seen that for increasing process times, there is a general decrease in throughputs. However, this is not surprising and is a predictable consequence. Further, it can be seen that the vehicle labeled CityAirbus usually achieves the highest throughput and thus appears to be the best vehicle. For increasing $t_{turn,passenger}$, on the other hand, the vehicle of eHang seems to gain importance, which is probably due to the small number of passengers. It can be further seen that increasing $t_{T\&L}$ negatively affects the achieved throughput of eHang. In particular,

eHang shows strength for short $t_{T\&L}$ and long $t_{turn,passenger}$. It can also be seen that the eHang vehicle experiences a faster drop in throughput as the area size increases compared to larger vehicles. It is also evident that passenger throughput for vehicles with a larger passenger capacity are less responsive to increasing $t_{T\&L}$ with decreasing throughputs. CityAirbus consistently shows higher throughputs than the Lilium Jet despite similar size and passenger capacity. The Lilium Jet accommodates 6 passengers, whereas CityAirbus accommodates 5. Size-wise, the MD from the Lilium Jet is 3 m larger than the MD from CityAirbus. This suggests that the size of the vehicle has a greater impact on passenger throughput than passenger capacity. This suspicion is reinforced by the fact that the two largest vehicles studied, that of Uber and the VoloCity consistently achieve the worst throughput values.

Figure 4.11 has the same structure as figure 4.10. It differs in that $t_{turn,fix}$ of 10 min is assumed compared to figure 4.11. Since $t_{turn,fix}$ of 5 min does not have much more value compared to $t_{turn,fix}$ of 10 min in the analysis, the results are not reported here. However, if interested, they can be found in appendix B.2.

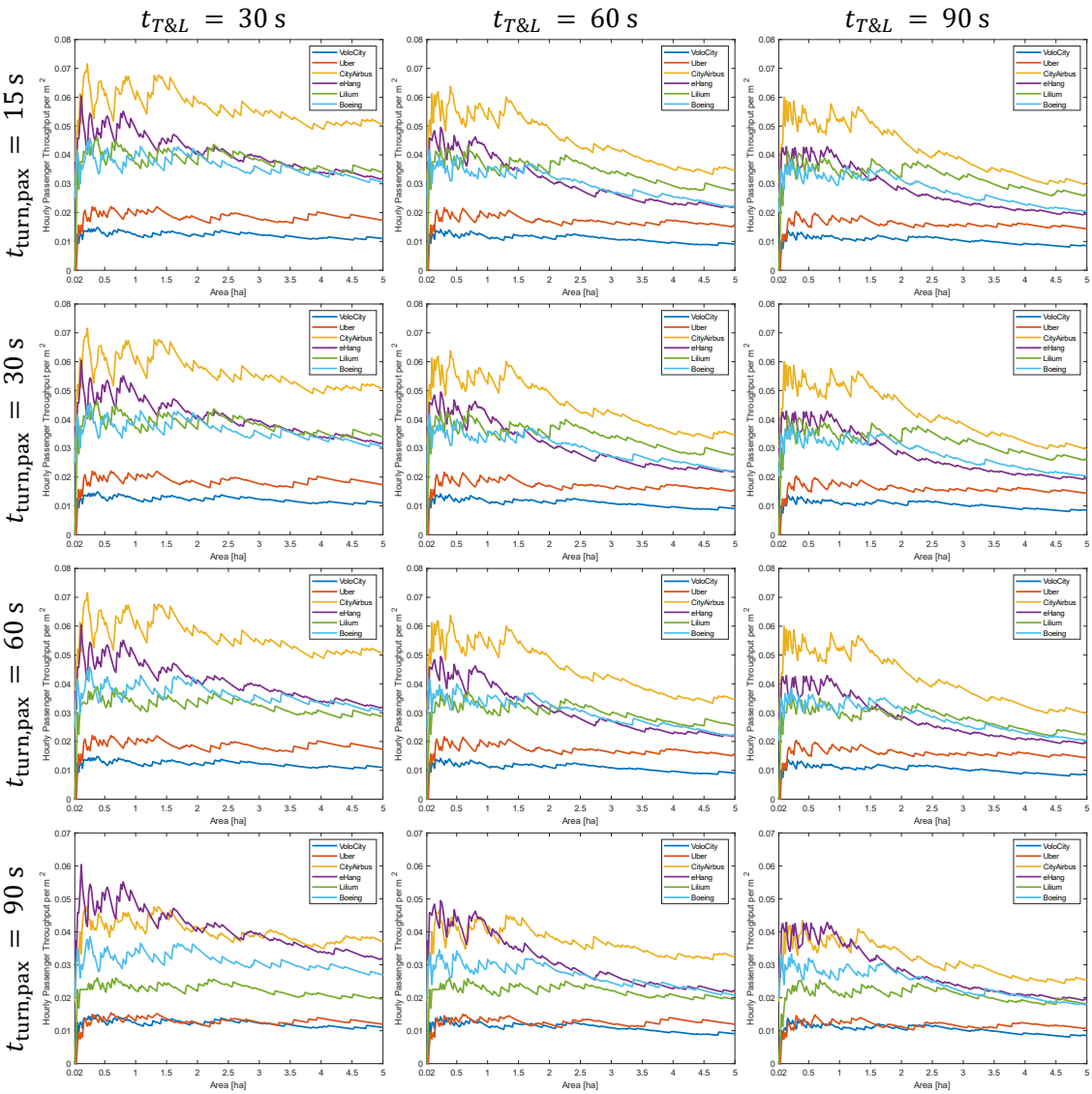

Figure 4.11: Hourly passenger throughput for different vehicles and process times and $t_{turn,fix} = 10\ min$

Due to the larger $t_{turn,fix}$, the dominance of CityAirbus continues to increase and it can be observed that the importance of eHang strongly decreases. Moreover, it can be seen that a change in $t_{turn,passenger}$ does not further affect the achievable throughput. This is due to the fact that the total turnaround time resulting from $t_{turn,passenger}$ is less than or equal to $t_{turn,fix}$. Accordingly, $t_{turn,passenger}$ is no longer the limiting factor in the turnaround process. This change can be observed when switching from $t_{turn,passenger} = 60\ s$ to $t_{turn,passenger} = 90\ s$. No change in throughput is observed

for the eHang vehicle with a passenger capacity of two. In contrast, the throughput of CityAirbus with a passenger capacity of five drops when $t_{turn,passenger}$ is increased, since $t_{turn,fix}$ is still smaller than the total turnaround time resulting due to $t_{turn,passenger}$. Further, it can be seen that the throughputs for increasing $t_{T\&L}$ and for short $t_{turn,passenger}$ of eHang and Lilium and Boeing are similar but for larger areas eHang starts to generate lower throughputs. For longer $t_{turn,passenger}$, eHang's lower passenger capacity allows it to play to its advantages. It is also interesting to note the similarity in generated throughputs observed for Lilium and Boeing, as both vehicles show greater variation in size and passenger capacity. This suggests that a kind of equilibrium has been established between size and passenger capacity. That is, the smaller size of the Boeing allows more pad and gate units to be placed, offsetting the lower passenger capacity.

Moreover, it can be observed that for further increasing $t_{turn,fix}$ less and less differences can be seen in changes of $t_{T\&L}$ and $t_{turn,passenger}$. For this, please refer to appendix B.2 for the results with $t_{turn,fix}$ of 15 min and with $t_{turn,fix}$ of 20 min.

4.1.2.4 Results Research Questions on resulting Layout

The following section will present the results based on research questions seven through eight, which have already been presented. For the sake of clarity, the questions are listed again here:

- What are the most common gate to pad ratios for each topology?
- How do different take-off and landing times influence the vertiport layout?
- How do different process times influence the vertiport layout?

These research questions focus on how the layout of each topology changes as process times change or the design is made for a different vehicle. By layout in this context is meant how the $gate2pad$ ratios change with varying the parameters. The changes in turnaround and vehicle process times are considered together because they are in direct influence to each other. On the one hand, the size of a vehicle affects the number of placeable gates through its dimensions. On the other hand, the

$t_{turn,passenger}$ that each passenger needs to enter and leave a vehicle can influence the turnaround time in a way that more or less gates per pad are desirable. The same is true for the take-off and landing time. In order to better evaluate the results, they were filtered according to the research questions. For these research questions, a x_{min} of 30 m was generally assumed. In addition, $t_{turn,fix}$ was set to 0 min. This measure is justified by the fact that varying $t_{turn,fix}$ as known from the previous result evaluation in section 4.1.2.3 would only cause the turnaround time to become vehicle independent beyond a certain $t_{turn,passenger}$. It should also be noted that all results are used for this study, since the individual topologies are considered separately. If the best results were used, it would lead to gaps in certain areas, since there is no best result for this topology and parameter set. However, the single topology is not considered, since the absence of gates in this topology would mean that the $gate2pad$ relation would not provide any new information. Table 4.6 provides an overview of the variables included in this study.

Table 4.6: Considered parameters for research questions on resulting layout of the area to throughput approach

Parameter	Values	Unit
Areas	all	m^2
Vehicles	all	-
Topologies	satellite; linear; pier	-
$t_{turn,passenger}$	15; 30; 60; 90	s
$t_{turn,fix}$	0	min
$t_{T\&L}$	30; 60; 90	s
x_{min}	30	m
Taximode	hover	-

The following figure 4.12 shows the results for the CityAirbus at a turnaround time per passenger of 30 s for the satellite topology. Along the x-axis of the plot the size of the area in hectares is plotted. Along the y-axis the $gate2pad$ ratio is plotted. The different $t_{T\&L}$ are color coded. It can be seen that the average gate to pad ratio varies for the different take-off and landing times. With two gates per pad, the smallest ratio

is present for a take-off and landing time of 90 s. For decreasing take-off and landing times, the gate to pad ratio increases. The largest number of gates is reached with an average of about 3.7 for an area of 5 ha and a take-off and landing time of 30s. For take-off and landing times of 60 and 90 s, the ratio does not change over the area. This can be due to the fact that because of to the long take-off and landing times, the bottleneck is quickly at the pad and thus with two and three gates the maximum of gates is already reached which makes sense for this constellation. In the case of the take-off and landing time of 30 s, on the other hand, fluctuations in the ratios can be observed. This can be explained by the fact that for some constellations it makes more sense to keep the gate as a bottleneck in order to be able to place more pads in total and thus achieve a higher total throughput.

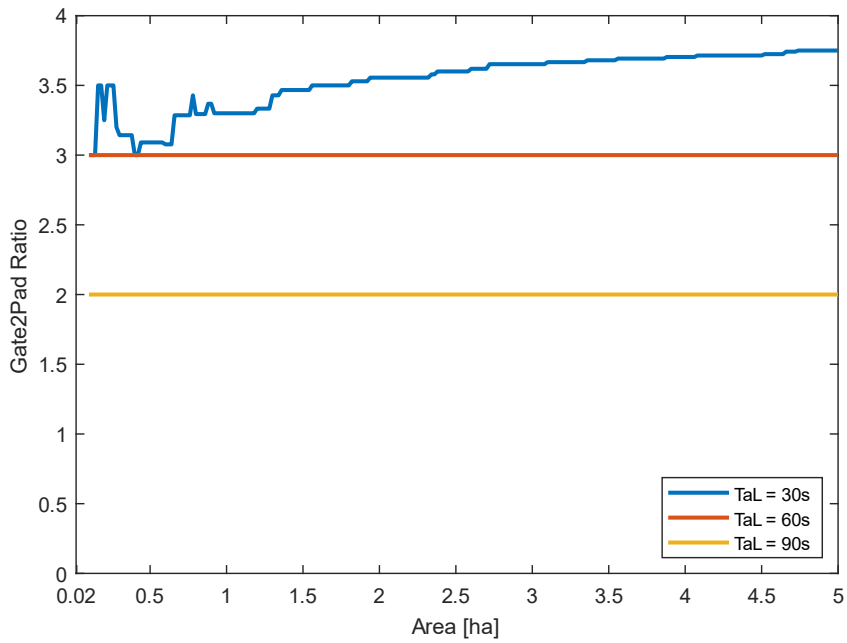

Figure 4.12: Topology layout for CityAirbus for $t_{turn,passenger} = 30\ s$ and $t_{turn,fix} = 0\ min$

In order to better compare the results for the different topologies and to analyze the effects of the different turnaround times per passenger, the results for the CityAirbus are summarized in figure 4.13. Along a row the different topologies are arranged. From left to right, the satellite, linear, and pier topology. The assumed $t_{turn,passenger}$ increases from top to bottom.

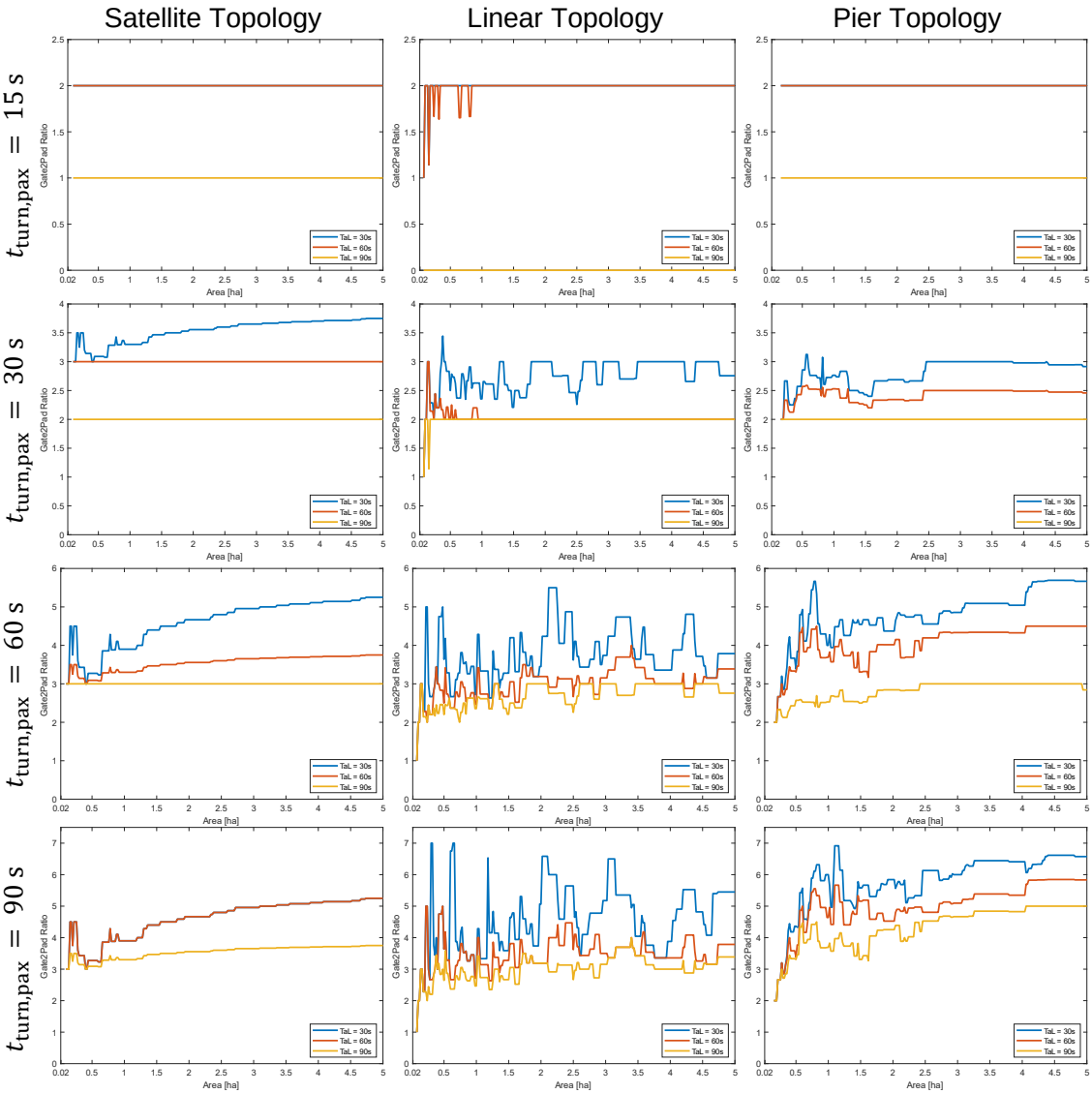

Figure 4.13: Topology layout for CityAirbus for different process times and $t_{turn,fix} = 0\ min$

When analyzing the results from figure 4.13, it can be seen that no results are yet available for small areas. It can be assumed that in these areas units from pad and gate are too large to be placed.

The satellite and also the pier topology show constant $t_{turn,passenger}$ ratios across the size of the surface for all three different $t_{T\&L}$. However, it is observed that the longest $t_{T\&L}$ has a smaller $gate2pad$ ratio than the other two. A ratio of one and two, respectively. A similar behavior is observed for the linear topology, but for areas up to one

hectare and smaller 90 s, fluctuations in the $gate2pad$ ratio are still observed before this takes a constant level. With respect to the components just mentioned, it can also be seen that as $t_{turn,passenger}$ increases and $t_{T\&L}$ decreases, the $gate2pad$ ratio shows greater fluctuations.

Further, it is shown that as $t_{turn,passenger}$ increases, the $gate2pad$ ratios become larger, regardless of the topology. For the linerar and pier topologie, a maximum of seven gates per pad is reached. For the satellite topology, the maximum is already around five. The reason for this is probably that the number of gates for the satellite topology is geometrically limited due to their arrangement around the pad, unlike the other topologies. Also to be seen is that with increasing $t_{T\&L}$ the $gate2pad$ ratio becomes smaller. For a linear topology with $t_{turn,passenger}$ of 15 s and $t_{T\&L}$ of 90 s it even turns out that excluding gates is reasonable.

To better understand the results, the results for the vehicle of eHang are used for comparison (see figure 4.14).

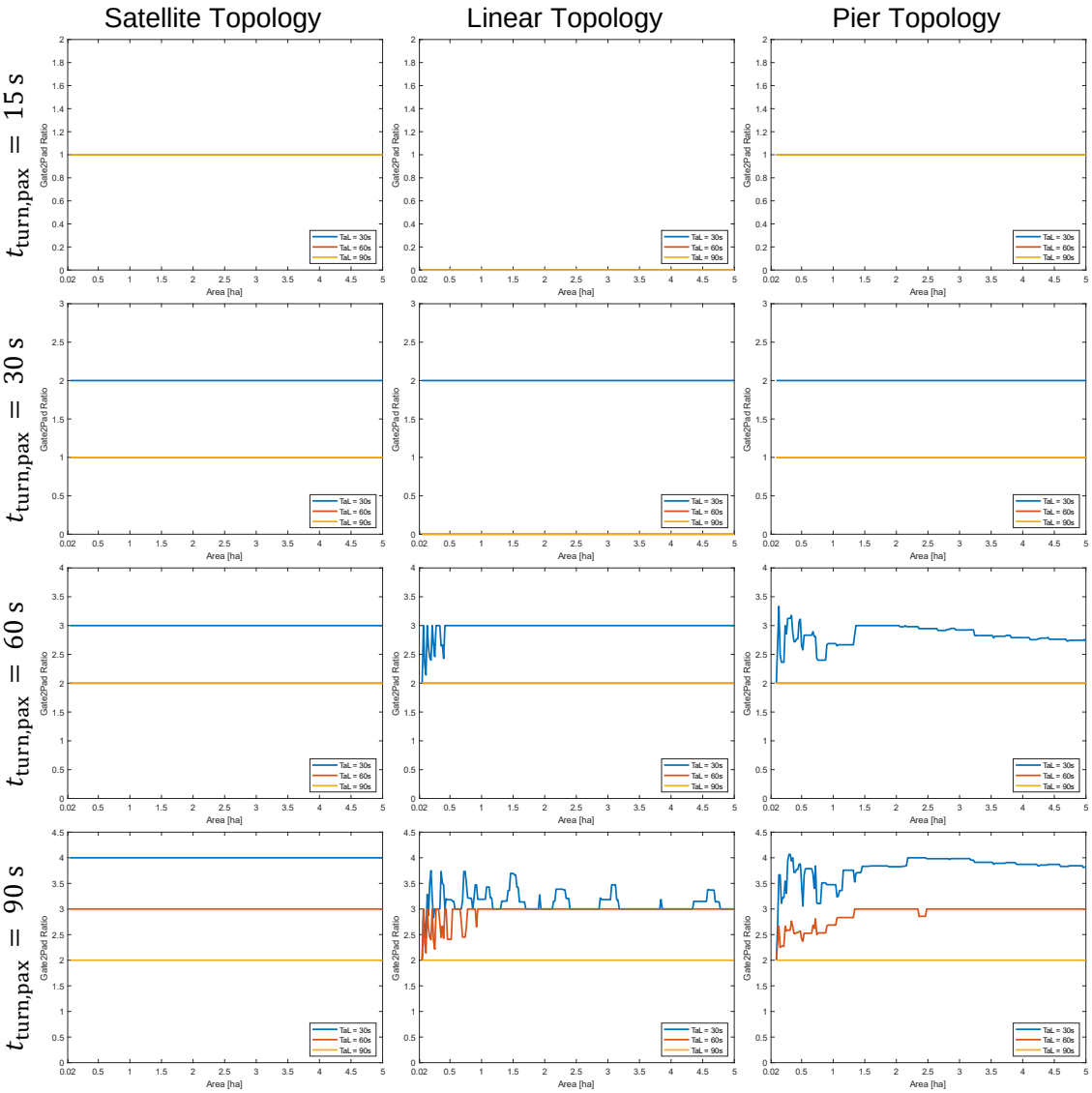

Figure 4.14: Topology layout for eHang for different process times and $t_{turn,fix} = 0\ min$

Again, it can be seen that for short $t_{turn,passenger}$ a constant $gate2pad$ ratio already sets in for small areas. This condition also occurs more frequently for longer $t_{turn,passenger}$ compared to the CityAirbus, especially for the satellite topology. This suggests that an 'optimal' $gate2pad$ ratio has been achieved, i.e. that the pad is the bottleneck, or in the case of the satellite topology it may be due to the fact that more gates cannot be placed. For vehicles with small passenger capacity, this can be achieved with smaller ratios than for larger ones. Also, a longer $t_{T\&L}$ seems to ensure that an optimum for

the $gate2pad$ ratio is reached faster. It is for the satellite topology with a $t_{turn,passenger}$ of 90 s that the effect of increasing $t_{T\&L}$ is particularly well seen. For larger $t_{T\&L}$, fewer gates per pad are needed to reach the pad as bottleneck. For $t_{turn,passenger}$ of 60 s, it can also be seen that for $t_{T\&L}$ of 30 s and of 60 s, an equal $gate2pad$ ratio is still proposed. However, with further increase of $t_{turn,passenger}$ also for the $t_{T\&L}$ of 30 s another gate is needed to keep the pad as bottleneck.

Further, it can be seen that the achieved maxima for the eHang are smaller than for CityAirbus, thus representing that vehicles with a higher passenger capacity require pads with more gates. The results for the other vehicles further reinforce these assumptions. However, they are not presented here. Nevertheless, if interested, they can be found in the appendix B.3.

4.1.2.5 Results Research Questions on Bottleneck of Layout

The following section will present the results based on research question ten. The question addresses which bottleneck occurs most frequently for different topologies and design parameters.

In order to better evaluate the results, they were filtered according to the research questions. The filtering was done according to that for research questions eight to ten (see section 4.1.2.4 and table 4.6), except that the $t_{T\&L}$ was set to 60 s. This value is consistent with the assumptions of Vascik and Hansman [89]. Based on the findings of section 4.1.2.4, the decision was made not to consider any further $t_{T\&L}$ in the investigation, as they would not provide any added value.

Figure 4.15 plots the bottlenecks for eHang's vehicle for a turnaround time of 90 s per passenger. Along the x-axis of the plots the size of the area in hectares is plotted. Along the y-axis the percentage of times a bottleneck occurs depending on the area is plotted . The three bottlenecks, pad, gate, and taxiway are color coded.

It can be seen that for most constellations the highest throughput can be achieved with the gate as bottleneck. Only for areas smaller than 0.2 ha it seems more effective to choose the pad as bottleneck. Since there is no classical taxiway in the satellite topology, it is logical that the taxiway is never the bottleneck. The reason that for small

areas the pad as bottleneck achieves the highest throughputs is probably due to the fact that in this size range it is not possible to place more units on the area by reducing the gate to pad ratio. Thus, it seems more effective that the existing units achieve the highest possible individual throughput.

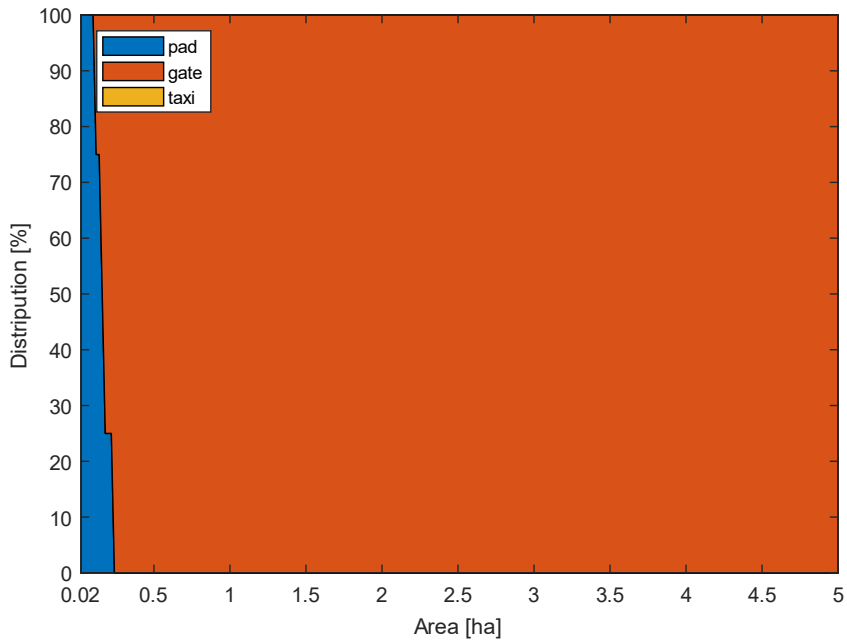

Figure 4.15: Bottleneck distribution for eHang for $t_{turn,passenger} = 90\ s$ and $t_{turn,fix} = 0\ min$ and $t_{T\&L} = 60\ s$

With the aim of comparing the bottleneck of the different topologies and investigating how the different turnaround times per passenger affect them, the results for the vehicle of eHang were summarized in figure 4.16. The different topologies are arranged along a row. From left to right, the satellite, linear, and pier topologie. The assumed $t_{turn,passenger}$ increases from top to bottom.

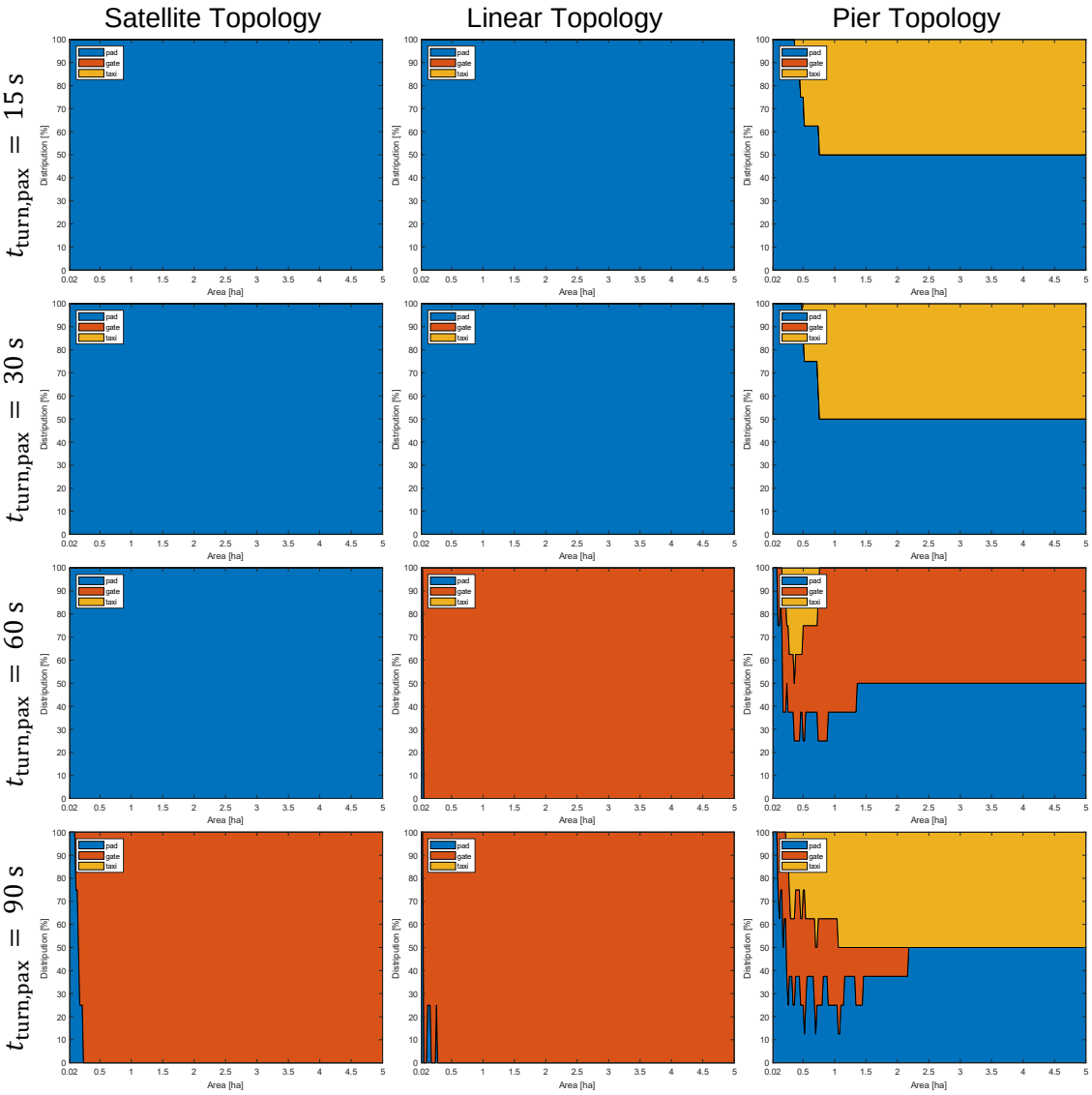

Figure 4.16: Bottleneck distribution for eHang for different process times and $t_{turn,fix} = 0\ min$ and $t_{T\&L} = 60\ s$

The analysis of the graphs shows that for the satellite and linear topology the pad, is the general bottleneck for $t_{turn,passenger}$ of up to 30 s. For the satellite topology, this holds up to $t_{turn,passenger}$ of up to 60 s. After that, it can be observed that the gate becomes the bottleneck.

For the pier topology, it can be seen that a subdivision gives that for $t_{turn,passenger}$ of up to 30 s for half of the results the pad is the bottleneck and for the other the taxiway. This is probably due to the fact that two approaches are considered in the pier

topology. One is that two pads share a taxiway and the other is that each pad has its own taxiway. The assumption is that by sharing a taxiway, it becomes congested and thus becomes the throughput limiting factor. For areas smaller than 0.8 ha this does not seem to be a problem yet. For $t_{turn,passenger}$ of up to 60 s the gate seems to be the bottleneck more often in the pier topology as well. The results for the bottlenecks confirm the assumptions made in section 4.1.2.4 regarding figure 4.14. The assumption states that an optimal ratio of gate to pad was achieved. This can be done by placing so many gates that the pad becomes the bottleneck or the geometric maximum of gates is reached, or in the case of the linear topology, an optimal ratio of space required and number of gates is obtained.

By comparison with the vehicle VoloCity (see figure 4.17) which has almost twice the MD for the same passenger capacity, it can be seen that the bottleneck does not depend on the size of a vehicle, but much more on the passenger capacity. However, one can also see that larger vehicles tend to have the pad as bottleneck more often as $t_{turn,passenger}$ increases.

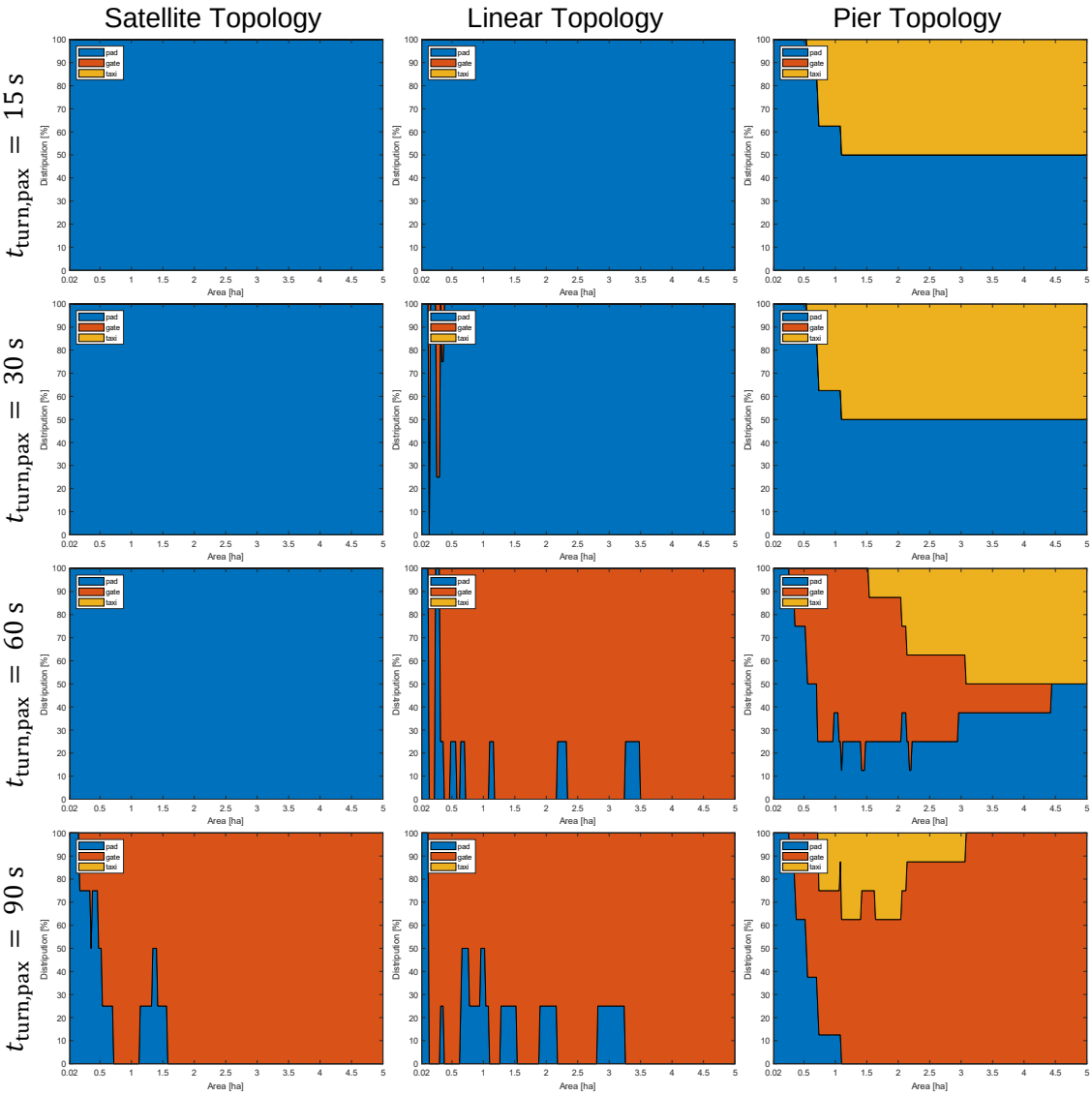

Figure 4.17: Bottleneck distribution for VoloCity for different process times and $t_{turn,fix} = 0\ min$ and $t_{T\&L} = 60\ s$

Taking further the results of the Lilium Jet (see figure 4.18), which has similar dimensions to the VoloCity but three times the passenger capacity, it can be seen that vehicles with a high passenger capacity are more likely to cause the gate to be the bottleneck. It can also be observed here that for about $25\ \%$ of the areas in the linear topology, the pad is the bottleneck. It is reasonable to assume that these are the areas with a side ratio of one to three. In this case, the longer length is more favorable to the linear topology.

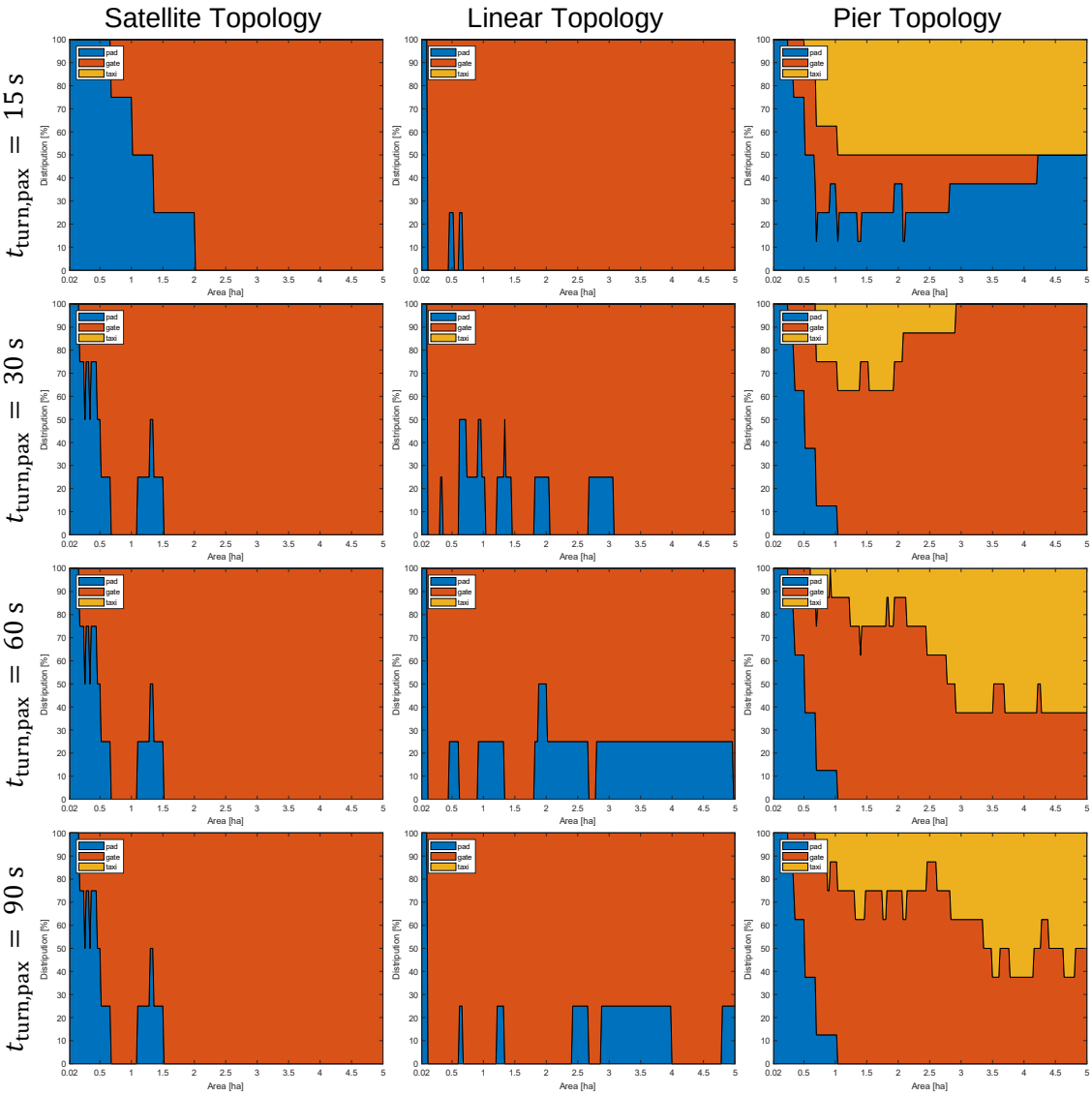

Figure 4.18: Bottleneck distribution for Lilium for different process times and $t_{turn,fix} = 0\ min$ and $t_{T\&L} = 60\ s$

The results of the other vehicles can be found in the appendix B.4.

4.2 Real World Scenario

The real world scenario study was conducted using the area to throughput tool and a summary of the experimental setup can be seen in appendix C.1. The main objective of this study is to determine if the developed method provides realistic results for real world areas. It was also intended to determine which vehicles would achieve the

best results in the real world environment and the potential throughput rates for the locations.

4.2.1 Experimental Setup

To find answers to these questions, the following parameters were varied (see table 4.7).

Table 4.7: Varied parameters for real world scenario of the area to throughput approach

Parameter	Value Range	Unit	Combinations
Area	3 areas out of (Berlin)	polygon	3
Vehicles (size & passengers)	6 representative	m & $n_{passengers}$	6
Topology	single; satellite; linear; pier;	-	4
Total			72

The core component in this study is the area. For this purpose, three possible locations in Berlin were selected that could span a UAM network as seen in figure 4.19.

It can be seen that if a UAM travel speed of 100 km/h on average is assumed, time savings in travel would already be possible compared to the travel times by car predicted by google maps [118]. For the routes studied, it is assumed that the travel time can be reduced to approximately one third. Turnaround times were not taken into account in this scenario; it was assumed that the journey begins with the take-off and ends after the approach, since no time for reaching the vehicle or similar is taken into account for the car journey either.

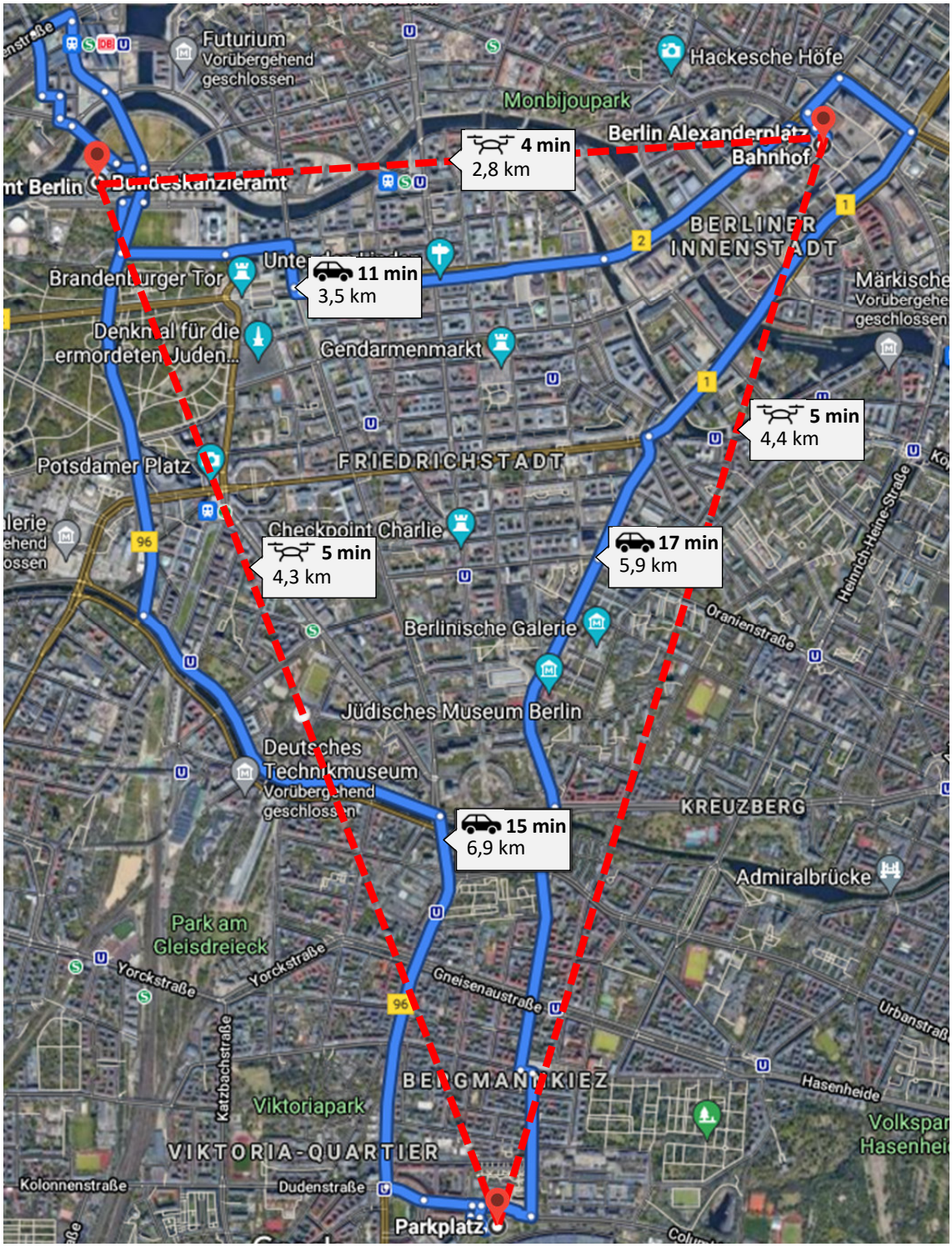

Figure 4.19: UAM network of real world scenario [118]

The selected locations are:

- Roof of the train station at Alexanderplatz with an area of 6187 m^2 (see fig-

ure 4.20a)

- Roof of the Bundeskanzleramt with an area of 2968 m^2 (see figure 4.20b)
- Parking at Berlin Tempelhof with an area of 4412 m^2 (see figure 4.20c)

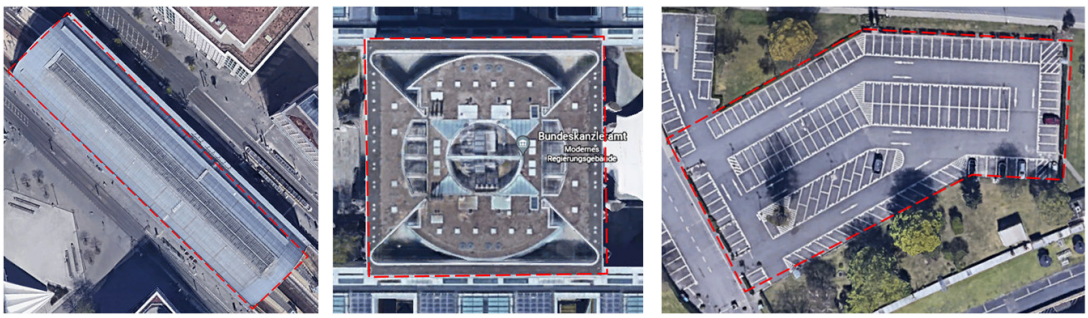

a) Alexanderplatz b) Kanzleramt c) Tempelhof

Figure 4.20: Locations of real world scenario [118]

In addition, the study was conducted with six different vehicles. These are already known from the study in section 4.1.2 (see table 4.1).

The other parameters were considered fixed and were not varied (see table 4.8).

Table 4.8: Fixed parameters for real world scenario of the area to throughput approach

Parameter	Value	Unit
x_{min}	30	m
$t_{T\&L}$	60	s
$t_{turn,passenger}$	30	s
$t_{turn,fix}$	10	min
Taximode	hover	-
$t_{prepare4taxi}$	0	s
$pad2taxi$	1	-
$taxi2gate$	0.5	-

In order to clarify the questions, the first step is to investigate which vehicle produces the highest throughputs for the given surfaces and then, using the developed GUI, the proposed results are visualized for this vehicle to confirm their validity.

4.2.2 Best Vehicle

Depending on the vehicle selected, different possible hourly passenger throughputs are apparent for each location. The different throughputs are summarized in table 4.9.

Table 4.9: Hourly throughput for different locations and vehicles

Vehicle	Alexanderplatz	Kanzleramt	Tempelhof	Total
Boeing	212 pax/h	92 pax/h	168 pax/h	472 pax/h
CityAirbus	335 pax/h	115 pax/h	230 pax/h	680 pax/h
eHang	234 pax/h	180 pax/h	270 pax/h	684 pax/h
Lilium	240 pax/h	120 pax/h	192 pax/h	552 pax/h
Uber	125 pax/h	75 pax/h	80 pax/h	280 pax/h
VoloCity	165 pax/h	100 pax/h	160 pax/h	425 pax/h

It can be seen that eHang's vehicle achieves the highest throughputs for the locations Kanzleramt and Tempelhof. In contrast, the Airbus vehicle exceeds the throughput of eHang for the Alexanderplatz location by almost 100 passengers per hour. Looking at throughputs for the entire network, CityAirbus and eHang achieve throughputs of 680 and 684 passengers per hour, respectively. Lilium's vehicle is in third place with a throughput that is about 130 passengers lower.

Accordingly, it seems that the vehicle of eHang is the most suitable for the given UAM network. However, it should be noted that for an eHang, due to the reduced passenger capacity, the vehicle throughput is also about 3 times that of Airbus. Consequently, the fleet of vehicles would have to be 3 times as large. Furthermore, it must be taken into account that the data refer to a full capacity utilization. In a real scenario, however, it can be assumed that there is not always a full capacity utilization and thus a large number of vehicles would not be used at eHang. For Airbus, on the other hand, it would most likely result in vehicles not operating their flights at full capacity. Thus, the choice for the best vehicle in this work falls on that of Airbus. According to the pure numbers, this vehicle performs slightly worse than the one from eHang, but in the personal opinion of the author, the factors just shown speak for

using the vehicle from Airbus for the planning of the UAM network. Due to the larger dimensions of the CityAirbus, it would also be possible to operate a vertiport based on it with the smaller eHang.

4.2.3 Resulting Designs

In the following, the vertiport designs created for the given locations based on the CityAirbus are presented.

It can be seen that for all designs, all elements can be placed in compliance with the minimum distances. This means that neither the minimum distance of 30 m between two pads with departure paths pointing in the same direction is violated, which would prevent parallel operation. At the same time, the safety zones of the elements are not penetrated. It follows that these results are feasible from a purely geometrical point of view.

In detail, one can see for the design for the locations Tempelhof (see figure 4.21) and Kanzleramt (see figure 4.22) a pier topology is proposed.

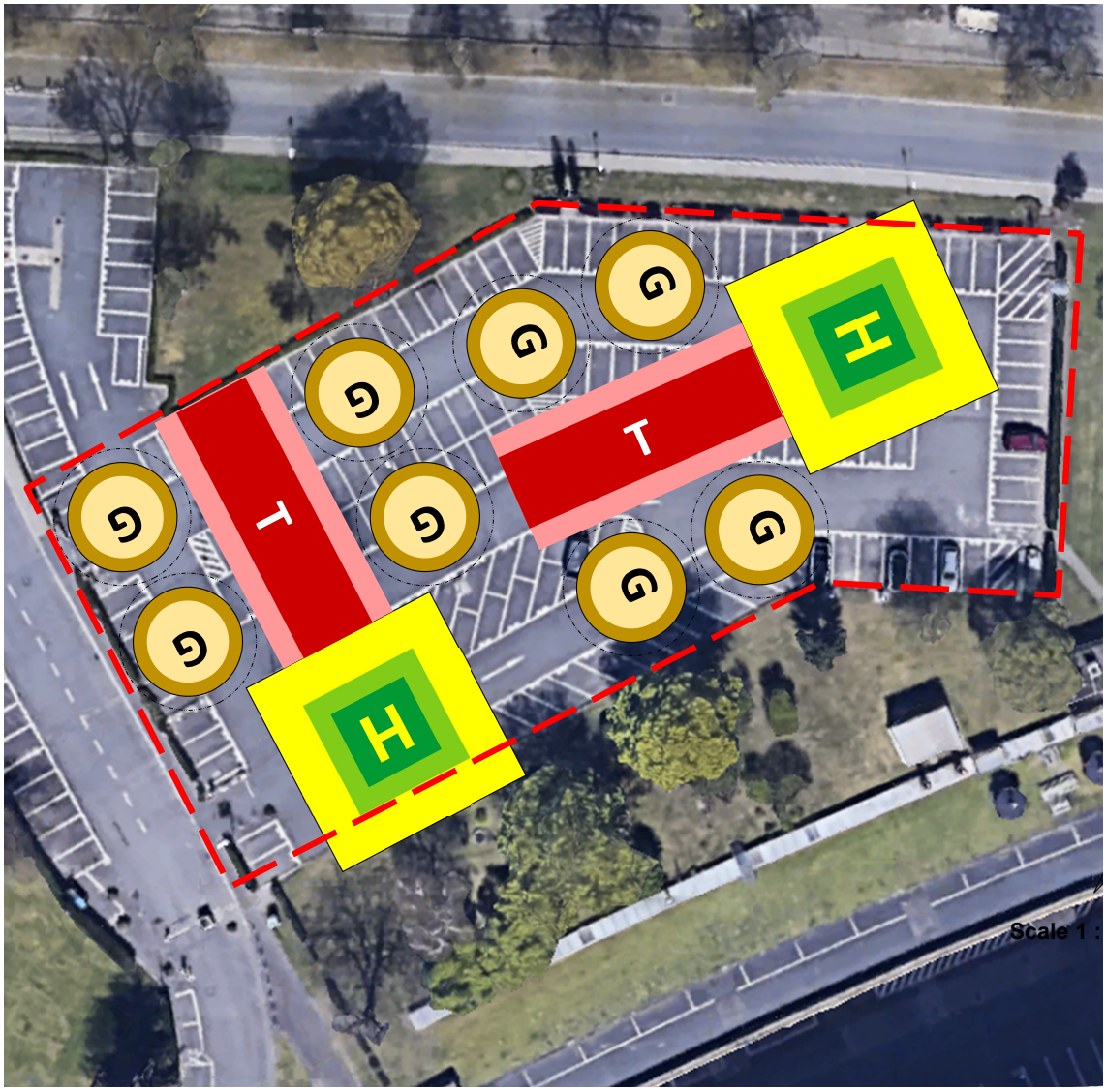

Figure 4.21: Pier topology layout for Tempelhof for CityAirbus

Two pads with four gates each will be placed at Tempelhof to handle a total throughput of 230 passengers per hour, which is limited by the number of gates. In addition, 46 car parking spaces are needed, which could be placed on one level below the airfield to meet the expected passenger throughput. It should be noted in the design that this is a ground level location and accordingly it would need to be built a minimum of one level in height for the proposed configuration. It can also be observed that due to the shape of the area, it is not possible to place both pads directly at the edge of the area. Rotating the right pad clockwise by about 25° would make up for this, but as it currently stands, no curved taxiways can be projected by the GUI.

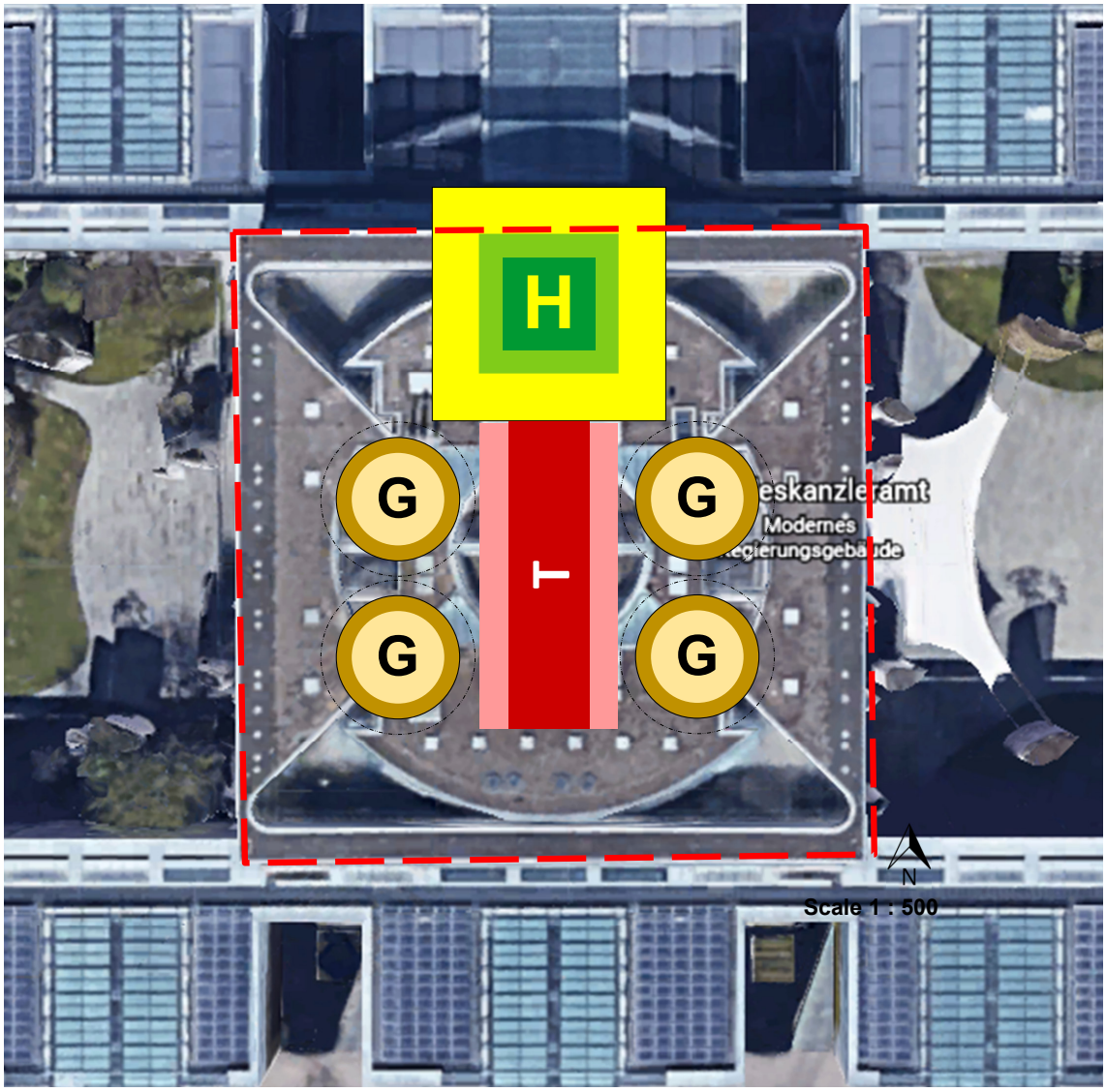

Figure 4.22: Pier topology layout for Kanzleramt for CityAirbus

As already mentioned, a pier topology is also proposed for the location on top of the Bundeskanzleramt in Berlin. This also has a gate to pad ratio of four. However, due to the reduced space, only one pad/gate unit is placed and an hourly passenger throughput of 115 is achieved. As in the previous constellation, the gate is the bottleneck. A closer look at the area and the individual components reveals that by rotating the pad/gate unit by 45°, another gate could be placed at the base of the taxiway, thus also increasing the potential throughput. This shows that the designed method is close to the possible maximum, but still has deficits. The 23 car parking spaces needed for this design could be placed on one level below the airfield.

For the last location examined, the train station at Alexanderplatz (see figure 4.23), a possible hourly passenger throughput of 335 is calculated. Unlike the other two locations, a linear topology is proposed here with a gate to pad ratio of one to three. Again, the gate represents the bottleneck. As already noted for the location at the Bundeskanzleramt, more gates could be positioned after visual inspection, but this would lead to a mixing of the linear and satellite topology, which is not possible according to the current state of the implemented method. On a positive note, however, this design is also feasible from a geometric standpoint and does not exceed the limits of the surface. Thus, it can be concluded that the results are sometimes somewhat conservative, but feasible.

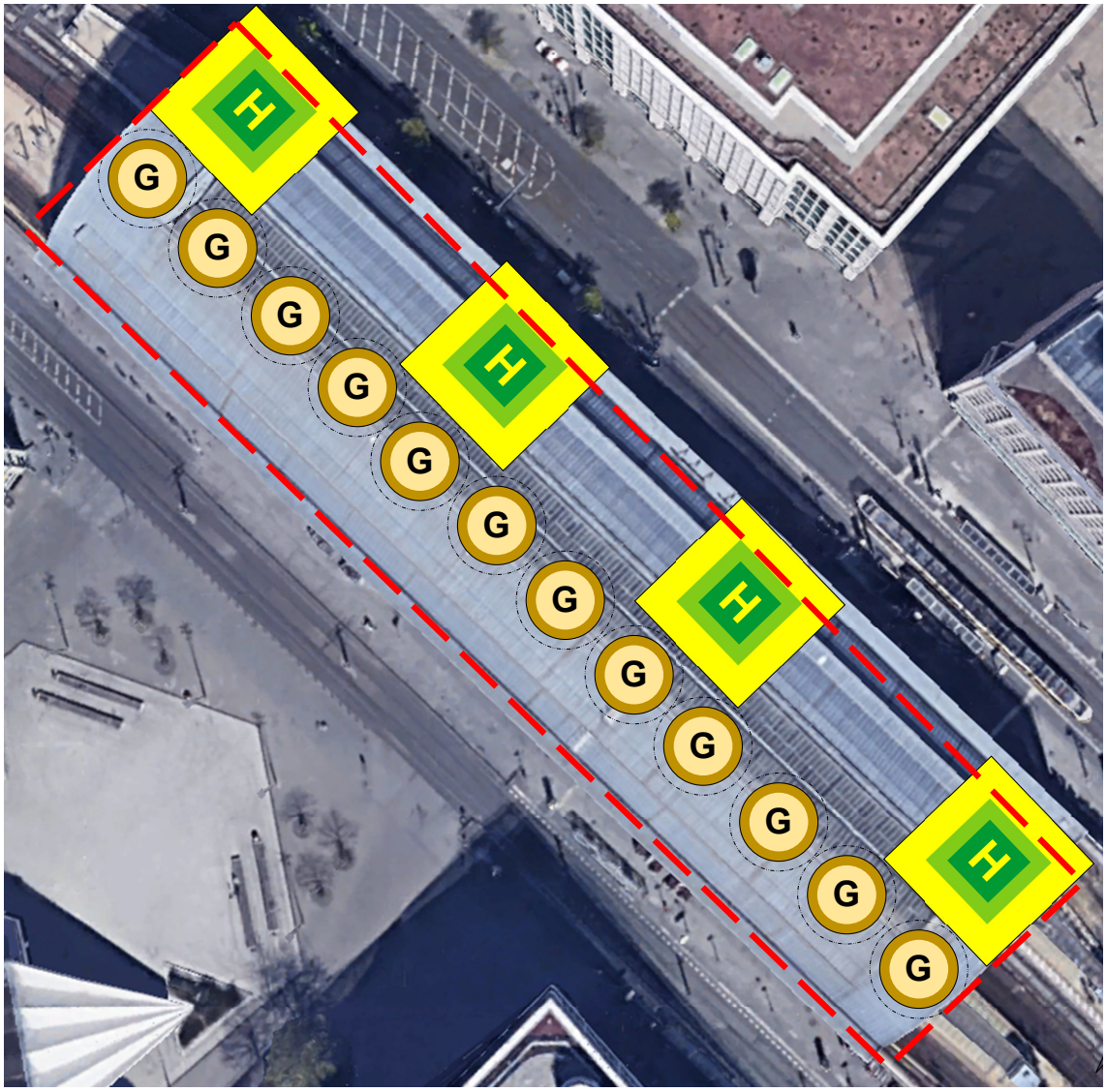

Figure 4.23: Linear topology layout for Alexanderplatz for CityAirbus

4.3 Throughput to Area

The sensitivity study presented below was conducted using the throughput to area method and a summary of the experimental setup can be seen in appendix D.1. The objective of the study is primarily to determine the impact of desired passenger throughputs in combination with varying process times, vehicles, and geometric specifications on the footprint required for a vertiport. In this context, three research questions were formulated:

1. Which topology has the highest throughput per area unit?

2. What is the influence of varying take-off and landing times as well as turnaround times on the required area?
3. Which vehicle requires the least area to achieve a given throughput?

The setup of the study is explained in more detail below.

4.3.1 Experimental Setup

To find answers to these questions, the following parameters were varied (see table 4.10).

Table 4.10: Varied parameters for sensitivity study with throughput to area approach

Parameter	Value Range	Unit	Combinations
Passenger throughput per hour	20 to 1000 in steps of 5	pax/h	197
Vehicles (size & passengers)	6 representative	m & $n_{passengers}$	6
$t_{T\&L}$	30; 60; 90;	s	3
$t_{turn,passenger}$	15; 30; 60; 90;	s	4
Topology	single; satellite; linear; pier;	-	4
Total			56736

For this study, the throughput is the central parameter. Therefore, it was increased from an initial throughput of 20 in steps of five to 1000 passengers per hour. In addition, the vehicles already known from the previous studies were used for this study (see table 4.1). To observe the impact of the different process parameters on the results, they were varied as shown in table 4.10. For the parameters listed in table 4.11, fixed values were assumed within the scope of the study.

Table 4.11: Fixed parameters for sensitivity study with throughput to area approach

Parameter	Value	Unit
x_{min}	30	m
$t_{turn,fix}$	10	min
Taximode	hover	-
$t_{prepare4taxi}$	0	s
$pad2taxi$	1	-
$taxi2gate$	0.5	-

A fixed turnaround time of 10 minutes was assumed for vehicle charging, as it is considered a desirable time for future vehicle operation. This prevents vehicles with a small passenger capacity from gaining an advantage over others by neglecting processes such as recharging. As already known from the other studies, all four topologies are also varied. This results in a total of 56736 parameter combinations, which took 5 minutes to process. In the following sections the results will be presented.

4.3.2 Results

When examining the results, the first step was to consider which topology, depending on the vehicle used, required the least area to achieve the desired throughput. For this purpose, the results were visualized in plots. The desired passenger throughput per hour was plotted along the x-axis and the percentage distribution of the best topology along the y-axis. The different topologies are color coded. No parameter combinations were filtered for these plots. Only the vehicles were distinguished. As a representative example, the plot of the results for the vehicle of Airbus is presented below. The best results, as shown in the diagram, are defined as the topology for which the highest ratio between desired throughput and required area has been achieved.

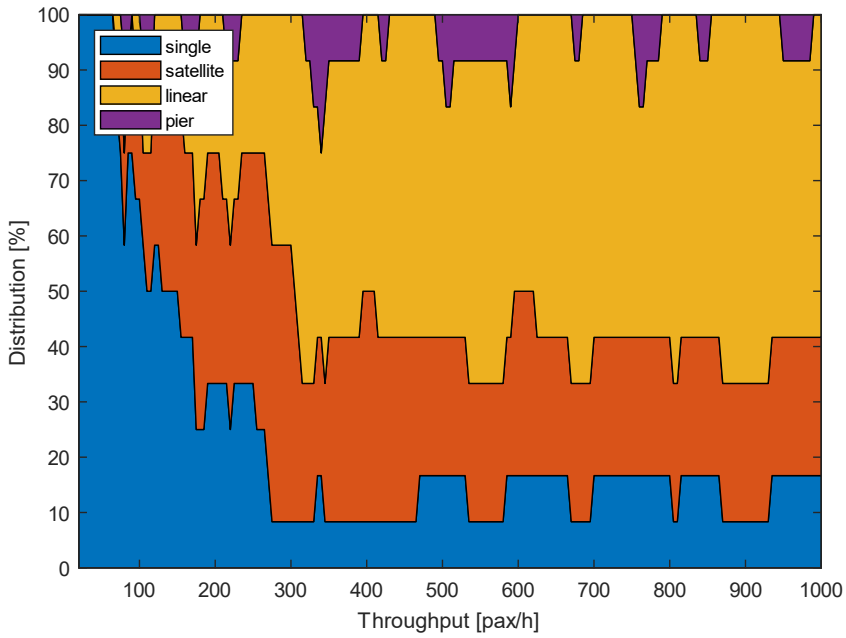

Figure 4.24: Best topology for desired throughput for vehicle of Airbus

It can be observed that for a desired throughput of up to about 100 passengers per hour, the single topology is the best choice. After that, the other topologies begin to gain in importance, but especially the satellite topology. From a desired throughput of about 280 passengers per hour, the single topology settles in its representation between 10 and 15 %. The satellite topology is represented by about 30 % and the linear topology seems to be the best option for about 50 % of the examined constellations. Thus, for the vehicle of Airbus from about a throughput of 280 are mostly the best choice, followed by the satellite and single topology. The pier topology seems to be the best choice for only a few constellations and in some cases is not even represented at all.

In order to put the results shown in relation to each other, the results of the individual vehicles are juxtaposed in the following figure 4.25.

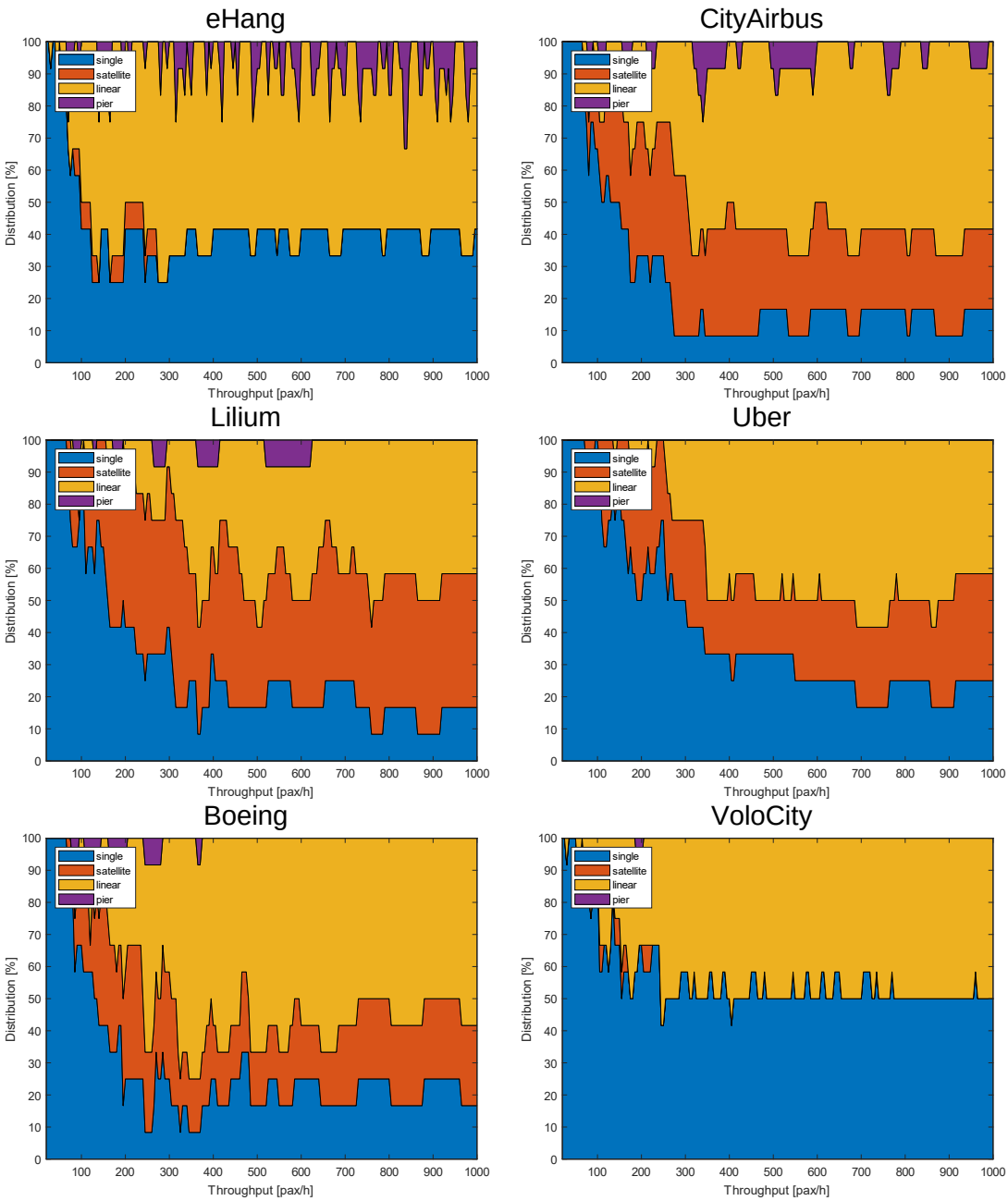

Figure 4.25: Best topology for desired throughput for all vehicles

Examination of the plots shows that, compared to the Airbus vehicle, the satellite topology is of little importance for the eHang and VoloCity vehicles. Instead, the single topology seems to be a good option for larger throughputs. For the VoloCity, the single topology is the best topology for almost $60\ \%$ of the constellations, depending on the desired throughput. However, for most desired throughputs for the VoloCity, the single

topology is the best for half of the parameter constellations and the linear topology for the other half. For the vehicle of eHang the linear topology is represented with about $50\ \%$ and the single topology with about $40\ \%$. However, it also shows that for some parameter constellations the pier topology can be advantageous. The vehicle of Lilium has a similar plot as the one of Airbus, however, with a somewhat larger share of satellite topology and a correspondingly reduced share of linear topology. For Boeing's vehicle, the linear topology seems to be the best choice in most cases. The pier topology is hardly represented here and the single and satellite topologies are represented by about $20\ \%$ each. Parallels can also be observed between Uber's vehicle and Lilium's vehicle. However, Uber has a larger share of constellations in which the single topology seems to be the best.

In the following, the focus of the investigation of the results is on how the different take-off and landing times as well as the turnaround times affect the required area and, associated with this, which vehicle delivers the best results. In the first plot, for an assumed take-off and landing time of 60 seconds each and a boarding and deboarding time per passenger of 30 seconds, the required areas are shown for the different vehicles to achieve the desired throughputs (see figure 4.26). Along the x-axis the different throughputs are plotted and along the y-axis the corresponding required areas. The vehicles are color coded. The plot always shows the result of the topology that achieves the highest ratio between desired throughput and required area.

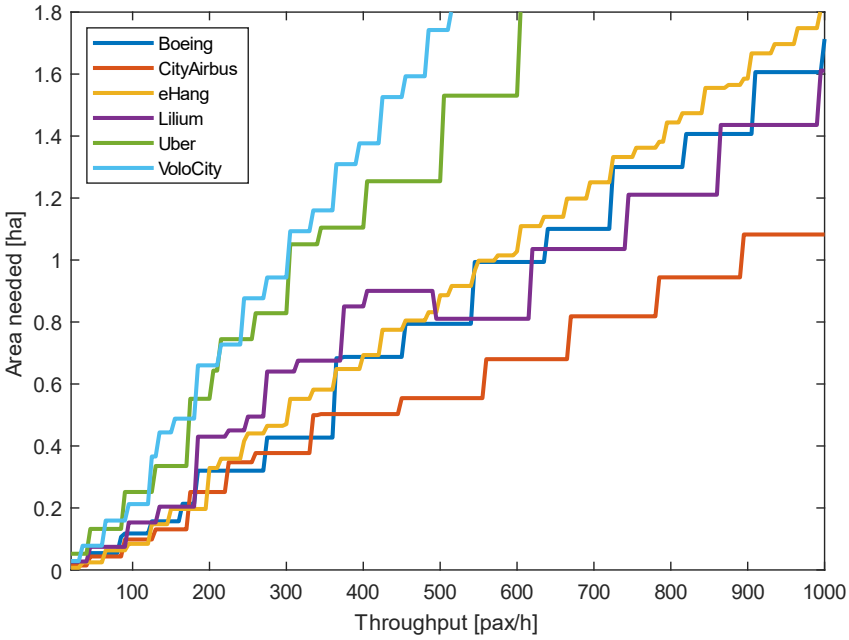

Figure 4.26: Comparison for area needed for $t_{T\&L} = 60\ s$ and $t_{turn,passenger} = 30\ s$

Up to a desired throughput of about 200 passengers per hour, it is hard to tell which vehicle achieves the best throughputs per required area. However, it can be seen that Uber's vehicle and the VoloCity perform the worst. This is almost certainly due to the fact that they are the vehicles with the largest dimensions. As the throughput increases, it can be seen that the curve of the CityAirbus has the lowest slope and thus requires the smallest areas as the desired throughput increases. Also providing good results are the Lilium and Boeing vehicles. Here, it can be observed that a change takes place at a desired throughput of slightly more than 500. Up to this threshold, the vehicle from Boeing delivered better results, then that from Lilium. Surprisingly, at a desired throughput of about 500 passengers per hour for Lilium's vehicle, a drop in the required area can be observed. This can be due to the choice of the best result, as it results from the ratio of desired throughput and required area. The reason for this assumption is that there are topology configurations that achieve a higher ratio between the achieved throughput and the required area but perform worse in terms of the desired throughput, and thus their strength only becomes apparent for larger desired throughputs.

In order to put the results shown in relation to each other, the results for the different

process times are juxtaposed in the following figure 4.27. In the figure, the turnaround time increases from top to bottom and the take-off and landing time from left to right.

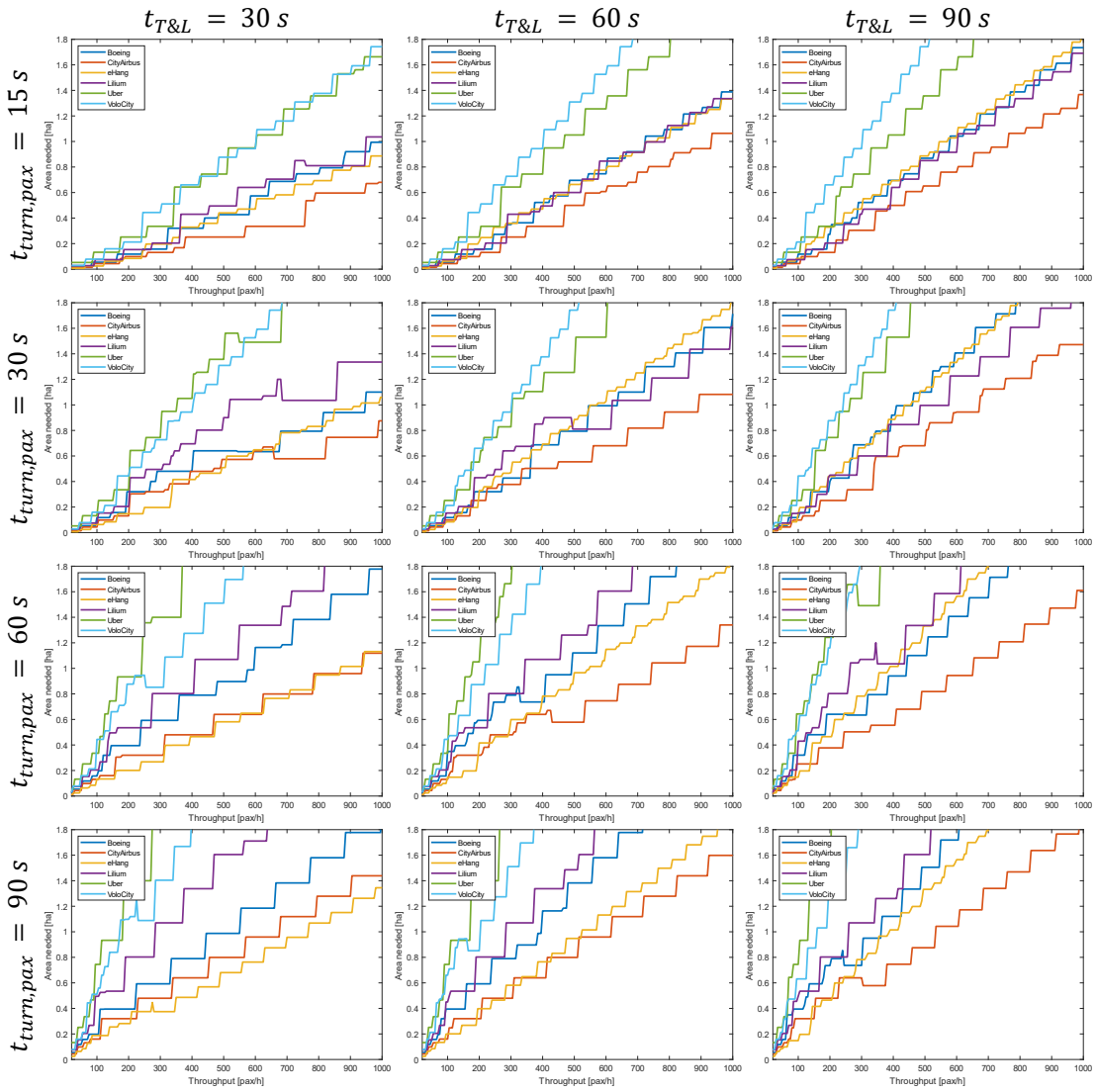

Figure 4.27: Comparison for area needed for different process times

Comparing the different plots, it can be seen that the vehicle of Airbus mostly gives the best results, followed by the vehicle of eHang, which is in line with the results from section 4.1.2. For short take-off and landing times in combination with increasing turnaround times, in some cases the vehicle of eHang is even better than the CityAirbus. This is due to the fact that because of the low passenger capacity and short take-off and landing time, more flights and thus overall a higher throughput can

be achieved. With increasing take-off and long times, it can also be observed that the performance of eHang deteriorates compared to Boeing and Lilium. Further examination of the Boeing and Lilium vehicles shows that the previously mentioned change also occurs when other process times are assumed. It should be noted, however, that it occurs earlier for shorter take-off and landing times and just as for increasing turnaround times. Further, it can be seen that for all constellations, the vehicle of Uber and the VoloCity provide the worst results, which is again in line with the results from section 4.1.2. In general, it can be observed that the longer the process times become, the larger the required areas become to achieve the desired throughputs. It should also be noted that longer take-off and landing times tend to favor vehicles with large passenger capacities. In contrast, vehicles with smaller passenger capacities are better suited for short take-off and landing times and long turnaround times.

5 Conclusion

After evaluating the results, it was shown that a functioning tool was developed with which it is possible to create feasible vertiport designs. Especially by applying it to the sites selected in Berlin, this can be confirmed.

Furthermore, the effects of different parameters on the resulting designs and expected throughputs can be investigated. Here it became apparent that by extending and detailing the area to throughput method, better insights into the effects of different framework parameters can be obtained. The first version of the method was severely limited in its freedom to deliver the best possible design by fixed constraints such as a maximum number of pads for the single or satellite topology and fixed gate to pad ratios. Although the extension to version 2 of the method has increased the degrees of freedom and thus provided more versatile results, it should be noted that a number of important parameters still remain unconsidered.

For example, the environment of the vertiports at the current stage of development is not taken into account. However, the environment has a great influence on how a vertiport should be designed. Especially regarding the position of the pads and the resulting approach and departure paths. For example, even if the space is available, no pads can be placed at certain locations because the approach is not possible due to surrounding buildings or unfavorable winds. Furthermore, the financial component as well as the infrastructure, which does not belong to the airfield, was left out. It was neglected that buildings are also needed for passenger handling or that some designs may generate high throughput but may not be financially viable.

Nevertheless, the results obtained enabled initial conclusions to be drawn that can play a key role in the future planning of vertiports. For example, some guidelines could already be derived, such as that for short turnaround times and long take-off and landing times, the single topology in particular has its strengths. However, this loses its advantages with increasing turnaround times and is replaced by the satellite, linear or pier topology. Which topology is the best choice here depends on the chosen vehicle.

It was not possible to provide fixed reference values for the throughput depending on a specific area, since the throughput depends on a large number of factors. Nevertheless, it was possible to specify guideline values for certain vehicles and frame parameters. Further, it was shown, for example, that vehicles with a large passenger capacity benefit from long fixed turnaround times. For example, a takeaway for the future would be that if problems such as long loading times of eVTOLS cannot be solved, vehicles with higher passenger capacities will provide the best results.

Based on the current results, the best vehicle for planning a vertiport seems to be the CityAirbus, as it provides the best results for most parameter constellations and thus gives a certain degree of planning certainty. However, it should also be noted here that the evaluation is based on the assumption of continuous demand, i.e., no empty flights or only with a partial load factor. Likewise, the turnaround time, which depends on the number of passengers, is determined by a fixed value per passenger. However, it can be the case that with increasing passenger capacity the assumed boarding and deboarding time per passenger decreases or can also increase. It would be possible that boarding one passenger would take one minute and boarding two passengers would take one and a half or even three minutes instead of the currently assumed two minutes. It should also be noted that a large number of parameters were not taken into account when considering the vehicles. The evaluation of the vehicles was based only on the size and passenger capacity of the vehicles. Thus, parameters such as range, travel speed, noise, safety, cost, etc. were not considered in the context of this thesis. However, a fully comprehensive evaluation of the vehicles is also only possible by simulating an entire UAM network, which would have exceeded the scope of this work.

Overall, it can be said that the work provides a good basis for further research into vertiport infrastructure, which can, however, still be refined in some areas. Also of advantage would be a mandatory regulation for vertiports, so that no further assumptions have to be derived from the already known commercial air traffic and heliport planning.

6 Summary

The thesis started with an introduction to the topic of UAM and showed its advantages and potential. Furthermore, it was explained that in order to exploit this potential, an development of the UAM infrastructure is necessary and that there is still a knowledge gap.

Furthermore, an overview of the state of the art was given. The infrastructure of a vertiport was presented in terms of the elements that make it up and how this can be constructed in the form of different topologies. In addition, due to the lack of guidelines for the planning and design of vertiports, it was discussed how this process is done for comparable infrastructure. Since vertiports can be defined as heliports with the passenger volume of a commercial airport, the design standards of a heliport according to FAA and ICAO were presented and an insight into the planning of an airport was given.

Subsequently, the methods developed in the course of this work were presented. First, however, a number of existing approaches and tools that have been developed for the design and planning of vertiports were presented in order to better classify the developed methods in the state of the art. Here it was shown that there are already approaches that support a siting of vertiports or even allow to simulate the processes that take place on them. However, there is not yet a method that makes it possible to automatically create the design of a vertiport for a given area. Here this work starts and develops a method based on a mixed integer programming approach, which allows to create a vertiport design from a given area under specification of different frame parameters and to calculate a possible throughput for it. Furthermore, a GUI was developed to visualize the calculated design. In the context of the work, the counterpart to the method just mentioned was also developed. This method calculates from a desired throughput how many pads and gates are needed in the context of a certain topology to achieve this throughput. In addition, the dimensions of the required area are output.

With these developed methods, sensitivity studies were subsequently carried out with the aim of determining the influence of different areas as well as vehicles and pro-

cess times on the throughput to be achieved and the choice of the topology to be used. In the study, the parameters were varied in such a way that a total of 29.92 million different combinations resulted. Among other things, the arrival and departure times as well as the turnaround times were varied, with the result that for most areas and also parameter combinations, the CityAirbus generates the highest throughputs. Depending on the process parameters and the available space, hourly throughputs of around 0.02 to 0.2 passengers per square meter can be achieved. In contrast, eHang's vehicle allows throughputs of up to 0.23 passengers per hour per square meter of area for small areas up to about 200 m^2. In addition, it was found that for short turnaround times per passenger, the single topology in particular delivers high throughputs. However, with increasing turnaround times, more gates are needed and therefore topologies such as the satellite, linear and pier topology gain importance. These can achieve gate to pad ratios of up to seven.

Furthermore, a real case scenario was run through in which a vertiport design was created for three locations in Berlin. The process parameters were defined beforehand and only the vehicles were varied in order to determine with which of the given vehicles the highest throughputs can be achieved for the designed UAM network. It was found that a total hourly throughput of 680 passengers per hour can be achieved in the network of three locations and the CityAirbus was selected as the best vehicle. In addition, this study visualized the designs using the developed GUI. The results proved that the designs proposed by the method are feasible.

Subsequently, a further study was carried out using the throughput to area method. In this study, the required areas were calculated for different passenger throughputs. A total of 197 throughputs from 20 to 1000 passengers per hour were examined. Here it was found that for most vehicles, for about 50 % of the cases, the linear topology required the least area to achieve the desired throughput. This was followed in importance by the single and satellite topologies. The pier topology was rarely suitable for achieving the desired throughputs with the smallest possible area. The CityAirbus also achieved the best results for this approach.

In the following, the results were discussed and it was found that they are suitable as

initial guidelines for the design of vertiports, but that further refinement of the methods is needed to make the results more precise and reliable. Possible ideas and approaches on how to achieve this are presented in the following chapter.

7 Outlook

As can be seen from chapter 5 'Conclusion', the developed methods already provide good results. These results can help to identify weak points in the planning and design of vertiports at an early stage. For example, a first vertiport design can be quickly created for a specific location, or a possible throughput can be directly derived, which can be used to determine the profitability of UAM to other means of transport or which aircraft should best be considered for the planning of the vertiport. In this context, it would also be desirable to extract a collection of guideline values with which it would be possible to directly deduce, with the knowledge of the size of an area, which throughput is to be expected, which tobology is most suitable and which type of vehicle is the best choice for high throughputs.

However, there is still room for improvement and extension, as some factors are not yet taken into account when creating the vertiport desing.

It would be conceivable to extend the area to throughput approach by an automated selection of suitable areas from OpenStreetMap (OSM) and a deep learning approach for the recognition of roof areas (see Krapf et al. [119]). This would make it possible to specify an area in which a vertiport is to be constructed and the program would automatically search for areas with a suitable size from OSM and use deep learning to recognize whether the roof area is free for construction projects. Furthermore, it would even be possible to select parking garages for these investigations using the tags stored in OSM. This approach would also have the advantage that surrounding buildings and other obstacles can be taken into account in the design of the vertiport, as these can be detected by computer vision.

Another plus point would be if the local weather conditions and especially the wind can be taken into account during the design creation, since this has an influence on the approach and departure paths of the vehicles, as usually the landing area should be approached against the wind.

Furthermore, it would be a gain if not only the airfield would be dimensioned, but the complete vertiport, for example also the necessary terminals as well as waiting areas

for the passengers.

In terms of determining potential throughputs, it would also be interesting to implement the demand of a particular region for UAM travel and not assume $100\ \%$ utilization. In addition, studies can be done to determine actual boarding and deboarding times or studies on charging times or the duration of security checks on the vehicle.

Another aspect that would add value to the analysis of the vertiport infrastructure is the cost. It would be interesting to know how much it would cost to install a gate or pad and optimize the vertiport not only in terms of throughput, but also in terms of the cost of construction. Since costs are usually the driving factor in the development of new technologies and thus deserve special attention.

In the area of visualization, it would be interesting to further automate this so that the individual elements are automatically placed in the best possible position and thus do not require human intervention. Another possible extension would be the creation of 3D designs as it would be possible with a CAD library [120].

The next step in developing the method would be to implement it in a comprehensive design pipeline. That is, an automated pipeline that selects sites, creates a vertiport design for them, visualizes these designs, and then simulates the resulting vertiport network and the individual vertiports within it. This would allow for a much larger set of variables to be considered in vertiport design and, in the future, for larger-scale studies in which infrastructure planning is done for entire cities or regions. These data can strengthen the acceptance of UAM in the population, as well as make the field of UAM infrastructure more accessible for investors and thus lay the foundation for a functioning UAM network of the future.

Bibliography

[1] The World Bank, “Urban Developement,” 2020. https://www.worldbank.org/en/topic/urbandevelopment/overview text#1.

[2] altran, “EN-Route to Urban Air Mobility: On the fast track to viable and safe on-demad air services,” 2020.

[3] US EPA, Sources of Greenhouse Gas Emissions | US EPA, 2015. https://www.epa.gov/ghgemissions/sources-greenhouse-gas-emissions (accessed: Mar. 31 2021).

[4] Cambridge Systematics, Inc., “Traffic Congestion and Reliability: Linking Solutions to Problems,” 2004.

[5] C. Adams, “London drivers spend 227 hours each year in traffic,” The Independent, 12 Feb., 2019. https://www.independent.co.uk/travel/news-and-advice/london-uk-most-congested-cities-traffic-hours-driving-roads-busy-birmingham-glasgow-manchester-a8775056.html (accessed: Mar. 31 2021).

[6] TomTom, Traffic congestion ranking | TomTom Traffic Index, 2021. https://www.tomtom.com/en_gb/traffic-index/ranking/ (accessed March 31, 2021).

[7] C. Brown, D. Das, M. Ahmed, and J. Anderson, “Aviation 2030: Disruption beyond COVID-19,” 2020.

[8] D. Schrank, B. Eisele, and T. Lomax, “2019 URBAN MOBILITY REPORT,” Texas Department of Transportation, 2019.

[9] CEBR, 50% Rise in Gridlock Costs by 2030, 2014. https://cebr.com/reports/the-future-economic-and-environmental-costs-of-gridlock/ (accessed Mar 31, 2021).

[10] C. M. Hoehner, C. E. Barlow, P. Allen, and M. Schootman, “Commuting distance, cardiorespiratory fitness, and metabolic risk,” American journal of preventive medicine, vol. 42, no. 6, pp. 571–578, 2012, doi: 10.1016/j.amepre.2012.02.020.

[11] J. Holden and N. Goel, “Fast-Forwarding to a Future of On-Demand Urban Air Transportation,” Uber Elevate, 2016.

[12] EIT, A European initiative to create liveable urban spaces, 2020. https://www.eiturbanmobility.eu/ (accessed Mar 31, 2021).

[13] H. Ritchie and M. Roser, “Urbanization,” Our World in Data, 2018. [Online]. Available: https://ourworldindata.org/urbanization#how-many-people-will-live-in-urban-areas-in-the-future

[14] Lilium Blog, Designing a scalable vertiport, 2020. https://lilium.com/newsroom-detail/designing-a-scalable-vertiport.

[15] M. Dodge and R. Brook, Infrastructure and the rebuilt city after the Second World War: Helicopter dreaming: the unrealised plans for city centre heliports in the post-war period. Birmingham, 2014.

[16] K. Hulme et al., “The Flying Car -Emergent Modeling & Simulation (M&S) Policies and Standards concerns,” in 2019.

[17] M. Taylor, A. Saldanli, and A. Park, “Design of a Vertiport Design Tool,” in 2020 Integrated Communications Navigation and Surveillance Conference (ICNS), Herndon, VA, USA, 2020, 2A2-1-2A2-12, doi: 10.1109/ICNS50378.2020.9222989.

[18] F. Reuter and R. Griemens, “The roadmap to scalable urban air mobility: White paper 2.0,” Mannheim DE257583335, 2021.

[19] W. Choi and S. Hampton, “Scenario-Based Strategic Planning for Future Civil Vertical Take-off and Landing (VTOL) Transport,” JAAER, 2020, doi: 10.15394/jaaer.2020.1808.

[20] A. Anand, H. Kaur, C. Y. Justin, T. Zaidi, and D. N. Mavris, “A Scenario-Based Evaluation of Global Urban Air Mobility Demand,” in AIAA Scitech 2021 Forum, VIRTUAL EVENT, 2021, doi: 10.2514/6.2021-1516.

[21] T. Duvall, A. Green, M. Langstaff, and K. Miele, “Air-mobility solutions: What they’ll need to take off,” 2019. https://www.mckinsey.com/∼/media/McKinsey/Industries/Capital%20Projects%20and%20Infrastructure/Our%20Insights/Air%20mobility%20solutions%20The%20infrastructure%20challenges%20ahead/Air-mobility-solutions.ashx.

[22] M. Hader, S. Baur, S. Kopera, T. Schönberg, and J.-P. Hasenberg, “Urban Air Mobility: USD 90 billion of potential: How to capture a share of the passenger drone market,” München, 2020. https://www.rolandberger.com/en/Insights/Publications/The-high-flying-industry-Urban-Air-Mobility-takes-off.html.

[23] Morgan Stanley Research, “Flying Cars: Investment Implications of Autonomous Urban Air Mobility,” 2018. https://www.morganstanley.com/ideas/autonomous-aircraft.

[24] Booz Allen Hamilton, “UAM Market Study - Technical Out Brief,” 2018.

[25] EHang, “EHang Holdings Limited: Investor Presentation,” 2020.

[26] E. Xu, “The Future of Transportation: White Paper on Urban Air Mobility Systems,” 2020.

[27] K. O. Ploetner et al., “Long-term application potential of urban air mobility com-

plementing public transport: an upper Bavaria example," CEAS aeronautical journal, pp. 1–17, 2020, doi: 10.1007/s13272-020-00468-5.

[28] V. Agouridas, "EIP-SUM-AC UAM Initiative," 2018. https://smart-cities-marketplace.ec.europa.eu/action-clusters-and-initiatives/action-clusters/sustainable-urban-mobility/urban-air-mobility-uam.

[29] L. Gipson, "Advanced Air Mobility National Campaign Overview," 2021. https://www.nasa.gov/aeroresearch/aam/description/.

[30] European Commission, What is Horizon 2020? - Horizon 2020 - European Commission, 2014. https://ec.europa.eu/programmes/horizon2020/what-horizon-2020#Article (accessed: Apr. 1 2021).

[31] European Commission, Towards sustainable urban air mobility: Publication Office/CORDIS, 2019. https://cordis.europa.eu/programme/id/H2020_MG-3-6-2020 (accessed: Apr. 1 2021).

[32] M. N. Postorino and G. M. L. Sarné, "Reinventing Mobility Paradigms: Flying Car Scenarios and Challenges for Urban Mobility," Sustainability, vol. 12, no. 9, p. 3581, 2020, doi: 10.3390/su12093581.

[33] BMVI, KI-basierte Planung von Vertiports und Vertistops unter Berücksichtigung der Anforderungen für urbane Start- und Landeplätze – INCity TakeOff, 2020. https://www.bmvi.de/SharedDocs/DE/Artikel/DG/UAV-Projekte/incity-takeoff.html.

[34] M. Klarner, Mobilität in der 3. Dimension: In der Region Ingolstadt soll die städtische Mobilität der Zukunft erprobt werden. Ingolstadt, 2018.

[35] P. Butterworth-Hayes, "The Global Urban Air Mobility project report," 2019. https://www.urbanairmobilitynews.com/wp-content/uploads/2019/03/Global-Urban-Air-Mobility-Report-7-March-2019.pdf.

[36] BMVI, eVertical-Start und Lande-Infrastruktur für Lufttaxis - EDMO-TUEF-VERTILU, 2019. https://www.bmvi.de/SharedDocs/DE/Artikel/DG/UAV-Projekte/edmo-tuef-vertilu.html.

[37] BMVI, Flughafen Köln/Bonn Flugtaxi Infrastruktur - FKBFTI, 2019. https://www.bmvi.de/SharedDocs/DE/Artikel/DG/UAV-Projekte/flughafen-koeln-bonn-flugtaxi-infrastruktur.html.

[38] BMVI, Studie zur Akzeptanz von Lufttaxis im urbanen Raum - AirTaxiS, 2019. https://www.bmvi.de/SharedDocs/DE/Artikel/DG/UAV-Projekte/airtaxis.html.

[39] O. Klug and T. Fröhlich, Uber Air-Lufttaxis: Uber präsentiert neue Partnerschaften, erste Kabine-Designs sowie Uber Copter als ersten Flugservice in New York | Uber Newsroom, 2019. https://www.uber.com/de/newsroom/elevate-summit-2019/ (accessed: Apr. 3 2021).

[40] R. Lineberger, A. Hussain, M. Metcalfe, and V. Rutgers, “Infrastructure barriers to the elevated future of mobility: Are cities ready with the infrastructure needed for urban air transportation?,” Deloitte, 2019.

[41] E. Feldhoff and G. Soares Roque, “Determining Infrastructure Requirements for an Air Taxi Service at Cologne Bonn Airport,” 2020. http://www.via.rwth-aachen.de/downloads/DLRK2020_530069_paper.pdf.

[42] D. F. Finger, F. Götten, C. Braun, and C. Bil, “Initial Sizing for a Family of Hybrid-Electric VTOL General Aviation Aircraft,” 2018, doi: 10.25967/480102.

[43] D. P. Thipphavong et al., “Urban Air Mobility Airspace Integration Concepts and Considerations,” in 18th AIAA Aviation Technology, Integration, and Operations Conference 2018: Atlanta, Georgia, USA, 25-29 June 2018 : held at the AIAA Aviation Forum 2018, Atlanta, Georgia, 2018, doi: 10.2514/6.2018-3676.

[44] R. Whittle, “Air Mobility Bonanza Beckons Electric VTOL Developers,” 2017.

[45] P. Nathen, “Architectural performance assessment of an electric vertical take-off and landing (e-VTOL) aircraft based on a ducted vectored thrust concept,” 2021.

[46] P. Pradeep and P. Wei, “Energy-Efficient Arrival with RTA Constraint for Multi-rotor eVTOL in Urban Air Mobility,” Journal of Aerospace Information Systems, vol. 16, no. 7, pp. 263–277, 2019, doi: 10.2514/1.I010710.

[47] A. Bacchini and E. Cestino, “Electric VTOL Configurations Comparison,” Aerospace, vol. 6, no. 3, p. 26, 2019, doi: 10.3390/aerospace6030026.

[48] E. S. Hendricks et al., “Multidisciplinary Optimization of a Turboelectric Tiltwing Urban Air Mobility Aircraft,” in AIAA Aviation 2019 Forum, Dallas, Texas, 2019, doi: 10.2514/6.2019-3551.

[49] M. D. Moore, “The joby S2 VTOL concept: Exploring the new degrees of design freedom of distributed electric propulsion,” vol. 60, pp. 22–24, 2014.

[50] A. M. Stoll, E. V. Stilson, J. Bevirt, and P. P. Pei, “Conceptual Design of the Joby S2 Electric VTOL PAV,” in 14th AIAA Aviation Technology, Integration, and Operations Conference, Atlanta, GA, 2014, doi: 10.2514/6.2014-2407.

[51] E. Allen and R. W. Simpson, “Ground facilities for a VTOL intercity air transportation system,” Department of Aeronautics and Astronautics, 1970.

[52] R. de Neufville, A. R. Odoni, P. Belobaba, and T. Reynolds, Airport systems: Planning, design, and management, 2nd ed. New York: McGraw-Hill, 2013.

[53] D. Stewart, “Airport Master Planning – Process & Update,” International Civil Aviation Organization (ICAO) Document 9184, 2018.

[54] A. Blumstein, “The Landing Capacity of a Runway,” Operations Research, vol. 7, no. 6, pp. 752–763, 1959, doi: 10.1287/opre.7.6.752.

[55] IATA, Airport development reference manual, 9th ed. Montreal, 2004.

[56] NATA, “Urban Air Mobility: Considerations for Vertiport Operation,” 2019.

[57] S. Bradford, “Concept of Operations: Urban Air Mobility (UAM),” Washington, 2020.

[58] P. Whitley, “Concept of Operations: Unmanned Aircraft System (UAS) Traffic Management (UTM),” Washington, 2020.

[59] P. Kopardekar, “Unmanned Aerial System (UAS) Traffic Management (UTM): Enabling Low-Altitude Airspace and UAS Operations,” 20140013436, 2014.

[60] P. Kopardekar, T. Prevot, J. Rios, J. E. Robinson III, M. Johnson, and J. Jung, “UAS Traffic Management (UTM) Concept of Operations to Safely Enable Low Altitude Flight Operations,” in AIAA Aviation: 16th AIAA Aviation Technology, Integration, and Operations Conference, Washington, D.C, 2016.

[61] P. Kopardekar, “Unmanned Aerial System (UAS) Traffic Management (UTM): Enabling Low-Altitude Airspace and UAS Operations,” 20140013436, 2014.

[62] T. Jiang, J. Geller, D. Ni, and J. Collura, “Unmanned Aircraft System traffic management: Concept of operation and system architecture,” 2046-0430, vol. 5, no. 3, pp. 123–135, 2016, doi: 10.1016/j.ijtst.2017.01.004.

[63] D. Geister and B. Korn, “Concept for Urban Airspace Integration DLR U-Space Blueprint: Integrating UAS into the future aviation system,” Institute of Flight Guidance, 2017.

[64] S. Kern, D. Geister, N. Peinecke, and B. Korn, “Demonstration of Traffic Management in Urban Airspace,” Institute of Flight Guidance, 2018.

[65] M. M. Cohen, “The Vertiport as an Urban Design Problem,” in SAE Technical Paper Series, 1996.

[66] D. J. Peisen and B. Sawyer, “Heliport/Vertiport MLS Precision Approaches,” 1994. http://www.tc.faa.gov/its/worldpac/techrpt/rd94-23.pdf.

[67] Peisen, D. J., Sampson, W. T., LaBelle, L. J., Sawyer, B., Ludders, R., Berardo, S., Dyment, R., Ferguson, S. W., Winick, R., and Bragdon, C., “Analysis of Vertiport Studies Funded by the Airport Improvement Program (AIP),” 1994. https://apps.dtic.mil/dtic/tr/fulltext/u2/a283249.pdf.

[68] D. J. Peisen and S. W. Ferguson, “Vertiport Design Characteristics for Advanced Rotorcraft Technology,” SAE Transactions, vol. 105, pp. 1313–1319, 1996. http://www.jstor.org/stable/44725620.

[69] Y.-M. Kim, P. Schonfeld, and J. Rakas, “Vertiport Capacity - Analysis Methods,” University of Maryland ADA298361, 1995.

[70] L. E. Mudd, “Vertiport Design (Cancelled),” AAS-100, Office of Airport Safety & Standards - Airport Engineering Division AC 150/5390-3, 1991.

[71] M. J. O’Donnell, “Heliport Design,” AAS-100, Office of Airport Safety & Standards - Airport Engineering Division AC 150/5390-2C, 2012.

[72] ICAO, “Heliport Manual: Volume II - Heliports,” Doc 9261-AN/903, 1995.

[73] ICAO, “Aerodromes - Annex 14: Volume II - Heliports,” 2009.

[74] ICAO, “Heliport Manual,” Doc 9261-AN/903, 2020.

[75] ICAO, “Aerodrome Design Manual: Part 2 – Taxiways, Aprons and Holding Bay,” Doc 9157-AN/901 Part 2, 2020.

[76] EASA, “Certification Specifications and Guidance Material for the design of

surface-level VFR heliports located at aerodromes that fall under the scope of Regulation (EU) 2018/1139," 2019.

[77] R. L. Mahr, "CVN FLIGHT/HANGAR DECKNATOPS MANUAL," NAVAIR 00-80T-120, 2010.

[78] C. M. Scaparrotti, "Joint Shipboard Helicopter and Tiltrotor Aircraft Operations," 2012.

[79] D. Schmaglowski and E. Mazeikis, "HELICOPTER OPERATIONS FROMSHIPS OTHER THAN AIRCRAFTCARRIERS (HOSTAC)," 2017.

[80] International Code Council, 2012 International fire code. Country Club Hills, IL: International Code Council, 2012.

[81] NFPA 418 - Standard for Heliports Scope, NFPA 418 - Standard for Heliports Scope, National Fire Protection Association (NFPA), 2021. [Online]. Available: https://www.nfpa.org/codes-and-standards/all-codes-and-standards/list-of-codes-and-standards/detail?code=418

[82] International Code Council, 2012 International Building Code: 2012 IBC ; a member of the International Code Family. Country Club Hills, Ill.: International Code Council, 2011.

[83] Caltrans, Ed., "California Airport Land Use Planning Handbook," State of California Department of Tarnsportation Division of Aeronautics, 2011.

[84] N. J. Ashford, S. A. Mumayiz, and P. H. Wright, Airport engineering: Planning, design, and development of 21st century airports. Hoboken, New Jersey: John Wiley & Sons, 2011. [Online]. Available: http://search.ebscohost.com/login.aspx?direct=true&scope=site&db=nlebk&db=nlabk&AN=364272, doi: 10.1002/9780470950074.

[85] P. Galis, “Airport Environmental Handbook,” APP-600, Office of Airport Safety & Standards - Airport Engineering Division 5050.4 A, 2006.

[86] R. Swayze, “Policies and Procedures for Considering Environmental Impacts,” AEE-400 Order 1050.1F, 2015.

[87] S. Salzwedel and D. Tutt, ““Innovation” podcast series (Ep. 3): eVTOL Power Density and Thermal Management,” Talking Aerospace Today, 2021. [Online]. Available: https://blogs.sw.siemens.com/podcasts/talking-aerospace-today/innovation-podcast-series-ep-3-evtol-power-density-and-thermal-management/

[88] L. Preis, “Quick Sizing, Throughput Estimating and Layout Planning for VTOL Aerodromes – A Methodology for Vertiport Design,” in AIAA AVIATION 2021 FORUM, doi: 10.2514/6.2021-2372.

[89] P. D. Vascik and R. J. Hansman, “Development of Vertiport Capacity Envelopes and Analysis of Their Sensitivity to Topological and Operational Factors,” in AIAA Scitech 2019 Forum, San Diego, California, 2019, doi: 10.2514/6.2019-0526.

[90] ICAO, “Operation of Aircraft - Anex 6: Part III - International Operations - Helicopters,” AN 6-3, 2018.

[91] L. W. Kohlman and M. D. Patterson, “System-Level Urban Air Mobility Transportation Modeling and Determination of Energy-Related Constraints,” in 18th AIAA Aviation Technology, Integration, and Operations Conference 2018: Atlanta, Georgia, USA, 25-29 June 2018 : held at the AIAA Aviation Forum 2018, Atlanta, Georgia, 2018, doi: 10.2514/6.2018-3677.

[92] K. Lippoldt, L. Preis, and K. Bogenberger, “Vertiport Locating and Sizing Method using Mobility Data and Heliport Design Guidelines,” 2020.

[93] A. Amirzada, “Implementation of a Simulation Framework for Vertiport Ground Operations in the Context of Urban Air Mobility,” Master Thesis, Institute for Aircraft Design, Technical University of Munich, München, 2021.

[94] A. Horni, K. Nagel, and K. W. Axhausen, The Multi-Agent Transport Simulation MATSim. s.l.: Ubiquity Press, 2016.

[95] P. Glaab, F. Wieland, M. Santos, R. Sharma, and P. U. Lee, “Simulating Fleet Noise for Notional UAM Vehicles and Operations in New York,” in 2019 IEEE/AIAA 38th Digital Avionics Systems Conference (DASC), 2019, pp. 1–10. [Online]. Available: https://www.researchgate.net/publication/341076135_Simulating_Fleet_Noise_for_Notional_UAM_Vehicles_and_Operations_in_New_York, doi: 10.1109/DASC43569.2019.9081670.

[96] N. M. Guerreiro, R. W. Butler, J. M. Maddalon, and G. E. Hagen, “Mission Planner Algorithm for Urban Air Mobility – Initial Performance Characterization,” in AIAA Aviation 2019 Forum, Dallas, Texas, 2019, doi: 10.2514/6.2019-3626.

[97] N. M. Guerreiro, G. E. Hagen, J. M. Maddalon, and R. W. Butler, “Capacity and Throughput of Urban Air Mobility Vertiports with a First-Come, First-Served Vertiport Scheduling Algorithm,” in AIAA AVIATION 2020 FORUM, VIRTUAL EVENT, 2020, doi: 10.2514/6.2020-2903.

[98] I. C. Kleinbekman, M. Mitici, and P. Wei, “Rolling-Horizon Electric Vertical Takeoff and Landing Arrival Scheduling for On-Demand Urban Air Mobility,” Journal of Aerospace Information Systems, vol. 17, no. 3, pp. 150–159, 2020, doi: 10.2514/1.I010776.

[99] M., Niklaß, N., Dzikus, M., Swaid, J., Berling, B., Lührs, A., Lau, I., Terekhov, and V., Gollnick, “A Collaborative Approach for an Integrated Modeling of Urban Air Transportation Systems,” Aerospace, vol. 7, no. 5, 2020, doi:

10.3390/aerospace7050050.

[100] R. Rothfeld, M. Balac, and C. Antoniou, “Modelling and evaluating urban air mobility – an early research approach,” Transportation Research Procedia, vol. 41, pp. 41–44, 2019, doi: 10.1016/j.trpro.2019.09.007.

[101] X. Yang, L. Deng, and P. Wei, “Multi-Agent Autonomous On-Demand Free Flight Operations in Urban Air Mobility,” in AIAA Aviation 2019 Forum, Dallas, Texas, 2019, doi: 10.2514/6.2019-3520.

[102] S. Rath and J. Y. J. Chow, “Air Taxi Skyport Location Problem for Airport Access,” Apr. 2019. [Online]. Available: https://arxiv.org/pdf/1904.01497

[103] S. Rajendran and J. Zack, “Insights on strategic air taxi network infrastructure locations using an iterative constrained clustering approach,” Transportation Research Part E: Logistics and Transportation Review, vol. 128, pp. 470–505, 2019, doi: 10.1016/j.tre.2019.06.003.

[104] S. Arellano, “A Data- and Demand-Based Approach at Identifying Accessible Locations for Urban Air Mobility Stations,” Masterthesis, Department of Civil, Geo, and Environmental Engineering, Technical University of Munich, München, 2020.

[105] D. N. Fadhil, “A GIS-based Analysis for Selecting Ground Infrastructure Locations for Urban Air Mobility,” Master Thesis, Department of Civil, Geo, and Environmental Engineering, Technical University of Munich, München, 2018. [Online]. Available: https://www.bgu.tum.de/fileadmin/w00blj/msm/theses/fadhil_2018.pdf

[106] D. N. Fadhil, R. Moeckel, and R. Rothfeld, “GIS-based Infrastructure Requirement Analysis for an Electric Vertical Take-off and Landing Vehicle-based Transportation System,” Transportation Research Procedia, vol. 41, pp. 101–103, 2019, doi: 10.1016/j.trpro.2019.09.020.

[107] J. N. Robinson, M.-D. R. Sokollek, C. Y. Justin, and D. N. Mavris, “Development of a Methodology for Parametric Analysis of STOL Airpark Geo-Density,” in 18th AIAA Aviation Technology, Integration, and Operations Conference 2018: Atlanta, Georgia, USA, 25-29 June 2018 : held at the AIAA Aviation Forum 2018, Atlanta, Georgia, 2018, doi: 10.2514/6.2018-3054.

[108] QGIS Development Team, “QGIS Geographic Information System,” 2009. [Online]. Available: http://qgis.osgeo.org/

[109] VBG, “Fachinfoblatt:Pkw-Stellplatz-Flächen,” 2013. https://www.vbg.de/SharedDocs/Medien-Center/DE/Faltblatt/Themen/Arbeitsstaetten_gestalten/fi_pkw_stell.html.

[110] S. P. Bradley, A. C. Hax, and T. L. Magnanti, Applied mathematical programming, 19th ed. Reading, Mass.: Addison-Wesley, 1992. [Online]. Available: http://web.mit.edu/15.053/www/AMP.htm

[111] T. H. Nguyen, S. Daniel, D. Guériot, C. Sintès, and J.-M. Le Caillec, “UNSUPERVISED AUTOMATIC BUILDING EXTRACTION USING ACTIVE CONTOUR MODEL ON UNREGISTERED OPTICAL IMAGERY AND AIRBORNE LIDAR DATA,” Int. Arch. Photogramm. Remote Sens. Spatial Inf. Sci., XLII-2/W16, pp. 181–188, 2019, doi: 10.5194/isprs-archives-XLII-2-W16-181-2019.

[112] H. Wang, Q. Meng, and X.-N. Zhang, “Park-and-Ride Network Equilibrium with Heterogeneous Commuters and Parking Space Constraint,” Transportation Research Record, vol. 2466, no. 1, pp. 87–97, 2014, doi: 10.3141/2466-10.

[113] K. Song, H. Yeo, and J.-H. Moon, “Approach Control Concepts and Optimal Vertiport Airspace Design for Urban Air Mobility (UAM) Operation,” Int. J. Aeronaut. Space Sci., vol. 22, no. 4, pp. 982–994, 2021, doi: 10.1007/s42405-020-00345-9.

[114] Volocopter GmbH, “VoloCity - Design specifications,” 2019.

[115] A. Thai, S. Grace, J. Sitaraman, and B. Roget, “Multirotor Trim using Loose Aerodynamic Coupling,” in 2020.

[116] Š. Klein, “Specification AeroMobil 3.0,” Viena, 2014.

[117] S. Zelinski, “Operational Analysis of Vertiport Surface Topology,” in 2020 AIAA/IEEE 39th Digital Avionics Systems Conference (DASC), San Antonio, TX, USA, 2020, pp. 1–10, doi: 10.1109/DASC50938.2020.9256794.

[118] Google LLC, Map and route of Berlin: Google LLC, 2005. https://www.google.de/maps (accessed August 18, 2021).

[119] S. Krapf, N. Kemmerzell, S. Khawaja Haseeb Uddin, M. Hack Vázquez, F. Netzler, and M. Lienkamp, “Towards Scalable Economic Photovoltaic Potential Analysis Using Aerial Images and Deep Learning,” Energies, vol. 14, no. 13, p. 3800, 2021, doi: 10.3390/en14133800.

[120] A. Rapisarda, Heliport CAD library: GrabCAD, 2015. [Online]. Available: https://grabcad.com/library/heliport-1

Eigenständigkeitserklärung

Hiermit versichere ich, dass ich die vorliegende Arbeit selbstständig und ausschließlich unter Zuhilfenahme der im Literaturverzeichnis angegebenen Quellen angefertigt habe. Aus anderen Publikationen und Veröffentlichungen entnommenen Ideen, Abbildungen und Textstellen sind als solche direkt kenntlich gemacht. Die Arbeit ist in gleicher oder ähnlicher Form noch keiner Prüfungsbehörde vorgelegt worden.

Garching, den 01. September 2021

Vorname Nachname

A Appendix: Vertiport Layouts

Here is a collection of different assumed vertiport layouts.

A.1 Layouts Single Topology

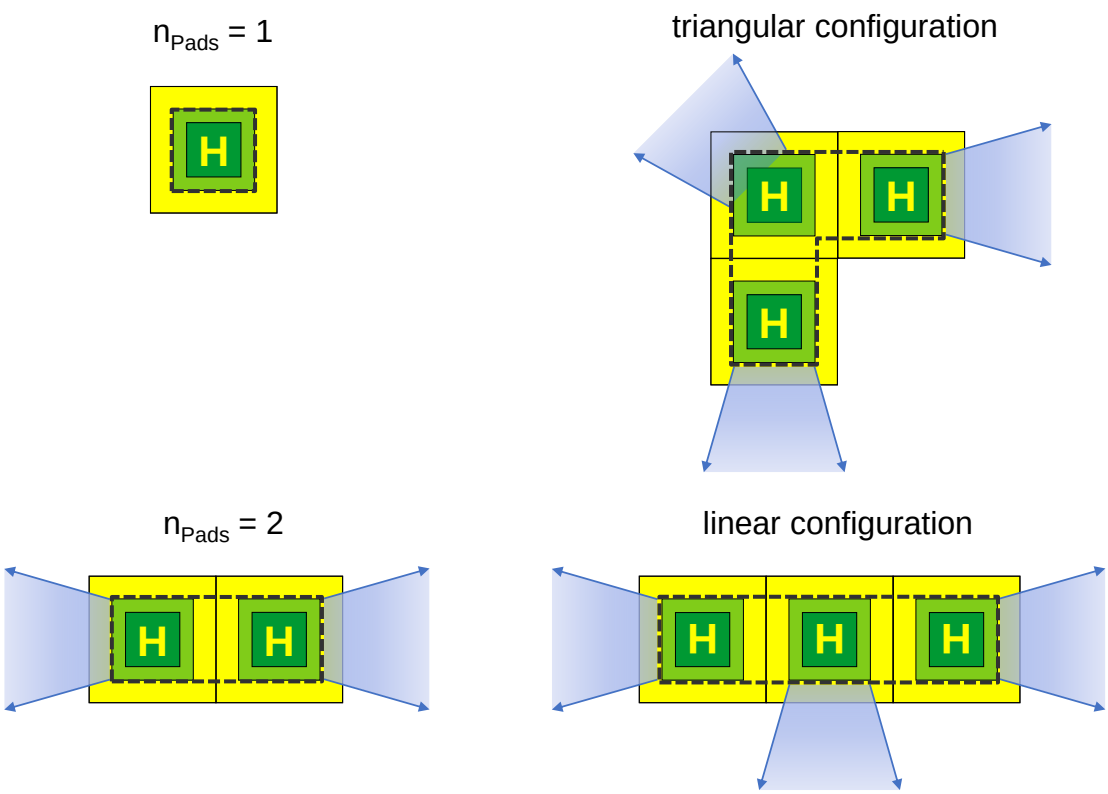

Figure A.1: Layouts single topology for one, two and three pads

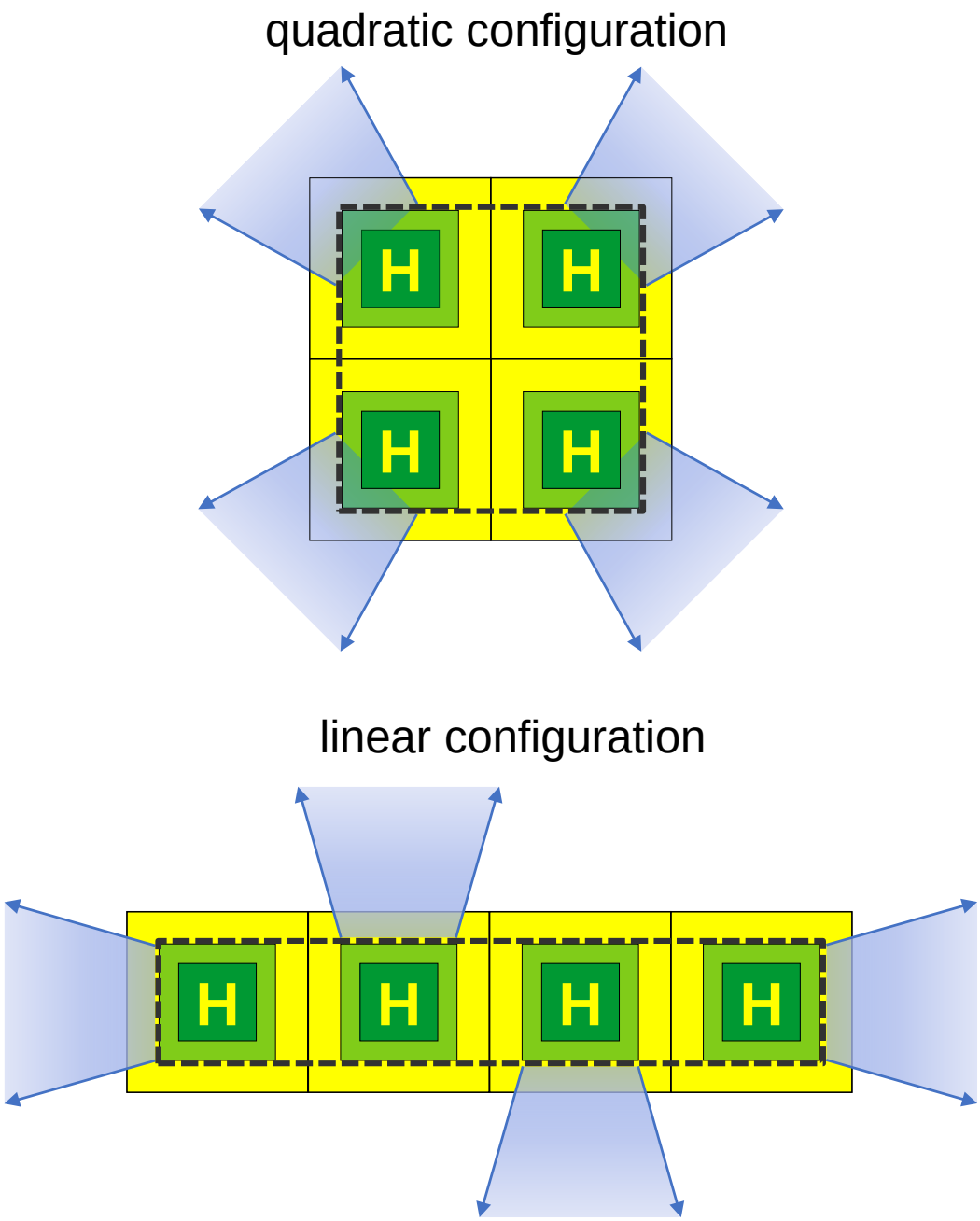

Figure A.2: Layouts single topology for four pads

A.2 Layouts Satellite Topology

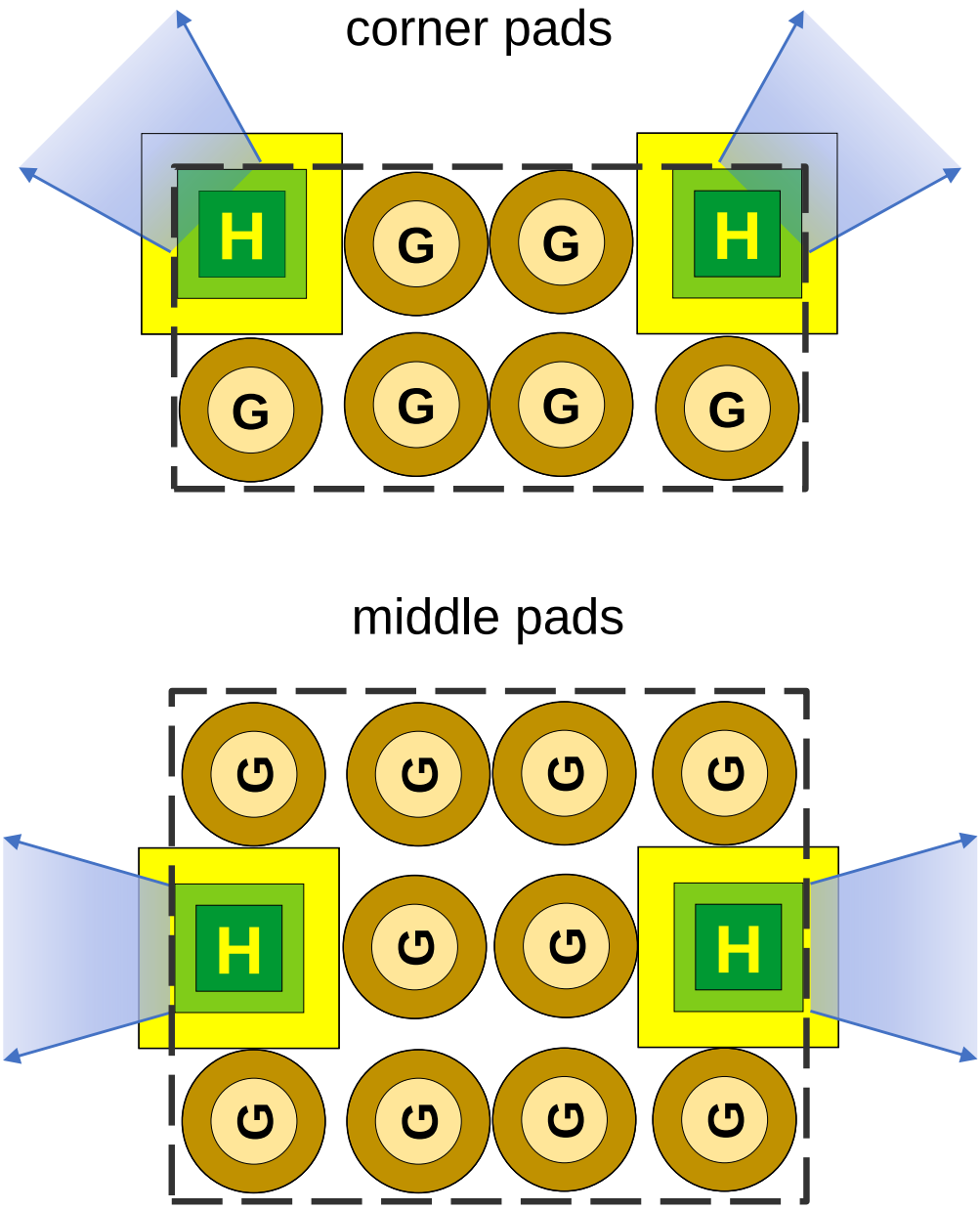

Figure A.3: Layouts satellite topology for two pads

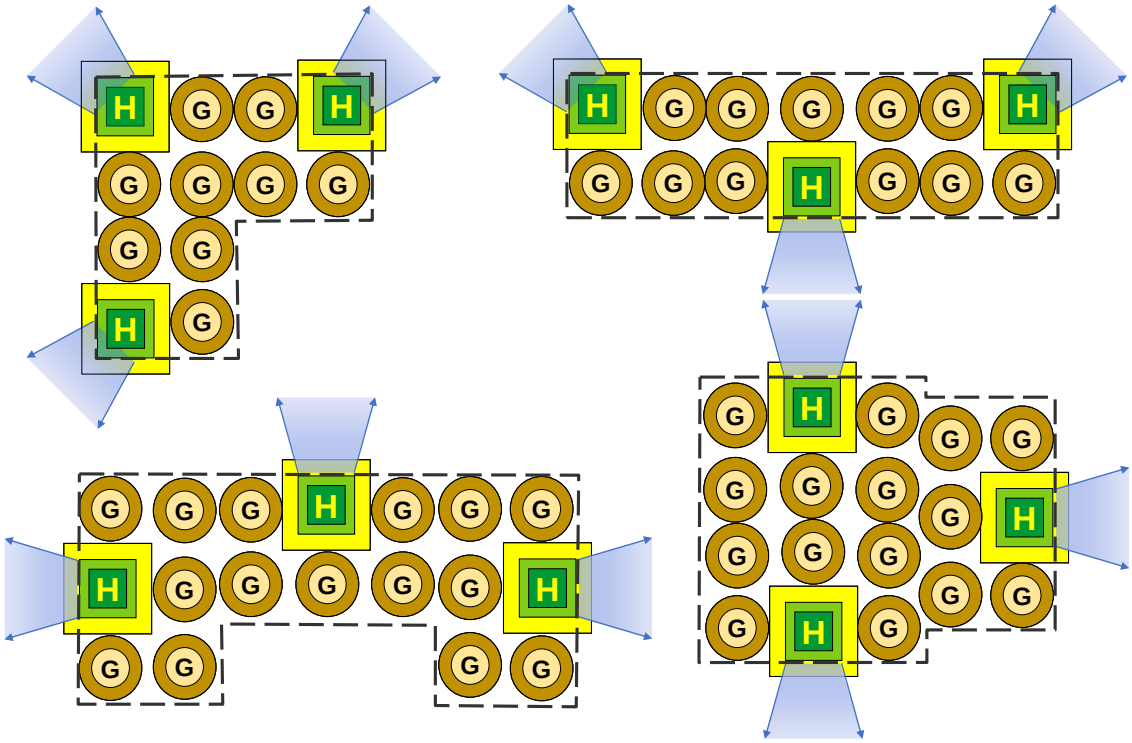
H
G
G
H
G
G
G
G
G
G
H
G
H
G
G
G
G
G
H
G
G
G
H
G
G
G
G
G
H
G
G
G
G
G
H
G
G
G
G
G
H
G
G
G
G
G
H
G
G
G
G
G
G

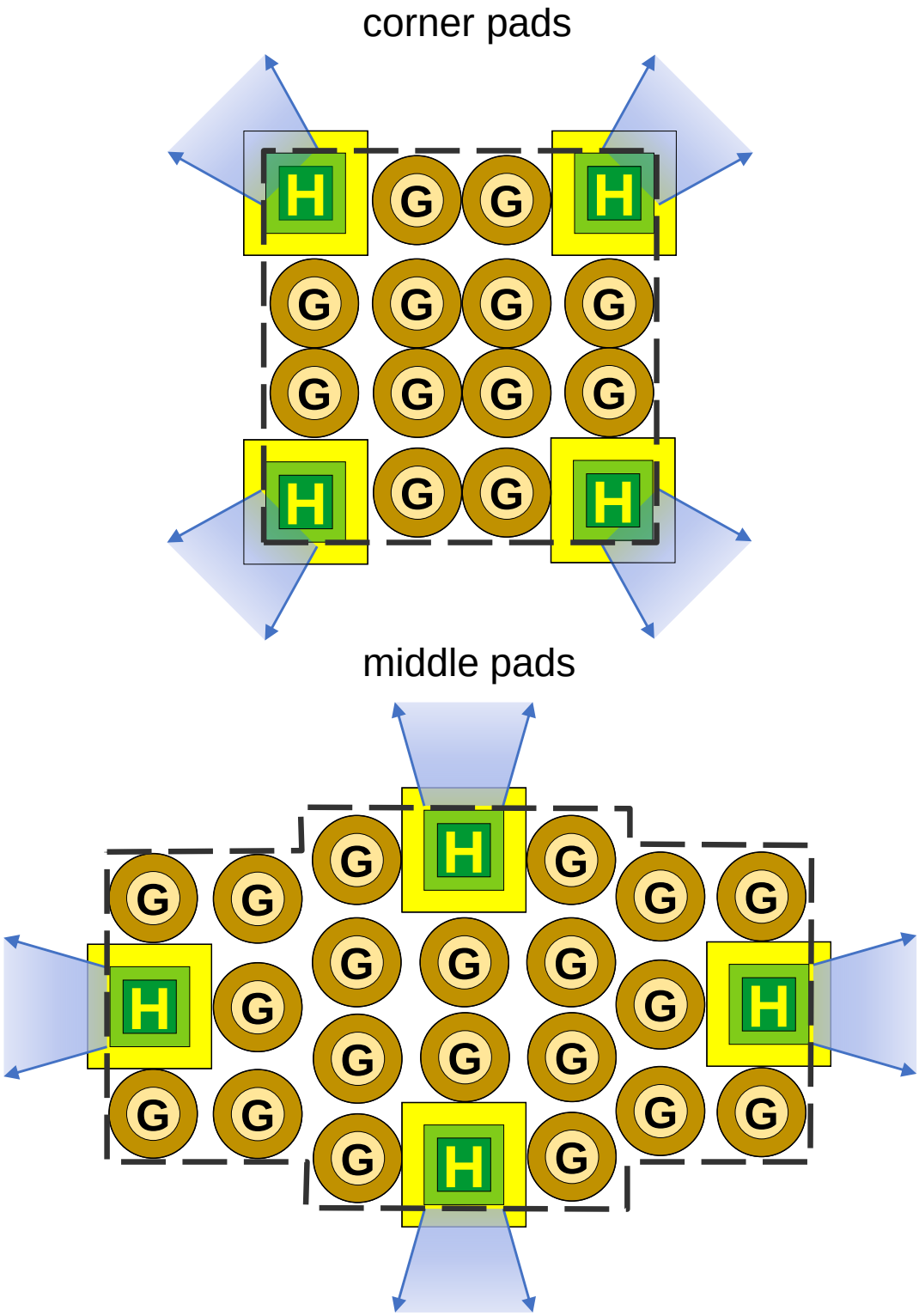

Figure A.5: Layouts satellite topology for four pads in quadratic configuration

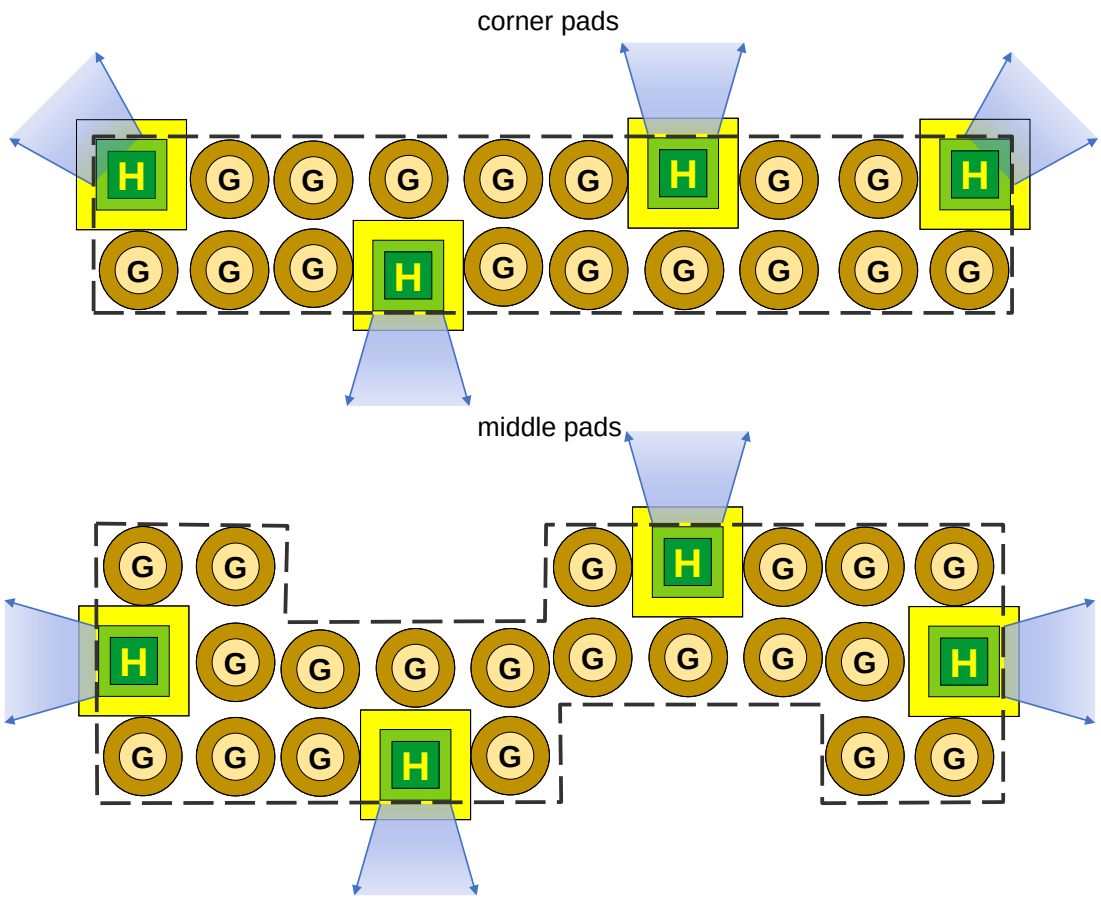

Figure A.6: Layouts satellite topology for four pads in linear configuration

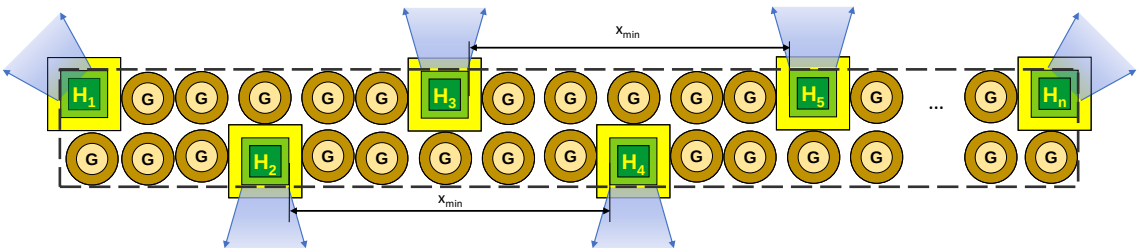

Figure A.7: Layouts satellite topology for n pads in linear configuration

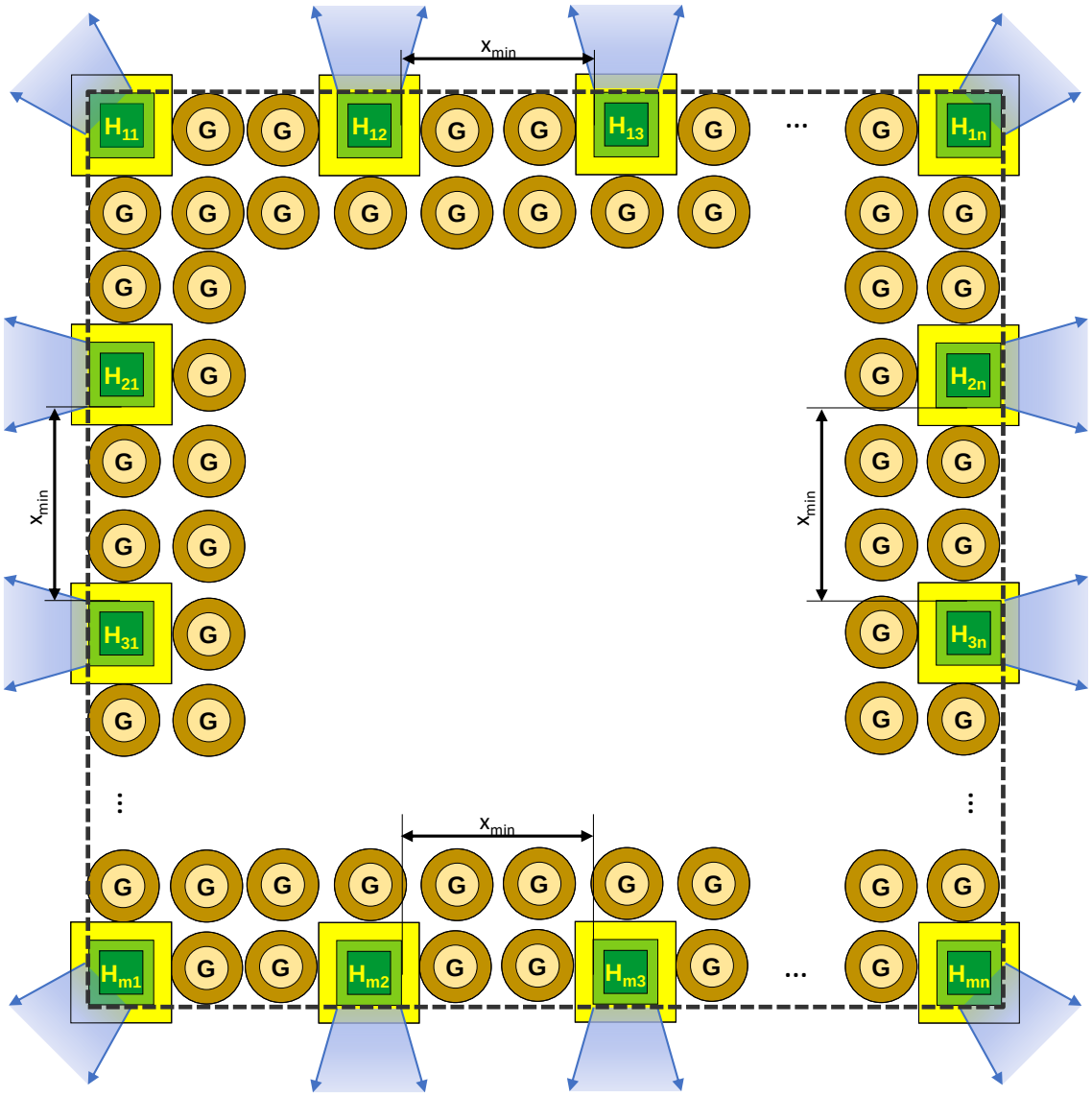

Figure A.8: Layouts satellite topology for n pads in quadratic configuration

A.3 Layouts Linear Topology

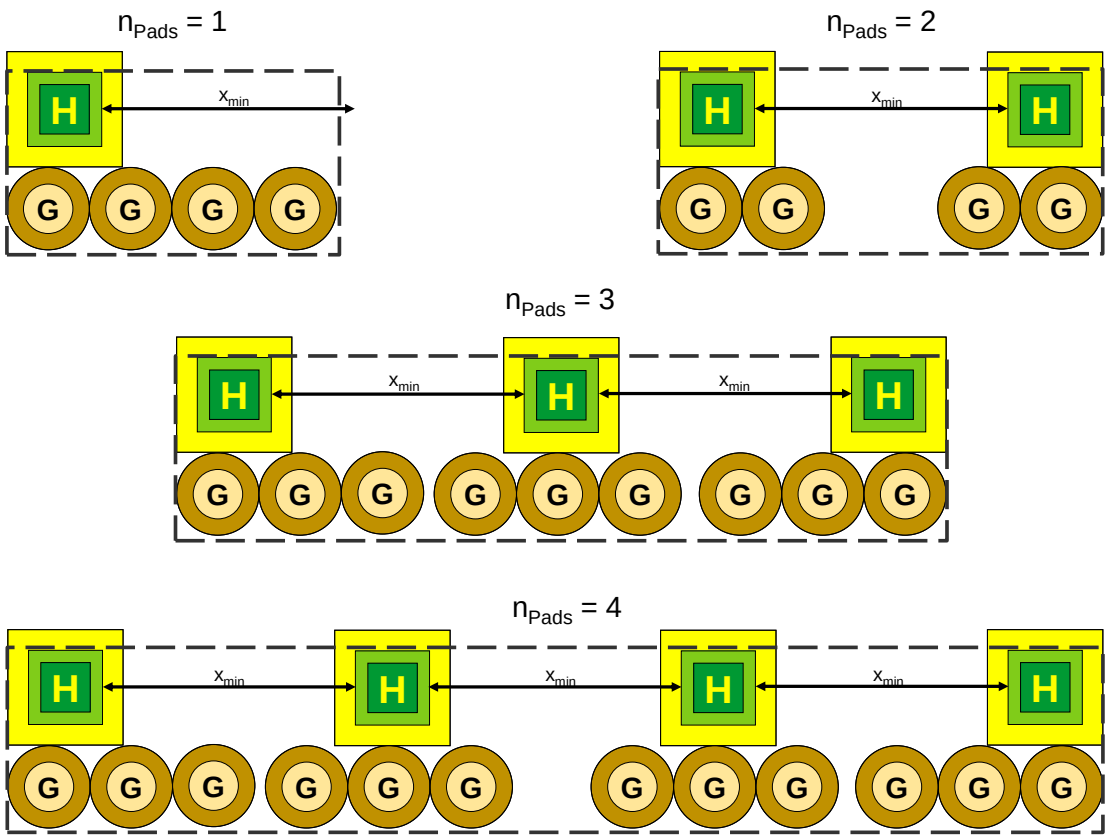

Figure A.9: Layouts linear topology for one, two, three and four pads in one row for given x_{min}

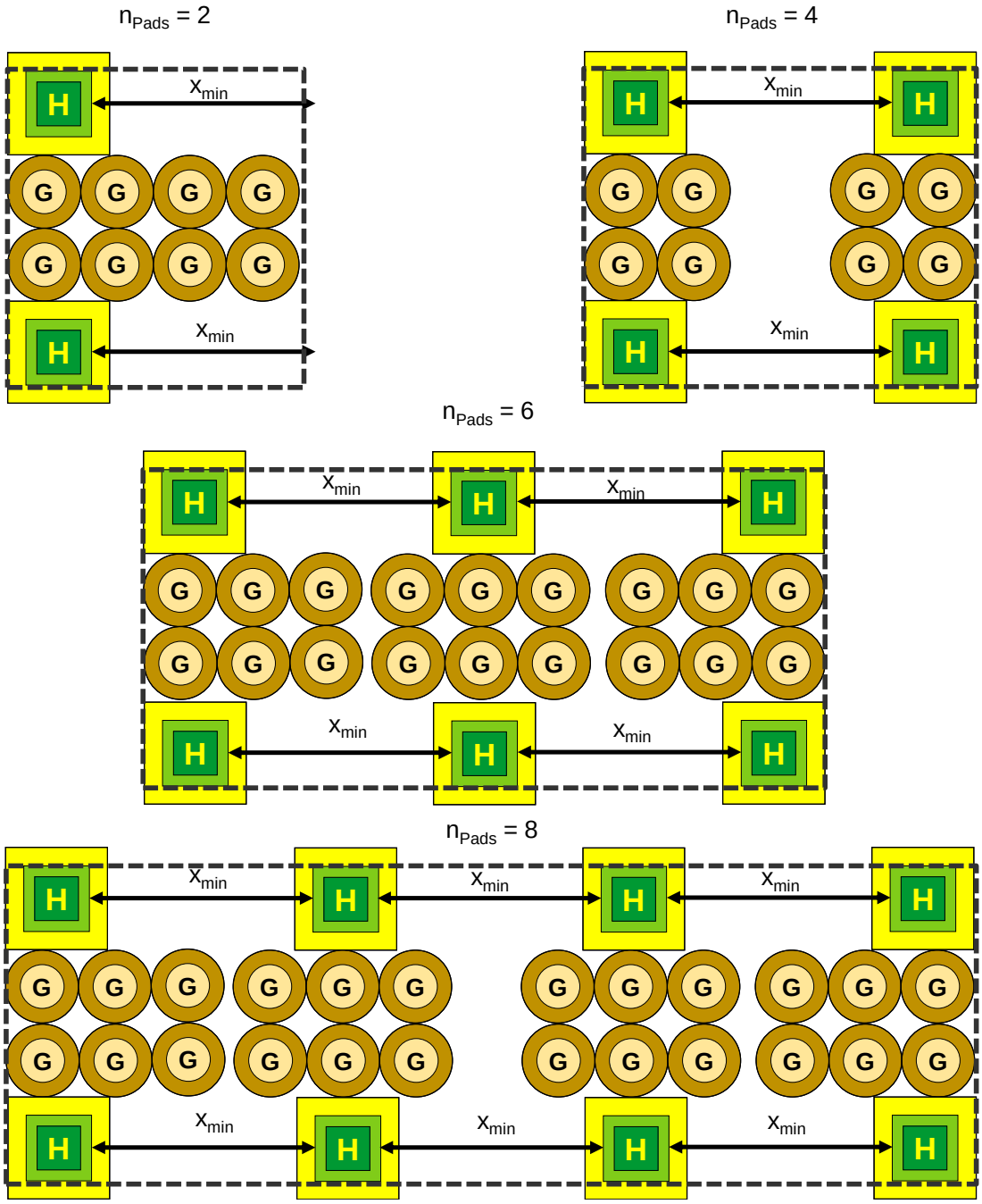

Figure A.10: Layouts linear topology for one, two, three and four pads in two rows for given x_{min}

A.4 Layouts Pier Topology

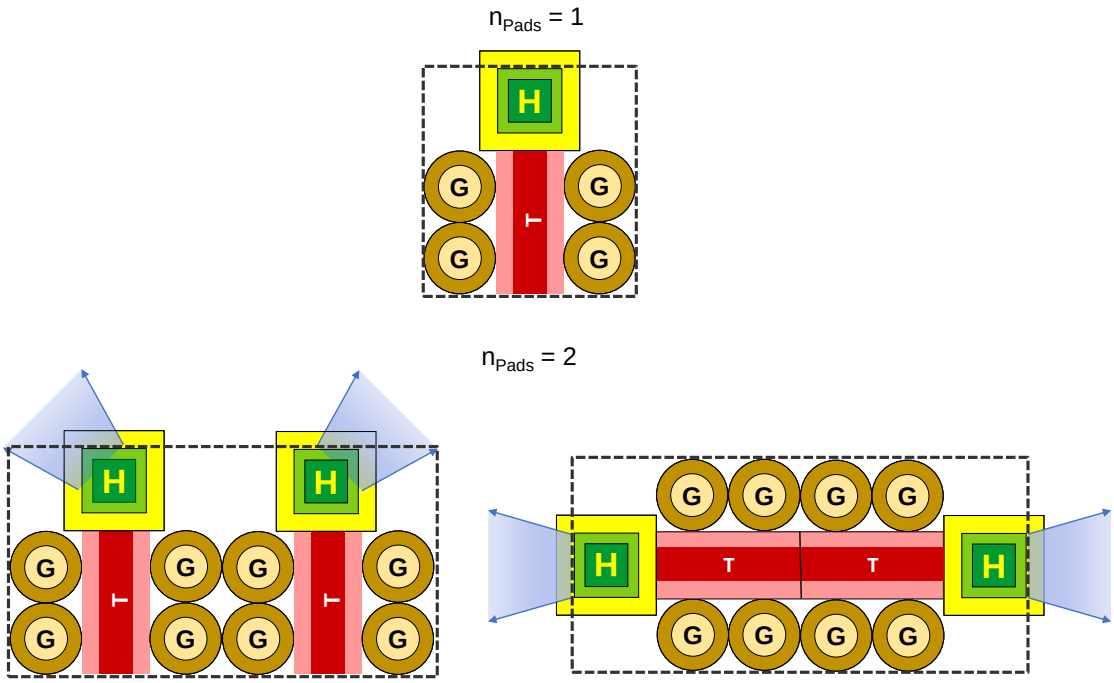

Figure A.11: Layouts pier topology for one and two pads for $pad2taxi = 1$

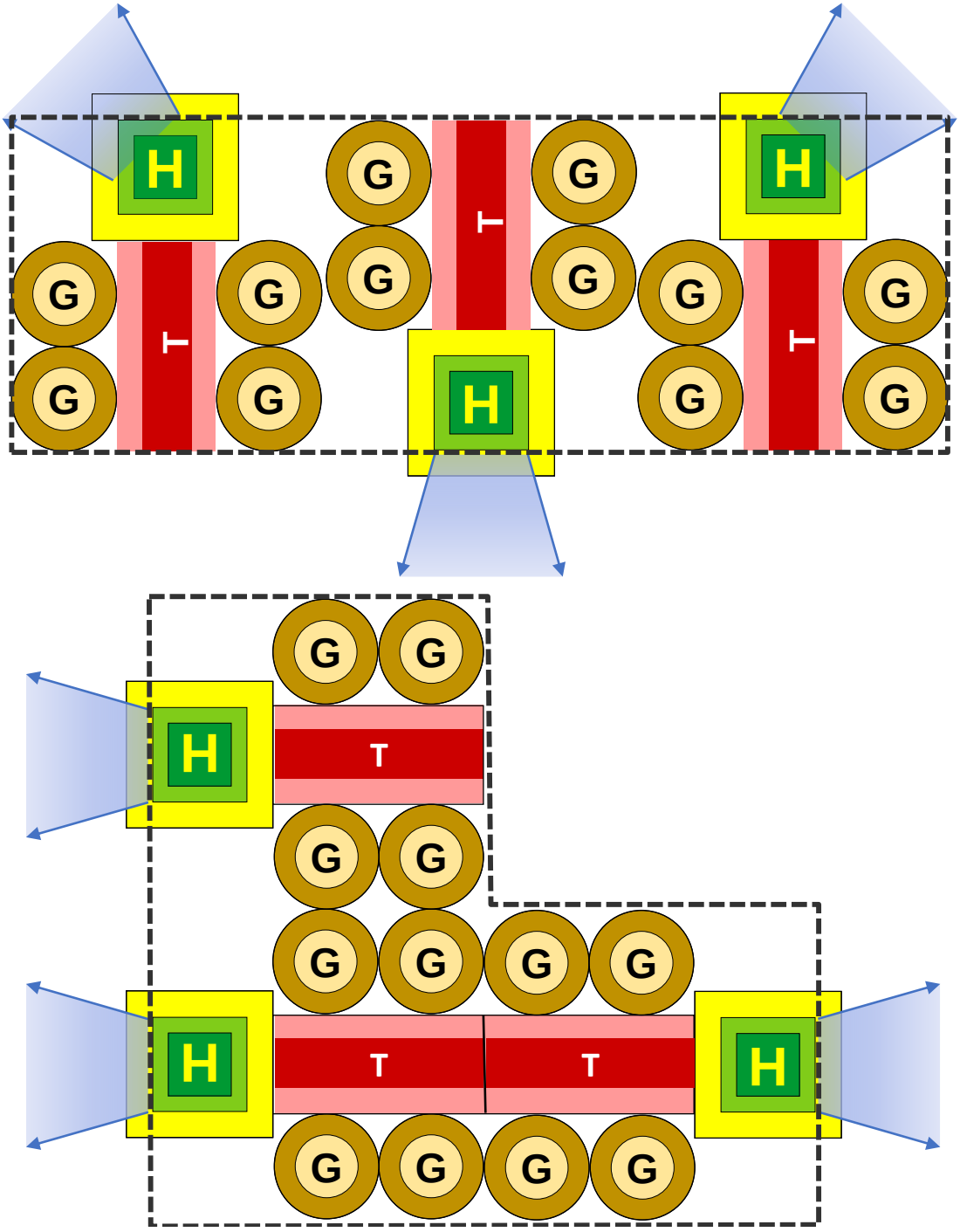

Figure A.12: Layouts pier topology for three pads for $pad2taxi = 1$

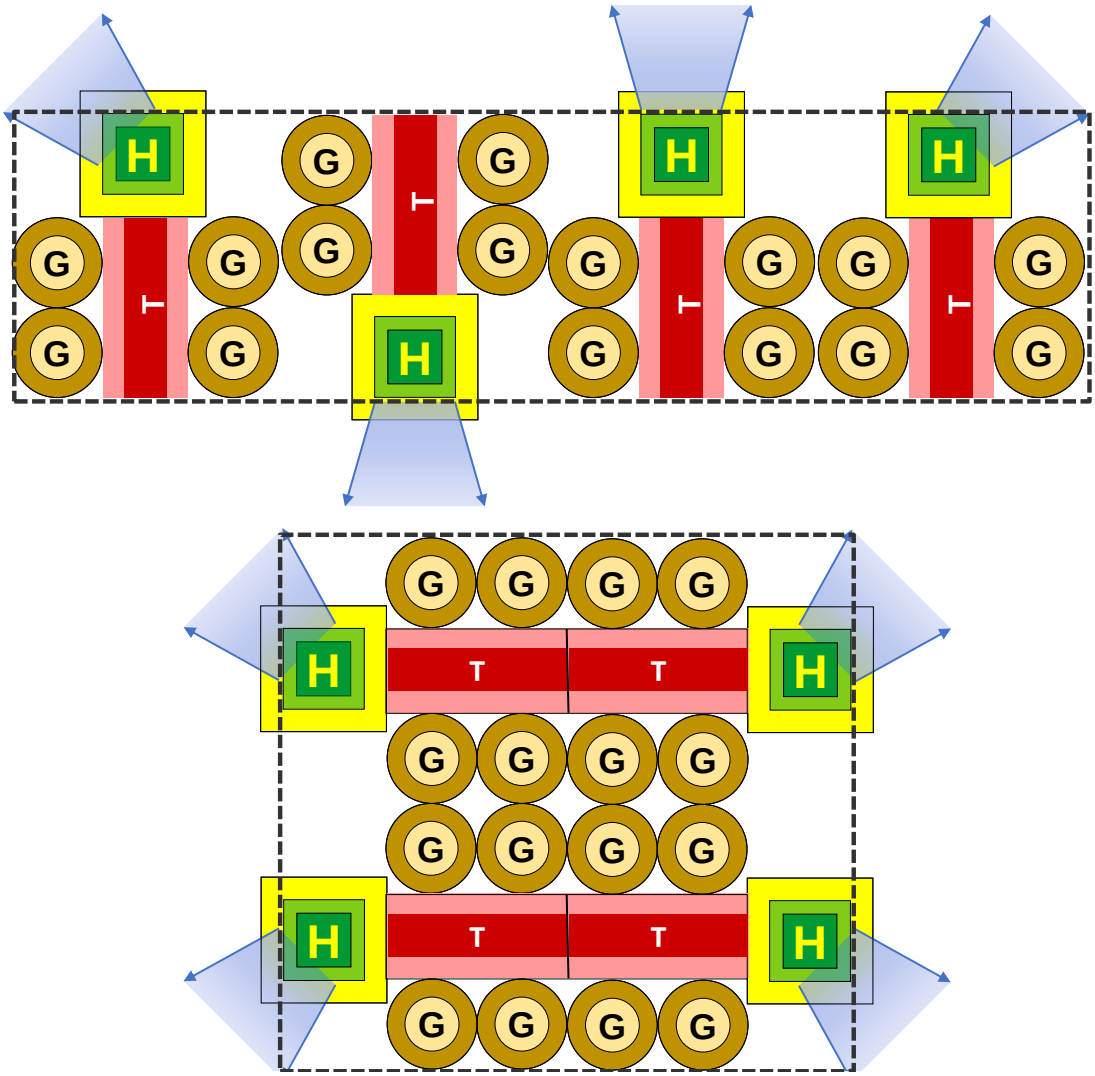

Figure A.13: Layouts pier topology for four pads for $pad2taxi = 1$

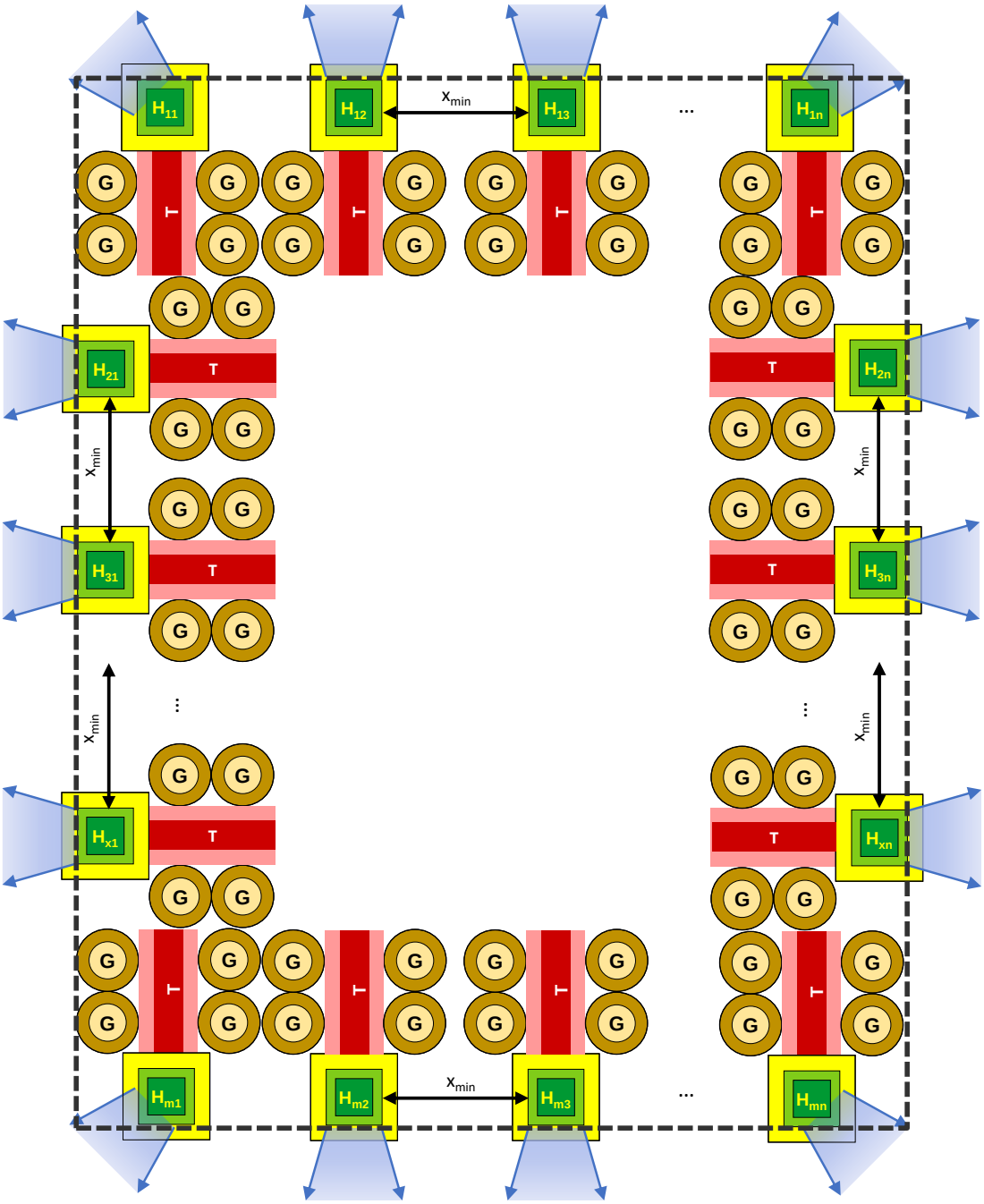

Figure A.14: Layouts pier topology for n pads for $pad2taxi = 1$

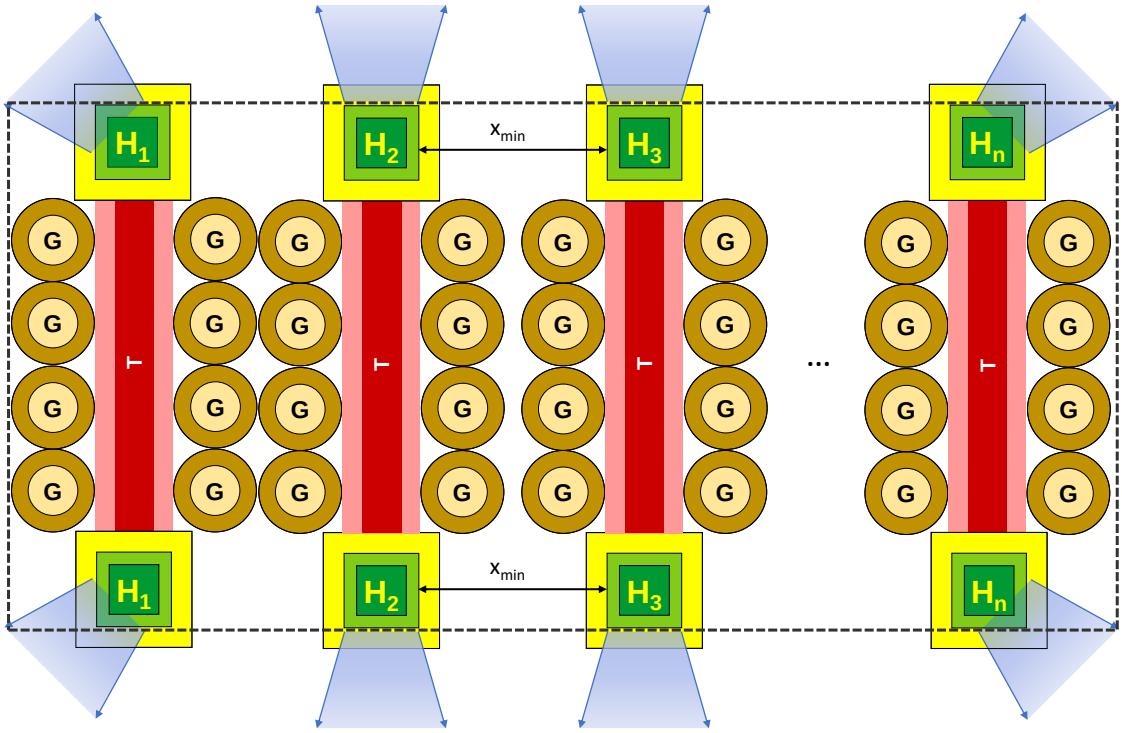

Figure A.15: Layouts pier topology for n units in linear configuration for $pad2taxi = 2$

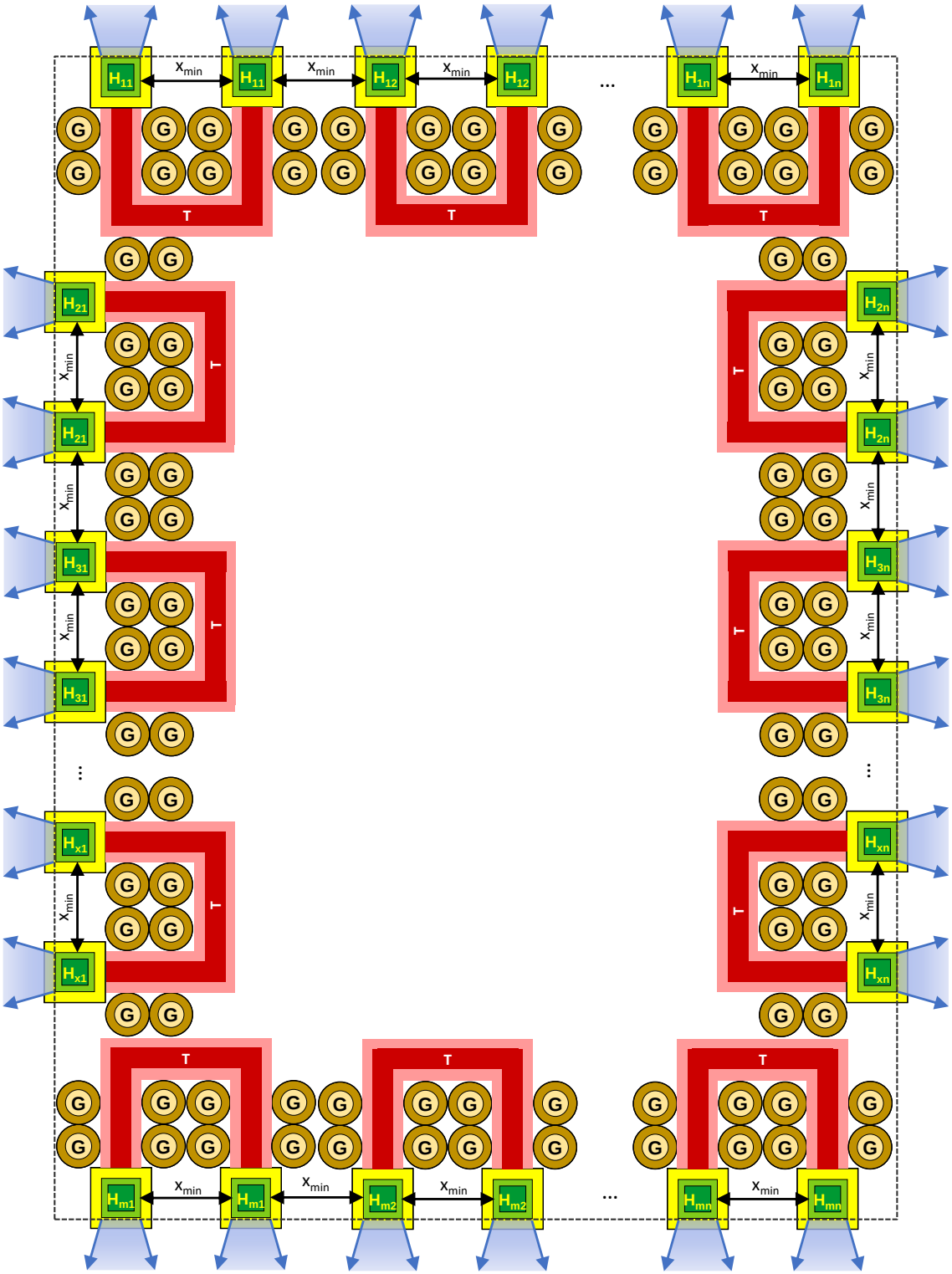

Figure A.16: Layouts pier topology for n units in quadratic configuration for $pad2taxi = 2$

B Appendix: Area to Throughput Study with improved version

All in relation to the area to throughput study conducted with the improved version.

B.1 Experimental Setup

STUDY-SHEET

Study name:	Study A2T v2.0
Date:	15.07.2021
Tool:	A2T v2.0

Research Questions

1. How does the area size and shape influence the Topology selection?
2. Which topology is favorable for which area?
3. How much is the throughput dependent on the area-shape?
4. Which vehicle leads to highest throughput based on variation of turnaround times and areas?
5. What is the influence of different $t_{turn,passenger}$ depending on the vehicle?
6. How is the influence of $t_{turn,\mathrm{fix}}$ vs $t_{turn,passenger}$?
7. How big is the impact of takeoff and landing time depending on the other process times and the vehicle?
8. What are the most common $\mathrm{gate2pad}$ ratios for each topology?
9. How do different takeoff and landing times influence the vertiport layout?
10. How do different process times influence the vertiport layout?
11. What is the most common bottleneck?

Research Hypothesis

1. A rule of thumb can be derived for the choice of topology depending on the given area.
2. A rule of thumb for the $\mathrm{gate2pad}$ ratio for each topology can be extracted.
3. A rule of thumb can be derived for the expected throughput depending on the given area.
4. There is a type of vehicle that is best suited depending on the given parameters.

Parameters

Parameter	Value Range	Unit	Combinations
Area (size)	200 – 50.000 in steps of 200	m^2	250
Area (side ratio)	1:1; 1:2; 1:3; 2:3	m	4
Vehicles (size/passengers)	6 representative	m & $n_{passengers}$	6
x_{min}	0; 30; 61	m	3
$t_{T\&L}$	30; 60; 90	s	3
$t_{turn,passenger}$	15; 30; 60; 90	s	4
$t_{turn,\mathrm{fix}}$	0; 5; 10; 15; 20	min	5
Taximode	hover; ground	-	2
$t_{prepare4taxi}$	0; 5; 90 (hover; wheels; passive)	s	3
$pad2taxi$	1; 2	-	2
$taxi2gate$	0.5	-	1
Topology	single; satellite; linear; pier	-	4
Total	-	-	25.92 million

Figure B.1: Eperimental setup of study with improved version of area to throughput

B.2 Results Research Questions on Throughput of Layout

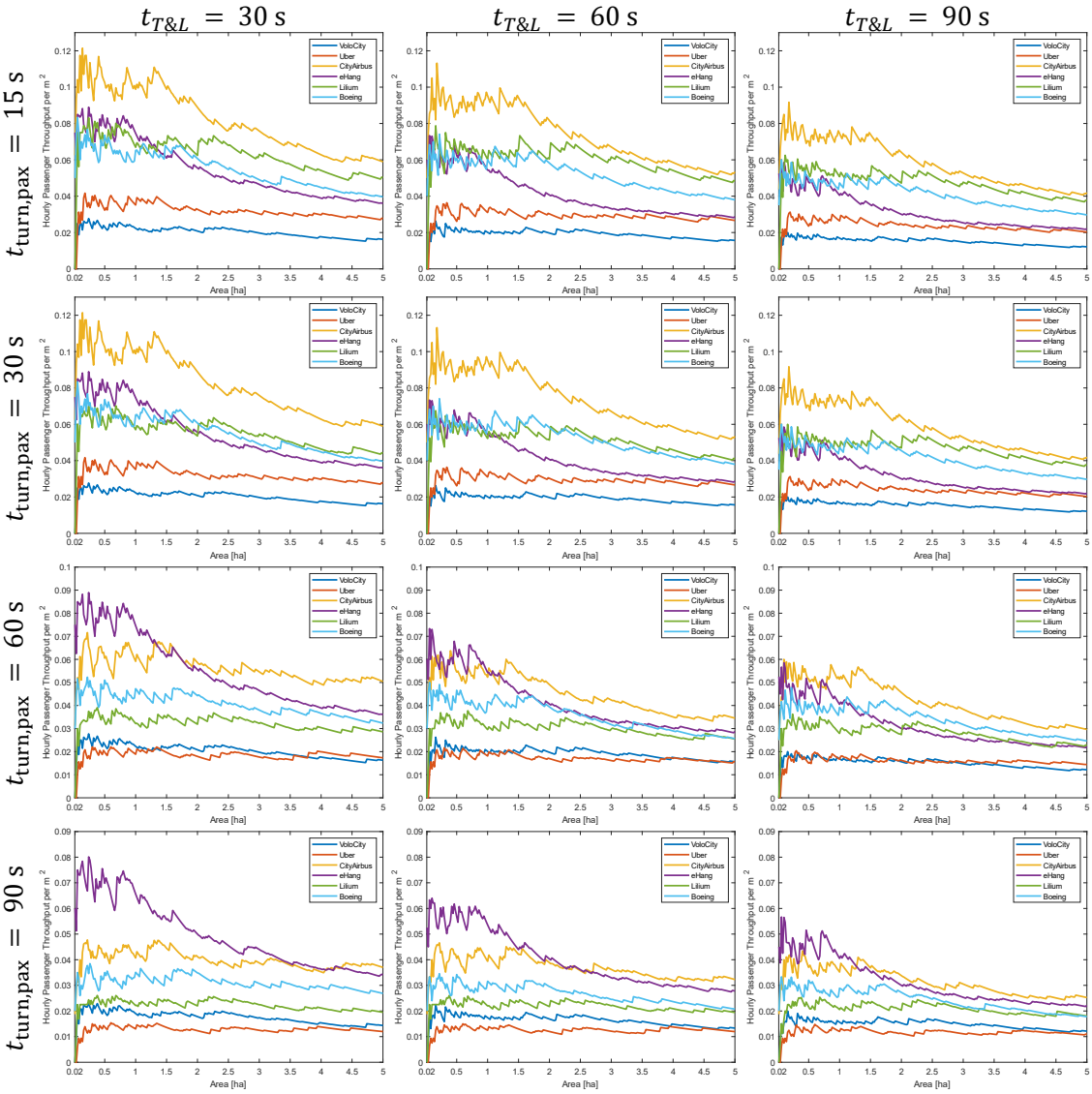

Figure B.2: Hourly passenger throughput for different vehicles and process times and $t_{turn,fix} = 5\ min$

Figure B.3: Hourly passenger throughput for different vehicles and process times and $t_{turn,fix} = 15\ min$

Figure B.4: Hourly passenger throughput for different vehicles and process times and $t_{turn,fix} = 20\ min$

B.3 Results Research Questions on resulting Layout

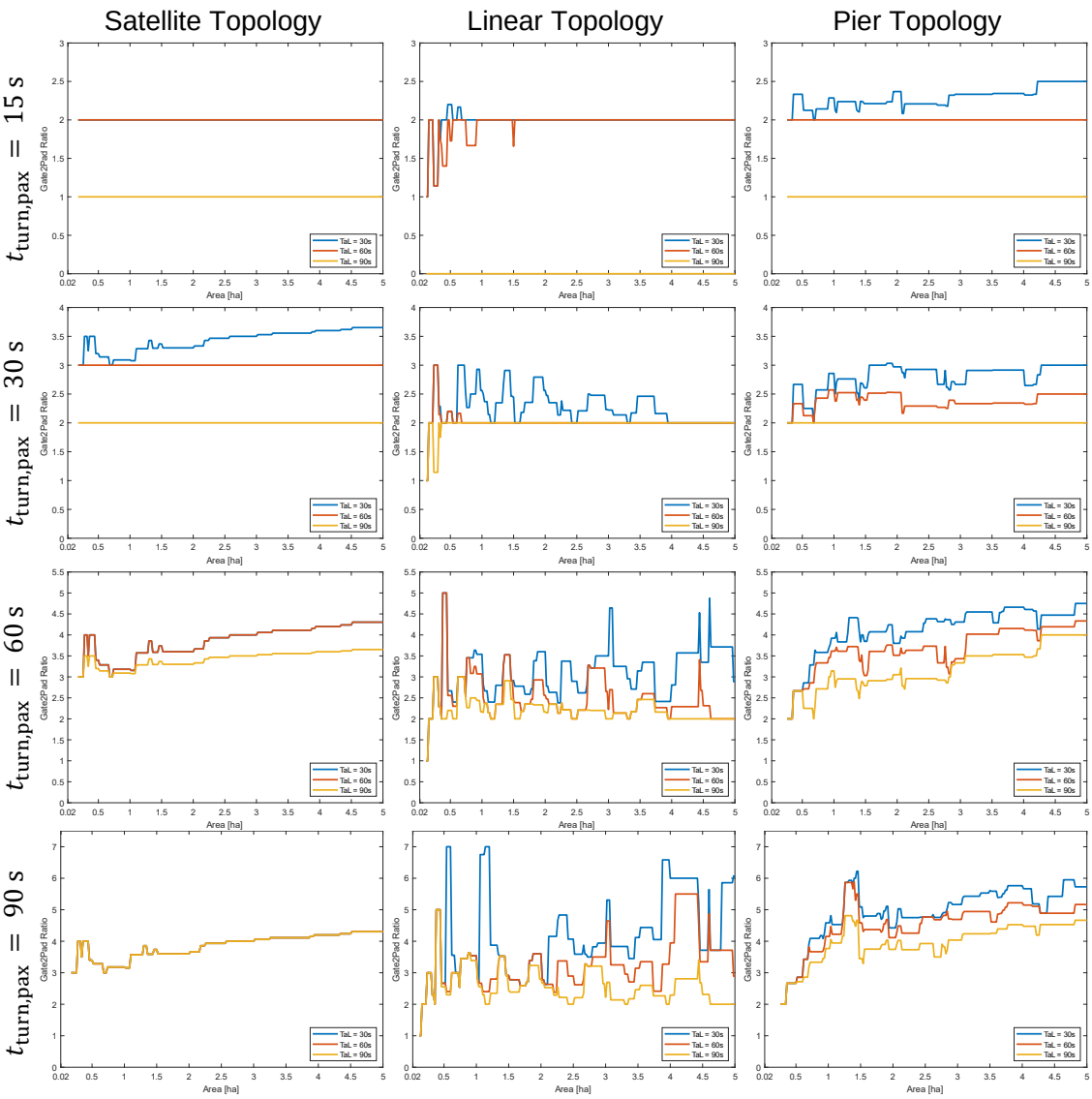

Figure B.5: Topology layout for Lilium for different process times and $t_{turn,fix} = 0\ min$

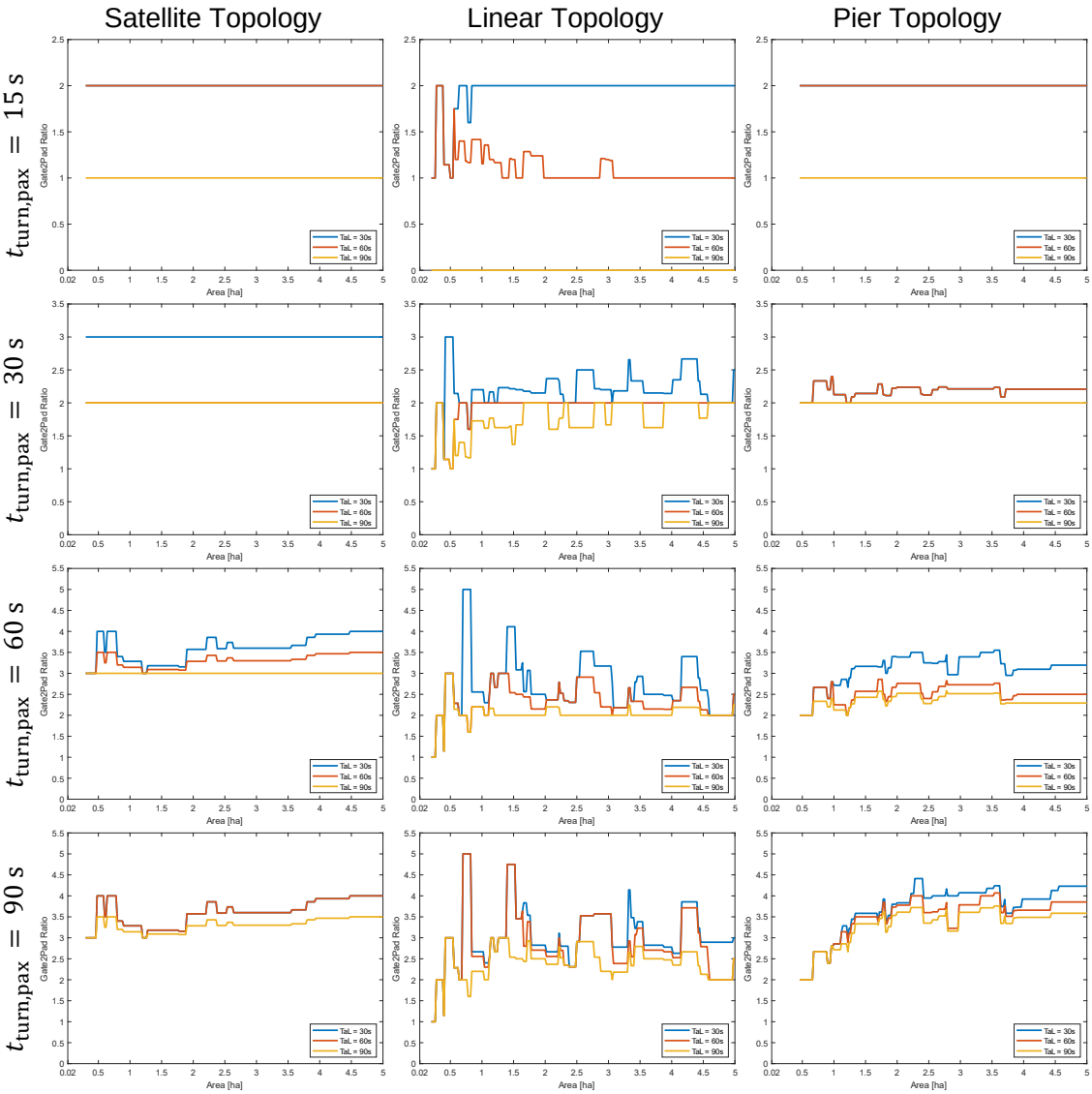

Figure B.6: Topology layout for Uber for different process times and $t_{turn,fix} = 0\ min$

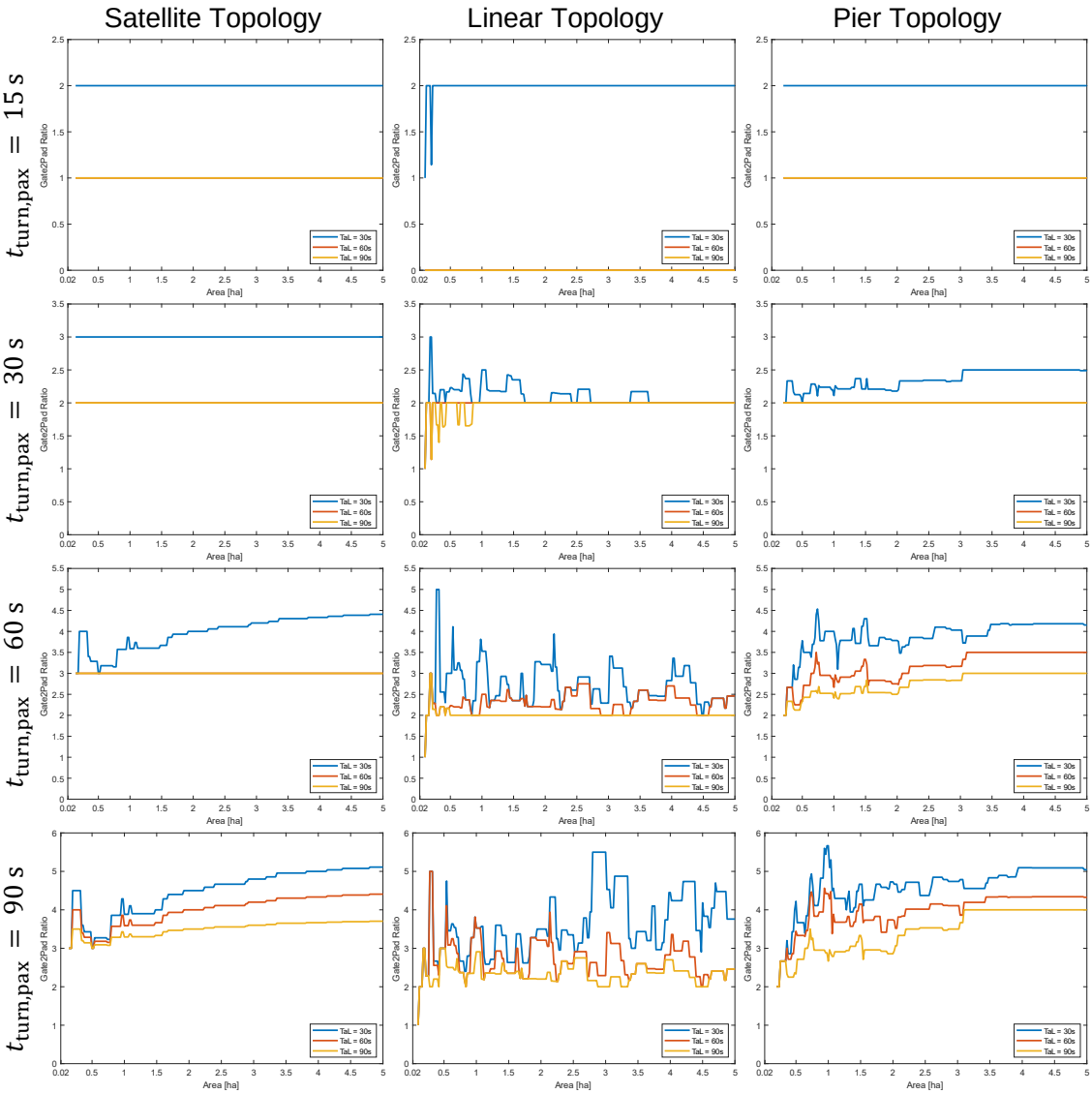

Figure B.7: Topology layout for Boeing for different process times and $t_{turn,fix} = 0\ min$

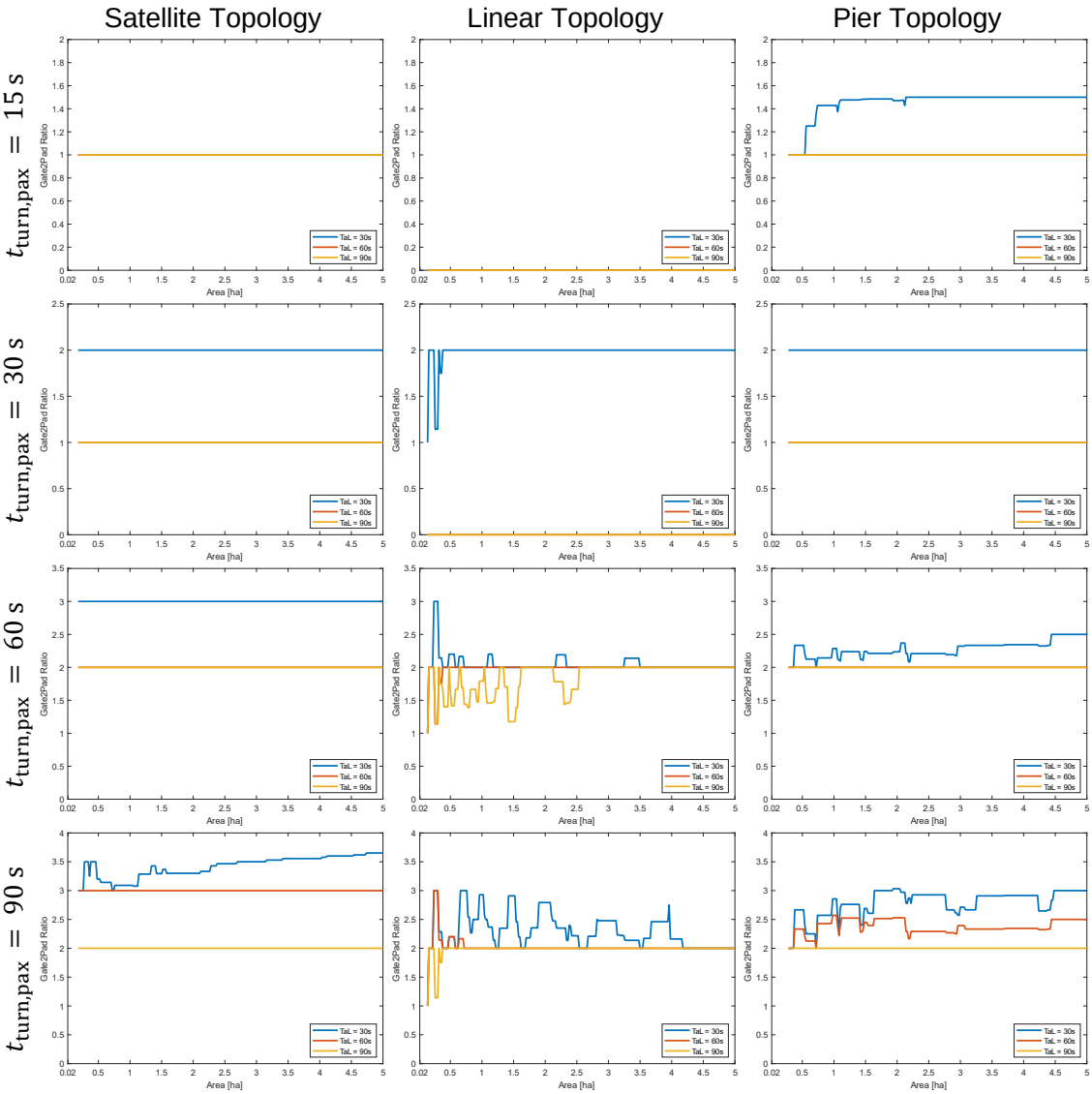

Figure B.8: Topology layout for VoloCity for different process times and $t_{turn,fix} = 0\ min$

B.4 Results Research Question on Bottleneck of Layout

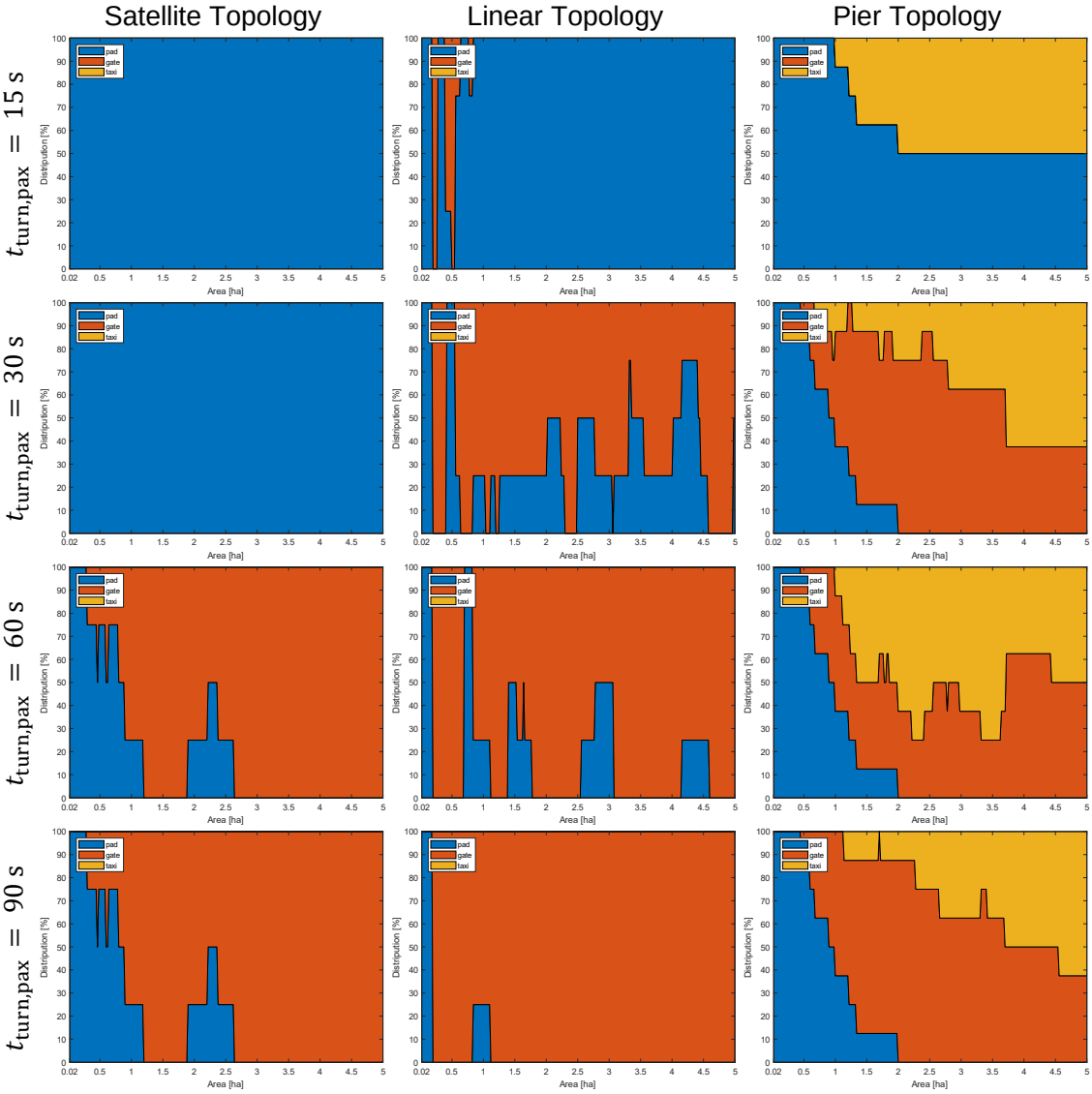

Figure B.9: Bottleneck distribution for Uber for different process times and $t_{turn,fix} = 0\ min$ and $t_{T\&L} = 60\ s$

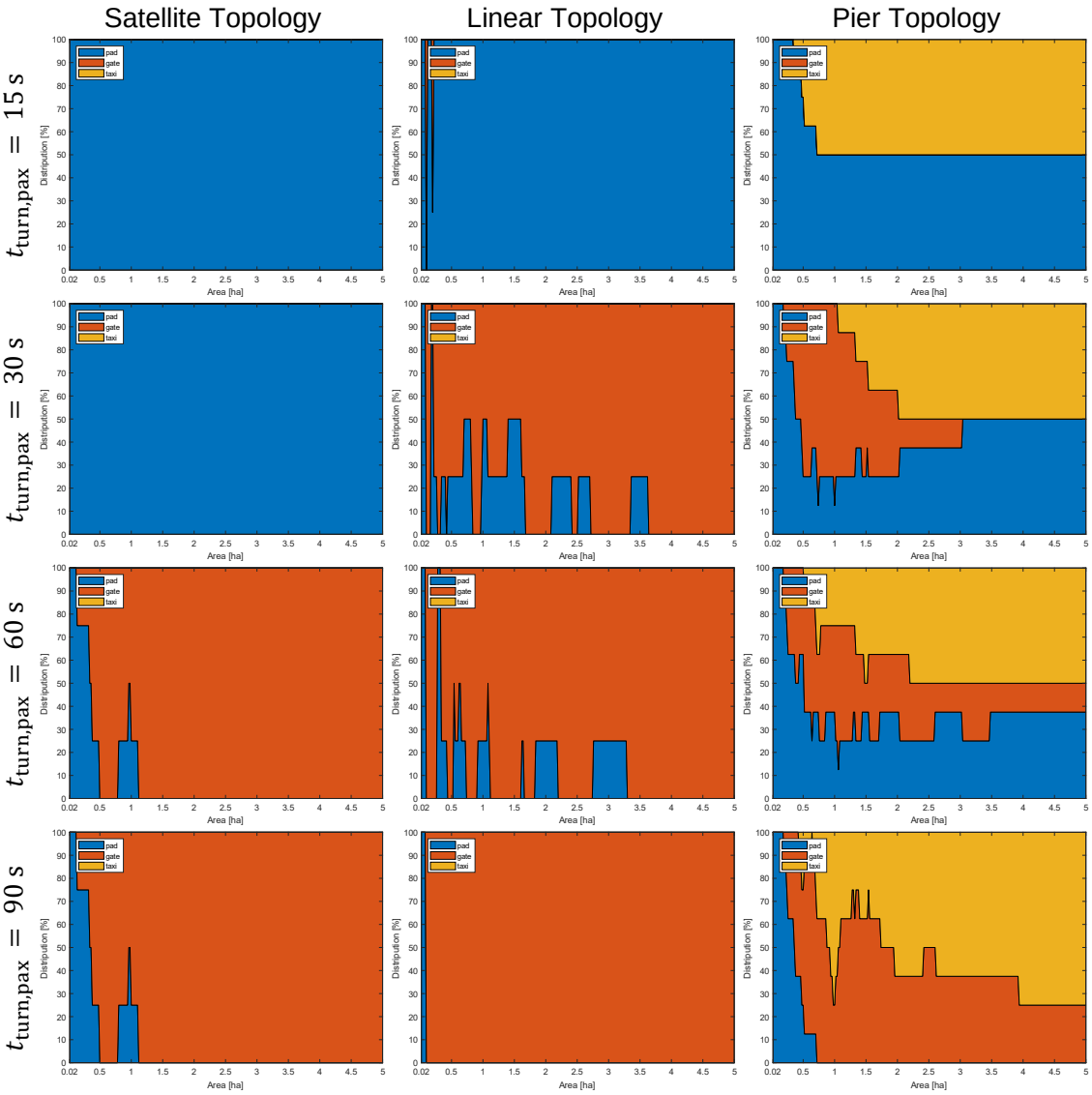

Figure B.10: Bottleneck distribution for Boeing for different process times and $t_{turn,fix} = 0\ min$ and $t_{T\&L} = 60\ s$

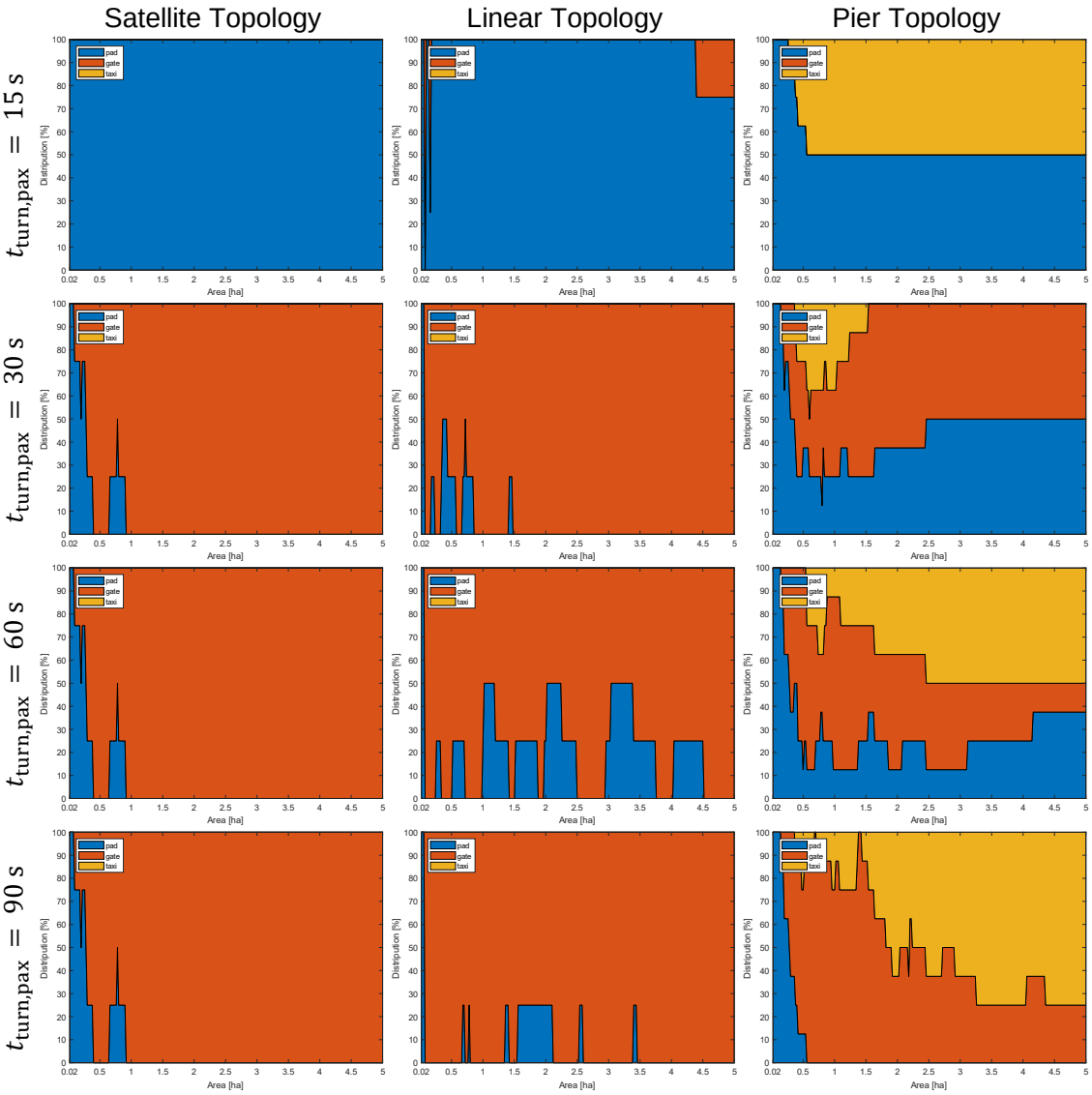

Figure B.11: Bottleneck distribution for CityAirbus for different process times and $t_{turn,fix} = 0\ min$ and $t_{T\&L} = 60\ s$

C Appendix: Area to Throughput Real World Scenario

All in relation to the area to throughput study regarding the real world scenario.

C.1 Experimental Setup

STUDY-SHEET

Study name:	Real World Study
Date:	15.07.2021
Tool:	A2T v2.0

Research Questions

1. Is the code applicable on real world scenarios?
2. Will the given design fit on the given area?
3. Which vehicle will work best for the buildings?
4. Are the results relatable to the rules of thumb from other study?
5. What is the possible throughput of the given locations?

Research Hypothesis

1. With the given code feasible vertiport designs can be created.

Parameters

Parameter	Value Range	Unit	Nr.
Area	3 areas out of (Berlin)	polygon	3
Vehicles (size/passengers)	6 representative	m & $n_{passengers}$	6
x_{min}	30	m	1
$t_{T\&L}$	60	s	1
$t_{turn,passenger}$	30;	s	1
$t_{turn,\mathrm{fix}}$	10	min	1
Taximode	hover	-	1
$t_{prepare4taxi}$	0	s	1
$pad2taxi$	1	-	1
$taxi2gate$	0.5	-	1
Topology	single; satellite; linear; pier	-	4
Total	-	-	72

Selected Areas

- Berlin Alexanderplatz Train station
- Bundeskanzleramt Berlin
- Parking Berlin Tempelhof

Figure C.1: Eperimental setup of real world scenario of area to throughput approach

D Appendix: Throughput to Area Study

All in relation to the throughput to area study.

D.1 Experimental Setup

STUDY-SHEET

Study name:	Study T2A
Date:	15.07.2021
Tool:	T2A

Research Questions

1. Which topology has the highest throughput per area unit?
2. What is the influence of varying take-off and landing times as well as turnaround times on the required area?
3. Which vehicle requires the least area to achieve a given throughput?

Parameters

Parameter	Value Range	Unit	Combinations
Passenger throughput per hour	20 to 1000 in steps of 5	pax/h	197
Vehicles (size/passengers)	6 representative	m & $n_{passengers}$	6
x_{min}	30	m	1
$t_{T\&L}$	30; 60; 90	s	3
$t_{turn,passenger}$	15; 30; 60; 90	s	4
$t_{turn,\mathrm{fix}}$	10	min	1
Taximode	hover	-	1
$t_{prepare4taxi}$	0	s	1
$pad2taxi$	1	-	1
$taxi2gate$	0.5	-	1
Topology	single; satellite; linear; pier	-	4
Total	-	-	56736

Figure D.1: Eperimental setup of throughput to area approach